Uncovering interactions between exported *Plasmodium falciparum* and human erythrocyte cytoskeleton proteins in the process of host cell remodeling

INAUGURALDISSERTATION

zur

Erlangung der Würde eines Doktors der Philosophie

vorgelegt der

Philosophisch-Naturwissenschaftlichen Fakultät

der Universität Basel

von

Jan Dominic Warncke

aus

Teufen (AR)

Basel, 2019

genehmigt von der Philosophisch-Naturwissenschaftlichen Fakultät auf Antrag von

Prof. Dr. Hans-Peter Beck und Prof. Dr. Kai Matuschewski

Basel, den 11. Dezember 2018

Prof. Dr. Martin Spiess

Dekan

Summary

The protozoan parasite *Plasmodium falciparum* causes the most severe form of human malaria, an infectious tropical disease of global public health importance. Despite efforts and means to prevent or treat this disease, there are still over 200 million cases and almost half a million deaths annually attributed to *P. falciparum*. Transmitted to the human host by female *Anopheles* mosquitos serving as vector, the parasite eventually invades erythrocytes and starts asexual replication. This stage causes the clinical symptoms of malaria.

The red blood cell is an interesting choice of a host cell for the intracellular parasite *P. falciparum* as it lacks a nucleus, protein transport machinery, and its nutrient channels are inactive. To survive within this host environment, the parasite therefore has to remodel its host cell. The extensive host cell remodelling of human erythrocytes during the course of *P. falciparum* infection is facilitated by a large number of proteins which the parasite exports into its host cell cytoplasm. The function of the majority of these proteins remains elusive. Existing data suggests that some of these exported parasite proteins target the host cytoskeleton and modulate its properties, as apparent in changed mechanical properties of the host cell.

The aim of this project was to identify interactions between host cytoskeleton and exported parasite proteins and to create a protein interaction network of the remodeled cytoskeleton. Identifying the key players and essential interactions in the process of host cell remodelling will lead to the identification of new targets in the fight against the malaria parasite. To this end, a number of exported proteins belonging to the PHIST family were selected. All selected PHIST proteins were exported into the host cell with most of them localizing in proximity to the erythrocyte cytoskeleton or membrane. The promiscuous biotin ligase BirA* (BioID) was fused to these proteins and upon addition of biotin proteins in the proximity were labelled with biotin. This allowed the pull-down using streptavidin-beads and identification of potential interaction partners of these transgenic, exported proteins by mass spectrometry. Based on the results from this study and additional data from previous projects, I generated a network of potential protein-protein interactions at the erythrocyte cytoskeleton.

A standard approach to verify potential protein interactions is to perform reverse protein pull-downs. Because erythrocytes lack a nucleus, the classical transgenic approach to add molecular tags to erythrocyte proteins or to modify them in any way is not possible. To circumvent this holdback and to facilitate immunoprecipitations with erythrocyte proteins as bait, I generated parasite lines which expressed and exported different tagged human cytoskeleton proteins. These transgenic human proteins were designed to be exported and to be soluble within the cytosol of

the infected erythrocyte. It was expected that these proteins would bind to their putative endogenous parasite binding partners while these are transported to their final destination within the host cell. These transgenic human proteins can then be used for immunoprecipitations to identify these binding partners. I tested several export sequences and showed that each of them resulted in efficient export of the intracellular loop of band 3 (residues 1-379) and the full-length band 4.1. In both of these cell lines, the majority of the protein was soluble in the host cytosol. Due to time constraints, these cell lines could not be further analyzed in detail.

While little is known about the function and role of exported proteins in host cell remodeling during asexual developmental stages, even less is known about these proteins and their functions during gametocyte development of *P. falciparum*. Until recently, it was difficult to obtain high numbers of gametocytes, making it difficult to study host cell remodeling in these stages. The availability of a transgenic cell line from the Voss lab at Swiss TPH, in which high sexual conversion rates can be induced, provides a great opportunity to study these interactions in gametocytes. Taking advantage of this cell line we characterized GEXP02, a member of the PHIST protein family which is expressed and exported in gametocytes. We confirmed the expression pattern and localized GEXP02 at the periphery of the gametocyte-infected erythrocyte. By immuno-precipitation and mass spectrometry we could identify cytoskeleton proteins as well as other exported proteins as potential interaction partners. Based on co-labelling of GEXP02 with PFI1780w and PF3D7_0424600, two other PHIST proteins, we could confirm these as likely interaction partners. In GEXP02 knock-out parasites, no obvious detrimental effect or phenotype could be observed in asexual parasites or during gametocyte development nor throughout the mosquito stages or in liver hepatocyte infectivity. Although no function could be assigned to this protein, our study is one of the first to characterize in great detail an exported protein in gametocytes and shows that the erythrocyte cytoskeleton is targeted by exported parasite proteins also during gametocyte development.

Furthermore, within the context of this present study, I conducted two extensive literature reviews. In one review I collected information on the functionally elusive PHIST family in the genus *Plasmodium*. The review on the PHIST protein family presents an in-depth overview on this protein family. It acts as a reference work for quick, but detailed information on these proteins that are thought to be involved in cytoskeleton remodelling. The other review concerned protein-protein interactions involved in host cytoskeleton remodeling of *P. falciparum*. By combining pieces of existing information, new insights were gained in this review. I could show that each

stage of the intraerythrocytic life cycle presents different challenges to the intracellular survival of the parasite. Consequently, *P. falciparum* remodels its host cell differently in the various stages to meet the specific needs.

In summary, this thesis provides new insight into host cell remodeling by the malaria parasite, shows the importance of exported proteins in this process, and offers a new tool in the study of interactions between erythrocyte cytoskeleton and exported parasite proteins.

Acknowledgements

This PhD project has been quite a journey and I am grateful that many people accompanied, supported, and motivated me and also walked alongside me during this journey. The work presented here has been carried out between March 2015 and December 2018.

First and foremost I want to thank Prof. Dr. Hans-Peter Beck for giving me the opportunity to conduct my PhD thesis work under his supervision and guidance. I highly appreciate the constant strive for scientific correctness and excellence. Thank you also for supporting my attendance at a number of interesting courses on bioinformatics.

I want to thank Armin Passecker for being a good friend and lab mate since we started our Master thesis work in the Mol Par Group.

Beatrice Schibler, it was a pleasure to work with you in the lab. I highly appreciate our conversations and the scientific input iI received from you. This encouraged me and provided me with the motivation needed to overcome some difficult times.

It was a great pleasure to be entrusted with four master students: Trang Nguyen, Anke Gabel, Sabina Beilstein, and Matthias Wyss. Furthermore, I had the chance to work with other master students that went through our lab: Eva Hitz, Laura Zurbrügg, Stephan Wichers, and Eron Rushiti. It was an enrichment to have you all of you in the lab, to talk to you, and to see you succeed in your projects. Working with you has been a great experience. Your many questions challenged me and helped me to understand things even better.

Thank you Alex Oberli for being a good supervisor during my Master studies, for teaching me the ins and outs of malaria culture and work in a molecular biology lab. This made the start into my PhD studies much easier.

A special thanks goes to Sebastian Rusch for answering so many of my questions in a helpful, professional, and patient way. This was a great and invaluable support. Thierry Brun and Fabien Haas from the Technical Services were an amazing support at keeping the lab together and running and fixing our lab equipment.

During the past few years, I had the chance to work with and learn from many other wonderful malaria researcher at the Swiss TPH and I am grateful for their input to my projects during lab meeting presentations or other conversations: Natalie Hofmann, Rahel Wampfler, Maria Grünberg, Igor Niederwieser, Till Voss, Ingrid Felger, and Esther Mundwiler-Pachlatko.

I am also grateful to Alexia Loynton-Ferrand and Kai Schleicher from the Imaging Core Facility at the Biozentrum of the University of Basel for assistance with image acquisition and analysis.

Lara Pérez-Martínez and Falk Butter from the Institute of Molecular Biology (IMB), Mainz, Germany, were instrumental in the mass spectrometric analysis of the many co-immunoprecipitations I performed. Thank you for this collaboration and also for the two great visits I had in Mainz.

Thank you Jemma Day, for the fun time in the lab. It was great to have you here for a while.

I want to acknowledge the generous support of the ‚Gesellschaft für experimentelle Zoologie' from which I received a travel stipend to attend the Molecular Parasitology Meeting 2018 in Woods Hole, USA.

Thanks to Sylwia Boltryk, Françoise Brand, and Clara Antunes-Muniz for the many great conversations we had during the past few years, our lunches, and the afternoon coffee breaks. I also enjoyed the activities we did outside of the lab, be it concerts, barbecues, watching the lunar eclipse, or playing fun games.

It is difficult to even find words that express how grateful I am to my family for their support during the past four years. Without you, I probably would not have made it. Your constant encouragement and love kept me going. Thanks for always believing in me and telling me that I could do it.

Table of Contents

Abbreviations

Abbreviation	Name
aa	amino acid
ACT	Artemisinin-based combination therapy
ATS	acidic terminal segment
bp	base pair
BSA	bovine serum albumin
BSD	Blasticidin-S-hydrochloride
CD36	cluster of differentiation 36
CSA	chondroitin sulfate
DAPI	4′,6′-diamino-2-phenylindole
DD	destabilization domain
DIC	differential interference contrast
DTT	dithiothreitol
EDTA	ethylenediaminetetraacedic acid
EPCR	endothelial protein C receptor
EPIC	exported protein-interacting complex
ER	endoplasmic reticulum
EXP2	exported protein 2
fw	forward
GAPDH	glyceraldehyde 3-phosphate dehydrogenase
GEXP	gametocyte exported protein
GFP	green fluorescent protein
GIE	gametocyte-infected erythrocyte
GlcN	glucosamine
GlcNAc	N-acetylglucosamine
h	hour
HA	hemagglutinin
hDHFR	human dehydrofolate reductase
hpi	hour post invasion
HR	homology region

Abbreviation	Name
HSP	heat shock protein
ICAM	intracellular adhesion molecule
iRBC	infected red blood cell membrane
KAHRP	knob-associated histidine rich protein
kDa	kilo Dalton
KO	knock-out
LDS	lithium dodecyl sulfate
LyMP	lysine-rich membrane associated PHISTb protein
MAHRP1/2	membrane-associated histidine rich protein
MC	Maurer's cleft
MESA	mature parasite-infected erythrocyte antigen
MS	mass spectrometry
myc	proto-oncogene named after the myelocytomatosis-associated gene
NPP	new permeation pathway
P. falciparum	*Plasmodium falciparum*
PAGE	polyacrylamide gel electrophoresis
PBS	phosphate buffered saline
PCM	parasite culture medium
PCR	polymerase chain reaction
PEXEL	*Plasmodium* Export Element
PfEMP1	*Plasmodium falciparum* Exported Membrane Protein 1
PfPTP	*Plasmodium falciparum* PFEMP1 transporting protein
PHIST	*Plasmodium* Helical Interspersed Subtelomeric
PIC	protease inhibitor complete/cocktail
PNEP	PEXEL negative protein
PPM	parasite plasma membrane
PRESAN	*Plasmodium* RESAN N-terminal
PSAC	*Plasmodial* surface anion channel
PTEX	*Plasmodium* translocon of exported proteins

Abbreviation	Name
PV	Parasitophorous vacuole
PVM	Parasitophorous vacuole membrane
RBC	red blood cell membrane
RESA	ring-infected erythrocyte surface antigen
rv	reverse
SBP1	skeleton-binding protein 1
SDS	sodium dodecyl sulfate
SERA	serine-repeat antigen
SLI	selection linked integration
SMFA	standard membrane feeding assay
TM	transmenbrane
Tris	Tris(hydroxymethyl)aminoethan
TRX2	thioredoxin 2
WHO	World Heath Organization

Chapter 1: Introduction

Malaria Epidemiology

Malaria is a tropical disease caused by the unicellular Apicomplexan parasite *Plasmodium*. Five *Plasmodium* species cause human malaria: *P. falciparum*, *P. vivax*, *P. malariae*, *P. ovale*, and *P. knowlesi*. While *P. vivax* is the most wide-spread species, *P. falciparum* causes the most severe form of malaria, called malaria tropica (1-3).

The 2017 WHO World Malaria Report shows progress made in the fight against malaria. Between 2010 and 2016, an increase was reported for the distribution of insecticide-treated nets, the number of febrile children seeking health care and being tested for malaria, as well as the number of pregnant women receiving preventive treatment. In the same time interval, the incidence rate decreased by 18% and a number of countries has reported zero cases for the last years or has been certified as malaria free (4).

Despite this progress and despite being a preventable and treatable disease, malaria still has a major global impact on health and economy. It has caused an estimated 216 million cases and 445'000 deaths in 2016, with half of the human population at risk of infection (4). Malaria remains endemic in 76 countries, most of which are located in subsaharan Africa, and the tropical regions of Southeast Asia and South America (Figure 1). 80% of all malaria cases were reported from 15 countries, all but one in subsaharan Africa, indicating that this region suffers the greatest malaria burden (4).

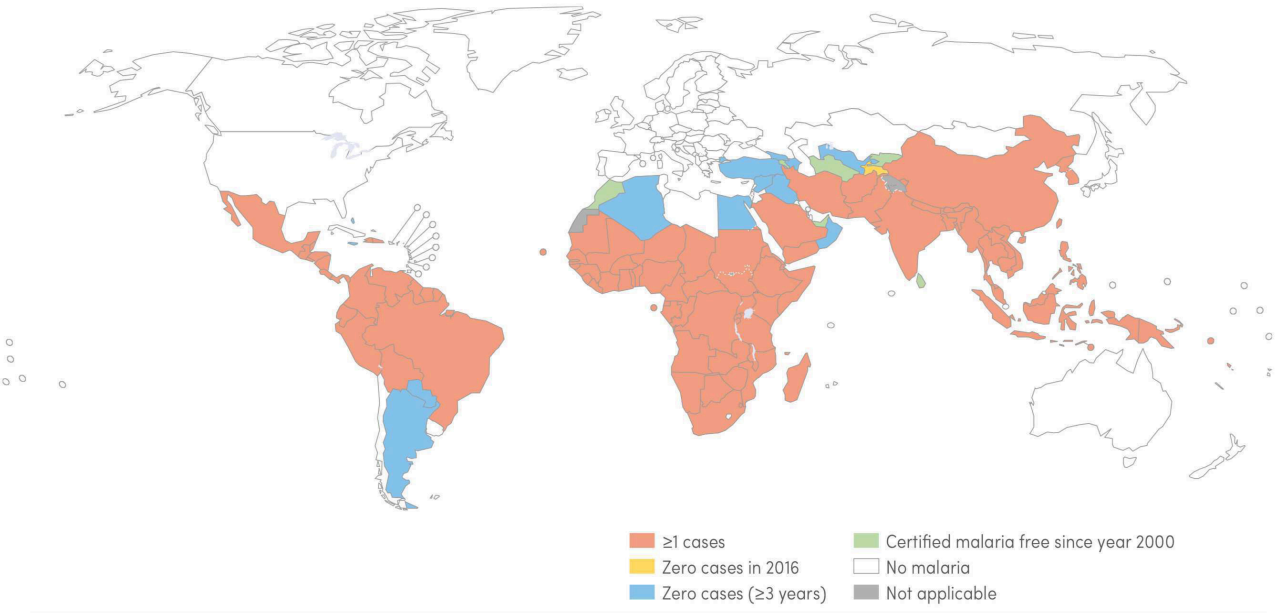

Figure 1. Malaria endemic countries. World map showing the 2016 status of countries with indigenous malaria cases in 2000. Figure adapted from WHO World Malaria Report 2017 (4).

Malaria Life Cycle

P. falciparum has a complex life cycle alternating between two different hosts, the human host and the arthropod vector. Upon the bite of an infected female *Anopheles* mosquito, a few sporozoites are injected into dermal tissue (Figure 2A). These sporozoites then migrate through the tissue by gliding motility until they reach the blood stream. From there, sporozoites eventually reach the liver, traverse through Kupffer cells hepatocytes, and finally invade liver hepatocytes (3). Once inside the hepatocyte, sporozoites start replication, at the end of which thousands of merozoites are formed (3, 5). Upon rupture of the hepatocyte, merosomes are released into the blood stream and subsequently release the merozoites which then invade erythrocytes (6). This starts the 48 hour asexual replication cycle (Figure 2B).

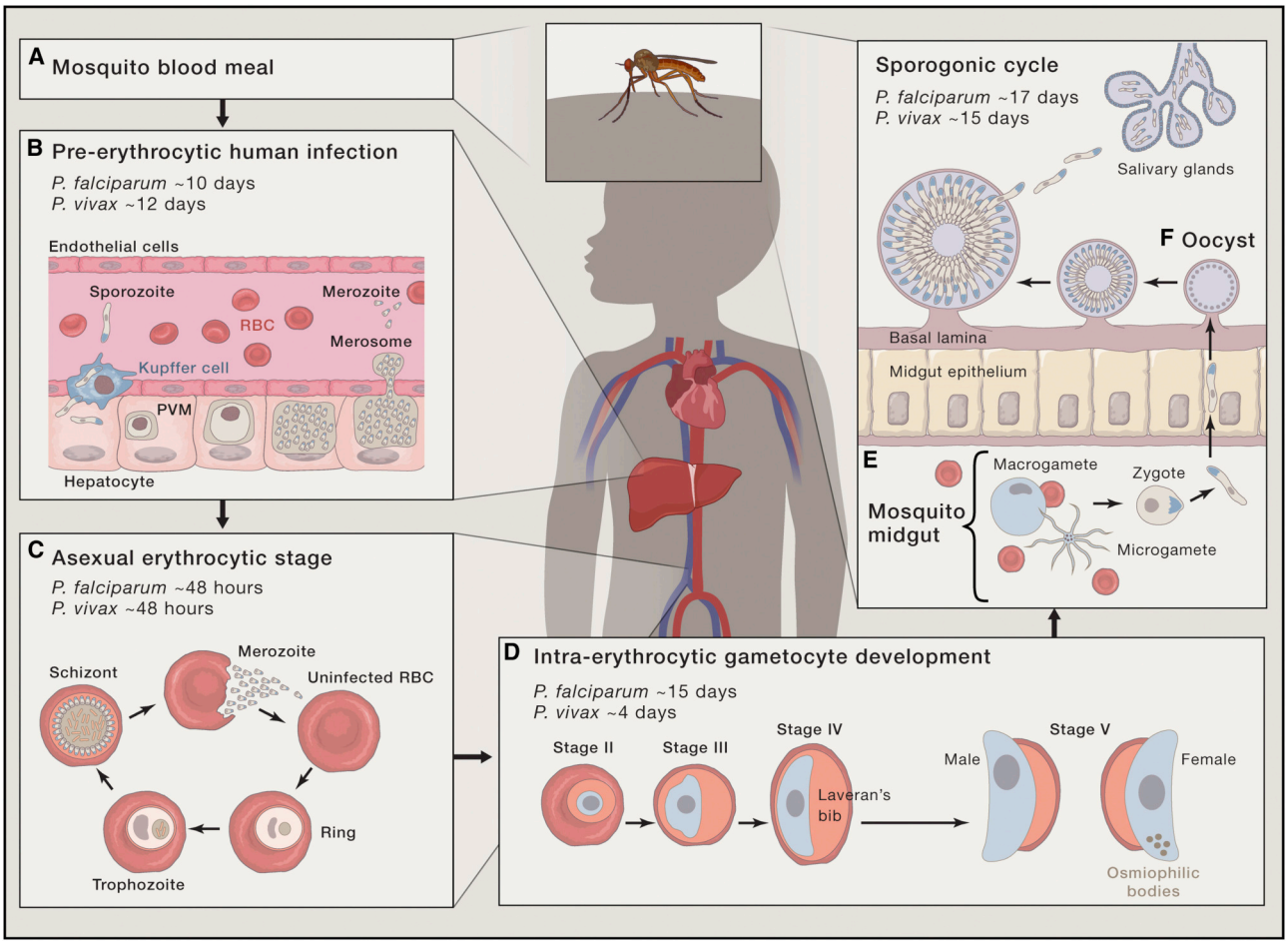

Figure 2. Life cycle of *P. falciparum*. The life cycle starts with the transmission event during a mosquito blood meal (A), followed by the liver stage (B) and the intra-erythrocytic stages consisting of asexual replication (C) and sexual development (D). After transmission to the mosquito, sexual replication occurs in the mosquito midgut (E) and then final developmental stages occur in the basal lamina (F). Figure adapted from Cowman et al. (3).

For the first half of the intra-erythrocytic cycle, the parasite is in the ring stage. This is followed by the trophozoite and schizont stages. Mature schizonts release merozoites into the blood stream in an event known as egress. These released merozoites start a new asexual replication cycle (Figure 2C) (3). During each asexual cycle, a few parasites commit to sexual development. Once these committed parasites reinvade a new host cell, they become gametocytes. Gametocytes sequester in the bone marrow. Sexual development can be divided into five distinct morphological stages, with stage V being mature gametocytes which re-enter the blood stream (7). Stage V gametocytes can be transmitted to the mosquito vector during a blood meal (Figure 2D). In the mosquito midgut, male and female gametocytes become gametes, fuse into a zygote, and undergo meiosis (Figure 2E). Following meiosis, ookinetes migrate into the midgut endothelium. There, they develop into oocysts inside which sporozoites are formed. Mature sporozoites migrate to the salivary gland and are ready for transmission to a new human host (Figure 2F) (3).

Clinical Symptoms, Treatment, and Prevention

Clinical symptoms are only caused during the asexual blood stages. The most common and also non-specific clinical symptoms are fever, nausea, vomiting, and muscle pain. In severe cases life-threatening complications such as cerebral malaria (coma), anaemia, and organ failure can occur (3, 8).

A number or antimalarial drugs are available. However, in recent years, resistance to some of these antimalarial drugs has been reported (9). For example, resistance against artemisinin has surfaced in Southeast Asia, conferred by the C580Y point mutation in Kelch 13, a proposed E3 adaptor protein (10). Emerging resistances threaten malaria control programs and elimination efforts and underline the need for further research in drug and vaccine development. To minimize the risk of resistance formation, WHO recommends Artemisinin-based combination therapies.

The most effective way to fight malaria and work towards its elimination would be vaccines. Albeit research for malaria vaccines is ongoing and various candidates are at different stages of clinical trials, none has yet been licensed for commercial use (11).

Early malaria diagnosis is essential for successful treatment and interrupting the transmission cycle. Different types of diagnostic tools are available, each of them bearing intrinsic advantages and disadvantages with regard to sensitivity, availability, and given infrastructures. The most

sensitive means of malaria diagnosis is PCR. Antigen-based rapid diagnostic tests and parasite detection by microscopy of Giemsa-stained blood smears are standard diagnostic tools in low resource or field settings (12).

Protein Export

Since the erythrocyte is a terminally differentiated cell that lacks both a nucleus and a secretory system/protein trafficking machinery, *P. falciparum* has to extensively remodel the red blood cell in order to turn it into a suitable host and ensure its survival. Exported parasite proteins and their interactions with host proteins are responsible for this remodeling. To reach their interaction partners and to fulfill their role, these parasite proteins have to cross two membranes: the parasite plasma membrane (PPM) and the parasitophorous vacuole membrane (PVM). Exported proteins are classified into two different groups, those with a known export signal, and those lacking such a signal.

A group of exported parasite proteins possesses a pentameric amino acid motif RxLxE/Q/D, with x representing any amino acid. The discovery of this *Plasmodium* Export Element (PEXEL) allowed for the prediction of about 460 exported proteins (13-16), accounting for approximately 10% of the parasite's proteome (17).

A number of exported proteins lack a known export signal and are thus called PEXEL-negative exported proteins (PNEP). Some PNEPs are associated with Maurer's clefts and PfEMP1 trafficking such as MAHRP1/2, SBP1, and REX1/2, indicating their significance in host cell remodeling (18). However, the lack of an export signal makes it impossible to predict their number, making PNEPs somewhat of a black box in these processes.

Proteins are translated in the parasite cytosol. Normally, co-translational entry into the ER and thus entry into the secretory pathway is mediated by a signal peptide, a hydrophobic region at the N-terminus of the nascent protein. Once inside the ER, the PEXEL motif is cleaved after the leucine residue by Plasmepsin V, the N-terminus is acetylated (19, 20), and proteins are folded by chaperones. Proteins destined for export are then transported by vesicles to the PPM and are secreted into the PV (21).

The next barrier to be crossed is the PVM. A multi-protein complex, the *Plasmodium* translocon of exported proteins (PTEX), translocates proteins across the PVM. The PTEX consists of three essential proteins EXP2, PTEX150, HSP101, as well as two non-essential proteins PTEX88

and TRX2. Multiple copies of EXP2 proteins form a pore that spans the PVM while multiple copies of PTEX150 and HSP101 extend the pore on the luminal side of the PV. Once unfolded, proteins are translocated by the PTEX from the PV lumen into the erythrocyte cytosol in an ATP-dependent process (22-25). The newly discovered Exported Protein-Interacting Complex (EPIC) is thought to shuttle proteins targeted for export to the PTEX and thus aid in translocation across the PVM (26). Chaperones assist in refolding and/or further trafficking of these proteins. Now in the host cell, exported proteins have to reach their final destination such as the iRBC cytoskeleton and membrane, Maurer's clefts, J-dots, vesicles, or the host cytosol (reviewed in (27)).

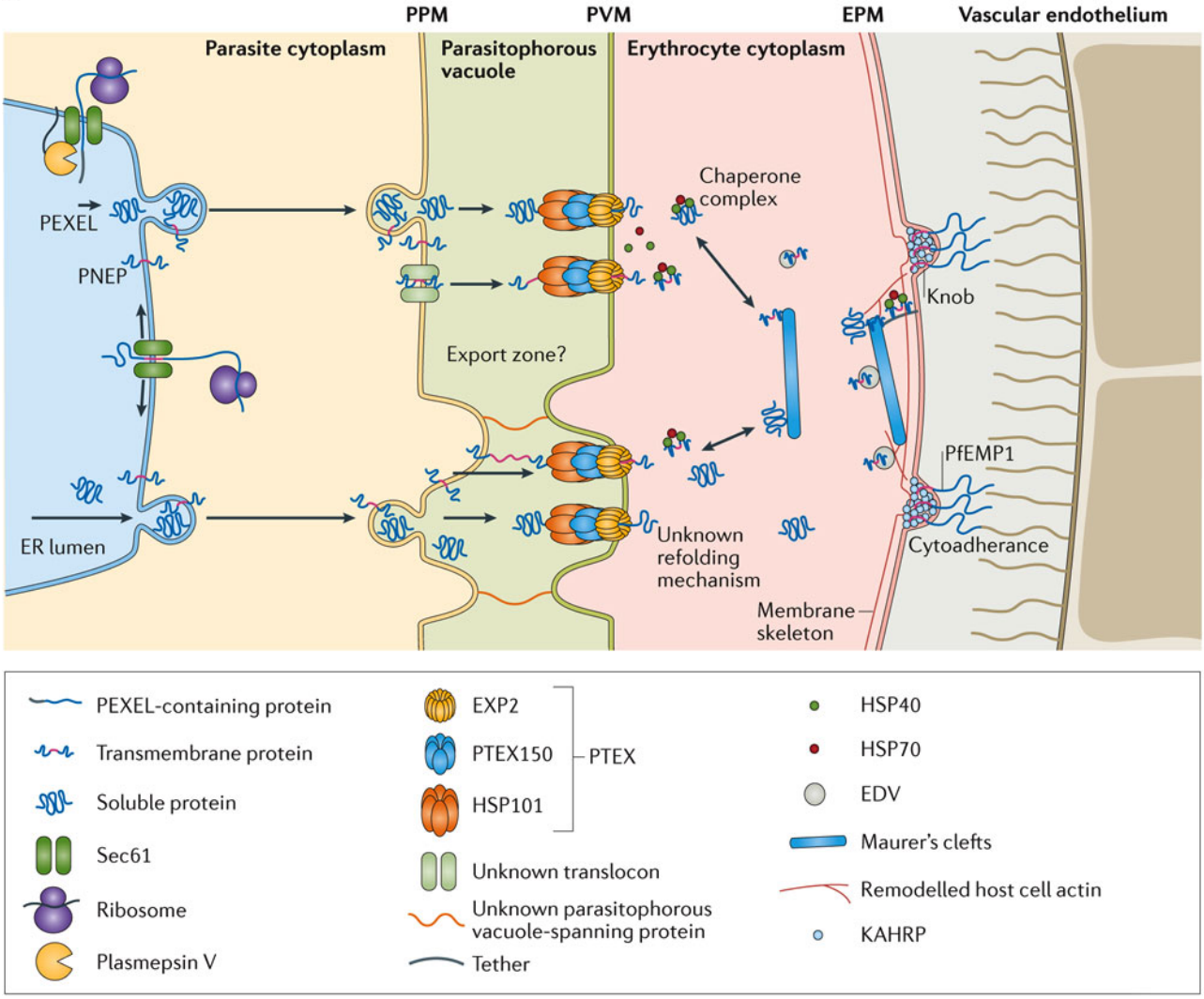

Figure 3. Protein export in *P. falciparum*. During their export from the parasite into the host, parasite proteins have to cross several membranes, including the parasite membrane (PM), the parasitophorous vacuole membrane (PVM), and in the case of secreted proteins also the erythrocyte plasma membrane (EPM). Vesicular transport, translocation through pore complexes, and chaperone-assisted protein refolding are some means involved in protein export. Figure adapted from De Koning-Ward et al. (27).

Functions of Exported Proteins

Exported proteins are central to the intracellular survival of *P. falciparum* and thus fulfil a variety of functions within the host cell. One of these functions is nutrient uptake. While the malaria parasite feeds on hemoglobin, this does not provide all amino acids as hemoglobin lacks for example isoleucine. To access required solutes and amino acids not (sufficiently) found within the host cytoplasm, the permeability of the iRBC membrane has to be increased, allowing uptake of nutrients from the extracellular environment and ion homeostasis. This new permeability pathway (NPP) consists of parasite-derived membrane channels called *Plasmodial* surface anion channel (PSAC). These channels are inserted into the PPM and facilitate solute uptake (28-30).

Many exported proteins assist in trafficking of others. On the way to their final destination, many exported proteins pass through Maurer's clefts, or are transported in vesicle-like structures or in protein complexes containing chaperones. Thus, some proteins are simply exported to establish the trafficking machinery for those exported proteins that interact with and modify the host (reviewed in (31, 32)). Gametocyte sequestration in the bone marrow requires parasite-induced alterations to host cytoskeleton deformability and rigidity. Apart from STEVOR (33), such a role for most exported proteins in gametocytes has yet to be confirmed (7).

PfEMP1, Immune Evasion, and Cytoskeleton Remodeling

The growing parasite has to avoid clearance by the spleen in order to ensure its survival and to continue in its life cycle. The evolutionary answer to this is cytoadhesion mediated by *P. falciparum* exported membrane protein 1 (PfEMP1), an exported transmembrane protein which is inserted into the iRBC membrane in surface protrusions referred to as knobs (34). The PfEMP1 ecto-domain mediates binding to cell receptors such as CD36, ICAM, CSA, and EPCR (35, 36). This binding between PfEMP1 and cell receptors is associated with severe malaria and thus plays a central role in the pathogenicity of *P. falciparum* (36-38). A number of exported parasite proteins are involved in local remodeling of the cytoskeleton to connect it to knobs and PfEMP1. Thus, exported proteins are central to the successful completion of the intra-erythrocytic development and to the continuation in the life cycle of *P. falciparum*. The processes and key players in the remodeling of the iRBC cytoskeleton are reviewed in detail in Chapter 2.

PHIST Proteins

Bioinformatics analyses identified eighty-nine *P. falciparum* proteins that share common features. They contain four consecutive alpha helices and conserved tryptophan residues. These proteins were grouped into the *Plasmodium* helical interspersed subtelomeric (PHIST) family. Based on the number and position of the conserved tryptophan residues, PHIST proteins are further divided into sub-categories: PHISTa, PHISTb, and PHISTc, with seven of the PHISTb proteins containing a DnaJ domain (39). Previous studies have shown that at least some of the PHIST proteins localize at the iRBC cytoskeleton. One PHIST protein was shown to interact with PfEMP1 and cytoskeletal proteins and was thus suggested to be involved in PfEMP1 anchoring (40-42). When investigating the sub-cellular localization of PHIST proteins, a number of them were found to localize to the iRBC periphery (43). Again another study detected a binding motif which in one protein is known to bind to cytoskeleton protein band 4.1, suggesting some of the PHISTs to possess a cytoskeleton binding capacity (44). An in-depth review on the PHIST protein family is found in Chapter 3.

Aims and Objectives

The overall aim of this thesis was to investigate the function and role of selected exported parasite proteins. Many exported proteins are directly or indirectly involved in the process of host cell remodeling, which leads to knob formation and PfEMP1 anchoring, and thus to morbidity and mortality. While a number of studies have focused on exported proteins, the majority of them still remain enigmatic. To close this knowledge gap, a set of ten PHIST proteins was selected to be investigated in more detail with special focus on their interaction partners. Understanding the function of exported proteins can help to identify new targets in the fight against malaria.

In the effort to identify potential interaction partners for proteins of interest, immunoprecipitations play a central role. As exported parasite proteins also target the iRBC cytoskeleton, reverse immunoprecipitations would need to be performed to verify proposed protein-protein interactions. Due to the interconnectivity of the cytoskeleton, these have proven difficult. Furthermore, with the erythrocyte being a terminally differentiated cell that lacks a nucleus, the genetic manipulation of erythrocyte proteins remains a challenge. Thus, a system needs to be designed that allows for genetic manipulation of erythrocyte proteins which are then exported into the host cell and that can then be used in assays such as immunoprecipitations.

There is an even greater knowledge gap on the function of exported proteins in host cytoskeleton remodeling during gametocyte development. Uncovering their potential role in the processes of altering cell deformability and sequestration could identify new ways to interfere with gametocyte development and thus interfere with transmission to the mosquito.

OBJECTIVE 1

Characterization of selected PHIST proteins as well as the identification and confirmation of potential interaction partners to generate a network of protein-protein interactions at the remodeled iRBC cytoskeleton (see Chapter 4).

OBJECTIVE 2

Generation of transgenic parasite lines that express and export (truncated versions of) human cytoskeleton proteins to be used in immunoprecipitations and the confirmation of potential interactions with exported parasite proteins as detected in Objective 1 (see Chapter 5).

OBJECTIVE 3

Characterization of a PHIST protein (GEXP02) that is expressed and exported during the gametocyte stages with regard to its possible role in host cytoskeleton remodeling during this developmental phase (see Chapter 6).

References

1. **Bousema T, Drakeley C**. 2011. Epidemiology and infectivity of Plasmodium falciparum and Plasmodium vivax gametocytes in relation to malaria control and elimination. Clin Microbiol Rev 24:377-410.
2. **Ahmed MA, Cox-Singh J**. 2015. Plasmodium knowlesi - an emerging pathogen. ISBT Sci Ser 10:134-140.
3. **Cowman AF, Healer J, Marapana D, Marsh K**. 2016. Malaria: Biology and Disease. Cell 167:610-624.
4. **WHO**. 2017. World Malaria Report 2017. WHO,
5. **Sturm A, Amino R, van de Sand C, Regen T, Retzlaff S, Rennenberg A, Krueger A, Pollok JM, Menard R, Heussler VT**. 2006. Manipulation of host hepatocytes by the malaria parasite for delivery into liver sinusoids. Science 313:1287-90.
6. **Baer K, Klotz C, Kappe SH, Schnieder T, Frevert U**. 2007. Release of hepatic Plasmodium yoelii merozoites into the pulmonary microvasculature. PLoS pathogens 3:e171.
7. **Tiburcio M, Sauerwein R, Lavazec C, Alano P**. 2015. Erythrocyte remodeling by Plasmodium falciparum gametocytes in the human host interplay. Trends Parasitol 31:270-8.
8. **Miller LH, Baruch DI, Marsh K, Doumbo OK**. 2002. The pathogenic basis of malaria. Nature 415:673-9.
9. **Haldar K, Bhattacharjee S, Safeukui I**. 2018. Drug resistance in Plasmodium. Nature Reviews Microbiology 16:156.
10. **Ariey F, Witkowski B, Amaratunga C, Beghain J, Langlois AC, Khim N, Kim S, Duru V, Bouchier C, Ma L, Lim P, Leang R, Duong S, Sreng S, Suon S, Chuor CM, Bout DM, Menard S, Rogers WO, Genton B, Fandeur T, Miotto O, Ringwald P, Le Bras J, Berry A, Barale JC, Fairhurst RM, Benoit-Vical F, Mercereau-Puijalon O, Menard D**. 2014. A molecular marker of artemisinin-resistant Plasmodium falciparum malaria. Nature 505:50-5.
11. **Laurens MB**. 2018. The Promise of a Malaria Vaccine-Are We Closer? Annu Rev Microbiol 72:273-292.
12. **Zimmerman PA, Howes RE**. 2015. Malaria diagnosis for malaria elimination. Curr Opin Infect Dis 28:446-54.
13. **Hiller NL, Bhattacharjee S, van Ooij C, Liolios K, Harrison T, Lopez-Estrano C, Haldar K**. 2004. A host-targeting signal in virulence proteins reveals a secretome in malarial infection. Science 306:1934-7.
14. **Marti M, Good RT, Rug M, Knuepfer E, Cowman AF**. 2004. Targeting malaria virulence and remodeling proteins to the host erythrocyte. Science 306:1930-3.
15. **Boddey JA, Carvalho TG, Hodder AN, Sargeant TJ, Sleebs BE, Marapana D, Lopaticki S, Nebl T, Cowman AF**. 2013. Role of plasmepsin V in export of diverse protein families from the Plasmodium falciparum exportome. Traffic 14:532-50.

16. **Schulze J, Kwiatkowski M, Borner J, Schluter H, Bruchhaus I, Burmester T, Spielmann T, Pick C**. 2015. The Plasmodium falciparum exportome contains non-canonical PEXEL/HT proteins. Mol Microbiol 97:301-14.

17. **Spielmann T, Gilberger TW**. 2015. Critical Steps in Protein Export of Plasmodium falciparum Blood Stages. Trends Parasitol 31:514-525.

18. **Heiber A, Kruse F, Pick C, Gruring C, Flemming S, Oberli A, Schoeler H, Retzlaff S, Mesen-Ramirez P, Hiss JA, Kadekoppala M, Hecht L, Holder AA, Gilberger TW, Spielmann T**. 2013. Identification of new PNEPs indicates a substantial non-PEXEL exportome and underpins common features in Plasmodium falciparum protein export. PLoS Pathog 9:e1003546.

19. **Chang HH, Falick AM, Carlton PM, Sedat JW, DeRisi JL, Marletta MA**. 2008. N-terminal processing of proteins exported by malaria parasites. Mol Biochem Parasitol 160:107-15.

20. **Boddey JA, O'Neill MT, Lopaticki S, Carvalho TG, Hodder AN, Nebl T, Wawra S, van West P, Ebrahimzadeh Z, Richard D, Flemming S, Spielmann T, Przyborski J, Babon JJ, Cowman AF**. 2016. Export of malaria proteins requires co-translational processing of the PEXEL motif independent of phosphatidylinositol-3-phosphate binding. Nat Commun 7:10470.

21. **Deponte M, Hoppe HC, Lee MC, Maier AG, Richard D, Rug M, Spielmann T, Przyborski JM**. 2012. Wherever I may roam: protein and membrane trafficking in P. falciparum-infected red blood cells. Mol Biochem Parasitol 186:95-116.

22. **Gehde N, Hinrichs C, Montilla I, Charpian S, Lingelbach K, Przyborski JM**. 2009. Protein unfolding is an essential requirement for transport across the parasitophorous vacuolar membrane of Plasmodium falciparum. Molecular Microbiology 71:613-628.

23. **de Koning-Ward TF, Gilson PR, Boddey JA, Rug M, Smith BJ, Papenfuss AT, Sanders PR, Lundie RJ, Maier AG, Cowman AF, Crabb BS**. 2009. A newly discovered protein export machine in malaria parasites. Nature 459:945-9.

24. **Beck JR, Muralidharan V, Oksman A, Goldberg DE**. 2014. PTEX component HSP101 mediates export of diverse malaria effectors into host erythrocytes. Nature 511:592-5.

25. **Elsworth B, Matthews K, Nie CQ, Kalanon M, Charnaud SC, Sanders PR, Chisholm SA, Counihan NA, Shaw PJ, Pino P, Chan J-A, Azevedo MF, Rogerson SJ, Beeson JG, Crabb BS, Gilson PR, de Koning-Ward TF**. 2014. PTEX is an essential nexus for protein export in malaria parasites. Nature 511:587-591.

26. **Batinovic S, McHugh E, Chisholm SA, Matthews K, Liu B, Dumont L, Charnaud SC, Schneider MP, Gilson PR, de Koning-Ward TF, Dixon MWA, Tilley L**. 2017. An exported protein-interacting complex involved in the trafficking of virulence determinants in Plasmodium-infected erythrocytes. Nat Commun 8:16044.

27. **de Koning-Ward TF, Dixon MW, Tilley L, Gilson PR**. 2016. Plasmodium species: master renovators of their host cells. Nat Rev Microbiol 14:494-507.

28. **Ginsburg H, Kutner S, Krugliak M, Cabantchik ZI**. 1985. Characterization of permeation pathways appearing in the host membrane of Plasmodium falciparum infected red blood cells. Mol Biochem Parasitol 14:313-22.

29. **Kirk K, Horner HA, Elford BC, Ellory JC, Newbold CI**. 1994. Transport of diverse substrates into malaria-infected erythrocytes via a pathway showing functional characteristics of a chloride channel. Journal of Biological Chemistry 269:3339-3347.

30. **Desai SA, Miller LH**. 2014. Malaria: Protein-export pathway illuminated. Nature 511:541-2.

31. **Mundwiler-Pachlatko E, Beck HP**. 2013. Maurer's clefts, the enigma of Plasmodium falciparum. Proc Natl Acad Sci U S A 110:19987-94.

32. **Spillman NJ, Beck JR, Goldberg DE**. 2015. Protein export into malaria parasite-infected erythrocytes: mechanisms and functional consequences. Annu Rev Biochem 84:813-41.

33. Sanyal S, Egee S, Bouyer G, Perrot S, Safeukui I, Bischoff E, Buffet P, Deitsch KW, Mercereau-Puijalon O, David PH, Templeton TJ, Lavazec C. 2012. Plasmodium falciparum STEVOR proteins impact erythrocyte mechanical properties. Blood 119:e1-8.

34. **Ganguly AK, Ranjan P, Kumar A, Bhavesh NS**. 2015. Dynamic association of PfEMP1 and KAHRP in knobs mediates cytoadherence during Plasmodium invasion. Sci Rep 5:8617.

35. **Baruch DI, Pasloske BL, Singh HB, Bi X, Ma XC, Feldman M, Taraschi TF, Howard RJ**. 1995. Cloning the P. falciparum gene encoding PfEMP1, a malarial variant antigen and adherence receptor on the surface of parasitized human erythrocytes. Cell 82:77-87.

36. **Turner L, Lavstsen T, Berger SS, Wang CW, Petersen JE, Avril M, Brazier AJ, Freeth J, Jespersen JS, Nielsen MA, Magistrado P, Lusingu J, Smith JD, Higgins MK, Theander TG**. 2013. Severe malaria is associated with parasite binding to endothelial protein C receptor. Nature 498:502-5.

37. **Rowe A, Obeiro J, Newbold CI, Marsh K**. 1995. Plasmodium falciparum rosetting is associated with malaria severity in Kenya. Infect Immun 63:2323-6.

38. **Jensen AT, Magistrado P, Sharp S, Joergensen L, Lavstsen T, Chiucchiuini A, Salanti A, Vestergaard LS, Lusingu JP, Hermsen R, Sauerwein R, Christensen J, Nielsen MA, Hviid L, Sutherland C, Staalsoe T, Theander TG**. 2004. Plasmodium falciparum associated with severe childhood malaria preferentially expresses PfEMP1 encoded by group A var genes. J Exp Med 199:1179-90.

39. **Sargeant TJ, Marti M, Caler E, Carlton JM, Simpson K, Speed TP, Cowman AF**. 2006. Lineage-specific expansion of proteins exported to erythrocytes in malaria parasites. Genome Biol 7:R12.

40. **Oberli A, Slater LM, Cutts E, Brand F, Mundwiler-Pachlatko E, Rusch S, Masik MF, Erat MC, Beck HP, Vakonakis I**. 2014. A Plasmodium falciparum PHIST protein binds the virulence factor PfEMP1 and comigrates to knobs on the host cell surface. FASEB J 28:4420-33.

41. **Proellocks NI, Herrmann S, Buckingham DW, Hanssen E, Hodges EK, Elsworth B, Morahan BJ, Coppel RL, Cooke BM**. 2014. A lysine-rich membrane-associated PHISTb protein involved in alteration of the cytoadhesive properties of Plasmodium falciparum-infected red blood cells. FASEB J 28:3103-13.

42. **Oberli A, Zurbrugg L, Rusch S, Brand F, Butler ME, Day JL, Cutts EE, Lavstsen T, Vakonakis I, Beck HP**. 2016. Plasmodium falciparum PHIST Proteins Contribute to

Cytoadherence and Anchor PfEMP1 to the Host Cell Cytoskeleton. Cell Microbiol doi: 10.1111/cmi.12583.

43. **Tarr SJ, Moon RW, Hardege I, Osborne AR**. 2014. A conserved domain targets exported PHISTb family proteins to the periphery of Plasmodium infected erythrocytes. Mol Biochem Parasitol 196:29-40.

44. **Kilili GK, LaCount DJ**. 2011. An erythrocyte cytoskeleton-binding motif in exported Plasmodium falciparum proteins. Eukaryot Cell 10:1439-47.

Chapter 2: Cytoskeleton Remodeling Review

Manuscript in preparation for submission

Host Cytokeleton Remodeling Throughout the Life Cycle of *Plasmodium falciparum* on a Molecular Level

Jan D. Warncke[a,b], Hans-Peter Beck[a,b*]

[a] Department of Medical Parasitology and Infection Biology, Swiss Tropical and Public Health Institute, Basel, Switzerland

[b] University of Basel, Basel, Switzerland

* corresponding author: Hans-Peter Beck, Swiss TPH, Socinstrasse 57, CH-4051 Basel, Switzerland, phone +41 61 284 81 16, fax: +41 61 284 81 01, hans-peter.beck@unibas.ch

ORCID IDs

Jan Warncke: 0000-0001-6852-4191

Hans-Peter Beck: 0000-0001-8326-4834

Abstract

The asexual intraerythrocytic development of *Plasmodium falciparum*, causing the most severe form of human malaria, is marked by extensive host cell remodeling. Throughout the processes of invasion, intracellular development, and egress, the erythrocyte membrane skeleton is remodeled by the parasite as required for each specific developmental stage. The remodeling is facilitated by a plethora of exported parasite proteins and the erythrocyte membrane skeleton is the interface of most of the observed interactions between parasite and host cell proteins.

Host cell remodeling mostly has been described in the context of protein export or for the description of parasite induced structures such as Maurer's clefts or knobs on the host cell surface. Here we attempt to go beyond this and review the molecular level of each host cell remodeling step at each stage of the intraerythrocytic development of *P. falciparum*. We describe key events such as invasion, knob formation, and egress, and identify the interactions between exported parasite proteins and the host cell cytoskeleton. We discuss each remodeling step with respect to time and specific requirement of the developing parasite to explain host cell remodeling in a stage-specific manner. Thus, we highlight the interaction with the host membrane skeleton as key event in parasite survival.

Introduction

Plasmodium

Malaria is caused by the intracellular apicomplexan parasite of the genus *Plasmodium*. This infectious disease is transmitted by the bite of an infected female *Anopheles* mosquito. Despite many efforts towards its elimination, malaria remains a major global health burden, causing roughly 430'000 deaths and 210 million infections per year, while 3.5 billion people live at risk of infection (1, 2).

Six *Plasmodium* species cause human malaria: *P. falciparum*, *P. vivax, P. ovale curtisi*, *P. ovale wallikeri*, *P. malariae*, and *P. knowlesi* (1, 3). Of these, *Plasmodium vivax* is the most widespread species, while the most severe form of malaria is caused by *P. falciparum* (4).

The Life Cycle of P. falciparum

Throughout its life cycle, *P. falciparum* alternates between two hosts, the arthropod vector and the human host. During a blood meal of an infected female *Anopheles* mosquito, extracellular sporozoites are transmitted into dermal tissue subsequently reaching blood vessels from where they are transported to the liver. Sporozoites transverse and invade hepatocytes where they replicate and develop into merozoites that are released into the peripheral blood. Once in the blood merozoites invade erythrocytes and the asexual replication cycle starts which is responsible for all clinical symptoms of malaria. During each intra-erythrocytic developmental cycle few parasites commit to sexual development and become gametocytes. Mature gametocytes are transmitted to mosquitoes during a blood meal. In the mosquito midgut, male and female gametocytes become gametes which then fuse into a zygote. After development in the mosquito sporozoites are formed, migrate to the salivary glands, and can be transmitted to the next human host (1, 5).

Why to remodel the host cell?

P. falciparum invades its host cell to replicate and to be transmitted and all changes during the 48 hours intraerythrocytic cycle are logical consequence for this. Host cell invasion requires the parasite to cross the erythrocyte membrane and cytoskeleton. Replication and formation of daughter cells leads to substantial increase of size and the once discoid red blood cell changes

into a more spherical infected red blood cell (iRBC) with the consequence that it can no longer pass through the spleen. To avoid splenic clearance the parasite sequesters at the endothelial lining of the capillaries in deep tissue. This cytoadhesion requires the parasite to insert antigens into the host cell membrane and to anchor them in knob complexes to the iRBC cytoskeleton in order to mediate adhesion. At the end of the intraerythrocytic cycle, the merozoites exit from their host cell and must cross the iRBC cytoskeleton and membrane again. Each stage therefore has its own requirements and through remodeling of the host cell the parasite fulfills those requirements and the exported parasite proteins play a key role in these processes.

A number of reviews mention how extensively *P. falciparum* remodels the host cell but focus on exported parasite proteins, the machinery required for export, and the establishment of exo-membrane structures which aid in protein trafficking (5-8). Despite such large body of information, the interaction of these exported proteins and the alteration of host proteins through these interactions are often neglected. Here we focus on the iRBC cytoskeleton because it is the target or interface of many known host-parasite interactions and it is continually remodeled throughout the intraerythrocytic asexual and sexual development (Figure 1). The erythrocyte cytoskeleton is remodeled during invasion, knob formation, egress, or during gametocyte maturation. Each step has been shown to require specific modifications of the cytoskeleton and here we review the different modifications and the key players involved in each stage or specific event. We highlight and discuss the specific steps involving host-parasite interactions at the iRBC cytoskeleton.

Protein Export

To initiate host cell changes the parasite must export a large number of proteins to refurbish the iRBC. In this process all exported proteins need to pass through the parasite and parasitophorous vacuole membranes. The identification of the *Plasmodium* export element (PEXEL), a pentameric amino acid motif, was a major breakthrough and allowed to predict a large number of exported proteins (9, 10). Currently, proteins carrying a PEXEL, a more relaxed PEXEL (11), or a non-canonical PEXEL (12), allowed the prediction of over 460 exported proteins. In addition there is another group of exported proteins lacking a known export motif and these are referred to as PEXEL negative exported proteins (PNEPs) (13). Exported proteins have been implicated in the genesis of new organelles or functional complexes/structures such as the PTEX (14), Maurer's clefts (MCs) (15), J-dots (16, 17), knobs (18), and the new permeability pathway (19,

20) as previously reviewed (8, 21, 22). Many of these proteins also are involved in remodeling of the cytoskeleton and export of these proteins leads to the pathology of falciparum malaria.

The human red blood cell cytoskeleton

The erythrocyte membrane skeleton is a two dimensional hexagonal lattice formed by $(\alpha 1\beta 1)_2$-spectrin tetramers (about 180 nm in length) which are connected at their ends by short actin filaments (35 nm). These junctions are stabilized by band 4.1, forming a ternary complex (23-26). Multiple other proteins either stabilize this meshwork or support its attachment to the red cell membrane. Proteins involved in actin binding and turn-over are adducin, tropomodulin, tropomyosin, and others as reviewed in (25). The spectrin-tetramer is bridged in its middle to band 3, an integral membrane protein via ankyrin, keeping the skeleton close to the cell membrane (23, 24, 27, 28). Another link between the skeleton and the membrane is formed by the interaction between the cytoplasmic face of Glycophorin A and band 4.1, which in turn associates with actin (23). An alternative vertical connection between membrane and skeleton is facilitated by p55 linking Glycophorin C and band 4.1 (29). The highly elastic properties and unique biconcave shape of the erythrocyte membrane skeleton allow for passive deformation which occurs during the passage through the spleen (23, 30).

Life cycle stage and event specific remodeling of the host cell cytoskeleton

In a simplified model the mature human erythrocyte can be divided into three major components: membrane, membrane skeleton, and cytosol, of which all are important sites for the intracellular development of the parasite. During invasion and egress, the cytoskeleton and erythrocyte membrane have to be crossed, and during other stages, the cytoskeleton and membrane need to be modified to accommodate the needs of a growing parasite that tries to evade the host immune system.

Invasion

Erythrocyte invasion is a fast and well-orchestrated process that is completed within less than two minutes (Figure 2). The initial contact is yet not well understood but the merozoite surface protein 1 (MSP1) seems to mediate the initial binding between merozoite and erythrocyte (31).

This causes a weak deformation of the erythrocyte at the site of merozoite attachment (31-34) and could be the result of cytoskeleton phosphorylation induced by increased Ca^{2+} (32, 35). Ca^{2+} concentration determines the shape of the erythrocyte through modulating protein phosphorylation which in turn regulates protein-protein interactions at the erythrocyte cytoskeleton.

The initial contact is followed by stronger binding mediated by members of two *Plasmodium* protein families, the erythrocyte binding-like proteins (EBL) or the *P. falciparum* reticulocyte-binding protein homologs (PfRh) to glycophorin A, B, C, or to the complement receptor 1 on the erythrocyte surface (31). This interaction between the Rh5-complex and Basigin leads to an influx of Ca^{2+} into the erythrocytes which triggers phosphorylation of membrane skeleton proteins (34) such as spectrin (36) or band 3 (37, 38). Once phosphorylated, band 3 dissociates from ankyrin and spectrin thereby weakening the cytoskeleton and detaching it from the membrane at the site of entry (37, 39). Binding of recombinant Rh5 to RBCs not only causes also increased phosphorylation of ankyrin and adducing leading to dissociation from the skeleton and its weakening but also increases the overall size of the spectrin meshwork (34). The importance of band 3 in invasion is evident in the higher resistance to *P. falciparum* invasion of ovalocytic erythrocytes which carry a 27 bp deletion in the band 3 gene (40, 41).

Another mechanism emerged for protein depletion and detachment of the cytoskeleton at the site of entry. Band 3 as well as ankyrin, adducin, or band 4.1 are proteolytically cleaved (42, 43) and proteases potentially involved are chymotrypsin-like protease (42), the parasite serine protease gp76 (44, 45), falcipain 1 (46), or plasmepsin II (47, 48). Some of these proteases are also found in schizonts and it is not clear whether they are involved in egress or if they are stored in apical organelles of newly formed merozoites to be used later. Some of these proteases have only been tested on substrates in vitro and their true function has not been clearly elucidated.

It is intriguing to note that band 4.1 can be proteolytically cleaved during the invasion process (43). However, when band 4.1 is already absent due to its gene deletion in hereditary elliptocytosis invasion of merozoites is less efficient. Band 4.1 links the spectrin-actin cytoskeleton to glycophorin C and thus to the membrane and gives it an important function in maintaining the structural integrity of the cytoskeleton (49). Elliptocytes also have been reported to display decreased membrane deformability and rigidity and in both, ovalocytosis and elliptocytosis, the altered structural integrity of the cytoskeleton impairs the invasion process.

Binding of EBA-175 to Glycophorin A induces phosphorylation of cytoskeletal proteins tropomodulin, adducin, ankyrin and band 4.1, leading to increased deformability of the erythrocyte, which is important for merozoite invasion. Blocking this phosphorylation prevents increase of deformability and thus prevents parasite invasion (31, 50). In contrast, Koch et al. reported that binding of EBA-175 to Glycophorin A increased the erythrocyte stiffness which seemed to enhance invasion probably as result of cross-linking of Glycophorin A to the membrane skeleton (39, 51).

It was also reported that elevated Ca^{2+} concentrations cause membrane budding or intake of vesicles into erythrocytes that normally do not phagocytose (52-54). This and the depletion of cytoskeletal proteins from the site of invasion resulting in loosening of the membrane from the cytoskeleton, could promote membrane wrapping which had been described to occur during invasion and could contribute to the energy needed for this process (36, 55). Membrane wrapping or budding presumably are the same processes in merozoite invasion and membrane wrapping around the merozoite leads to budding and subsequent intake of the parasite. At the same time the parasite becomes enclosed within the parasitophorous vacuole membrane (PVM).

Most of the cytoskeleton remodeling occurs at the very initial phase of contact between the merozoite and the erythrocyte with the purpose to facilitate entry and PVM formation. After successful invasion the membrane is resealed and the cytoskeleton is most likely restored (55). RBC membrane and cytoskeleton pose an obstacle to merozoite invasion but in the best interest of the merozoite these barriers are crossed without causing permanent damage to the host cell.

Ring Stage

The first half of the intraerythrocytic developmental cycle is referred to as the ring stage, a name inspired by its typical shape or morphology as seen by Giemsa staining (56). Within minutes after invasion, the parasite starts exporting proteins into the host cell (5), a continuous process until the end of the 48 h developmental cycle. One of the earliest exported proteins is the PHIST (*Plasmodium* helical interspersed subtelomeric) protein RESA, which is discharged from dense granules into the parasitophorous vacuole and then exported into the host cell (57). Malaria induces fever episodes episode (58) and stability of the spectrin network decreases as temperature increases (59). Hence, binding of phosphorylated RESA to repeat 16 of β-spectrin conveys protection against thermally induced denaturation by increasing the rigidity of the iRBC to have a protective effect, while still remaining sufficiently deformable to allow for splenic

passage (57, 59-63). This stabilizing effect might be mediated by the DnaJ chaperone domain of RESA which could prevent unfolding of spectrin (64).

Several high molecular weight proteins (RhopH) are discharged from the rhoptries during invasion and are found throughout the entire intraerythrocytic cycle at the iRBC periphery. Multiple host cytoskeleton and exported parasite proteins have been identified as potential interaction partners suggesting that RhopH proteins might be involved in host cell remodeling. While no functional analyses supporting this conclusion have been provided (65, 66) this clearly indicates that parasite proteins are present in the host cell from the moment of invasion. However, it is possible that these proteins are involved in invasion and simply remain in the host cell not having any known function anymore.

While almost no phosphorylation is found during the ring stage, band 3 was shown to be phosphorylated at tyrosine residues (67) coinciding with a reduced lateral mobility (68). At the same time, this indicates that proteins phosphorylated during invasion are actively dephosphorylated during the ring stage otherwise they still would be detected. This also supports the notion that cytoskeleton modifications observed during invasion are reversible and non-destructive. Little is known about further modifications of the iRBC cytoskeleton during the next hours until the transition from ring to trophozoite stage which is accompanied by major remodeling processes. There is little further information on the first half of the intraerythrocytic life cycle. It is unclear whether there are slowly progressing modifications but the rest of this part of the cycle seems to be quite uneventful. As the host's fever episode lasts throughout almost the entire ring stage, cytoskeletal modifications other than protection against thermally induced stress would be detrimental and probably are not possible. Any modifications which would further increase the deformability of the host cell would put the iRBC cytoskeleton at risk of collapsing. Similarly, increasing rigidity too much would cause the circulating iRBC to be cleared out by the spleen. Therefore, this stage seems to prepare for major changes occurring when the parasite develops into the trophozoite stage. Transcriptome analysis of the early stage shows genes up-regulated that are involved in transcription translation and in metabolic processes (69). Structures such as the PTEX (14), MCs (15), J-dots (16, 17) and other components of the protein export and trafficking machinery are generated at this stage. Many proteins are synthesized and exported to MCs, where they are stored until trafficked to their final destination. MCs seem to be larger in size during ring stage than in trophozoites (70), suggesting a possible function as storage organelles. Many exported proteins accumulate in MCs, but do not yet interact with the host cell

cytoskeleton, but they are present in large quantities and in close proximity to their destination from where they may be discharged when needed. The reduced size of MCs in trophozoites (70) could imply that transiently stored cargo has been discharged and could explain the rapid changes occurring during the transition to trophozoites.

Transition from Ring to Trophozoite Stage

During the first hours of infection *P. falciparum* establishes a fully functional protein trafficking machinery enabling transport of proteins to various subcellular localizations. The transition from ring to trophozoite stage around 16-24 hours post invasion the parasite is marked by multiple changes in the iRBC. The parasite exports proteins that target the cytoskeleton changing its properties and structure, knobs appear on the surface of the host cell, and the mobile MCs are tethered to the cytoskeleton. All these changes described in detail below occur to facilitate cytoadherence to avoid splenic clearance and to prepare for future growth, replication, and formation of daughter cells.

Reorganization of the iRBC cytoskeleton

During this transition phase, RESA disappears from the cytoskeleton and seems to be replaced by MESA, although they do not share the same binding partner or site (59, 71). As described earlier, RESA seems to protect the host cell cytoskeleton against thermal damage which is no longer needed since at this stage of infection body temperature decreases to normal (58). Whilst RESA stabilizes the cytoskeleton, binding of MESA alters its stability by competing with the host protein p55 for binding to band 4.1, a protein involved in stabilizing the spectrin-actin network. A 19 amino acid motif of phosphorylated MESA interacts with a 51 aa motif encoded by exon 10 of band 4.1 (72-75). The interaction at the ternary complex between band 4.1, actin, and spectrin seems to be regulated through the level of phosphorylation. In iRBCs band 4.1 shows an increased level of phosphorylation, which weakens its interaction with the cytoskeleton (76). MESA and band 4.1 are phosphorylated independently but this modification is important for their interaction (72, 77, 78). The removal of p55 weakens the spectrin-actin interaction and free spectrin ends are generated and used to anchor knobs to the cytoskeleton. At the same time free actin becomes available and is used to grow filaments to connect MCs with the cytoskeleton. It is unclear whether MESA competes with every single p55 molecule or if this competition takes place

only in focal spots where knobs are being formed. Actin is absent from knobs but is still found in close proximity (79-81) suggesting that the site of actin mining and knob formation are identical. The presence of a band 4.1-binding motif in 13 other exported parasite proteins (75) suggests that MESA is most likely not the only protein involved in restructuring the iRBC cytoskeleton.

Knob formation and Cytoadhesion

Knobs are protrusions on the iRBC surface formed by an electron-dense layer underneath the iRBC membrane consisting of a protein complex dominated by KAHRP (18, 82) and an underlying spiral scaffold (81). Knobs were reported in association with cytoskeletal junctions, although not all junctions showed presence of knobs (18, 83, 84). KAHRP self-assembles underneath the iRBC membrane, is essential for knob formation (82, 85), and binds spectrin, actin, and band 4.1 (86-88). A 72 amino-acid stretch of KAHRP binds α-spectrin at repeat 4 (88) while the 5′ repeat region of KAHRP binds β-spectrin at repeats 10-14. This binding is strengthened through complementary isoelectric charges and takes place adjacent to the spectrin-ankyrin interaction site at repeats 14-15 of β-spectrin (82, 89, 90). This interaction takes place close to ankyrin and KAHRP also interacts with ankyrin. As a result, each knob is connected to four to eight spectrin tetramers leading to a higher spectrin density in knob areas than anywhere else in the skeleton (84). Presumably, the spectrin ends connected to the knobs were generated during actin mining. Neither the composition of the knob spiral scaffold (spectrin was excluded as a component) nor the exact interactions to link this spiral to the erythrocyte cytoskeleton are known, but it was proposed that the spiral would give knobs their shape and provide mechanical stability (81). A detailed model of knobs has been described by Cutts et al. (90).

Probably the most important function of knobs is to anchor PfEMP1 which accumulates at the iRBC surface around 16-20 hpi (91). PfEMP1 mediates cytoadhesion to the endothelial lining of the capillaries (92-96) and iRBC sequestration is linked to severe malaria (97, 98) making PfEMP1 the major virulence factor of *P. falciparum*. A large number of proteins seem to be exported only to build knobs and remodel the host cytoskeleton conferring these adherent properties which allows the parasite to massively grow and replicate.

A number of other exported proteins localize close to the knobs and might cross-link or anchor them to the cytoskeleton and play a role in structural integrity and shape of knobs. PHIST proteins have been implicated as linkers between cytoskeletal and exported parasite proteins (63, 99). PFE1605w (LyMP), a member of the PHIST family interaction has been shown with band 3

(100) and a number of ATS domains of PfEMP1 (100-102). PFI1780w, another PHIST protein, also has been shown to bind the ATS domain of some PfEMP1 molecules (99). The same ATS domain of PfEMP1 was shown to interact also with α-spectrin via its repeat 17 (90). There is controversial evidence that KAHRP anchors PfEMP1 to the knobs (87, 103), while an interaction with actin potentially provides another link to the cytoskeleton (104). Some of these interactions have only been observed in vitro and have not been confirmed otherwise.

Anchoring of Maurer's clefts

In ring stage parasites MCs are mobile and become arrested during the transition to trophozoites around 20-24 hpi (105, 106). The tethering to the cytoskeleton was proposed already a decade ago but no mechanism could be shown (91, 107). Recently, two links of MCs to the cytoskeleton have been described, one being mediated by actin filaments. In the erythrocyte cytoskeleton actin filaments are quite short with only 35-37 nm in length, connecting multiple ends of spectrin tetramers in the junctional complexes (25). At the transition to trophozoites actin mining causes these filaments to shorten and the free actin is used to generate 40-950 nm long filaments which extend inwards into the iRBC making the skeleton three dimensional (79, 107, 108). These new actin filaments show branching points normally not seen in uninfected erythrocytes (25, 79) and cryo-electron tomography showed that these remodeled actin filaments often start close to knobs and connect to MCs (79, 80, 108). The capacity of PfEMP1 and KAHRP to bind actin could indicate their involvement in anchoring the remodeled actin filaments to the iRBC cytoskeleton (82, 86, 104). At the MCs two proteins, PfPTP1 and Pf332 have been found to be essential for the attachment of the remodeled actin filament (80, 109-112). Both proteins show peak expression during the transition phase and have been detected in MCs at transition until egress (80, 112, 113). PfPTP1 not only links MCs to actin filaments but seem to play a role in remodeling and organizing these filaments (80). Pf332 has been shown to bind actin in a non-competing way with PfEMP3 which additionally also binds spectrin (111, 114). The MC resident protein SBP1 shares its expression pattern and localization with PfPTP1 and Pf332 (110, 115) and it was proposed that these three proteins form a complex (80). Phosphorylated SBP1 further interacts with LANCL1, a human protein that is recruited to MCs (116, 117). Another MCs protein PFE60, also known as PIESP2, interacts with MAHRP1, SBP1, and Pf332, but was shown not co-localize to PfEMP3 in immunofluorescence assays, indicating that PfEMP3 localizes to another sub-cellular location (118) most probably to the iRBC cytoskeleton. The role of PfEMP3 remains elusive

but it possibly could bind native actin filaments or it could provide the anchoring point of remodeled actin filaments to the cytoskeleton. Figure 3 presents a possible scenario how the actin filaments are anchored to the MCs and the cytoskeleton (Figure 3). The question remains how newly growing actin filaments are directed towards MCs and how they are stabilized? One potential candidate is PfHRP2 which has the capacity to stabilize and bind to actin filaments at acidic pH and also localizes to the iRBC periphery (119).

The importance of actin remodeling and the link to MCs is supported by observations with hemoglobinopathic erythrocytes. Oxidative stress on hemoglobinopathic iRBCs impaired the growth of actin filaments, caused MCs to be distorted, and to retain their mobility during mature stages. This coincides with decreased replication rate, reduced levels of protein export to the iRBC skeleton and membrane, and no PfEMP1 was found on the iRBC surface. It has been proposed that cargo vesicles would be moved along actin filaments towards the iRBC membrane by actin treadmilling (70, 79, 80, 108, 120, 121).

Another connection of MCs to the cytoskeleton is mediated by tethers consisting mainly of the exported small MAHRP2 protein (7, 122, 123) but neither anchor point at MCs or at the cytoskeleton is known and no further function has been assigned to these structures.

Both events, linking the MCs to the cytoskeleton and knob formation, seem to occur at the same time and we propose that knob formation and MCs arrest require free spectrin ends for stabilization and anchoring which in turn locally frees up actin which is repurposed into filaments responsible for vesicular cargo transport to the cytoskeleton. Because this would weaken the skeletal stability, exported parasite proteins must interact with cytoskeletal proteins to enhanced stability. The number of exported proteins targeting the iRBC skeleton at this life cycle stage is coherent with the model. In this refurbishing process of the iRBC a number of questions remains such as what triggers these, how is it orchestrated, and could potentially a drug target interfere with this process?

Further changes during ring to trophozoite transition

Once MCs are arrested, knobs are formed, and the iRBC cytoadheres, the parasite starts its rapid growth. The completion of these modifications of the host cell is seen as the end of the transition phase (70, 105).

Trophozoite

As a result of the cytoskeletal modifications, the spectrin network size increases in trophozoites (68). Computer modeling suggested that additional linkages between the cytoskeleton and the membrane which are caused by knob structures can account for the observed increased rigidity (Figure 4) (124).

Similar to the ring stage, during the trophozoite stage little major changes to the host cell seem to occur. It is rather the parasite's most metabolically active phase during the intraerythrocytic cycle (125) and prepares the parasite for replication and formation of daughter cells. Although most cytoskeleton remodeling occurs during the transition between ring to trophozoite, some of these changes gradually continue throughout the trophozoite stage and probably even until egress. First knobs appear around 20 hpi and their numbers increase linearly while their size decreases until 36 hpi (126, 127), which marks the end of the trophozoite stage (56). This constant remodeling indicates that protein export still occurs and that those proteins accumulate within the iRBC or at its cytoskeleton.

Schizont

During the schizont stage, daughter cells are being produced which subsequently will reinvade new host cells. A series of genome replications and nuclear divisions occur and individual merozoites are formed by segmentation (128). Proteins synthesis during this phase is focused on merozoite proteins and proteins that are required for invasion (69). At this time the number of knobs decreases (126, 127) and there is some evidence that the erythrocyte cytoskeleton is dismantled starting up to 15 hours prior to egress which corresponds to onset of the schizont stage. Proteins associated with junctional complexes such as adducin and tropomyosin are lost from the cytoskeleton, indicating that some remodeling or dismantling occurs. This is accompanied by an increased spectrin mesh size and the temporal appearance of holes in the cytoskeleton (129, 130). It is unclear why this happens so early since the structural integrity must still be maintained until egress. However, recent literature suggests that cytoskeleton degradation only occurs immediately before egress (131).

Egress

Parasite egress has been described by different models but irrespective of the model the actual processes all require degradation of the PVM and the iRBC cytoskeleton and membrane to release the newly formed merozoites. In contrast to invasion, egress is a rather destructive event and the iRBC cytoskeleton and membrane are now degraded by proteases to release the merozoites. At the end erythrocytic life cycle SERA6, a PV resident protein, is cleaved and activated by SUB1 (128, 132, 133) and subsequently crosses the now partially degraded PVM and localizes to the iRBC cytoskeleton. There it cleaves β-spectrin at its actin-binding site, leading to disrupting of the connection between the spectrin tetramers and the junctional complex. This is essential for the breakdown of the iRBC cytoskeleton and the final release of merozoites (131, 134). Interestingly, SERA8, another member of the SERA family, was found to be essential in egress of sporozoites from oocysts, indicating that SERA proteases might play a general role during egress of infective *P. falciparum* stages (135). A number of other proteins are proteolytically cleaved during egress of which most are associated with or are part of the iRBC cytoskeleton (129). Besides SERA6, SUB1 was also reported to cleave spectrin and probably band 3 (31, 131). MESA, ankyrin, and band 4.1 were also found to be degraded during egress (136, 137). Other proteases implicated in egress are calpain-1, falcipain, and plasmepsins (48, 129, 137-139). Falcipain and some plasmepsins which usually localize in the food vacuole (140) are also found to degrade the cytoskeleton during egress. The same processes that perforate the PVM might also perforate the food vacuole and thus releasing these proteases into the iRBC cytosol where they might assist in cytoskeleton breakdown. Curling of the host membrane has been described as part of egress and mechano-physical models suggested that the degradation and restructuring of the cytoskeleton contributes to membrane curling observed *in vivo* (141-143).

As reviewed in (144-146) other models of egress have been suggested but the model presented here summarizes the most current information and is likely correct as all effector proteins involved in egress are stored in merozoite organelles and can be rapidly discharged to start the cascade of events that result in the release of merozoites. This ensures that degradation of the host cytoskeleton occurs only when merozoites have been formed, making egress a fast and regulated process.

Gametocytes

During each intraerythrocytic developmental cycle, a few *P. falciparum* parasites commit to sexual development and develop into gametocytes. Five developmental stages have been defined and after completion (10-12 days) mature gametocytes re-enter the blood stream to be transmitted to mosquitos where they complete sexual development (1, 147). Much less is known of what modifications occur at the host cytoskeleton during the development of gametocytes.

Whilst host cytoskeleton remodeling causes morphological changes in asexual stages, morphological changes in gametocytes seem to be caused mostly by changes of the parasite's own cytoskeleton and its inner membrane complex (148). Changes of its own skeleton mostly seem to contribute to changes in cellular rigidity during sexual development (68, 148, 149). Also during gametocyte development many parasite proteins are exported but their function and potential role in the host cell remain elusive (147, 150). Great morphological differences between mature gametocytes and asexual stages suggest that different remodeling processes and targets might be involved in the generation of those differently shaped intracellular parasites.

Gametocyte stages I-IV

The cytoskeleton of gametocyte-infected erythrocytes (GIE) is targeted during sexual development with actin remodeling occurring when stage III and V gametocytes were investigated but there is no evidence of actin mining as observed in trophozoites and MCs are not tethered to the cytoskeleton via actin filaments. The number of actin junctions is reduced by 18% in stage III as compared to stage I, the size of the spectrin meshwork increases considerably until stage III, and lateral mobility of band 3 is reduced, all leading to decreased deformability of the GIEs (68). The degree of reduced deformability is similar to trophozoites (Figure 5) (148). It has been shown that the serine residue S_{324} of STEVOR, which binds to host cell cytoskeleton, is phosphorylated during stages I-IV (151). It has to be seen whether this PKA-mediated phosphorylation is the sole contributor to increased rigidity of gametocytes.

During gametocyte development from stage I to IV morphological changes are accompanied by a constant increase of rigidity (152) leading to sequestration in the bone marrow and spleen (147). The process of gametocytes sequestration until the end of stage IV is mostly unknown but PfEMP1 is observed in very low levels in stage I and GIEs have no knobs on the surface. Hence, it is likely that STEVORs might play an essential role in gametocyte sequestration (151, 153).

Gametocyte stage V

Stage V gametocytes, however must reach the blood circulation again to be taken up by mosquitoes during a blood meal to assure transmission. In order to circulate GIEs must become flexible again and previous remodeling steps up to stage III seemed to be reversed in stage V. In stage V the width of the spectrin network decreases (68), a sudden increase in deformability happens (152), and the lateral mobility of band 3 and the number of actin junctions increase again to levels comparable to uninfected RBCs (68). Hence, modifications in gametocytes seem to be mostly reversible, even the previously phosphorylated S_{324}-residue of STEVOR becomes dephosphorylated (151) and dissociates from the GIE membrane (152). It becomes important to understand this process to identify potential targets to block transmission.

Types and mechanisms of cytoskeleton remodeling

Phosphorylation

Phosphorylation and dephosphorylation by a number of human kinases such as cAMP-dependent kinase (131) or protein kinase C (77) modulate the properties of the erythrocyte cytoskeleton and membrane (76, 154-157). *P. falciparum* hijacks the human system to alter the iRBC skeleton according to its needs (54) in a stage-specific manner (67, 158). In addition, the parasite exports some of its own kinases into the host cell such as members of the FIKK family or a casein kinase (159).

During merozoite invasion phosphorylation plays an important role (24, 34, 36, 37, 50, 160) when phosphorylation of cytoskeletal proteins causes the cytoskeleton to locally detach from the membrane at the site of merozoite attachment (Figures 1, 2 and 4). This promotes membrane wrapping pushing the merozoite inwards (36, 52-55) and facilitates invasion without destruction of the cytoskeleton. Most host cytoskeleton proteins seem to be dephosphorylated during early parasite development (161), suggesting that phosphorylation and further modifications of cytoskeletal proteins does not play a major role during the first half of the life cycle.

As described above, transition from ring to trophozoite stage is accompanied by extensive remodeling of the cytoskeleton and is mediated by interaction of exported parasite proteins with host proteins. Some of these protein-protein interactions require phosphorylation and the level of phosphorylation (161), such as serine and tyrosine phosphorylation increases at this time (67). Accordingly, Treeck et al. identified in a proteomic study hundreds of phosphoproteins, both

human and parasite proteins (162), including proteins associated with the cytoskeleton or knobs (67).

Despite the large number of phosphorylated proteins little is known about kinases and phosphatases involved in this process. At least 20 parasite kinases are thought to be exported (159) and FIKK4.2, one of the exported kinases, shows peak expression during late ring and early trophozoite stages (159, 163), coinciding with the transition phase when all structural changes and host cell remodeling occur. Depletion of FIKK4.2 causes increased iRBC rigidity, reduced knob count on the iRBC surface, and impaired host cell remodeling (163). Because phosphorylation is linked to cytoskeleton remodeling and knob formation it was proposed to influence cytoadhesion (71, 78, 159).

At the end of the intra-erythrocytic development proteins begin to become dephosphorylated (67), most likely partially reversing previous cytoskeleton remodeling steps and thus weakening of the cytoskeleton in preparation of merozoite release (67). Phosphorylation plays a central role in modulating host cell alterations at the beginning of the asexual life cycle and dephosphorylation at the end of the cycle. A similar dynamic of phosphorylation is also observed during gametocyte development (164-166).

Altered Rigidity and Deformability

The ability of a cell to change its shape under predefined conditions without hemolysis is defined as deformability (149) but terms such as rigidity and stiffness are used interchangeably in this review. The structural integrity and deformability of the host cell cytoskeleton are important for the survival of *P. falciparum* and stage-specifically modulated at each stage of the life cycle (Figures 4 and 5).

During invasion a temporary increase in iRBC deformability is required (31, 50) and the degree thereof correlates with the success of invasion (33). As phosphorylation is reversed after invasion deformability is reverted to the original state. There is limited membrane stiffening mostly attributed to the effect of RESA interaction with the spectrin network (62). But no further cytoskeleton remodeling during the first half of the asexual life cycle is known and ring stage-iRBCs circulate and passage through the spleen despite this reduced deformability (167, 168).

In trophozoite and schizont stages the shape of the host cell changes and it sequesters to the endothelial capillary lining. There is an increase in phosphorylation (161) but in contrast to

phosphorylation during invasion, there is no partial dissociation and weakening of the cytoskeleton but it facilitates protein-protein interactions which contribute to increased rigidity (167, 168). In addition, metabolic products from the parasite exert oxidative stress which also contributes to the rigidification of the iRBC cytoskeleton (108, 169).

Exported proteins

Computer simulations suggested that the stiffening effect during the trophozoite and schizont stage is mainly caused by newly formed knobs providing vertical linkages between the spectrin cytoskeleton and the membrane rather than by direct remodeling of the spectrin network (124). Since several knob-resident proteins interact directly with spectrin, the formation of knobs seems to depend on cytoskeleton remodeling. Knobless parasites also show an increase in rigidity, albeit much less than knob-positive parasites (170) which suggests that other factors are involved in changes of cytoskeletal deformability. Over the years, reverse genetic studies have identified a number of interactions of exported proteins which in most cases lead to increased rigidity (28, 62, 109, 171, 172).

Chaperones

Although not directly binding to or interacting with the cytoskeleton, chaperones are also of importance to host cytoskeleton remodeling. Amongst the exported *P. falciparum* proteins are several chaperones (17) and seven PHISTb proteins containing a DnaJ domain (173). DnaJ domains have been shown to interact with or recruit parasite heat shock proteins for use in the remodeling process (174). A parasite cell line deficient of Hsp70-x, an exported parasite chaperone, showed higher retention rates in microsphiltration indicating increased rigidity (175) and suggests that chaperones might play a role in remodeling the cytoskeleton.

Protein Carbonylation

Reactive oxygen species lead to protein carbonylation (176) and although not controlled by the parasite, carbonylation of host membrane and cytoskeleton proteins can affect the integrity of the cytoskeleton. Carbonylation of iRBCs has been observed at the transition from ring to trophozoite and lasting throughout the entire trophozoite stage. This correlates in time with

hemoglobin metabolism and generation of free radicals. All major cytoskeleton proteins such as spectrin, actin, ankyrin, band 4.1, and band 4.2 were found to be carbonylated (177). Hence, through hemoglobin metabolism the parasite indirectly influences the rigidification of the host membrane and some of the remodeling mediated by exported parasite proteins might counteract the effects of carbonylation.

Protein Features

Many exported proteins contain motifs or charge distributions that can target exported parasite proteins to the cytoskeleton. The MEC motif found in MESA is present in a number of other exported proteins, some of which have been shown to localize to the iRBC cytoskeleton or to have an effect on rigidity (75). Similarly, lysine-rich repeats in a group of exported proteins were identified and shown or predicted to target the cytoskeleton (178). In several exported proteins (e.g. Pf332, SURFIN, and PfEMP1) tryptophan-rich domains interact with actin and spectrin (179, 180). A large number of exported proteins share a *Plasmodium* helical interspersed subtelomeric (PHIST) domain and several PHISTb members with an extended PHIST domain were targeted to the iRBC periphery (181). Finally, other exported parasite proteins were found to contain an amino acid sequence which mediates binding to band 4.1 (182). Overall, many proteins have been identified through molecular or bioinformatics approaches to be potentially involved in cytoskeleton remodeling, however, there is a significant redundancy of interacting proteins and each might not necessarily be involved in a particular interaction. Thus, many of these direct interactions need to be confirmed in the future.

Summary

Host cell remodeling by *P. falciparum* with regard to the cytoskeleton can be divided into three different phases: invasion, the transition phase between ring and trophozoite stages, and egress. During invasion, the erythrocyte plasma membrane as barrier has to be crossed in a conservative way that restores its properties and allows intracellular growth. This also includes the cytoskeleton stabilization when the cell is exposed to fever-induced thermal stress. At the transition phase of asexual growing parasites knobs are formed, conveying cytoadhesive properties to the infected cell. In contrast, sequestration of gametocytes must be reversible and

hence requires different modifications at the host cell cytoskeleton. During egress the parasite crosses the cytoskeleton again but this time in a more destructive way.

Cytoskeleton remodeling has been shown to be the key actor for these events, but little is known about events occurring between these steps. Available data suggest that the cytoskeleton is in a dynamic steady state.

Here we have shown that the iRBC cytoskeleton is the interface of most host-parasite protein-protein interactions that are essential for intracellular development of *P. falciparum*. The identification of key players involved in these major remodeling events could potentially provide new targets both to inhibit growth of the malaria parasite but also to inhibit transmission.

Funding Information

JW and HPB were supported by the Swiss National Science Foundation Grant Number SNF 31003A_169347. The funders had no role in determining the content of the paper or in the decision to submit this work for publication.

Acknowledgement

We would like to thank Armin Passecker, Beatrice Schibler, Sabina Beilstein, and Matthias Wyss for fruitful discussions as well as for careful and critical reading and commenting of the manuscript.

Author contributions

JW conducted the literature research, wrote the manuscript, and designed the figures. JW and HPB revised and finalized the manuscript.

Conflict of Interest

The authors claim no conflicting interest.

Bibliografie

1. **Cowman AF, Healer J, Marapana D, Marsh K.** 2016. Malaria: Biology and Disease. Cell **167:**610-624.
2. **WHO.** 2016. World Malaria Report 2016. WHO,
3. **Ahmed MA, Cox-Singh J.** 2015. Plasmodium knowlesi - an emerging pathogen. ISBT Sci Ser **10:**134-140.
4. **Bousema T, Drakeley C.** 2011. Epidemiology and infectivity of Plasmodium falciparum and Plasmodium vivax gametocytes in relation to malaria control and elimination. Clin Microbiol Rev **24:**377-410.
5. **Boddey JA, Cowman AF.** 2013. Plasmodium nesting: remaking the erythrocyte from the inside out. Annu Rev Microbiol **67:**243-269.
6. **Haldar K, Mohandas N.** 2007. Erythrocyte remodeling by malaria parasites. Curr Opin Hematol **14:**203-209.
7. **Hanssen E, McMillan PJ, Tilley L.** 2010. Cellular architecture of Plasmodium falciparum-infected erythrocytes. Int J Parasitol **40:**1127-1135.
8. **de Koning-Ward TF, Dixon MW, Tilley L, Gilson PR.** 2016. Plasmodium species: master renovators of their host cells. Nat Rev Microbiol **14:**494-507.
9. **Hiller NL, Bhattacharjee S, van Ooij C, Liolios K, Harrison T, Lopez-Estrano C, Haldar K.** 2004. A host-targeting signal in virulence proteins reveals a secretome in malarial infection. Science **306:**1934-1937.
10. **Marti M, Good RT, Rug M, Knuepfer E, Cowman AF.** 2004. Targeting malaria virulence and remodeling proteins to the host erythrocyte. Science **306:**1930-1933.
11. **Boddey JA, Carvalho TG, Hodder AN, Sargeant TJ, Sleebs BE, Marapana D, Lopaticki S, Nebl T, Cowman AF.** 2013. Role of plasmepsin V in export of diverse protein families from the Plasmodium falciparum exportome. Traffic **14:**532-550.
12. **Schulze J, Kwiatkowski M, Borner J, Schluter H, Bruchhaus I, Burmester T, Spielmann T, Pick C.** 2015. The Plasmodium falciparum exportome contains non-canonical PEXEL/HT proteins. Mol Microbiol **97:**301-314.
13. **Heiber A, Kruse F, Pick C, Gruring C, Flemming S, Oberli A, Schoeler H, Retzlaff S, Mesen-Ramirez P, Hiss JA, Kadekoppala M, Hecht L, Holder AA, Gilberger TW, Spielmann T.** 2013. Identification of new PNEPs indicates a substantial non-PEXEL exportome and underpins common features in Plasmodium falciparum protein export. PLoS Pathog **9:**e1003546.
14. **de Koning-Ward TF, Gilson PR, Boddey JA, Rug M, Smith BJ, Papenfuss AT, Sanders PR, Lundie RJ, Maier AG, Cowman AF, Crabb BS.** 2009. A newly discovered protein export machine in malaria parasites. Nature **459:**945-949.
15. **Mundwiler-Pachlatko E, Beck HP.** 2013. Maurer's clefts, the enigma of Plasmodium falciparum. Proc Natl Acad Sci U S A **110:**19987-19994.

16. **Kulzer S, Rug M, Brinkmann K, Cannon P, Cowman A, Lingelbach K, Blatch GL, Maier AG, Przyborski JM.** 2010. Parasite-encoded Hsp40 proteins define novel mobile structures in the cytosol of the P. falciparum-infected erythrocyte. Cell Microbiol **12:**1398-1420.

17. **Külzer S, Charnaud S, Dagan T, Riedel J, Mandal P, Pesce ER, Blatch GL, Crabb BS, Gilson PR, Przyborski JM.** 2012. Plasmodium falciparum−encoded exported hsp70/hsp40 chaperone/co−chaperone complexes within the host erythrocyte. Cell Microbiol **14:**1784-1795.

18. **Taylor DW, Parra M, Chapman GB, Stearns ME, Rener J, Aikawa M, Uni S, Aley SB, Panton LJ, Howard RJ.** 1987. Localization of Plasmodium falciparum histidine-rich protein 1 in the erythrocyte skeleton under knobs. Mol Biochem Parasitol **25:**165-174.

19. **Alkhalil A, Cohn JV, Wagner MA, Cabrera JS, Rajapandi T, Desai SA.** 2004. Plasmodium falciparum likely encodes the principal anion channel on infected human erythrocytes. Blood **104:**4279-4286.

20. **Desai SA.** 2014. Why do malaria parasites increase host erythrocyte permeability? Trends Parasitol **30:**151-159.

21. **Spillman NJ, Beck JR, Goldberg DE.** 2015. Protein export into malaria parasite-infected erythrocytes: mechanisms and functional consequences. Annu Rev Biochem **84:**813-841.

22. **Przyborski JM, Nyboer B, Lanzer M.** 2016. Ticket to ride: export of proteins to the Plasmodium falciparum-infected erythrocyte. Mol Microbiol **101:**1-11.

23. **Bennett V.** 1985. The membrane skeleton of human erythrocytes and its implications for more complex cells. Annu Rev Biochem **54:**273-304.

24. **Mitchell GH, Bannister LH.** 1988. Malaria parasite invasion: interactions with the red cell membrane. Crit Rev Oncol Hematol **8:**225-310.

25. **Fowler VM.** 2013. The human erythrocyte plasma membrane: a Rosetta Stone for decoding membrane-cytoskeleton structure. Curr Top Membr **72:**39-88.

26. **Lux SEt.** 2016. Anatomy of the red cell membrane skeleton: unanswered questions. Blood **127:**187-199.

27. **Marchesi VT.** 1983. The red cell membrane skeleton: recent progress. Blood **61:**1-11.

28. **Glenister FK, Coppel RL, Cowman AF, Mohandas N, Cooke BM.** 2002. Contribution of parasite proteins to altered mechanical properties of malaria-infected red blood cells. Blood **99:**1060-1063.

29. **Alloisio N, Dalla Venezia N, Rana A, Andrabi K, Texier P, Gilsanz F, Cartron JP, Delaunay J, Chishti AH.** 1993. Evidence that red blood cell protein p55 may participate in the skeleton-membrane linkage that involves protein 4.1 and glycophorin C. Blood **82:**1323-1327.

30. **Mohandas N, Gallagher PG.** 2008. Red cell membrane: past, present, and future. Blood **112:**3939-3948.

31. **Cowman AF, Tonkin CJ, Tham WH, Duraisingh MT.** 2017. The Molecular Basis of Erythrocyte Invasion by Malaria Parasites. Cell Host Microbe **22:**232-245.

32. **Gilson PR, Crabb BS.** 2009. Morphology and kinetics of the three distinct phases of red blood cell invasion by Plasmodium falciparum merozoites. Int J Parasitol **39:**91-96.

33. **Weiss GE, Gilson PR, Taechalertpaisarn T, Tham WH, de Jong NW, Harvey KL, Fowkes FJ, Barlow PN, Rayner JC, Wright GJ, Cowman AF, Crabb BS.** 2015. Revealing the sequence and resulting cellular morphology of receptor-ligand interactions during Plasmodium falciparum invasion of erythrocytes. PLoS Pathog **11:**e1004670.

34. **Aniweh Y, Gao X, Hao P, Meng W, Lai SK, Gunalan K, Chu TT, Sinha A, Lescar J, Chandramohanadas R, Li HY, Sze SK, Preiser PR.** 2017. P. falciparum RH5-Basigin interaction induces changes in the cytoskeleton of the host RBC. Cell Microbiol **19**.

35. **Lew VL, Tiffert T.** 2007. Is invasion efficiency in malaria controlled by pre-invasion events? Trends Parasitol **23:**481-484.

36. **Zuccala ES, Satchwell TJ, Angrisano F, Tan YH, Wilson MC, Heesom KJ, Baum J.** 2016. Quantitative phospho-proteomics reveals the Plasmodium merozoite triggers pre-invasion host kinase modification of the red cell cytoskeleton. Sci Rep **6:**19766.

37. **Fernandez-Pol S, Slouka Z, Bhattacharjee S, Fedotova Y, Freed S, An X, Holder AA, Campanella E, Low PS, Mohandas N, Haldar K.** 2013. A bacterial phosphatase-like enzyme of the malaria parasite Plasmodium falciparum possesses tyrosine phosphatase activity and is implicated in the regulation of band 3 dynamics during parasite invasion. Eukaryot Cell **12:**1179-1191.

38. **Acharya P, Garg M, Kumar P, Munjal A, Raja KD.** 2017. Host-Parasite Interactions in Human Malaria: Clinical Implications of Basic Research. Front Microbiol **8:**889.

39. **Koch M, Baum J.** 2016. The mechanics of malaria parasite invasion of the human erythrocyte - towards a reassessment of the host cell contribution. Cell Microbiol **18:**319-329.

40. **Genton B, al-Yaman F, Mgone CS, Alexander N, Paniu MM, Alpers MP, Mokela D.** 1995. Ovalocytosis and cerebral malaria. Nature **378:**564-565.

41. **Kidson C, Lamont G, Saul A, Nurse GT.** 1981. Ovalocytic erythrocytes from Melanesians are resistant to invasion by malaria parasites in culture. Proc Natl Acad Sci U S A **78:**5829-5832.

42. **McPherson RA, Donald DR, Sawyer WH, Tilley L.** 1993. Proteolytic digestion of band 3 at an external site alters the erythrocyte membrane organisation and may facilitate malarial invasion. Mol Biochem Parasitol **62:**233-242.

43. **Raphael P, Takakuwa Y, Manno S, Liu SC, Chishti AH, Hanspal M.** 2000. A cysteine protease activity from Plasmodium falciparum cleaves human erythrocyte ankyrin. Mol Biochem Parasitol **110:**259-272.

44. **Braun-Breton C, Rosenberry TL, da Silva LP.** 1988. Induction of the proteolytic activity of a membrane protein in Plasmodium falciparum by phosphatidyl inositol-specific phospholipase C. Nature **332:**457-459.

45. **Roggwiller E, Betoulle ME, Blisnick T, Braun Breton C.** 1996. A role for erythrocyte band 3 degradation by the parasite gp76 serine protease in the formation of the

parasitophorous vacuole during invasion of erythrocytes by Plasmodium falciparum. Mol Biochem Parasitol **82:**13-24.

46. **Greenbaum DC, Baruch A, Grainger M, Bozdech Z, Medzihradszky KF, Engel J, DeRisi J, Holder AA, Bogyo M.** 2002. A role for the protease falcipain 1 in host cell invasion by the human malaria parasite. Science **298:**2002-2006.

47. **Le Bonniec S, Deregnaucourt C, Redeker V, Banerjee R, Grellier P, Goldberg DE, Schrevel J.** 1999. Plasmepsin II, an acidic hemoglobinase from the Plasmodium falciparum food vacuole, is active at neutral pH on the host erythrocyte membrane skeleton. J Biol Chem **274:**14218-14223.

48. **Cooke BM, Mohandas N, Coppel RL.** 2004. Malaria and the red blood cell membrane. Semin Hematol **41:**173-188.

49. **Chishti AH, Palek J, Fisher D, Maalouf GJ, Liu SC.** 1996. Reduced invasion and growth of Plasmodium falciparum into elliptocytic red blood cells with a combined deficiency of protein 4.1, glycophorin C, and p55. Blood **87:**3462-3469.

50. **Sisquella X, Nebl T, Thompson JK, Whitehead L, Malpede BM, Salinas ND, Rogers K, Tolia NH, Fleig A, O'Neill J, Tham WH, David Horgen F, Cowman AF.** 2017. Plasmodium falciparum ligand binding to erythrocytes induce alterations in deformability essential for invasion. Elife **6**.

51. **Koch M, Wright KE, Otto O, Herbig M, Salinas ND, Tolia NH, Satchwell TJ, Guck J, Brooks NJ, Baum J.** 2017. Plasmodium falciparum erythrocyte-binding antigen 175 triggers a biophysical change in the red blood cell that facilitates invasion. Proc Natl Acad Sci U S A **114:**4225-4230.

52. **Ben-Bassat I, Bensch KG, Schrier SL.** 1972. Drug-induced erythrocyte membrane internalization. J Clin Invest **51:**1833-1844.

53. **Allan D, Billah MM, Finean JB, Michell RH.** 1976. Release of diacylglycerol-enriched vesicles from erythrocytes with increased intracellular (Ca2+). Nature **261:**58-60.

54. **Zuccala ES, Baum J.** 2011. Cytoskeletal and membrane remodelling during malaria parasite invasion of the human erythrocyte. Br J Haematol **154:**680-689.

55. **Dasgupta S, Auth T, Gov NS, Satchwell TJ, Hanssen E, Zuccala ES, Riglar DT, Toye AM, Betz T, Baum J, Gompper G.** 2014. Membrane-wrapping contributions to malaria parasite invasion of the human erythrocyte. Biophys J **107:**43-54.

56. **Bannister LH, Hopkins JM, Fowler RE, Krishna S, Mitchell GH.** 2000. A brief illustrated guide to the ultrastructure of Plasmodium falciparum asexual blood stages. Parasitol Today **16:**427-433.

57. **Silva MD, Cooke BM, Guillotte M, Buckingham DW, Sauzet JP, Le Scanf C, Contamin H, David P, Mercereau-Puijalon O, Bonnefoy S.** 2005. A role for the Plasmodium falciparum RESA protein in resistance against heat shock demonstrated using gene disruption. Mol Microbiol **56:**990-1003.

58. **Crutcher JM, Hoffman SL.** 1996. Malaria. *In* Baron S (ed), Medical Microbiology, 4th ed. University of Texas Medical Branch at Galveston, Galveston (TX).

59. **Pei X, Guo X, Coppel R, Bhattacharjee S, Haldar K, Gratzer W, Mohandas N, An X.** 2007. The ring-infected erythrocyte surface antigen (RESA) of Plasmodium falciparum stabilizes spectrin tetramers and suppresses further invasion. Blood **110:**1036-1042.

60. **Foley M, Tilley L, Sawyer WH, Anders RF.** 1991. The ring-infected erythrocyte surface antigen of Plasmodium falciparum associates with spectrin in the erythrocyte membrane. Mol Biochem Parasitol **46:**137-147.

61. **Da Silva E, Foley M, Dluzewski AR, Murray LJ, Anders RF, Tilley L.** 1994. The Plasmodium falciparum protein RESA interacts with the erythrocyte cytoskeleton and modifies erythrocyte thermal stability. Mol Biochem Parasitol **66:**59-69.

62. **Mills JP, Diez-Silva M, Quinn DJ, Dao M, Lang MJ, Tan KS, Lim CT, Milon G, David PH, Mercereau-Puijalon O, Bonnefoy S, Suresh S.** 2007. Effect of plasmodial RESA protein on deformability of human red blood cells harboring Plasmodium falciparum. Proc Natl Acad Sci U S A **104:**9213-9217.

63. **Warncke JD, Vakonakis I, Beck HP.** 2016. Plasmodium Helical Interspersed Subtelomeric (PHIST) Proteins, at the Center of Host Cell Remodeling. Microbiol Mol Biol Rev **80:**905-927.

64. **Bork P, Sander C, Valencia A, Bukau B.** 1992. A Module of the Dnaj Heat-Shock Proteins Found in Malaria Parasites. Trends Biochem Sci **17:**129-129.

65. **Counihan NA, Kalanon M, Coppel RL, de Koning-Ward TF.** 2013. Plasmodium rhoptry proteins: why order is important. Trends Parasitol **29:**228-236.

66. **Counihan NA, Chisholm SA, Bullen HE, Srivastava A, Sanders PR, Jonsdottir TK, Weiss GE, Ghosh S, Crabb BS, Creek DJ, Gilson PR, de Koning-Ward TF.** 2017. Plasmodium falciparum parasites deploy RhopH2 into the host erythrocyte to obtain nutrients, grow and replicate. Elife **6**.

67. **Pantaleo A, Ferru E, Carta F, Mannu F, Giribaldi G, Vono R, Lepedda AJ, Pippia P, Turrini F.** 2010. Analysis of changes in tyrosine and serine phosphorylation of red cell membrane proteins induced by P. falciparum growth. Proteomics **10:**3469-3479.

68. **Dearnley M, Chu T, Zhang Y, Looker O, Huang C, Klonis N, Yeoman J, Kenny S, Arora M, Osborne JM, Chandramohanadas R, Zhang S, Dixon MW, Tilley L.** 2016. Reversible host cell remodeling underpins deformability changes in malaria parasite sexual blood stages. Proc Natl Acad Sci U S A **113:**4800-4805.

69. **Bozdech Z, Llinas M, Pulliam BL, Wong ED, Zhu J, DeRisi JL.** 2003. The transcriptome of the intraerythrocytic developmental cycle of Plasmodium falciparum. PLoS Biol **1:**E5.

70. **Kilian N, Dittmer M, Cyrklaff M, Ouermi D, Bisseye C, Simpore J, Frischknecht F, Sanchez CP, Lanzer M.** 2013. Haemoglobin S and C affect the motion of Maurer's clefts in Plasmodium falciparum-infected erythrocytes. Cell Microbiol **15:**1111-1126.

71. **Coppel R, Lustigman S, Murray L, Anders R.** 1988. MESA is a Plasmodium falciparum phosphoprotein associated with the erythrocyte membrane skeleton. Molecular and Biochemical Parasitology **31:**223-231.

72. **Lustigman S, Anders RF, Brown GV, Coppel RL.** 1990. The mature-parasite-infected erythrocyte surface antigen (MESA) of Plasmodium falciparum associates with the erythrocyte membrane skeletal protein, band 4.1. Mol Biochem Parasitol **38:**261-270.

73. **Bennett BJ, Mohandas N, Coppel RL.** 1997. Defining the minimal domain of the Plasmodium falciparum protein MESA involved in the interaction with the red cell membrane skeletal protein 4.1. J Biol Chem **272:**15299-15306.

74. **Waller KL, Nunomura W, An X, Cooke BM, Mohandas N, Coppel RL.** 2003. Mature parasite-infected erythrocyte surface antigen (MESA) of Plasmodium falciparum binds to the 30-kDa domain of protein 4.1 in malaria-infected red blood cells. Blood **102:**1911-1914.

75. **Kilili GK, LaCount DJ.** 2011. An erythrocyte cytoskeleton-binding motif in exported Plasmodium falciparum proteins. Eukaryot Cell **10:**1439-1447.

76. **Eder PS, Soong CJ, Tao M.** 1986. Phosphorylation reduces the affinity of protein 4.1 for spectrin. Biochemistry **25:**1764-1770.

77. **Chishti AH, Maalouf GJ, Marfatia S, Palek J, Wang W, Fisher D, Liu SC.** 1994. Phosphorylation of protein 4.1 in Plasmodium falciparum-infected human red blood cells. Blood **83:**3339-3345.

78. **Magowan C, Liang J, Yeung J, Takakuwa Y, Coppel RL, Mohandas N.** 1998. Plasmodium falciparum: influence of malarial and host erythrocyte skeletal protein interactions on phosphorylation in infected erythrocytes. Exp Parasitol **89:**40-49.

79. **Cyrklaff M, Sanchez CP, Kilian N, Bisseye C, Simpore J, Frischknecht F, Lanzer M.** 2011. Hemoglobins S and C interfere with actin remodeling in Plasmodium falciparum-infected erythrocytes. Science **334:**1283-1286.

80. **Rug M, Cyrklaff M, Mikkonen A, Lemgruber L, Kuelzer S, Sanchez CP, Thompson J, Hanssen E, O'Neill M, Langer C, Lanzer M, Frischknecht F, Maier AG, Cowman AF.** 2014. Export of virulence proteins by malaria-infected erythrocytes involves remodeling of host actin cytoskeleton. Blood **124:**3459-3468.

81. **Watermeyer JM, Hale VL, Hackett F, Clare DK, Cutts EE, Vakonakis I, Fleck RA, Blackman MJ, Saibil HR.** 2016. A spiral scaffold underlies cytoadherent knobs in Plasmodium falciparum-infected erythrocytes. Blood **127:**343-351.

82. **Rug M, Prescott SW, Fernandez KM, Cooke BM, Cowman AF.** 2006. The role of KAHRP domains in knob formation and cytoadherence of P falciparum-infected human erythrocytes. Blood **108:**370-378.

83. **Oh SS, Chishti AH, Palek J, Liu SC.** 1997. Erythrocyte membrane alterations in Plasmodium falciparum malaria sequestration. Curr Opin Hematol **4:**148-154.

84. **Shi H, Liu Z, Li A, Yin J, Chong AG, Tan KS, Zhang Y, Lim CT.** 2013. Life cycle-dependent cytoskeletal modifications in Plasmodium falciparum infected erythrocytes. PLoS One **8:**e61170.

85. **Crabb BS, Cooke BM, Reeder JC, Waller RF, Caruana SR, Davern KM, Wickham ME, Brown GV, Coppel RL, Cowman AF.** 1997. Targeted gene disruption shows that knobs

enable malaria-infected red cells to cytoadhere under physiological shear stress. Cell **89:**287-296.

86. **Kilejian A, Rashid MA, Aikawa M, Aji T, Yang YF.** 1991. Selective association of a fragment of the knob protein with spectrin, actin and the red cell membrane. Mol Biochem Parasitol **44:**175-181.

87. **Oh SS, Voigt S, Fisher D, Yi SJ, LeRoy PJ, Derick LH, Liu S, Chishti AH.** 2000. Plasmodium falciparum erythrocyte membrane protein 1 is anchored to the actin-spectrin junction and knob-associated histidine-rich protein in the erythrocyte skeleton. Mol Biochem Parasitol **108:**237-247.

88. **Pei X, An X, Guo X, Tarnawski M, Coppel R, Mohandas N.** 2005. Structural and functional studies of interaction between Plasmodium falciparum knob-associated histidine-rich protein (KAHRP) and erythrocyte spectrin. J Biol Chem **280:**31166-31171.

89. **Weng H, Guo X, Papoin J, Wang J, Coppel R, Mohandas N, An X.** 2014. Interaction of Plasmodium falciparum knob-associated histidine-rich protein (KAHRP) with erythrocyte ankyrin R is required for its attachment to the erythrocyte membrane. Biochim Biophys Acta **1838:**185-192.

90. **Cutts EE, Laasch N, Reiter DM, Trenker R, Slater LM, Stansfeld PJ, Vakonakis I.** 2017. Structural analysis of P. falciparum KAHRP and PfEMP1 complexes with host erythrocyte spectrin suggests a model for cytoadherent knob protrusions. PLoS Pathog **13:**e1006552.

91. **Kriek N, Tilley L, Horrocks P, Pinches R, Elford BC, Ferguson DJ, Lingelbach K, Newbold CI.** 2003. Characterization of the pathway for transport of the cytoadherence-mediating protein, PfEMP1, to the host cell surface in malaria parasite-infected erythrocytes. Mol Microbiol **50:**1215-1227.

92. **Baruch DI, Pasloske BL, Singh HB, Bi X, Ma XC, Feldman M, Taraschi TF, Howard RJ.** 1995. Cloning the P. falciparum gene encoding PfEMP1, a malarial variant antigen and adherence receptor on the surface of parasitized human erythrocytes. Cell **82:**77-87.

93. **Su XZ, Heatwole VM, Wertheimer SP, Guinet F, Herrfeldt JA, Peterson DS, Ravetch JA, Wellems TE.** 1995. The large diverse gene family var encodes proteins involved in cytoadherence and antigenic variation of Plasmodium falciparum-infected erythrocytes. Cell **82:**89-100.

94. **Gardner JP, Pinches RA, Roberts DJ, Newbold CI.** 1996. Variant antigens and endothelial receptor adhesion in Plasmodium falciparum. Proceedings of the National Academy of Sciences of the United States of America **93:**3503-3508.

95. **Kyes S, Horrocks P, Newbold C.** 2001. Antigenic variation at the infected red cell surface in malaria. Annu Rev Microbiol **55:**673-707.

96. **Turner L, Lavstsen T, Berger SS, Wang CW, Petersen JE, Avril M, Brazier AJ, Freeth J, Jespersen JS, Nielsen MA, Magistrado P, Lusingu J, Smith JD, Higgins MK, Theander TG.** 2013. Severe malaria is associated with parasite binding to endothelial protein C receptor. Nature **498:**502-505.

97. **Dondorp AM, Ince C, Charunwatthana P, Hanson J, van Kuijen A, Faiz MA, Rahman MR, Hasan M, Bin Yunus E, Ghose A, Ruangveerayut R, Limmathurotsakul D, Mathura**

K, White NJ, Day NP. 2008. Direct in vivo assessment of microcirculatory dysfunction in severe falciparum malaria. J Infect Dis **197:**79-84.

98. **Wahlgren M, Goel S, Akhouri RR.** 2017. Variant surface antigens of Plasmodium falciparum and their roles in severe malaria. Nat Rev Microbiol **15:**479-491.

99. **Mayer C, Slater L, Erat MC, Konrat R, Vakonakis I.** 2012. Structural analysis of the Plasmodium falciparum erythrocyte membrane protein 1 (PfEMP1) intracellular domain reveals a conserved interaction epitope. J Biol Chem **287:**7182-7189.

100. **Oberli A, Zurbrugg L, Rusch S, Brand F, Butler ME, Day JL, Cutts EE, Lavstsen T, Vakonakis I, Beck HP.** 2016. Plasmodium falciparum PHIST Proteins Contribute to Cytoadherence and Anchor PfEMP1 to the Host Cell Cytoskeleton. Cell Microbiol doi: 10.1111/cmi.12583.

101. **Oberli A, Slater LM, Cutts E, Brand F, Mundwiler-Pachlatko E, Rusch S, Masik MF, Erat MC, Beck HP, Vakonakis I.** 2014. A Plasmodium falciparum PHIST protein binds the virulence factor PfEMP1 and comigrates to knobs on the host cell surface. FASEB J **28:**4420-4433.

102. **Proellocks NI, Herrmann S, Buckingham DW, Hanssen E, Hodges EK, Elsworth B, Morahan BJ, Coppel RL, Cooke BM.** 2014. A lysine-rich membrane-associated PHISTb protein involved in alteration of the cytoadhesive properties of Plasmodium falciparum-infected red blood cells. FASEB J **28:**3103-3113.

103. **Waller KL, Cooke BM, Nunomura W, Mohandas N, Coppel RL.** 1999. Mapping the binding domains involved in the interaction between the Plasmodium falciparum knob-associated histidine-rich protein (KAHRP) and the cytoadherence ligand P. falciparum erythrocyte membrane protein 1 (PfEMP1). J Biol Chem **274:**23808-23813.

104. **Waller KL, Nunomura W, Cooke BM, Mohandas N, Coppel RL.** 2002. Mapping the domains of the cytoadherence ligand Plasmodium falciparum erythrocyte membrane protein 1 (PfEMP1) that bind to the knob-associated histidine-rich protein (KAHRP). Mol Biochem Parasitol **119:**125-129.

105. **Gruring C, Heiber A, Kruse F, Ungefehr J, Gilberger TW, Spielmann T.** 2011. Development and host cell modifications of Plasmodium falciparum blood stages in four dimensions. Nat Commun **2:**165.

106. **McMillan PJ, Millet C, Batinovic S, Maiorca M, Hanssen E, Kenny S, Muhle RA, Melcher M, Fidock DA, Smith JD, Dixon MW, Tilley L.** 2013. Spatial and temporal mapping of the PfEMP1 export pathway in Plasmodium falciparum. Cell Microbiol **15:**1401-1418.

107. **Taraschi TF, O'Donnell M, Martinez S, Schneider T, Trelka D, Fowler VM, Tilley L, Moriyama Y.** 2003. Generation of an erythrocyte vesicle transport system by Plasmodium falciparum malaria parasites. Blood **102:**3420-3426.

108. **Cyrklaff M, Sanchez CP, Frischknecht F, Lanzer M.** 2012. Host actin remodeling and protection from malaria by hemoglobinopathies. Trends Parasitol **28:**479-485.

109. **Glenister FK, Fernandez KM, Kats LM, Hanssen E, Mohandas N, Coppel RL, Cooke BM.** 2009. Functional alteration of red blood cells by a megadalton protein of Plasmodium falciparum. Blood **113:**919-928.

110. **Hodder AN, Maier AG, Rug M, Brown M, Hommel M, Pantic I, Puig-de-Morales-Marinkovic M, Smith B, Triglia T, Beeson J, Cowman AF.** 2009. Analysis of structure and function of the giant protein Pf332 in Plasmodium falciparum. Mol Microbiol **71:**48-65.

111. **Waller KL, Stubberfield LM, Dubljevic V, Buckingham DW, Mohandas N, Coppel RL, Cooke BM.** 2010. Interaction of the exported malaria protein Pf332 with the red blood cell membrane skeleton. Biochim Biophys Acta **1798:**861-871.

112. **Nilsson S, Angeletti D, Wahlgren M, Chen QJ, Moll K.** 2012. Plasmodium falciparum Antigen 332 Is a Resident Peripheral Membrane Protein of Maurer's Clefts. Plos One **7:**e46980.

113. **Moll K, Chene A, Ribacke U, Kaneko O, Nilsson S, Winter G, Haeggstrom M, Pan W, Berzins K, Wahlgren M, Chen Q.** 2007. A novel DBL-domain of the P. falciparum 332 molecule possibly involved in erythrocyte adhesion. PLoS One **2:**e477.

114. **Waller KL, Stubberfield LM, Dubljevic V, Nunomura W, An X, Mason AJ, Mohandas N, Cooke BM, Coppel RL.** 2007. Interactions of Plasmodium falciparum erythrocyte membrane protein 3 with the red blood cell membrane skeleton. Biochim Biophys Acta **1768:**2145-2156.

115. **Blisnick T, Eugenia M, Betoulle M, Barale JC, Uzureau P, Berry L, Desroses S, Fujioka H, Mattei D, Breton CB.** 2000. Pfsbp 1, a Maurer's cleft Plasmodium falciparum protein, is associated with the erythrocyte skeleton. Mol Biochem Parasitol **111:**107-121.

116. **Blisnick T, Vincensini L, Barale JC, Namane A, Breton CB.** 2005. LANCL1, an erythrocyte protein recruited to the Maurer's clefts during Plasmodium falciparum development. Molecular and biochemical parasitology **141:**39-47.

117. **Blisnick T, Vincensini L, Fall G, Braun−Breton C.** 2006. Protein phosphatase 1, a Plasmodium falciparum essential enzyme, is exported to the host cell and implicated in the release of infectious merozoites. Cellular microbiology **8:**591-601.

118. **Zhang M, Faou P, Maier AG, Rug M.** 2018. Plasmodium falciparum exported protein PFE60 influences Maurer's clefts architecture and virulence complex composition. Int J Parasitol **48:**83-95.

119. **Benedetti CE, Kobarg J, Pertinhez TA, Gatti RM, de Souza ON, Spisni A, Meneghini R.** 2003. Plasmodium falciparum histidine-rich protein II binds to actin, phosphatidylinositol 4,5-bisphosphate and erythrocyte ghosts in a pH-dependent manner and undergoes coil-to-helix transitions in anionic micelles. Mol Biochem Parasitol **128:**157-166.

120. **Kilian N, Srismith S, Dittmer M, Ouermi D, Bisseye C, Simpore J, Cyrklaff M, Sanchez CP, Lanzer M.** 2015. Hemoglobin S and C affect protein export in Plasmodium falciparum-infected erythrocytes. Biol Open **4:**400-410.

121. **Cyrklaff M, Srismith S, Nyboer B, Burda K, Hoffmann A, Lasitschka F, Adjalley S, Bisseye C, Simpore J, Mueller AK, Sanchez CP, Frischknecht F, Lanzer M.** 2016. Oxidative insult can induce malaria-protective trait of sickle and fetal erythrocytes. Nat Commun **7:**13401.

122. **Hanssen E, Sougrat R, Frankland S, Deed S, Klonis N, Lippincott-Schwartz J, Tilley L.** 2008. Electron tomography of the Maurer's cleft organelles of Plasmodium falciparum-infected erythrocytes reveals novel structural features. Mol Microbiol **67:**703-718.

123. **Pachlatko E, Rusch S, Muller A, Hemphill A, Tilley L, Hanssen E, Beck HP.** 2010. MAHRP2, an exported protein of Plasmodium falciparum, is an essential component of Maurer's cleft tethers. Mol Microbiol **77:**1136-1152.

124. **Zhang Y, Huang C, Kim S, Golkaram M, Dixon MW, Tilley L, Li J, Zhang S, Suresh S.** 2015. Multiple stiffening effects of nanoscale knobs on human red blood cells infected with Plasmodium falciparum malaria parasite. Proc Natl Acad Sci U S A **112:**6068-6073.

125. **Bannister L, Mitchell G.** 2003. The ins, outs and roundabouts of malaria. Trends Parasitol **19:**209-213.

126. **Gruenberg J, Allred DR, Sherman IW.** 1983. Scanning electron microscope-analysis of the protrusions (knobs) present on the surface of Plasmodium falciparum-infected erythrocytes. J Cell Biol **97:**795-802.

127. **Quadt KA, Barfod L, Andersen D, Bruun J, Gyan B, Hassenkam T, Ofori MF, Hviid L.** 2012. The density of knobs on Plasmodium falciparum-infected erythrocytes depends on developmental age and varies among isolates. PLoS One **7:**e45658.

128. **Yeoh S, O'Donnell RA, Koussis K, Dluzewski AR, Ansell KH, Osborne SA, Hackett F, Withers-Martinez C, Mitchell GH, Bannister LH, Bryans JS, Kettleborough CA, Blackman MJ.** 2007. Subcellular discharge of a serine protease mediates release of invasive malaria parasites from host erythrocytes. Cell **131:**1072-1083.

129. **Millholland MG, Chandramohanadas R, Pizzarro A, Wehr A, Shi H, Darling C, Lim CT, Greenbaum DC.** 2011. The malaria parasite progressively dismantles the host erythrocyte cytoskeleton for efficient egress. Mol Cell Proteomics **10:**M111 010678.

130. **Nunez-Iglesias J, Blanch AJ, Looker O, Dixon MW, Tilley L.** 2018. A new Python library to analyse skeleton images confirms malaria parasite remodelling of the red blood cell membrane skeleton. PeerJ **6:**e4312.

131. **Thomas JA, Tan MSY, Bisson C, Borg A, Umrekar TR, Hackett F, Hale VL, Vizcay-Barrena G, Fleck RA, Snijders AP, Saibil HR, Blackman MJ.** 2018. A protease cascade regulates release of the human malaria parasite Plasmodium falciparum from host red blood cells. Nat Microbiol doi:10.1038/s41564-018-0111-0.

132. **Koussis K, Withers-Martinez C, Yeoh S, Child M, Hackett F, Knuepfer E, Juliano L, Woehlbier U, Bujard H, Blackman MJ.** 2009. A multifunctional serine protease primes the malaria parasite for red blood cell invasion. EMBO J **28:**725-735.

133. **Ruecker A, Shea M, Hackett F, Suarez C, Hirst EM, Milutinovic K, Withers-Martinez C, Blackman MJ.** 2012. Proteolytic activation of the essential parasitophorous vacuole cysteine protease SERA6 accompanies malaria parasite egress from its host erythrocyte. J Biol Chem **287:**37949-37963.

134. **Hale VL, Watermeyer JM, Hackett F, Vizcay-Barrena G, van Ooij C, Thomas JA, Spink MC, Harkiolaki M, Duke E, Fleck RA, Blackman MJ, Saibil HR.** 2017. Parasitophorous

vacuole poration precedes its rupture and rapid host erythrocyte cytoskeleton collapse in Plasmodium falciparum egress. Proc Natl Acad Sci U S A **114:**3439-3444.

135. **Aly AS, Matuschewski K.** 2005. A malarial cysteine protease is necessary for Plasmodium sporozoite egress from oocysts. J Exp Med **202:**225-230.

136. **Coppel RL, Culvenor JG, Bianco AE, Crewther PE, Stahl HD, Brown GV, Anders RF, Kemp DJ.** 1986. Variable antigen associated with the surface of erythrocytes infected with mature stages of Plasmodium falciparum. Mol Biochem Parasitol **20:**265-277.

137. **Hanspal M, Dua M, Takakuwa Y, Chishti AH, Mizuno A.** 2002. Plasmodium falciparum cysteine protease falcipain-2 cleaves erythrocyte membrane skeletal proteins at late stages of parasite development. Blood **100:**1048-1054.

138. **Dua M, Raphael P, Sijwali PS, Rosenthal PJ, Hanspal M.** 2001. Recombinant falcipain-2 cleaves erythrocyte membrane ankyrin and protein 4.1. Mol Biochem Parasitol **116:**95-99.

139. **Chandramohanadas R, Davis PH, Beiting DP, Harbut MB, Darling C, Velmourougane G, Lee MY, Greer PA, Roos DS, Greenbaum DC.** 2009. Apicomplexan parasites co-opt host calpains to facilitate their escape from infected cells. Science **324:**794-797.

140. **Banerjee R, Liu J, Beatty W, Pelosof L, Klemba M, Goldberg DE.** 2002. Four plasmepsins are active in the Plasmodium falciparum food vacuole, including a protease with an active-site histidine. Proc Natl Acad Sci U S A **99:**990-995.

141. **Kabaso D, Shlomovitz R, Auth T, Lew VL, Gov NS.** 2010. Curling and local shape changes of red blood cell membranes driven by cytoskeletal reorganization. Biophys J **99:**808-816.

142. **Callan-Jones A, Albarran Arriagada OE, Massiera G, Lorman V, Abkarian M.** 2012. Red blood cell membrane dynamics during malaria parasite egress. Biophys J **103:**2475-2483.

143. **Abkarian M, Massiera G, Berry L, Roques M, Braun-Breton C.** 2011. A novel mechanism for egress of malarial parasites from red blood cells. Blood **117:**4118-4124.

144. **Rayner JC.** 2006. Erythrocyte exit: Out, damned merozoite! Out I say! Trends Parasitol **22:**189-192.

145. **Blackman MJ.** 2008. Malarial proteases and host cell egress: an 'emerging' cascade. Cell Microbiol **10:**1925-1934.

146. **Dowse TJ, Koussis K, Blackman MJ, Soldati-Favre D.** 2008. Roles of proteases during invasion and egress by Plasmodium and Toxoplasma. Subcell Biochem **47:**121-139.

147. **Tiburcio M, Sauerwein R, Lavazec C, Alano P.** 2015. Erythrocyte remodeling by Plasmodium falciparum gametocytes in the human host interplay. Trends Parasitol **31:**270-278.

148. **Dearnley MK, Yeoman JA, Hanssen E, Kenny S, Turnbull L, Whitchurch CB, Tilley L, Dixon MW.** 2012. Origin, composition, organization and function of the inner membrane complex of Plasmodium falciparum gametocytes. J Cell Sci **125:**2053-2063.

149. **Lavazec C.** 2017. Molecular mechanisms of deformability of Plasmodium-infected erythrocytes. Curr Opin Microbiol **40:**138-144.

150. **Silvestrini F, Lasonder E, Olivieri A, Camarda G, van Schaijk B, Sanchez M, Younis Younis S, Sauerwein R, Alano P.** 2010. Protein export marks the early phase of gametocytogenesis of the human malaria parasite Plasmodium falciparum. Mol Cell Proteomics **9:**1437-1448.

151. **Naissant B, Dupuy F, Duffier Y, Lorthiois A, Duez J, Scholz J, Buffet P, Merckx A, Bachmann A, Lavazec C.** 2016. Plasmodium falciparum STEVOR phosphorylation regulates host erythrocyte deformability enabling malaria parasite transmission. Blood **127:**e42-53.

152. **Tiburcio M, Niang M, Deplaine G, Perrot S, Bischoff E, Ndour PA, Silvestrini F, Khattab A, Milon G, David PH, Hardeman M, Vernick KD, Sauerwein RW, Preiser PR, Mercereau-Puijalon O, Buffet P, Alano P, Lavazec C.** 2012. A switch in infected erythrocyte deformability at the maturation and blood circulation of Plasmodium falciparum transmission stages. Blood **119:**e172-180.

153. **Tiburcio M, Silvestrini F, Bertuccini L, Sander AF, Turner L, Lavstsen T, Alano P.** 2013. Early gametocytes of the malaria parasite Plasmodium falciparum specifically remodel the adhesive properties of infected erythrocyte surface. Cell Microbiol **15:**647-659.

154. **Lu PW, Soong CJ, Tao M.** 1985. Phosphorylation of ankyrin decreases its affinity for spectrin tetramer. J Biol Chem **260:**14958-14964.

155. **Ling E, Danilov YN, Cohen CM.** 1988. Modulation of red cell band 4.1 function by cAMP-dependent kinase and protein kinase C phosphorylation. J Biol Chem **263:**2209-2216.

156. **Manno S, Takakuwa Y, Nagao K, Mohandas N.** 1995. Modulation of erythrocyte membrane mechanical function by beta-spectrin phosphorylation and dephosphorylation. J Biol Chem **270:**5659-5665.

157. **Ferru E, Giger K, Pantaleo A, Campanella E, Grey J, Ritchie K, Vono R, Turrini F, Low PS.** 2011. Regulation of membrane-cytoskeletal interactions by tyrosine phosphorylation of erythrocyte band 3. Blood **117:**5998-6006.

158. **Nunes MC, Okada M, Scheidig-Benatar C, Cooke BM, Scherf A.** 2010. Plasmodium falciparum FIKK kinase members target distinct components of the erythrocyte membrane. PLoS One **5:**e11747.

159. **Nunes MC, Goldring JP, Doerig C, Scherf A.** 2007. A novel protein kinase family in Plasmodium falciparum is differentially transcribed and secreted to various cellular compartments of the host cell. Mol Microbiol **63:**391-403.

160. **Rangachari K, Dluzewski A, Wilson RJ, Gratzer WB.** 1986. Control of malarial invasion by phosphorylation of the host cell membrane cytoskeleton. Nature **324:**364-365.

161. **Murray MC, Perkins ME.** 1989. Phosphorylation of erythrocyte membrane and cytoskeleton proteins in cells infected with Plasmodium falciparum. Mol Biochem Parasitol **34:**229-236.

162. **Treeck M, Sanders JL, Elias JE, Boothroyd JC.** 2011. The phosphoproteomes of Plasmodium falciparum and Toxoplasma gondii reveal unusual adaptations within and beyond the parasites' boundaries. Cell Host Microbe **10:**410-419.

163. **Kats LM, Fernandez KM, Glenister FK, Herrmann S, Buckingham DW, Siddiqui G, Sharma L, Bamert R, Lucet I, Guillotte M, Mercereau-Puijalon O, Cooke BM.** 2014. An exported kinase (FIKK4.2) that mediates virulence-associated changes in Plasmodium falciparum-infected red blood cells. Int J Parasitol **44:**319-328.

164. **Jones GL, Edmundson HM.** 1990. Protein phosphorylation during the asexual life cycle of the human malarial parasite Plasmodium falciparum. Biochim Biophys Acta **1053:**118-124.

165. **Suetterlin BW, Kappes B, Franklin RM.** 1991. Localization and stage specific phosphorylation of Plasmodium falciparum phosphoproteins during the intraerythrocytic cycle. Mol Biochem Parasitol **46:**113-122.

166. **Wu Y, Nelson MM, Quaile A, Xia D, Wastling JM, Craig A.** 2009. Identification of phosphorylated proteins in erythrocytes infected by the human malaria parasite Plasmodium falciparum. Malar J **8:**105.

167. **Cranston HA, Boylan CW, Carroll GL, Sutera SP, Williamson JR, Gluzman IY, Krogstad DJ.** 1984. Plasmodium falciparum maturation abolishes physiologic red cell deformability. Science **223:**400-403.

168. **Nash GB, O'Brien E, Gordon-Smith EC, Dormandy JA.** 1989. Abnormalities in the mechanical properties of red blood cells caused by Plasmodium falciparum. Blood **74:**855-861.

169. **Dondorp AM, Kager PA, Vreeken J, White NJ.** 2000. Abnormal blood flow and red blood cell deformability in severe malaria. Parasitol Today **16:**228-232.

170. **Paulitschke M, Nash GB.** 1993. Membrane rigidity of red blood cells parasitized by different strains of Plasmodium falciparum. J Lab Clin Med **122:**581-589.

171. **Maier AG, Rug M, O'Neill MT, Brown M, Chakravorty S, Szestak T, Chesson J, Wu Y, Hughes K, Coppel RL, Newbold C, Beeson JG, Craig A, Crabb BS, Cowman AF.** 2008. Exported proteins required for virulence and rigidity of Plasmodium falciparum-infected human erythrocytes. Cell **134:**48-61.

172. **Sanyal S, Egee S, Bouyer G, Perrot S, Safeukui I, Bischoff E, Buffet P, Deitsch KW, Mercereau-Puijalon O, David PH, Templeton TJ, Lavazec C.** 2012. Plasmodium falciparum STEVOR proteins impact erythrocyte mechanical properties. Blood **119:**e1-8.

173. **Sargeant TJ, Marti M, Caler E, Carlton JM, Simpson K, Speed TP, Cowman AF.** 2006. Lineage-specific expansion of proteins exported to erythrocytes in malaria parasites. Genome Biol **7:**R12.

174. **Gilson PR, Chisholm SA, Crabb BS, de Koning-Ward TF.** 2017. Host cell remodelling in malaria parasites: a new pool of potential drug targets. International Journal for Parasitology **47:**119-127.

175. **Charnaud SC, Dixon MWA, Nie CQ, Chappell L, Sanders PR, Nebl T, Hanssen E, Berriman M, Chan JA, Blanch AJ, Beeson JG, Rayner JC, Przyborski JM, Tilley L, Crabb BS, Gilson PR.** 2017. The exported chaperone Hsp70-x supports virulence functions for Plasmodium falciparum blood stage parasites. PLoS One **12:**e0181656.

176. **Suzuki YJ, Carini M, Butterfield DA.** 2010. Protein carbonylation. Antioxid Redox Signal **12:**323-325.

177. **Mendez D, Linares M, Diez A, Puyet A, Bautista JM.** 2011. Stress response and cytoskeletal proteins involved in erythrocyte membrane remodeling upon Plasmodium falciparum invasion are differentially carbonylated in G6PD A- deficiency. Free Radic Biol Med **50:**1305-1313.

178. **Davies HM, Thalassinos K, Osborne AR.** 2016. Expansion of Lysine-rich Repeats in Plasmodium Proteins Generates Novel Localization Sequences That Target the Periphery of the Host Erythrocyte. J Biol Chem **291:**26188-26207.

179. **Frech C, Chen N.** 2013. Variant surface antigens of malaria parasites: functional and evolutionary insights from comparative gene family classification and analysis. BMC Genomics **14:**427.

180. **Zhu X, He Y, Liang Y, Kaneko O, Cui L, Cao Y.** 2017. Tryptophan-rich domains of Plasmodium falciparum SURFIN4.2 and Plasmodium vivax PvSTP2 interact with membrane skeleton of red blood cell. Malar J **16:**121.

181. **Tarr SJ, Moon RW, Hardege I, Osborne AR.** 2014. A conserved domain targets exported PHISTb family proteins to the periphery of Plasmodium infected erythrocytes. Mol Biochem Parasitol **196:**29-40.

182. **Lanzillotti R, Coetzer TL.** 2004. Myosin-like sequences in the malaria parasite Plasmodium falciparum bind human erythrocyte membrane protein 4.1. Haematologica **89:**1168-1171.

183. **Hanssen E, Hawthorne P, Dixon MW, Trenholme KR, McMillan PJ, Spielmann T, Gardiner DL, Tilley L.** 2008. Targeted mutagenesis of the ring-exported protein-1 of Plasmodium falciparum disrupts the architecture of Maurer's cleft organelles. Mol Microbiol **69:**938-953.

Figure Legends

Figure 1 - Overview of intraerythrocytic cycle of P. falciparum.

Some changes occurring at the erythrocyte cytoskeleton throughout the stages are highlighted.

Figure 2 - Invasion

Individual steps of invasion are shown, focusing on changes to the erythrocyte cytoskeleton.

Figure 3 – Changes during transition phase

Changes occurring during the transition from ring to trophozoite with focus on MC arrest. Figure in part inspired by (118) and additional information from (80, 183).

Figure 4 – Cytoskeleton Time Course in Asexual Stages

Changes in phosphorylation level and cellular rigidity over the course of the intraerythrocytic asexual development of *P. falciparum* (upper panel) are approximations. The lower panel depicts the changes occurring in the spectrin network over the course of development as described in (39, 84, 172).

Figure 5 - Cytoskeleton Time Course During Gametocyte Development

Changes in phosphorylation level and cellular rigidity over the course of gametocyte development (upper panel) are approximations. The lower panel depicts the changes occurring in the spectrin network over the course of development as described in (68).

Figure 1

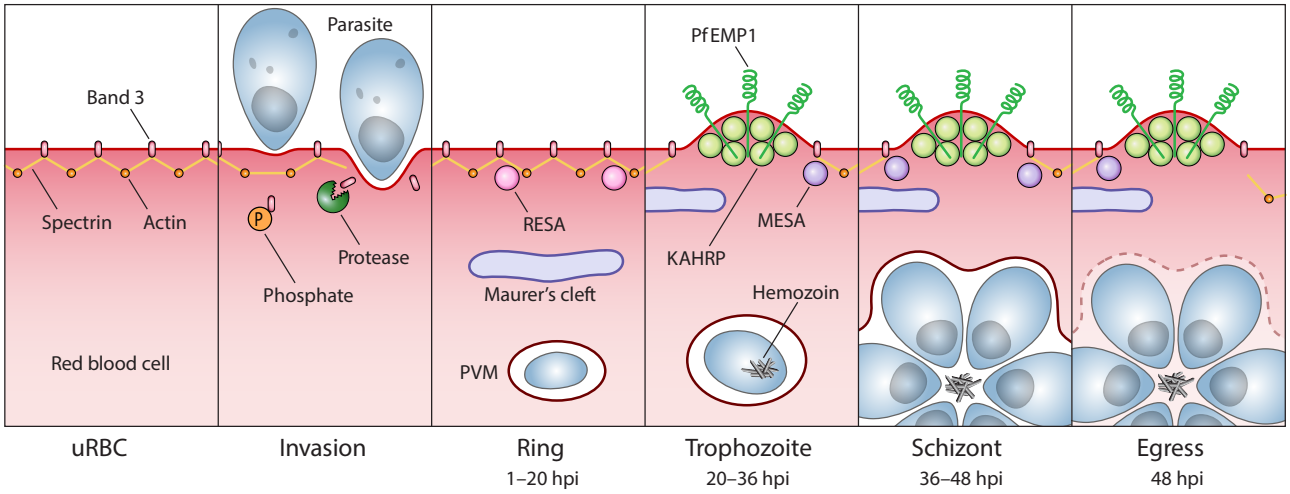
Band 3
Spectrin
Actin
Red blood cell
Parasite
P
Phosphate
Protease
RESA
Maurer's cleft
PVM
PfEMP1
KAHRP
MESA
Hemozoin
uRBC
Invasion
Ring
1–20 hpi
Trophozoite
20–36 hpi
Schizont
36–48 hpi
Egress
48 hpi

Figure 2

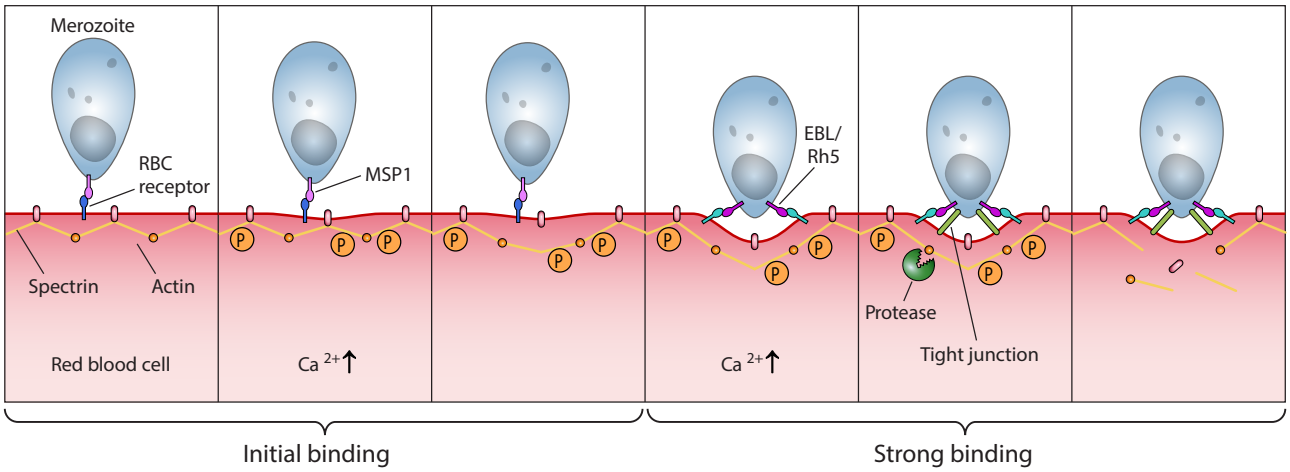
Merozoite
RBC receptor
Spectrin
Actin
Red blood cell
MSP1
Ca 2+
EBL/ Rh5
Ca 2+
Protease
Tight junction
Initial binding
Strong binding

Figure 3

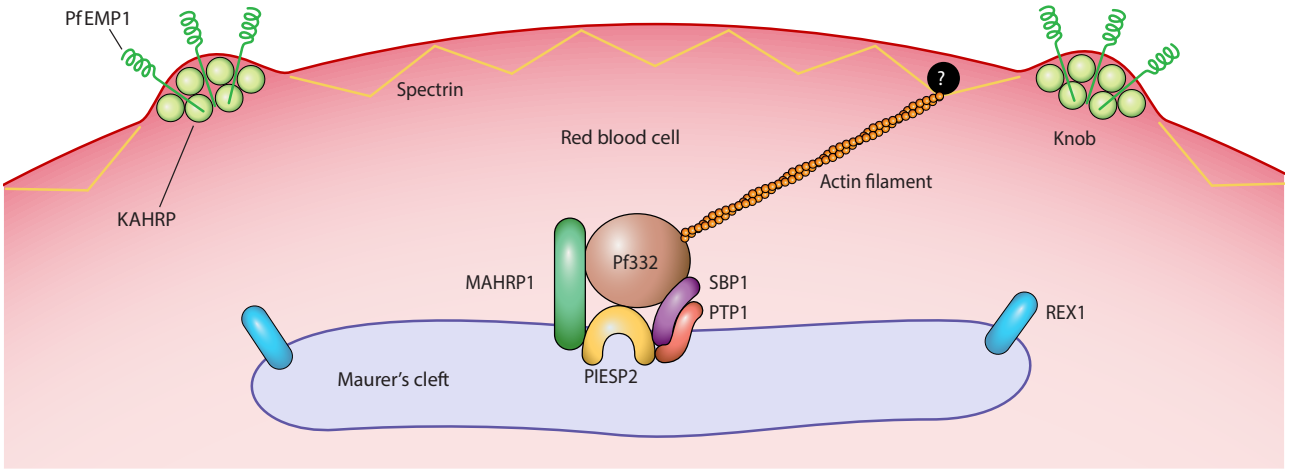
PfEMP1
Spectrin
Red blood cell
Knob
?
Actin filament
KAHRP
MAHRP1
Pf332
SBP1
PTP1
REX1
Maurer's cleft
PIESP2

Figure 4

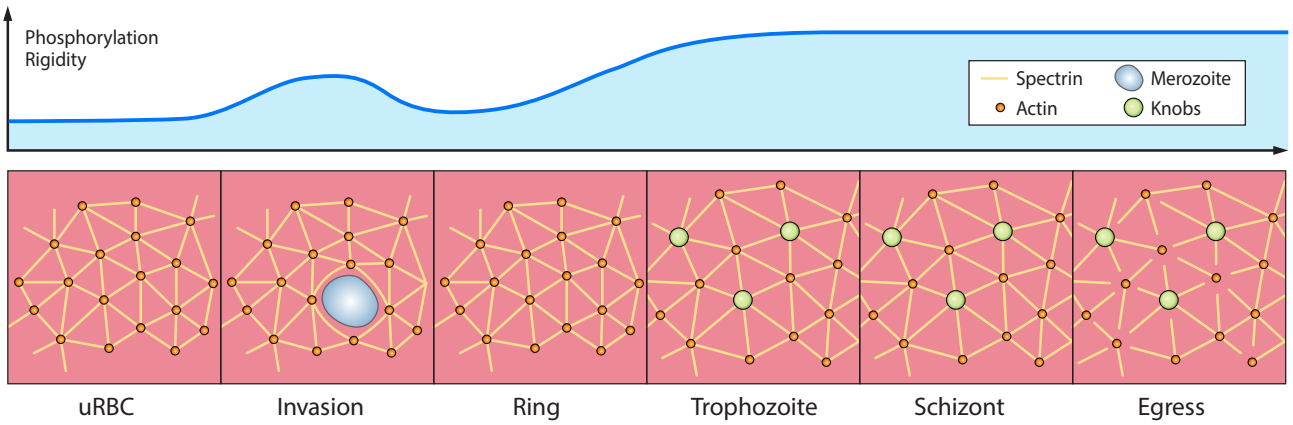
Phosphorylation
Rigidity
Spectrin
Actin
Merozoite
Knobs
uRBC
Invasion
Ring
Trophozoite
Schizont
Egress

Figure 5

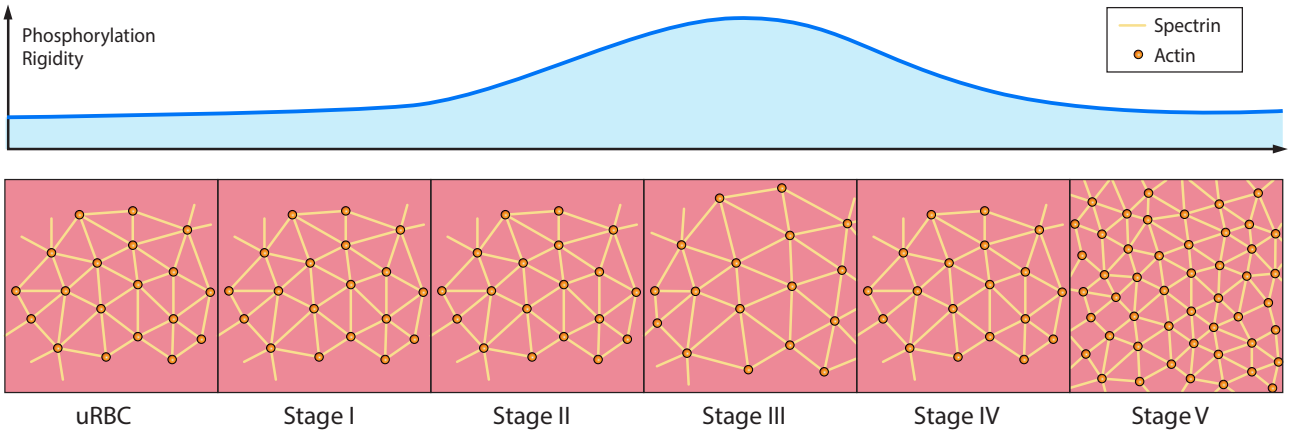
Phosphorylation
Rigidity
Spectrin
Actin
uRBC
Stage I
Stage II
Stage III
Stage IV
Stage V

Chapter 3: PHIST Review

AMERICAN SOCIETY FOR MICROBIOLOGY | Microbiology and Molecular Biology Reviews

Plasmodium Helical Interspersed Subtelomeric (PHIST) Proteins, at the Center of Host Cell Remodeling

Jan D. Warncke,[a,b] Ioannis Vakonakis,[c] Hans-Peter Beck[a,b]

Swiss Tropical and Public Health Institute, Basel, Switzerland[a]; University of Basel, Basel, Switzerland[b]; Department of Biochemistry, University of Oxford, Oxford, United Kingdom[c]

SUMMARY

During the asexual cycle, *Plasmodium falciparum* extensively remodels the human erythrocyte to make it a suitable host cell. A large number of exported proteins facilitate this remodeling process, which causes erythrocytes to become more rigid, cytoadherent, and permeable for nutrients and metabolic products. Among the exported proteins, a family of 89 proteins, called the *Plasmodium* helical interspersed subtelomeric (PHIST) protein family, has been identified. While also found in other *Plasmodium* species, the PHIST family is greatly expanded in *P. falciparum*. Although a decade has passed since their first description, to date, most PHIST proteins remain uncharacterized and are of unknown function and localization within the host cell, and there are few data on their interactions with other host or parasite proteins. However, over the past few years, PHIST proteins have been mentioned in the literature at an increasing rate owing to their presence at various localizations within the infected erythrocyte. Expression of PHIST proteins has been implicated in molecular and cellular processes such as the surface display of PfEMP1, gametocytogenesis, changes in cell rigidity, and also cerebral and pregnancy-associated malaria. Thus, we conclude that PHIST proteins are central to host cell remodeling, but despite their obvious importance in pathology, PHIST proteins seem to be understudied. Here we review current knowledge, shed light on the definition of PHIST proteins, and discuss these proteins with respect to their localization and probable function. We take into consideration interaction studies, microarray analyses, or data from blood samples from naturally infected patients to combine all available information on this protein family.

INTRODUCTION

Malaria is an infectious disease caused by the protozoan parasite *Plasmodium* and is transmitted by female *Anopheles* mosquitoes to humans during a blood meal. Of the five *Plasmodium* species that cause human malaria, two are of major public health interest: *P. falciparum* causes the most severe form of malaria, while *P. vivax* is the most widespread *Plasmodium* species (1, 2). The success of *P. vivax* is due to the presence of undetectable

Published 31 August 2016

Citation Warncke JD, Vakonakis I, Beck H-P. 2016. *Plasmodium* helical interspersed subtelomeric (PHIST) proteins, at the center of host cell remodeling. Microbiol Mol Biol Rev 80:905–927. doi:10.1128/MMBR.00014-16.

Address correspondence to Hans-Peter Beck, hans-peter.beck@unibas.ch.

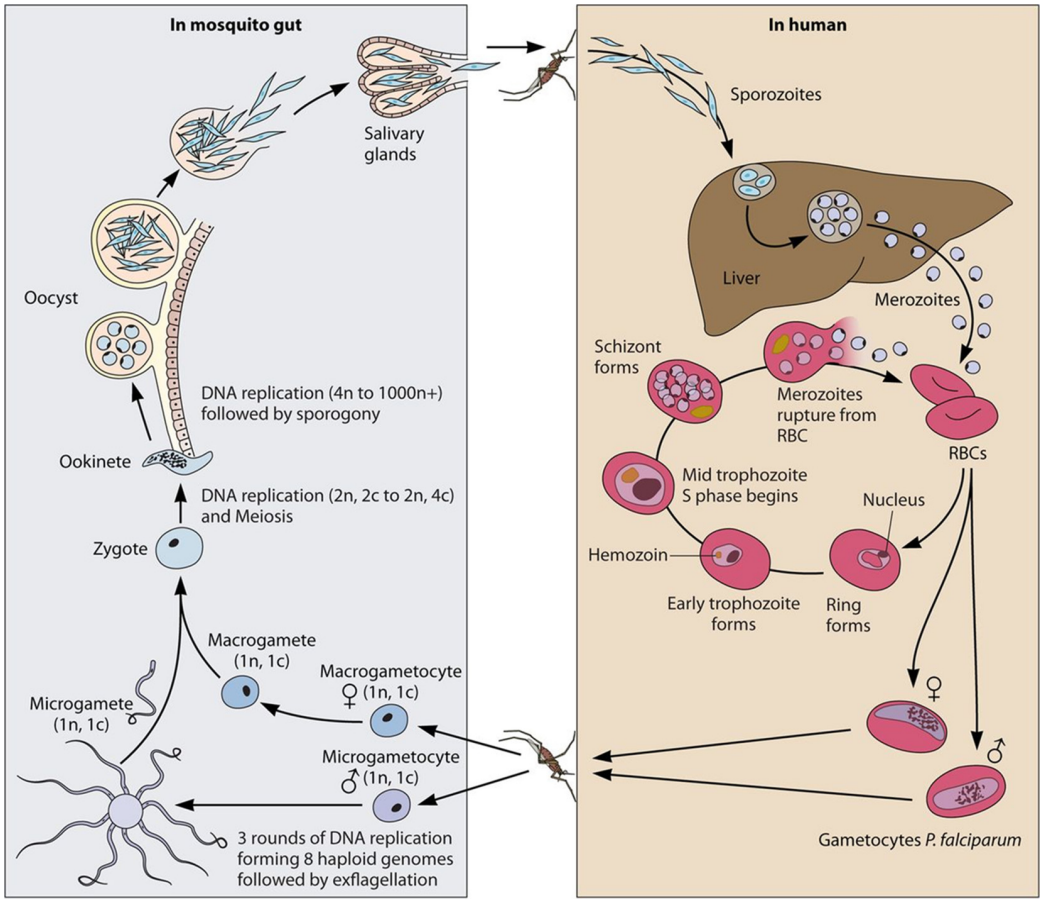

FIG 1 Life cycle of *P. falciparum*. (Right) Upon the bite of a *Plasmodium falciparum*-infected female *Anopheles* mosquito, sporozoites are injected into the dermal tissue of the human host. Sporozoites quickly enter the bloodstream and are transported to the liver, where they invade liver cells and develop into liver schizonts. Through merosomes, thousands of merozoites are released into the bloodstream, where they invade erythrocytes, starting the asexual replication cycle. Each cycle, a few parasites cease replicating, commit to the sexual cycle, and develop into gametocytes. (Left) Mature gametocytes are taken up by a mosquito during a blood meal; rapidly develop into male and female gametes, which fuse together in the gut of the mosquito; form an ookinete that penetrates the gut wall; and undergo sexual replication in the oocyst, producing thousands of sporozoites. At the end, sporozoites migrate to the salivary gland and are ready to be transmitted to a human host during the next blood meal. (Adapted from reference 148.)

hypnozoites, which represent dormant stages in the liver and pose a huge problem for malaria control. With half of the human population at risk, roughly 200 million malaria cases, and an estimated 438,000 deaths in 2015, malaria still remains a major threat to public health (3).

Plasmodium has a complex life cycle, alternating between the arthropod vector and its vertebrate host (Fig. 1) (1). During the bite of an infected female *Anopheles* mosquito, sporozoites are injected into dermal tissue and transported through the bloodstream to the liver. There, the sporozoites penetrate and invade hepatocytes, which is followed by several rounds of asexual replication. Subsequently, thousands of merozoites are released into the bloodstream through so-called merosomes, starting the blood stage cycle (4, 5).

Once in the bloodstream, merozoites invade erythrocytes and multiply during an ~48-h intraerythrocytic development cycle. At the end of the cycle, ~16 to 32 merozoites are released and reinvade new erythrocytes, starting the cycle anew. Once a merozoite has invaded the erythrocyte, it extensively refurbishes and remodels the host cell. This remodeling of the cell ensures parasite ion homeostasis within the cell, allows nutrient uptake, and is accompanied by changes in host cell membrane structure and rigidity. All this is achieved by the export of a large number of proteins from the parasite into the host cell, leading to dramatic changes of infected erythrocytes. Since such a remodeled erythrocyte would be eliminated in the spleen, the parasite also exports the major virulence factor *P. falciparum* erythrocyte membrane protein 1 (PfEMP1), which conveys binding of infected cells to endothelial receptors such as CD36, intracellular adhesion molecule (ICAM), or endothelial protein C receptor (EPCR) (6, 7). PfEMP1 is displayed on the surface of the infected red blood cell (iRBC) and is considered to be the key factor for morbidity and mortality. Overall, these refurbishing processes are considered to be responsible for most symptoms and the pathology of malaria (1, 8). Hence, recently, research focusing on exported proteins and processes involved in this host cell remodeling has attracted increased attention.

Protein Export

Because exported proteins of *P. falciparum* play such a central role in the remodeling of infected red blood cells, the description of the

pentameric amino acid motif RxLxE/Q/D, called the *Plasmodium* export element (PEXEL) (9, 10), was a breakthrough that allowed the prediction of ~400 exported proteins. The PEXEL motif was recently expanded into a more relaxed PEXEL motif (RxLxxE) (11) or a noncanonical motif (K/HxL/IxE/Q/D) (12), resulting in a total number of >460 proteins predicted to be exported in *P. falciparum*. This "exportome" provides the basis to study exported proteins and their involvement in the pathology of remodeled infected erythrocytes much more specifically. Besides the defined PEXEL exportome, there are additional exported proteins that lack a known or discernible export element, referred to as PEXEL-negative proteins (PNEPs) (13, 14). Although the definitive number of proteins exported into the erythrocyte is unknown, it is without doubt that they play important roles in pathology through the significant changes that they induce in infected erythrocytes and that they are major contributors to disease. Figure 2 shows a schematic representation of differences in cytoskeleton organization between uninfected and infected erythrocytes and the localization of exported proteins during the asexual replicative blood stage of *P. falciparum*.

PHIST PROTEINS

Methodology for Review

We focused on *P. falciparum* and included all *Plasmodium* helical interspersed subtelomeric (PHIST) proteins and genes that were either identified by Sargeant and colleagues (15) or later identified as PHIST proteins by Frech and Chen (16). We did not attempt to identify new PHIST proteins but compiled only data already reported. Gene identifications in PlasmoDB have changed over time; therefore, some PHIST proteins have two or even three gene identifications, and various articles use different gene identifications, although they refer to the same protein or gene. We also scanned supplemental material for information on PHISTs. which in some instances was found only there and would not be available through a standard literature search. We compiled any available information on each member of the PHIST family by using all gene identifications or names used now or previously. Complete lists of PHIST proteins or genes found in the literature and reviewed here are shown in Tables 1 to 5 and represent an in-depth description of this important protein family.

The PHIST Protein Family

In the large number of exported proteins, Sargeant and colleagues (15) identified a new protein family, which they termed the PHIST protein family. This protein family is characterized by a conserved domain of ~150 amino acids predicted to form four consecutive alpha helices (determined by Fugue [17]). Some members of this family comprise little more than an export signal sequence, the PEXEL motif, and the PHIST domain, whereas other members are substantially elongated and include additional domains, such as a DnaJ domain (Fig. 3). Based on the presence and position of several conserved tryptophan residues within the PHIST domain, the PHIST protein family has been further divided into three subgroups: PHISTa, PHISTb, and PHISTc (15). With more recent data included, PlasmoDB has annotated additional PHIST domains in proteins, resulting in a total of 89 currently known PHIST proteins in *P. falciparum* (15, 16). Some of the newly added PHIST proteins were not grouped into the already existing subgroups but were classified as PHISTa-like or simply PHIST proteins. Thus, PlasmoDB annotations give the impression that there are more than three PHIST subgroups. However, a phylogenetic tree based on a multiple-sequence alignment shows that PHISTa-like and PHIST proteins cluster with the PHISTa subgroup and the PHISTb-DnaJ protein group among the PHISTb subgroup, giving rise to three distinct PHIST subgroups (Fig. 3).

When the protein family was first described, Sargeant and colleagues used the presence and position of conserved tryptophan residues in the amino acid sequence of the PHIST domain to distinguish between the three subgroups (15). Comparison of multiple-sequence alignments for each subgroup in which PHISTb-DnaJ and PHISTa-like/PHIST proteins were treated as individual subgroups reveals a unique pattern of the conserved tryptophan residues for each of the subgroups (Fig. 4 and 5A). For each subgroup, a different positional pattern of conserved tryptophan residues was found, with PHISTa and PHISTa-like/PHIST proteins possessing only two conserved tryptophan residues within the PHIST domain and the remaining subgroups having four. There is only slight variation in the positions of these residues between the PHISTb and PHISTb-DnaJ subgroups and between the PHISTa and PHISTa-like/PHIST subgroups. We therefore use the original three subgroups introduced by Sargeant and colleagues unless otherwise stated.

Tables 1 to 5 list all 89 proteins that we identified as PHIST proteins in *P. falciparum*, 64 of which contain a classical PEXEL motif and are thus predicted to be exported (11, 15). Although PlasmoDB lists 19 *phist* genes as pseudogenes in reference strain 3D7, some have been found to be present as proteins or transcripts in other studies. Thus, PHISTs represent a substantial group of exported proteins comprising ~14% of all PEXEL proteins or nearly 2% of the complete *P. falciparum* proteome. Despite their potentially important role in host cell remodeling and (in)direct involvement in pathogenicity, most PHIST proteins remain completely uncharacterized, rendering it difficult to assign specific functions or roles to the PHIST protein family and/or the three subgroups.

Comparison of PHIST and PRESAN Domains

There has been confusion in the literature on the definition of PHIST and *Plasmodium* ring-infected erythrocyte antigen (RESA) N-terminal (PRESAN) domains, which in fact are virtually identical. The confusion was generated when, independent of the sequence analysis reported by Sargeant and colleagues (15), transcriptome analysis of *P. falciparum* parasites grown at elevated temperatures mimicking febrile conditions revealed a number of upregulated genes that coded for proteins containing a DnaJ domain (Pfam family PF00226) (18). Subsequent alignments identified an extended protein family with at least 67 members, all sharing a particular N-terminal domain, with a DnaJ domain being present in only some members. Because some of the DnaJ domain-containing proteins showed similarity to the RESA, this N-terminal domain was termed the PRESAN domain (Pfam family PF09687). Examination of the sequence alignments by Sargeant and colleagues (15) and Oakley and colleagues (18) revealed that the domain boundaries of the PHIST and PRESAN domains are virtually identical. Secondary-structure predictions by Oakley and colleagues (18) suggested the presence of six α-helices in PRESAN domains; however, these α-helices overlapped the predicted four α-helices of the PHIST domain (15). Thus, the PRESAN domain can be regarded as being highly similar to the

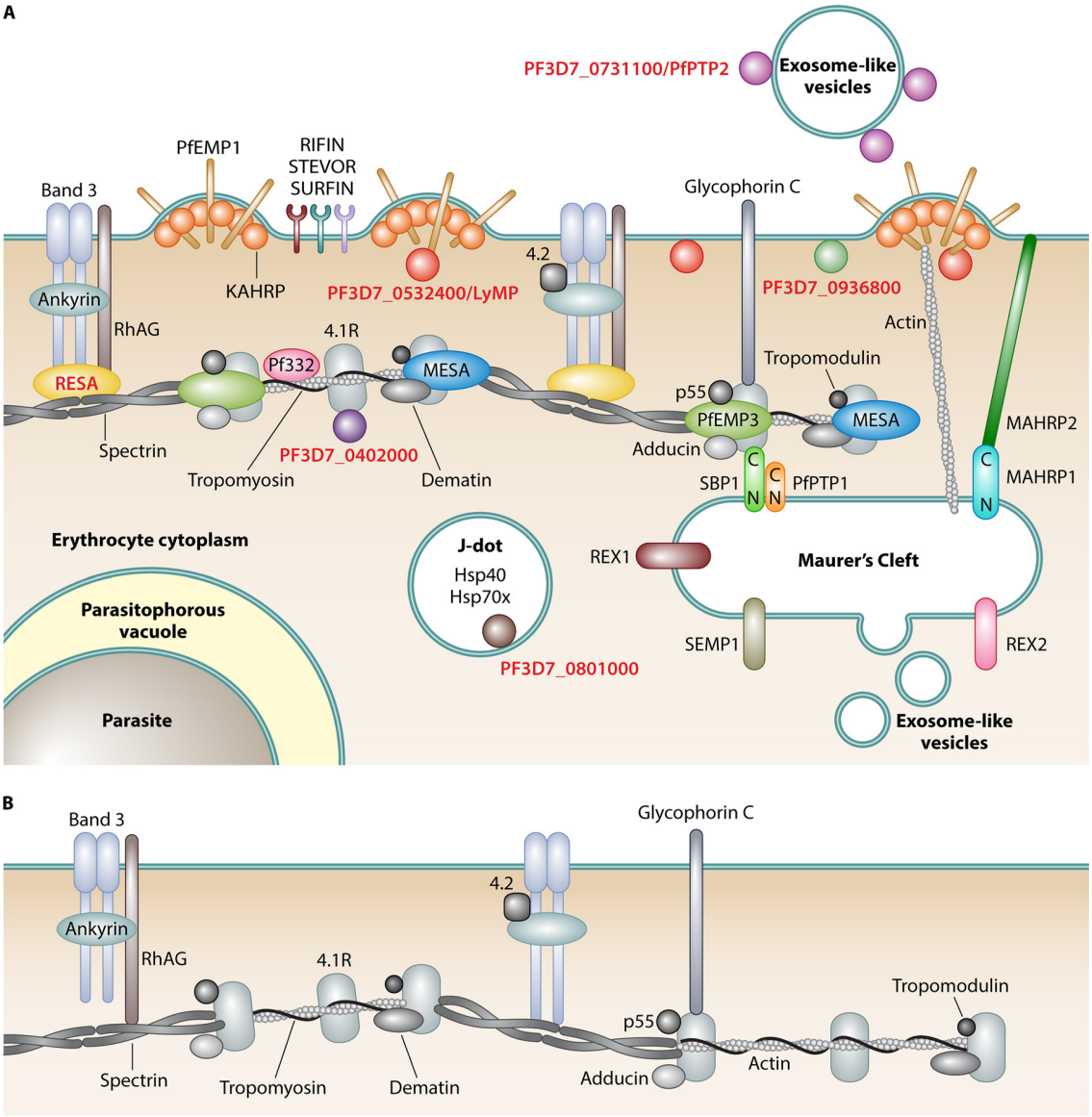

FIG 2 PHIST proteins in the remodeled iRBC. (A) Remodeled iRBC. During the asexual blood stage of *P. falciparum*, human erythrocytes are subject to extensive remodeling. All erythrocyte proteins are shown in gray (reviewed in reference 59). Parasite structures, compartments, and organelles are labeled in boldface type. PHIST proteins are labeled in red boldface type, and all parasite proteins are represented by colored shapes. References for PHIST proteins are indicated in the text. Knobs are parasite-derived protrusions in the host cell membrane, with knob-associated histidine-rich protein (KAHRP) being a prominent protein of these structures (149, 150). Maurer's clefts (reviewed in reference 151) are parasite-derived membranous structures in the iRBC cytoplasm involved in protein trafficking and are connected with knobs via actin filaments (152, 153). Maurer's cleft-associated histidine-rich protein 1 (MAHRP1) is a Maurer's cleft-resident protein (154) that potentially interacts with MAHRP2, the tether protein anchoring Maurer's clefts to the iRBC membrane (155). REX1 (156), REX2 (107), SEMP1 (157), SBP1 (158), and PfPTP1 (159) are other exported parasite proteins that localize to Maurer's clefts, with the latter two being located in a high-molecular-weight complex (159) and SBP1 interacting with the erythrocyte cytoskeleton proteins spectrin and band 4.1R (160). J dots are mobile, dot-like structures in iRBCs (161, 162). PfPTP2 is associated with exosomes, which are parasite-derived vesicles that are involved in cell-cell communication between iRBCs (43). RhAG, rhesus-associated antigen. (B) Cytoskeleton of an uninfected red blood cell (reviewed in reference 59). (Inspired by references 42 and 100.)

PHIST domain, with differences depending mainly on the prediction algorithms. An example of such close similarity is shown with the PHIST/PRESAN protein PF3D7_0532400 (Fig. 5B). The overall domain structure of all expressed PHIST proteins is shown in Fig. 3. Crystallographic and nuclear magnetic resonance (NMR) studies provided clear evidence that the PHIST/PRESAN domain forms a four-helix bundle (19). Subsequently, Tarr and colleagues (20) defined an "extended PRESAN" domain, which was N terminal to the original PHIST domain and which was thought to comprise a domain targeting membranes. This extended domain includes additional helix-forming sequences.

Confusingly, the current InterPro database uses the term "PHIST domain" (accession number IPR006526) to refer to a small protein fragment spanning approximately the N-terminal half of the PHIST/PRESAN domains, as defined by the original authors (15, 18). In contrast, the InterPro (accession number

TABLE 1 PHISTa genes

Gene identification[a]	Other gene identification(s) or name(s)[b]	Presence of PEXEL[c]	Gene status[d]	Molecular mass (kDa)[e]	Length (aa)[e]	KO[f]	Description (source or reference[s])[g]
PF3D7_0102000	PFA0100c, MAL1P1.11		PG	30.4	252		
PF3D7_0115100	PFA0735w, MAL1P4.22	x		28.6	239		Only 5-aa difference compared to PF3D7_0800600 (PlasmoDB)
PF3D7_0402000	PFD0090c, MAL4P1.18	x		41.7	357	x	Interaction between band 4.1R (58), not silenced in the 3D7 strain (28), overexpressed in samples from patients with cerebral malaria (34)
PF3D7_0424900	PFD1185w, MAL4P1.232	x		25.3	216		
PF3D7_0425300	PFD1210w, MAL4P1.237		PG	27.5	232		Exported despite the lack of any export signal (79)
PF3D7_0425400	PFD1215w, MAL4P1.238	x		19.5	164		
PF3D7_0601700	PFF0085w, MAL6P1.21	x	PG	26.3	222		
PF3D7_0800600	MAL8P1.163	x		28.3	237		Adjacent to a PfEMP1 variant on the gene locus; weak binding to the ATS domain of PfEMP1 compared to other PHIST proteins tested (19), only 5-aa difference compared to PF3D7_0115100 (PlasmoDB)
PF3D7_1001100.1	PF10_0014, PF10_0015, acyl-CoA binding protein			36.5	313	x	Grouped as PHISTa (15), deleted in parasites with PfCRT mutations, annotated as a putative lipid transporter (80), upregulated under lumefantrine pressure and deletion of the gene found under chloroquine pressure (81), unusual PHIST member with an N-terminal acyl-CoA binding protein domain (16)
PF3D7_1001100.2	PF10_0014, PF10_0015, acyl-CoA binding protein			31.0	267	x	Same as PF3D7_1001100.1
PF3D7_1001300	PF10_0017	x		22.8	190		Diffuse localization in the RBC cytosol (20), differentially expressed in parasites under lumefantrine pressure (81)
PF3D7_1100600	PF11_0012		PG	33.3	281		
PF3D7_1149700	PF11_0514			10.5	85		Once mentioned in relation to PHISTa structure (58)
PF3D7_1253100	PFL2555w, MAL12P1.506	x		26.5	221		HSP40 chaperone with a DnaJ domain (82), used as a negative control in an interaction study (58)
PF3D7_1253300	PFL2565w, MAL12P1.508	x	PG	18.3	157		Not silenced in 3D7 (28)
PF3D7_1253800	PFL2590w, MAL12P1.513	x		26.2	219		
PF3D7_1253900	PFL2595w, 2600w, MAL12P1.514	x	PG	24.3	207		Once mentioned in relation to PHISTa structure (58)
PF3D7_1301100	MAL13P1.11, MAL13P1.11a	x	PG	24.6	203		
PF3D7_1301500	MAL13P1.59			37.5	308		Downstream of a *clag* gene, and its expression is affected by H3K9me3 acetylation (83); not located in the telomeric region (27)
PF3D7_1372000	MAL13P1.470	x		41.0	349		String database mining suggested interaction with PFI1785w, PFB0115w, and PFL0050c (84)
PF3D7_1400900	PF14_0009	x	PG	24.6	209		
PF3D7_1477700	PF14_0748, Pfg14-748			34.5	291		Highest transcript concn in bone marrow comparing different organs (37); marker for early and midgametocytes, and its promoter can drive gametocyte-specific gene expression (36, 37); expressed in sexually committed schizonts with >100-fold upregulation (27); used as a marker for sexual commitment (85)
PF3D7_1478000	PF14_0752, GEXP17	x		25.5	215		Overexpressed in field samples compared to 3D7, suggested surface protein (30); differentially expressed in different 3D7 clones (33)
PF3D7_1478500	PF14_0757	x	PG	25.1	215		
PF3D7_1479200	PF14_0763	x		26.2	219		
PF3D7_1479300	PF14_0764 PF14_0765	x	PG	24.6	209		

[a] Current gene identification from PlasmoDB.
[b] Other/previous names.
[c] The presence of a PEXEL motif is indicated by "x," as identified in reference 15 or 1.
[d] Annotated as a pseudogene (PG) in PlasmoDB.
[e] For proteins with a PEXEL motif, molecular mass and length were calculated for the PEXEL-cleaved form of the protein (the molecular mass for PEXEL-cleaved proteins was calculated by using the ExPASy Web tool [http://web.expasy.org/compute_pi/]). aa, amino acids.
[f] Existing viable knockout (KO) parasites or natural gene deletions are indicated by "x" (see reference 44 or the reference[s] indicated).
[g] Information or references referring to the corresponding gene or protein.

TABLE 2 PHISTb genes

Gene identification[a]	Other gene identification(s) or name(s)[b]	Presence of PEXEL[c]	Gene status[d]	Molecular mass (kDa)[e]	Length (aa)[e]	KO[f]	Description (reference[s] or source)[g]
PF3D7_0201600	PFB0080c, PF02_0016	x		48.0	394	x	Affected by large chromosome break, which causes a loss of cytoadherence and permanent expression of var2csa, regulates *var2csa* and *var* gene expression (86); displayed on iRBC surface (86); cytosolic localization with weak accumulation at the erythrocyte periphery (20); PHISTb domain-containing RESA-like protein 1 (PlasmoDB); overexpressed in samples from patients with cerebral malaria (34)
PF3D7_0401800	PFD0080c, MAL4P1.16, PfD80	x		54.8	512		Upregulated within 90 min after artesunate treatment (87), suggested to interact with PFD0985w based on data mining (88), putative Maurer's cleft protein (89, 90), differentially expressed in Pf-FRC parasites selected for CSA or CD36 binding (91), among the most significantly upregulated genes in children with *P. falciparum* malaria (92), discrepancy observed between RNA and protein levels (93, 94)
PF3D7_0402100	PFD0095c, MAL4P1.19	x		61.7	522		*var* gene *chr4var7* showed recombination with PFD0100c (95), essential for *in vitro* growth (44), apparently linked to invasion ligand RH1 abundance in FCR3 (80, 95), contains a MEC motif (39)
PF3D7_0424600	PFD1170c, MAL4P1.229	x		26.2	221	x	Required for correct KAHRP transport and knob formation, and deletion has an effect similar to that in KAHRP KO parasites but does not affect PfEMP1 transport (44); protein shows peripheral localization (20); no interaction with the ATS of PfEMP1 (19); involved in knob formation and cytoadherence (96); present in peripheral blood of malaria patients (77)
PF3D7_0424800	PFD1180w, MAL4P1.231	x		31.1	266		
PF3D7_0532300	PFE1600w, MAL5P1.314	x		49.9	419		Exported and tyrosine phosphorylated in the RBC cytoplasm (97), shown on immunoblots with candidate vaccine antigens (98), shown in an interaction cluster with PFE1605w (99)
PF3D7_0532400	PFE1605w, MAL5P1.315, LyMP	x		50.6	439		Showed interaction with ATS of PfEMP1 variants localized to the knobs (19); localization at membrane cytoskeleton between knobs (40); recently reviewed, indicating both knob and membrane localizations (100); referred to as Hsp40 protein, with interaction with MSP1 (101); HSP40 protein with J domain (102); yeast two-hybrid interaction with SBP1 and PFE1600w (102); also computationally predicted to be a nuclear pore protein and to be part of a signaling pathway in the FIKK protein family (103)
PF3D7_0601500	PFF0075c, MAL6P1.19	x		50.0	417		Has two MEC motifs, with only a 1-aa difference compared to PF3D7_0631100 (39)
PF3D7_0631100	PFF1510w	x		49.9	416		Has two MEC motifs, with only a 1-aa difference compared to PF3D7_0601500 (39)
PF3D7_0702100	MAL7P1.7	x	PG	69.1	586		Part of an interaction network with SBP in the center (99), hexadecyl-trimethyl-ammonium bromide treatment changed its expression (104), identified as a RESA-like protein (82), identified as a RESA-like protein but not HSP40 (105)
PF3D7_0731300	MAL7P1.174, Pfg174	x		31.6	263	x	Putative Maurer's cleft protein (89, 90), suggested location of a surface protein (106), soluble protein (107)
PF3D7_0831000	MAL8P1.2, GEXP09			51.0	426		Listed as an HSP40 chaperone with a J domain (102)
PF3D7_0902700	PFI0130c	x	PG	44.0	372		Silencing of this gene resulted in inhibition of apoptosis without affecting parasite growth (108), potentially links an unknown surface protein to the iRBC cytoskeleton (109), contains a MEC motif (39)
PF3D7_0936900	PFI1785w	x	PG	32.9	274		Particularly abundant protein in samples from pregnant women but not in samples from children (49, 110, 111), affected by deletions on chromosome 9 (112, 113), String database mining suggested interaction with var2csa and MAL13P1.470-1 (84), one of the earliest-upregulated genes in the asexual cycle (28), often mentioned together with PFD1140w

(Continued on following page)

TABLE 2 (Continued)

Gene identification[a]	Other gene identification(s) or name(s)[b]	Presence of PEXEL[c]	Gene status[d]	Molecular mass (kDa)[e]	Length (aa)[e]	KO[f]	Description (reference[s] or source)[g]
PF3D7_0937000	PFI1790w			43.0	357	x	Yeast two-hybrid interaction with band 4.1R (99, 114), potential involvement in host cytoskeleton remodeling (39), located in a region prone to deletion in *P. falciparum* strains IT and FCR3 (113), contains a MEC motif (39)
PF3D7_1102500	PF11_0037, GEXP2	x		64.6	547	x	Immunoprecipitation using this protein pulled down *Plasmodium* translocon of exported proteins (PTEX) components HSP101, PTEX150, and EXP2 (45); differentially expressed in HP1-depleted parasites (53); involved in cytoadherence (109)
PF3D7_1201000	PFL0050c, MAL12P1.10	x		71.7	605	x	Putative Maurer's cleft protein (89, 90), String database mining suggests interaction with var2csa and MAL13P1.470-1 (84)
PF3D7_1252700	PFL2535w, MAL12P1.502	x		42.1	363		RESA-like protein (115)
PF3D7_1252800	PFL2540w, MAL12P1.503	x		66.6	559		Contains a MEC motif (39)
PF3D7_1372100	MAL13P1.475, GEXP04	x		67.0	558	x	Frequently deleted in field samples, affected by the same deletion as HRP2 and HRP3 (116, 117)
PF3D7_1401600	PF14_0018	x		45.7	391	x	Knockout resulted in less rigid but viable parasites (39, 44), putative TM domain or GPI anchor (118), contains a MEC motif (39)
PF3D7_1476200	PF14_0731 or PF14_0730	x		49.3	410		Upregulated *in vitro* when cultured with human serum compared to AlbuMAX (119)
PF3D7_1476300	PF14_0732	x		61.5	514	x	Frequently deleted in HB3 and other strains (120)
PF3D7_1477500	PF14_0746	x		49.9	411		

[a] Current gene identification from PlasmoDB.
[b] Other/previous names.
[c] The presence of a PEXEL motif is indicated by "x," as identified in reference 15 or 1.
[d] Annotated as a pseudogene (PG) in PlasmoDB.
[e] For proteins with a PEXEL motif, molecular mass and length were calculated for the PEXEL-cleaved form of the protein (the molecular mass for PEXEL-cleaved proteins was calculated by using the ExPASy Web tool [http://web.expasy.org/compute_pi/]).
[f] Existing viable knockout (KO) parasites or natural gene deletions are indicated by "x" (see reference 44 or the reference[s] indicated).
[g] Information or references referring to the corresponding gene or protein. TM, transmembrane; GPI, glycosylphosphatidylinositol.

IPR019111) and Pfam (family PF09687) entries for the PRESAN domain are identical to these original alignments. This discrepancy needs correction urgently. In this review, we refer to this conserved domain type as the PHIST domain.

PHIST Proteins in Other *Plasmodium* Species

PHIST proteins are found exclusively in the genus *Plasmodium*, and the protein family has been significantly expanded in *P. falciparum* and in the laveranian species *P. reichenowi*, in which there is a one-to-one representation of the PHIST genes (21). While little is known about PHIST proteins in *P. falciparum*, even less is known about PHIST proteins in other *Plasmodium* species. There are fewer PHIST proteins in other plasmodia, but their exact number is not yet clear, and different publications report various counts. Initially, Sargeant et al. reported 39 PHIST proteins for *P. vivax* (15), but the complete analysis of the *P. vivax* genome (22) revealed the presence of a gene family (Pv_fam_e), which contained 44 *rad* genes and 21 *phist* genes, with both groups showing structural similarities. However, PlasmoDB currently has only 18 genes annotated as *phist* (PlasmoDB) for *P. vivax*. Supplemental material in two publications provided expression data for *P. vivax* PHIST proteins (23, 24). For *P. knowlesi*, Sargeant and colleagues (15) initially reported 27 PHIST proteins, but this has been reannotated to 38 proteins by Pain et al. (25), and PlasmoDB currently lists 39 records. For the monkey malaria parasite *P. cynomolgi*, 21 PHIST genes were identified, while the number of PHIST genes in the rodent malaria parasite is unclear and varies in different publications or databases. For *P. berghei*, 1 to 3 *phist* genes have been found, and 1 to 2 have been found in both *P. chabaudi* and *P. yoelii* (15, 16, 26). Moreira et al. recently characterized two PHIST proteins in *P. berghei* and demonstrated potentially similar roles for these PHIST proteins, as has been attributed to *P. falciparum* PHIST proteins (26). So far, to our knowledge, no *phist* genes have been identified in the avian *Plasmodium* lineage. Whether there are other gene families with a similar structure or function in these species remains to be seen.

Except for CVC-81$_{95}$, a PHIST protein of *P. vivax* that has been investigated in more detail, we do not further discuss PHIST proteins in other plasmodia.

The PHIST Subfamilies

PHISTa. Proteins of the PHISTa subgroup are very short and besides the PHIST domain consist of only a signal sequence and a PEXEL motif if present. PHISTa proteins are found exclusively in *P. falciparum* (15) and currently amount to 26 different proteins (Table 1). In contrast to the other subgroups, PHISTa and PHISTa-like proteins possess only two conserved tryptophan residues (Fig. 4). These proteins were previously grouped together and described as a subtelomeric protein superfamily (27), although two of them, PF3D7_1301500 and PF3D7_1301300, are not located subtelomerically and are referred to as PHISTa-like proteins today (Table 5).

Except for PF3D7_0402000 and PF3D7_1253300, PHISTa proteins have been reported to be transcriptionally silent in reference strain 3D7 (15, 28). Initially, it was proposed that this transcriptional silencing might be caused by mutually exclusive expression (15). However, as shown in the heat map in Fig. 6, several studies recently showed that other PHISTa proteins are upregu-

TABLE 3 PHISTb genes with a DnaJ domain

Gene identification[a]	Other gene identification(s) or name(s)[b]	Presence of PEXEL[c]	Gene status[d]	Molecular mass (kDa)[e]	Length (aa)[e]	KO[f]	Description (reference[s] or source)[g]
PF3D7_0102200	PFA0110w, MAL1P1.13, Pf155, RESA			126.5	1,085	x	RESA-KO iRBCs have reduced cell rigidity (44, 65), RESA stiffens iRBCs and protects them from cell damage at febrile temperatures (71), binds to spectrin (68), expressed in ring stages of early gametocytes (51), part of an interaction network with SBP in the center (99), found in peripheral blood of malaria patients (77), RESA-positive and parasite-free RBCs observed (121), subject of research in vaccine development (search term, *Plasmodium* Pf155 vaccine)
PF3D7_0201700	PFB0085c, PF02_0017	x		99.7	846	x	Part of an upregulated gene cluster in C4S binding parasites but suggested to be nonessential for PfEMP1 expression (86); HSP40 chaperone with a DnaJ domain, RESA-like protein (82); chromosomal deletion also affecting KAHRP and resulting in the absence of knobs and reduced cytoadherence (15, 122)
PF3D7_0220100	PFB0920w, PF02_0188	x		106.8	909	x	Identified as type III HSP40 (105, 123), deletion leads to increased rigidity and increased CS2 binding (44), putative DnaJ protein (PlasmoDB)
PF3D7_1038800	PF10_0378	x		96.8	822	x	Coprecipitated full-length band 4.1R (39), identified as type III HSP40 (123), RESA-like protein with PHIST and DnaJ domains (PlasmoDB)
PF3D7_1149200	PF11_0509, RESA 3	x		117.2	1,003		Part of an interaction network with SBP in the center but also present in a different interaction network with RESA, SBP1, and other PHISTs (99); identified as type IV HSP40 (105); absent in parasites treated with T4, which causes arrest of the cell cycle (124); less abundant in proteomic data than RESA (65); described as an essential gene by Maier et al. (44); expression peak in late ring, early trophozoite stage (125); high level of sequence homology with RESA (126)
PF3D7_1149500	PF11_0512, RESA 2	x	PG	89.0	839	x	Although annotated as a pseudogene, it has been found to be poorly translated, with very low protein levels, function is not known, protein might be degraded (127); identified as RESA2 (65); mutation T1526C frequently found in cases of severe malaria, upregulated *in vivo* (128); identified as type IV HSP40 (105); not expressed in laboratory strains according to Maier et al. (42) but highly upregulated when two isogenic 3D7 strains were compared (33); peak expression in trophozoite stage (125); overexpressed in *in vivo* samples (30); transcript found at high levels in samples from patients with cerebral malaria from Malawi (129) (data not shown)
PF3D7_1201100	PFL0055c, MAL12P1.11	x		96.2	806		Identified as type III HSP40 (105, 123), RESA-like protein with PHIST and DnaJ domains (PlasmoDB), contains a MEC motif (39)

[a] Current gene identification from PlasmoDB.
[b] Other/previous names.
[c] The presence of a PEXEL motif is indicated by "x," as identified in reference 15 or 1.
[d] Annotated as a pseudogene (PG) in PlasmoDB.
[e] For proteins with a PEXEL motif, molecular mass and length were calculated for the PEXEL-cleaved form of the protein (the molecular mass for PEXEL-cleaved proteins was calculated by using the ExPASy Web tool [http://web.expasy.org/compute_pi/]).
[f] Existing viable knockout (KO) parasites or natural gene deletions are indicated by "x" (see reference 44 or the reference[s] indicated).
[g] Information or references referring to the corresponding gene or protein.

lated in pregnancy-associated malaria or in cerebral malaria (29–34). Additional studies reported that members of the PHISTa group are differentially expressed in parasites committed to becoming gametocytes (27, 35–37). Whether the transcriptional silencing of PHISTa proteins in 3D7 is an adaptation to *in vitro* growth remains to be tested, but PHISTa proteins in natural infections seem to play an important role in pathogenesis.

PHISTb. With 24 members, PHISTb proteins make the second largest subgroup (Table 2). Members of this subgroup are slightly longer than PHISTa proteins, with 300 to 600 residues. Characteristic of the PHISTb subgroup is a unique, long, C-terminal amino acid stretch that follows the PHIST domain (15) and that might indicate a unique and different function of these proteins compared to that of proteins of the other PHIST subgroups. It is conceivable that the PHIST domain provides a general binding motif, while the C terminus might provide a more specific interaction domain. Such a dual binding capacity was recently shown by Oberli and colleagues (38) for the PHIST protein

TABLE 4 PHISTc genes

Gene identification[a]	Other gene identification(s) or name(s)[b]	Presence of PEXEL[c]	Gene status[d]	Molecular mass (kDa)[e]	Length (aa)[e]	KO[f]	Description (reference[s] or source)[g]
PF3D7_0202100	PFB0105c, LSAP2	x		25.4	216		Not recognized by pooled immune sera (98); continuously upregulated, with predicted TM, granular pattern in immunofluorescence assays (IFA) of older parasites, expressed in liver stages (130); located at periphery in liver stage parasites similarly to circumsporozoite protein (CSP) (131); polymorphic gene with SNPs (80); differentially expressed in parasites under lumefantrine pressure (81)
PF3D7_0219700	PFB0900c, PF02_0184, GEXP20			35.3	295		
PF3D7_0219800	PFB0905c, PF02_0185	x		31.9	263		
PF3D7_0424000	PFD1140w, MAL4P1.223	x		35.2	296	x	Antigenic properties, antibody recognition in several reports, potential vaccine candidate (29, 49, 111, 132, 133); stronger expression in culture supplemented with albumin instead of human serum (119); String database mining suggests interaction with var2csa and PFB0115w (84); often referred to together with PFI1785w
PF3D7_0532200	PFE1595c, MAL5P1.313			27.3	226		Involved in response to chloroquine treatment (134, 135)
PF3D7_0731100	MAL7P1.172, GEXP11 PfPTP2	x		92.5	799	x	Involved in cell-cell communication and plasmid transfer, located on budding vesicles from Maurer's clefts (43); knockout with very reduced levels of surface PfEMP1, which was trapped in Maurer's clefts, no cytoadherence to CSA (44); indirect evidence for PfPTP2 being located inside the lumen of Maurer's clefts (44); coprecipitated with plasmepsin V (136); RESA-like protein found among soluble proteins from parasitophorous vacuole (PV) lumen and iRBC cytosol (82)
PF3D7_0801000	PF08_0137	x		147.1	1,127		Found among soluble proteins from PV lumen and iRBC cytosol (82), coprecipitated PTEX components such as HSP101 and PTEX150 (45), associated with J dots (J. Przyborski, personal communication), *P. yoelii* orthologue is annotated as a putative dentin phosphoryn protein possibly involved in mineral nucleation or functions as an extracellular matrix protein (137), contains a relaxed PEXEL motif (1), elicits an immune response (138)
PF3D7_0830600	MAL8P1.4	x		45.1	380		Located in Maurer's clefts, no interaction with the ATS of PfEMP1 (19); expression downregulated in HB3, 3D7, and Dd2 (28); expression upregulated with treatment with histone deacetylase inhibitors (trichostatin A, suberoylanilide hydroxamic acid) (139)
PF3D7_0936600	PFI1770w, GEXP5	x		25.2	212		Originally classified as PHISTb (15); reclassified as PHISTc (16); sole "PHISTb" that showed only cytosolic localization (20); upregulated in gametocytes (107, 140); earliest-known postinvasion gametocyte marker, expressed at 14 h postinvasion and independent of major gametocyte marker, cannot promote gametocyte maturation alone when other factors are not present (51)
PF3D7_0936800	PFI1780w	x		38.6	324		Protein of unknown function, several TM domains predicted (15); interacts with the ATS of PfEMP1 (56); located at the iRBC periphery with PfEMP1 but not cotransported with PfEMP1 (19); stuttering motif identified not found in any other PHIST protein (141); noncanonical PEXEL motif that is correctly cleaved (12); suggested presence in figure displaying exported proteins (100)
PF3D7_1001700	PF10_0021	x		27.6	226		Significantly downregulated after chloroquine treatment (80)
PF3D7_1001800	PF10_0022	x		23.8	204		Corrected gene model with adjusted exon and intron sizes (142, 143)
PF3D7_1016500	PF10_0161	x		81.3	675		Wrongly annotated as PF3D7_1016600 previously (15), evidence for sumoylation (144)
PF3D7_1016600	PF10_0161 or PF10_0161a	x		27.8	226		Had been annotated together with PF3D7_1016500 (15), evidence for sumoylation (144), IFA shows bright punctuate pattern in iRBCs (20)
PF3D7_1016700	PF10_0162			98.8	830		
PF3D7_1016800	PF10_0163	x		30.0	241		
PF3D7_1148700	PF11_0503, GEXP12	x		38.1	323		
PF3D7_1200900	PFL0045c, MAL12P1.9	x		37.6	310		Noncanonical PEXEL, localizes to small dotted structures in iRBCs (12)

[a] Current gene identification from PlasmoDB.
[b] Other/previous names.
[c] The presence of a PEXEL motif is indicated by "x," as identified in reference 15 or 1.
[d] Annotated as a pseudogene (PG) in PlasmoDB.
[e] For proteins with a PEXEL motif, molecular mass and length were calculated for the PEXEL-cleaved form of the protein (the molecular mass for PEXEL-cleaved proteins was calculated by using the ExPASy Web tool [http://web.expasy.org/compute_pi/]).
[f] Existing viable knockout (KO) parasites or natural gene deletions are indicated by "x" (see reference 44 or the reference[s] indicated).
[g] Information or references referring to the corresponding gene or protein. LSAP2, liver stage-associated protein 2; SNPs, single-nucleotide polymorphisms.

PF3D7_0532400. C-terminal interaction motifs have indeed been identified in several other PHISTb proteins (39). In this respect, it is important to note that all PHISTb proteins characterized today were localized at and might interact with the host cell cytoskeleton (19, 20, 39, 40).

The non-PHIST protein mature parasite-infected erythrocyte surface antigen (MESA) (PF3D7_0500800) interacts via an N-terminal 19-amino-acid motif with band 4.1R. This motif has been termed the MESA erythrocyte cytoskeleton binding (MEC) motif (39) and has been found in 14 other exported *P. falciparum* pro-

TABLE 5 PHISTa-like and PHIST proteins

Gene identification[a]	Other gene identification(s) or name(s)[b]	Presence of PEXEL[c]	Gene status[d]	Molecular mass (kDa)[e]	Length (aa)[e]	KO[f]	Description (reference[s] or source)[g]
PF3D7_0831300	MAL8P1.205, GEXP13	(x)		93.0	770		Classified as a PHIST protein (16), although no PHIST domain identified in InterPro; detected in early gametocytes (35); has a PEXEL motif (RKLSE), although this is not yet indicated in any publication
PF3D7_0831500				39.1	335		
PF3D7_0831750			PG	34.0	288		
PF3D7_0831900	MAL7P1.230		PG	33.5	287	x	Deletion in field samples from South America (116), no deletion in samples from Central America (117)
PF3D7_0832200.1	MAL7P1.225			33.5	286		One of the earliest-upregulated genes in the asexual cycle (28), one splice form of MAL7P1.225 (GeneDB)
PF3D7_0832200.2	MAL7P1.225			34.3	293		Same as PF3D7_0832200.1
PF3D7_0832300	MAL7P1.224			30.8	259		Upregulated during the commitment phase for the sexual developmental cycle (53, 145)
PF3D7_0832700	MAL7P1.220		PG	30.8	260		
PF3D7_1000700	PF10_0007, PF10_0008	x	PG	26.1	209		Both old gene identifications have different domains (27), PHISTa protein with N-terminal PHIST domain (15)
PF3D7_1201200	PFL0060w, MAL12P1.12	x		16.0	134		Downregulated in several strains (28), PHISTa-like protein (15)
PF3D7_1301300	MAL13P1.58		PG	28.9	247		Not located in telomeric region (27)
PF3D7_1372300				24.2	206		
PF3D7_1477300	PF14_0744, Pfg14-744	x		22.8	196		Strongly upregulated at gametocytogenesis (27); expression peak in stage I gametocytes but also present at stage II (85, 145, 146); grouped as PHIST or PHISTa-like protein (1, 15, 16); tested as a gametocyte marker (129); expressed as early as in committed schizont stage, regulated by AP2-G, and HP1 is reported to have a silencing effect (54)
PF3D7_1477400	PF14_0745			36.2	303		Expressed in parasites committed to the sexual cycle (27), found in the nuclear proteomic fraction (147), classified as a PHIST protein (16)

[a] Current gene identification from PlasmoDB.
[b] Other/previous names.
[c] The presence of a PEXEL motif is indicated by "x," as identified in reference 15 or 1. A newly identified PEXEL is indicated by "(x)."
[d] Annotated as a pseudogene (PG) in PlasmoDB.
[e] For proteins with a PEXEL motif, molecular mass and length were calculated for the PEXEL-cleaved form of the protein (the molecular mass for PEXEL-cleaved proteins was calculated by using the ExPASy Web tool [http://web.expasy.org/compute_pi/]).
[f] Existing viable knockout (KO) parasites or natural gene deletions are indicated by "x" (see reference 44 or the reference[s] indicated).
[g] Information or references referring to the corresponding gene or protein.

teins, 9 of which belong to the PHISTb/PHISTb-DnaJ subfamily (Tables 2 and 3). Each of these 9 PHIST proteins has a MEC motif in the C terminus downstream of the PHIST domain and in two cases is followed by a DnaJ domain. Three of these PHIST proteins also have been found to bind to inside-out vesicles (IOVs), suggesting an interaction between the MEC motif and a cytoskeleton interaction partner. Coprecipitation with the MEC motif of the PHISTb-DnaJ protein PF3D7_1038800 revealed band 4.1R as an interaction partner (39). Although these PHIST proteins were not further functionally characterized, the presence of a MEC motif, with its capacity to bind to band 4.1R, suggests their involvement in the remodeling of the iRBC cytoskeleton and, thus, a possible contribution to the pathology of malaria.

Seven PHISTb members (Table 3), including the well-known RESA, also comprise a DnaJ domain referred to as PHISTb-DnaJ. Proteins with a DnaJ domain belong to the HSP40 family. The J domains can act as cochaperones for proteins of the DnaK/HSP70 families and can associate with unfolded polypeptide chains to prevent their aggregation (18, 41). PHISTb and PHISTb-DnaJ differ in only one of the four conserved tryptophan positions (Fig. 4 and 5A), indicating their close relatedness. Another characteristic that sets the PHISTb-DnaJ proteins apart from the PHISTb subgroup is the extended length ranging from ~800 to 1,100 amino acids (15).

Several PHISTb proteins have been shown to localize at the host cell periphery, and solubility assays with green fluorescent

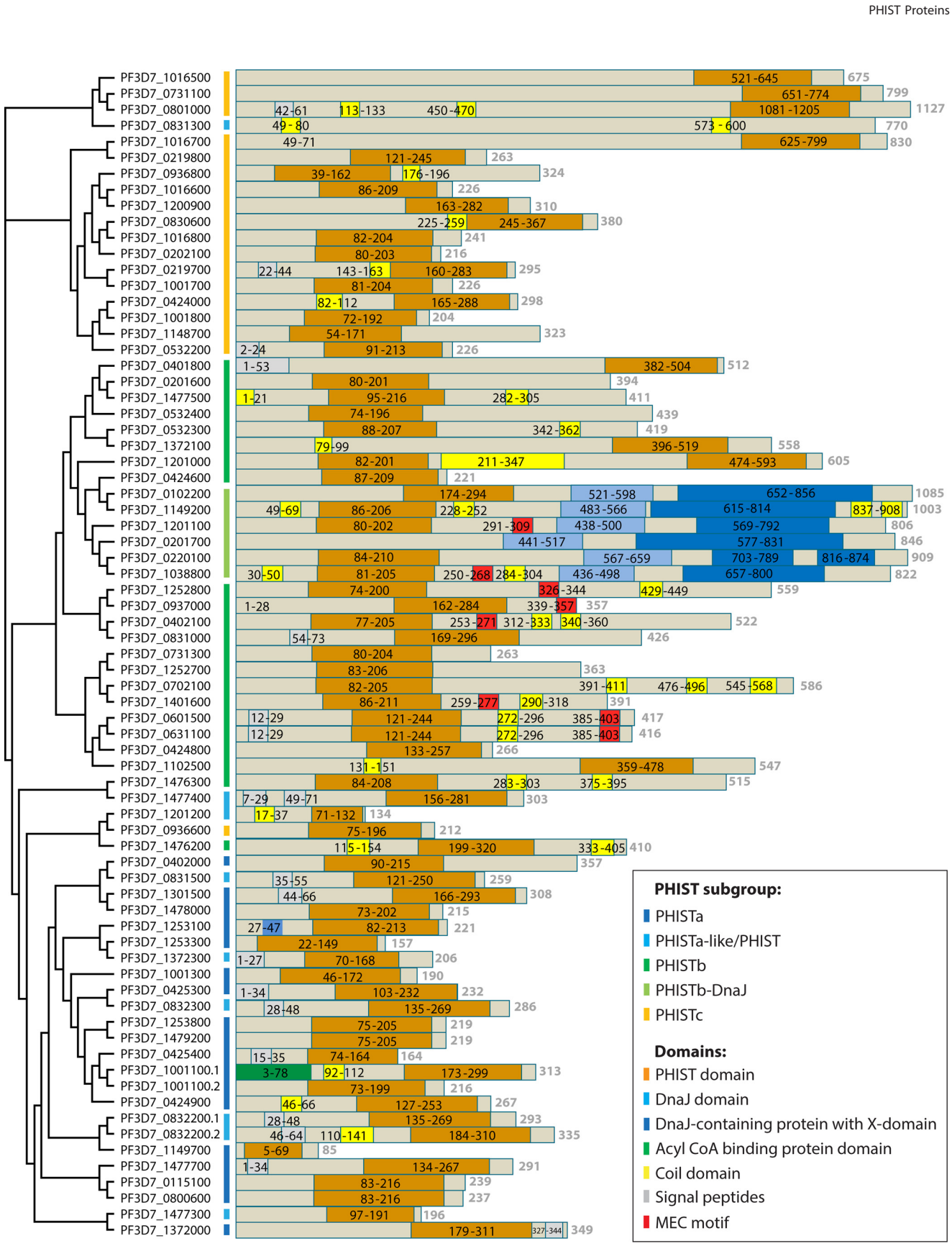
PHIST Proteins
PF3D7_1016500
PF3D7_0731100
PF3D7_0801000
PF3D7_0831300
PF3D7_1016700
PF3D7_0219800
PF3D7_0936800
PF3D7_1016600
PF3D7_1200900
PF3D7_0830600
PF3D7_1016800
PF3D7_0202100
PF3D7_0219700
PF3D7_1001700
PF3D7_0424000
PF3D7_1001800
PF3D7_1148700
PF3D7_0532200
PF3D7_0401800
PF3D7_0201600
PF3D7_1477500
PF3D7_0532400
PF3D7_0532300
PF3D7_1372100
PF3D7_1201000
PF3D7_0424600
PF3D7_0102200
PF3D7_1149200
PF3D7_1201100
PF3D7_0201700
PF3D7_0220100
PF3D7_1038800
PF3D7_1252800
PF3D7_0937000
PF3D7_0402100
PF3D7_0831000
PF3D7_0731300
PF3D7_1252700
PF3D7_0702100
PF3D7_1401600
PF3D7_0601500
PF3D7_0631100
PF3D7_0424800
PF3D7_1102500
PF3D7_1476300
PF3D7_1477400
PF3D7_1201200
PF3D7_0936600
PF3D7_1476200
PF3D7_0402000
PF3D7_0831500
PF3D7_1301500
PF3D7_1478000
PF3D7_1253100
PF3D7_1253300
PF3D7_1372300
PF3D7_1001300
PF3D7_0425300
PF3D7_0832300
PF3D7_1253800
PF3D7_1479200
PF3D7_0425400
PF3D7_1001100.1
PF3D7_1001100.2
PF3D7_0424900
PF3D7_0832200.1
PF3D7_0832200.2
PF3D7_1149700
PF3D7_1477700
PF3D7_0115100
PF3D7_0800600
PF3D7_1477300
PF3D7_1372000
PHIST subgroup:
PHISTa
PHISTa-like/PHIST
PHISTb
PHISTb-DnaJ
PHISTc
Domains:
PHIST domain
DnaJ domain
DnaJ-containing protein with X-domain
Acyl CoA binding protein domain
Coil domain
Signal peptides
MEC motif

protein (GFP)-tagged PHISTb proteins suggested an interaction with components of the host cytoskeleton (20). The authors of this study also investigated sequence requirements for peripheral localization and showed that the PHIST domain or the N-terminal region of the PHIST domain alone is not sufficient for peripheral localization. The PHIST domain together with parts of the N-terminal region, however, conferred peripheral localization (20). This was shown for the PHISTb protein PF3D7_0401800 and the PHISTb-DnaJ protein PF3D7_0102200, and it remains to be confirmed whether this applies to all PHISTb proteins and the precise sequence or structural requirements that are necessary. It also needs to be shown whether PHIST proteins of the other subfamilies have similar requirements for correct localization. Although localization does not predict function, these observations in general confirm that PHISTb proteins tend to associate with the iRBC cytoskeleton.

PHISTc. Most information is available for the PHISTc subgroup, which is entirely shared with *P. vivax* and *P. knowlesi* (15), indicating that the expansion of this subgroup occurred before the lineage diverged. The PHISTc subgroup is also the most diverse group in length, with lengths varying from <200 to >1,200 amino acids. In most of the 18 PHISTc proteins (Table 4), the PHIST domain is found very near the C terminus of the protein (Fig. 3), similarly to the PHISTa subgroup. In contrast to PHISTb proteins, which are associated mostly with the iRBC cytoskeleton, several PHISTc proteins have been found at structures such as Maurer's clefts (19, 42) and exosome-like vesicles (43) and are thought to be involved in protein trafficking (44, 45). There is recent evidence for PF3D7_0936800 (PFI1780w) to also be localized at the host cell membrane (19).

Other PHIST proteins. PlasmoDB lists 14 additional proteins that are annotated as PHISTa-like or simply PHIST proteins but originally were not included in the PHIST family (Table 5). Some of the PHISTa-like proteins were included in the subtelomeric protein superfamily identified by Eksi et al. (27), most of which have now been included in the PHISTa subgroup. There seems to be a close relationship between the PHISTa and the PHISTa-like proteins, indicated by sequence alignment and the pattern of conserved tryptophan residues (Fig. 4 and 5A).

PHIST Gene Expression

Transcriptome analysis of the *P. falciparum* 3D7 strain showed that most *phist* genes were expressed at an early stage during the intraerythrocytic development cycle. Throughout the second half of the cycle, almost all *phist* genes were switched off, while some were upregulated again toward the very end of the cycle (Fig. 6) (46). Genes with similar expression patterns were described to be involved in parasite-specific processes such as host cell invasion (47). In *Plasmodium*, the presence of the protein is often delayed after transcription, and the appearance of PHIST proteins was delayed on average by ~11 h (48). Thus, most PHIST proteins are present and exported during the first half of the intraerythrocytic development cycle, again strongly suggesting an important role of PHIST proteins in host cell remodeling.

Some *phist* genes have been reported to be differentially expressed, for example, during gametocytogenesis (35), in pregnancy-associated malaria (29, 49), or in cerebral malaria (32). Variable expression generally has also been observed in field isolates (50).

Figure 6 presents expression data obtained only from asexual blood stage parasites, but a proteomic study revealed that a number of PHIST proteins are enriched in early gametocytes, the sexual blood stage of *P. falciparum*. Of 26 putatively exported proteins enriched during early gametocyte stages, 9 belong to the PHIST protein family (35) (Fig. 6, yellow boxes). Two of these proteins, namely, GEXP5 (PF3D7_0936600) and PfEMP1-trafficking protein 2 (PfPTP2) (PF3D7_0731100), have been shown by microscopy to localize to gametocytes, with the former having been shown to be expressed exclusively in gametocytes (51). A function during sexual development remains to be shown (43, 51). The presence of some PHIST proteins in gametocytes suggests transcriptional upregulation, and indeed, the expression of ~20 *phist* genes, including GEXP5 (PF3D7_0936600), was shown to be under PfHP1 regulation (52). HP1 is a negative regulator of AP2-G, a transcription factor needed for sexual conversion, which binds to a promoter motif common to several early gametocyte genes, including the *phist* gene PF3D7_1477300 (53, 54). This provides strong evidence that gene regulation by HP1 affects the expression of *phist* genes and their involvement in gametocytogenesis.

Almelli et al. (32) compared transcriptional differences of samples from patients with cerebral malaria and samples from asymptomatic malaria cases from the 3D7 reference strain. A number of *phist* genes from all subfamilies were differentially either up- or downregulated (Fig. 6).

Mackinnon et al. (50) compared gene expression levels of the *P. falciparum* 3D7 strain with those of field isolates and also showed that a number of genes were differentially expressed. Among the 20 most regulated genes were also 7 *phist* genes (PF3D7_0202100, PF3D7_0424000, PF3D7_0702100, PF3D7_0832200.1, PF3D7_0936600, PF3D7_0936800, and PF3D7_1477700), suggesting that some PHIST proteins might be dispensable in culture but not for *in vivo* growth.

It has also been shown that 14 *phist* genes were variably expressed in *P. falciparum* 3D7 (Fig. 6) (55), indicating an active role

FIG 3 Phylogenetic tree and protein domain prediction for PHIST proteins. The amino acid sequences of all 89 PHIST proteins were obtained from PlasmoDB. Of 19 PHIST proteins annotated as pseudogenes, 16 contained one or more premature stop codons in the amino acid sequence and were removed from the list. All those of the remaining 73 PHIST proteins with a PEXEL motif were PEXEL cleaved *in silico* by using the PEXEL motifs provided by Sargeant et al. (15), Boddey et al. (11), or Schulze et al. (12). The amino acid sequences were aligned with MUSCLE (163). The alignment is represented in a phylogenetic tree using the phylogenic tree tool built into MUSCLE at the EMBL-EBI website (164). The branch lengths are drawn in cladogram style and do not represent actual phylogenetic distances. The colored bars next to the gene identifications represent different PHIST subgroups, as indicated. The structure of the amino acid sequences was then analyzed with InterPro (https://www.ebi.ac.uk/interpro/) (165). A schematic representation of the results for each PHIST protein is shown next to its respective gene identification. The following different domains are highlighted: the PHIST domain, the DnaJ domain as defined by Pfam (family PF00226), the DnaJ-containing protein with an X domain as defined by InterPro (accession number IPR026894) or Pfam (family PF14308), the acyl coenzyme A (CoA) binding protein domain as defined by Pfam (family PF00887), coil domains as identified by InterPro, signal peptides as defined by SignalP or transmembrane domains, and the MEC motif as defined by Kilili and LaCount (39).

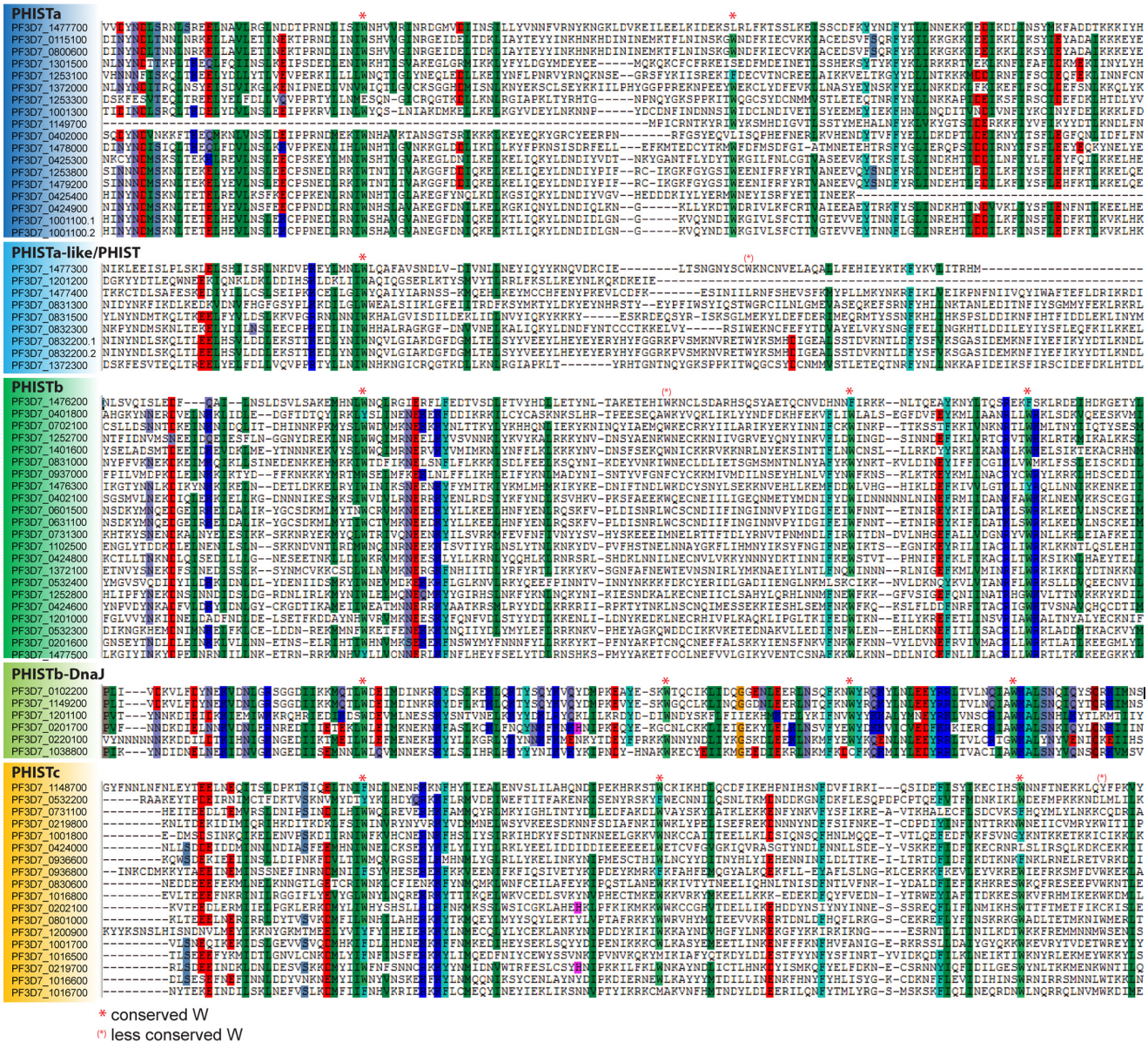

FIG 4 Sequence alignment of PHIST proteins. The processed amino acid sequences as described in the legend of Fig. 3 were sorted into PHIST subgroups, and individual alignments for each subgroup were obtained with CLUSTAL (166). The output was analyzed by using BioEdit (167). Conserved amino acids at a threshold of 83% are highlighted. Shown is the core of the alignment using the position of the first conserved tryptophan to align the different alignment blocks of the subgroups. Tryptophan residues conserved above or below the 83% threshold are marked as indicated.

in adaptation to changing environments such as heat shock (febrile illness) or nutrient depletion.

All of these studies were performed on the transcriptome or proteome level and reported general patterns and trends in gene expression or protein abundance. These studies repeatedly showed that *phist* genes or proteins are involved in different processes and support the notion that PHIST proteins play a central role in host cell remodeling. However, the functional and physical characterization of these proteins lags far behind. So far, we know that PHIST proteins are involved in cellular processes in iRBCs and in disease-associated functions, but our understanding of their actual function and interactions is very limited, at least for the large majority of them.

Below, we review and discuss individual PHIST proteins for which more detailed information is available, with most of them belonging to the PHISTb or PHISTc subgroup. Further information on other PHIST proteins is summarized in Tables 1 to 5.

PF3D7_0532400 (LyMP)

The PHISTb lysine-rich membrane-associated protein (LyMP) (PF3D7_0532400 or PFE1605w) is a PEXEL-containing PHISTb protein that is exported during the first half of the intraerythrocytic development cycle to the erythrocyte membrane, where it can localize at parasite-induced protrusions on the red blood cell membrane called knobs. Its transient localization at Maurer's clefts prior to its final destination correlates in space and time with

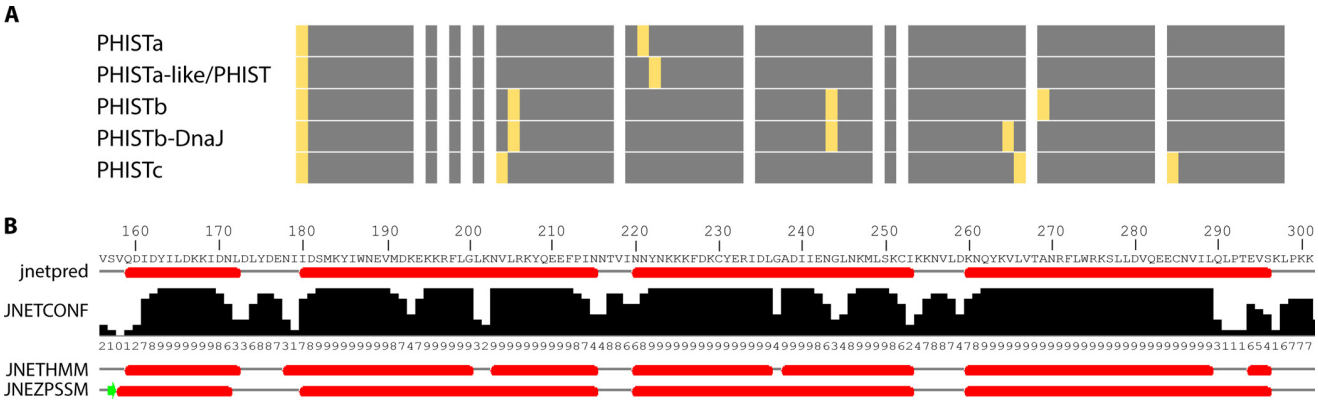

FIG 5 PHIST domain modeling. (A) Visual representation of the positions of the conserved tryptophan residues of the PHIST subgroups, treating PHISTb and PHISTb-DnaJ as well as PHISTa and PHISTa-like/PHIST domains as separate subgroups to show the slight variations between them. A consensus sequence was generated for each subgroup alignment from Fig. 4. The consensus sequence was then split into blocks of 10 residues represented by gray boxes (boxes containing no tryptophans were shortened). The positions of the tryptophan residues conserved within a subgroup are marked by yellow bars. (B) To exemplify the differences in structure prediction, the Jpred4 (168, 169) output is shown for the PHIST protein PF3D7_0532400. The top sequence is the consensus sequence used for PHIST identification by Sargeant et al. (15). JNetPRED displays the consensus prediction: helices are marked with red tubes. JNetCONF provides confidence estimates for the prediction. High values mean high confidence. For the JNetHMM profile-based prediction, the six predicted helices are marked as red tubes. For the JNETPSSM-based prediction, the four helices are marked as red tubes, and sheets are marked with a green arrow.

that of PfEMP1 (19). The PHIST domain of LyMP (amino acids 122 to 335) interacts with the intracellular acidic terminal segment (ATS) of PfEMP1. Conditional downregulation of LyMP reduced binding to CD36 by >60%, indicating that the interaction between the PHIST domain of LyMP and the ATS domain of PfEMP1 is important for the cytoadhesive properties of iRBCs (19, 38, 40, 56). A similar conditional downregulation of LyMP in iRBCs preselected for binding to different adhesion receptors displaying different PfEMP1 variants on the surface strongly differed in the reduction of cytoadherence (38), which led to the hypothesis that different PHIST proteins might be responsible for anchoring different PfEMP1 variants to the cytoskeleton.

It was further shown that the C-terminal segment of LyMP (amino acids 319 to 528) was able to bind IOVs, which are used to study protein interactions involving cytoskeletal proteins (40). Recently, we were able to show that this part of LyMP binds directly to human membrane protein band 3, which is linked to the cytoskeleton via ankyrin (38). Together with the ATS interaction mediated by the LyMP PHIST domain (19), it is evident that LyMP can act as a linker between the virulence complex of *P. falciparum* PfEMP1 and the host cytoskeleton.

PF3D7_0936800

PF3D7_0936800 (PFI1780w) is a PHISTc protein that was also shown to interact with the ATS domain of PfEMP1 albeit much more weakly than LyMP (56). A crystallographic structure of its PHIST domain (residues 85 to 247) has been obtained and is the first available structure for any PHIST protein. It confirms the predicted four-alpha-helix structure of the PHIST domain with a very short first alpha helix. The remaining three helices form a three-helix bundle with weak structural similarity to spectrin (19, 56).

PF3D7_0936800 has been classified as a noncanonical PEXEL protein with the first position of its PEXEL motif rendered from K to R, which was recently shown to be correctly cleaved and N-acetylated, confirming that this PHIST protein is correctly exported from parasites into iRBCs (12).

PF3D7_0936800 localizes underneath the iRBC membrane but is absent from knobs (19). It is speculated that it contains an interaction epitope for binding of iRBC membrane/cytoskeleton components (12). Here it is also noteworthy that PF3D7_0936800 has been found to be variantly expressed in 3D7 (55) and that there has been no reported PF3D7_0936800 knockout (PF3D7_0936800-KO) parasite.

PF3D7_0731100 (PfPTP2)

The PHISTc protein PF3D7_0731100 (PfEMP1 trafficking protein 2, PfPTP2) seems to play a role in PfEMP1 trafficking or surface display. Depletion of this protein leads to PfEMP1 accumulation in Maurer's clefts and its absence from knobs. Under flow conditions, PfPTP2-KO parasites do not adhere to chondroitin sulfate A (CSA), suggesting that the main role of PfPTP2 might be the trafficking of PfEMP1 from Maurer's clefts to knobs (42, 44).

Recently, PfPTP2 was also described to be located at exosome-like vesicles of ~70 nm that are involved in cell-cell communication and allow nucleic acid transfer between *Plasmodium* parasites. PfPTP2-deficient parasites showed reduced cell-cell communication, and Regev-Rudzki et al. (43) suggested that PfPTP2 is essential for cell-cell communication between *P. falciparum*-infected erythrocytes, leading to increased gametocytogenesis *in vitro*. PfPTP2 was the only protein involved in knob formation or PfEMP1 display (besides skeleton binding protein 1 [SBP1] [57]) but was also found to be enriched in early gametocytes (35, 43). In contrast, transcriptional analysis shows that PfPTP2 is downregulated in gametocytes; thus, PfPTP2 abundance in early gametocytes might be acquired through exosome-like vesicles, and this might in turn induce sexual conversion. Such a hypothetical model would accommodate the fact that PfPTP2 is upregulated in asexual stages but also enriched in gametocytes.

Immunoelectron microscopy and proteinase K assays revealed the localization of PfPTP2 on the cytosolic face of Maurer's clefts, on budding vesicles, and on the surface of exosome-like vesicles (43, 44).

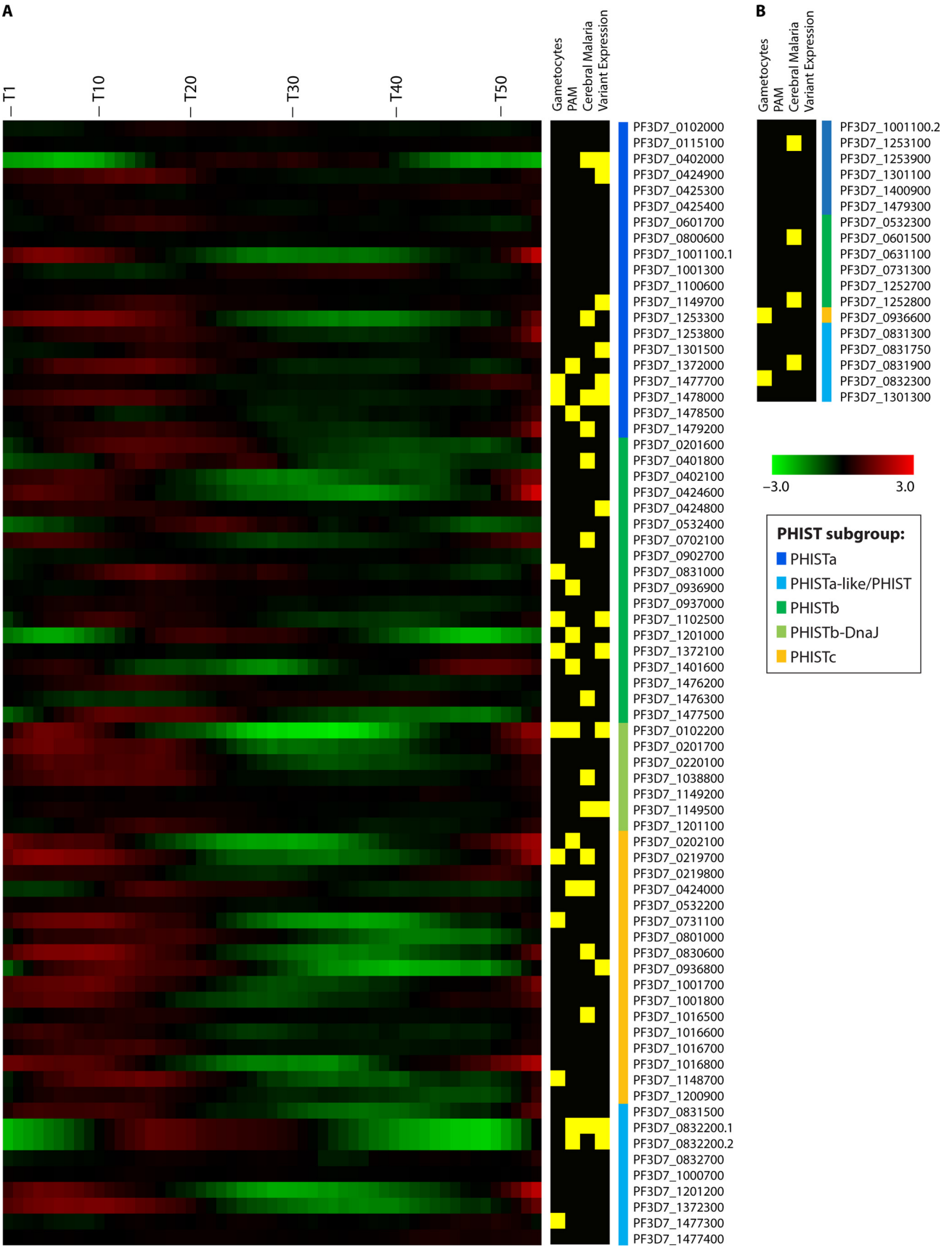
A
T1
T10
T20
T30
T40
T50
Gametocytes
PAM
Cerebral Malaria
Variant Expression
PF3D7_0102000
PF3D7_0115100
PF3D7_0402000
PF3D7_0424900
PF3D7_0425300
PF3D7_0425400
PF3D7_0601700
PF3D7_0800600
PF3D7_1001100.1
PF3D7_1001300
PF3D7_1100600
PF3D7_1149700
PF3D7_1253300
PF3D7_1253800
PF3D7_1301500
PF3D7_1372000
PF3D7_1477700
PF3D7_1478000
PF3D7_1478500
PF3D7_1479200
PF3D7_0201600
PF3D7_0401800
PF3D7_0402100
PF3D7_0424600
PF3D7_0424800
PF3D7_0532400
PF3D7_0702100
PF3D7_0902700
PF3D7_0831000
PF3D7_0936900
PF3D7_0937000
PF3D7_1102500
PF3D7_1201000
PF3D7_1372100
PF3D7_1401600
PF3D7_1476200
PF3D7_1476300
PF3D7_1477500
PF3D7_0102200
PF3D7_0201700
PF3D7_0220100
PF3D7_1038800
PF3D7_1149200
PF3D7_1149500
PF3D7_1201100
PF3D7_0202100
PF3D7_0219700
PF3D7_0219800
PF3D7_0424000
PF3D7_0532200
PF3D7_0731100
PF3D7_0801000
PF3D7_0830600
PF3D7_0936800
PF3D7_1001700
PF3D7_1001800
PF3D7_1016500
PF3D7_1016600
PF3D7_1016700
PF3D7_1016800
PF3D7_1148700
PF3D7_1200900
PF3D7_0831500
PF3D7_0832200.1
PF3D7_0832200.2
PF3D7_0832700
PF3D7_1000700
PF3D7_1201200
PF3D7_1372300
PF3D7_1477300
PF3D7_1477400
B
Gametocytes
PAM
Cerebral Malaria
Variant Expression
PF3D7_1001100.2
PF3D7_1253100
PF3D7_1253900
PF3D7_1301100
PF3D7_1400900
PF3D7_1479300
PF3D7_0532300
PF3D7_0601500
PF3D7_0631100
PF3D7_0731300
PF3D7_1252700
PF3D7_1252800
PF3D7_0936600
PF3D7_0831300
PF3D7_0831750
PF3D7_0831900
PF3D7_0832300
PF3D7_1301300
−3.0
3.0
PHIST subgroup:
PHISTa
PHISTa-like/PHIST
PHISTb
PHISTb-DnaJ
PHISTc

PF3D7_0402000

The PHISTa protein PF3D7_0402000 was identified in a yeast two-hybrid assay to determine potential interaction partners of the human erythrocyte cytoskeleton protein band 4.1R. The protein interacted with the N and alpha lobes of the FERM (four-point-one, ezrin, radixin, and moesin) domain (Pfam family PF00373) of band 4.1R through helices 2 and 3 of the PHIST domain, but the entire domain was required for maximal interaction (58). The host cytoskeleton protein band 4.1R binds to actin filaments and links these to membrane proteins such as band 3 and glycophorin C, maintaining the biconcave shape (reviewed in references 58 and 59). In this context, it is noteworthy that other *P. falciparum* proteins, e.g., MESA (PF3D7_0500800), which is not a PHIST protein, bind to this host cell cytoskeleton interaction hub (60). In immunofluorescence imaging analyses, subpopulations of both band 4.1R and PF3D7_0402000 were shown to colocalize at the parasitophorous vacuole membrane (58). The role that PF3D7_0402000 plays in changes of membrane rigidity or host actin recruitment remains unclear.

PF3D7_0936600 (GEXP5)

GEXP5 (gametocyte exported protein 5) was originally classified as PHISTb (15) but is now grouped among the PHISTc proteins (16), which is confirmed by the position of its conserved tryptophan residues (Fig. 4). GEXP5 was the first PHIST protein detected in gametocytes. A GEXP5-GFP fusion protein, when episomally expressed under the control of the endogenous promoter in asexual stages, was not detected by fluorescence imaging (51) but could be detected when expressed under the *pfcam* promoter, confirming a cytosolic localization (20). This indicated that endogenous GEXP5 is expressed and exported only in sexual stages and is found in the iRBC cytosol of stage I to IV gametocytes. Its uniform distribution throughout the iRBC and its presence in the soluble protein fraction suggest that it is a soluble protein (51). GEXP5 is already found at 14 h postinvasion in ring stage parasites committed to gametocytogenesis and is now considered to be the earliest gametocyte marker (51). This early appearance of GEXP5 in committed parasites might explain the presence of transcripts in the expression data sets in PlasmoDB.

The expression and export of GEXP5 are independent of transcription factors normally associated with gametocytogenesis, such as PfAP2-G, but GEXP5 is not able to drive gametocyte maturation alone in the absence of these transcription factors (51). It is therefore assumed that GEXP5 is not involved in processes driving gametocytogenesis but is used to remodel or prepare the host cell to accommodate sexual development.

PF3D7_0102200 (RESA)

RESA (ring-infected erythrocyte surface antigen) contains both PHIST and DnaJ domains and is one of seven members of the PHISTb-DnaJ subgroup. Its name is a misnomer since RESA is an intracellular exported protein (20).

RESA is expressed in mature-stage parasites (61) and is stored in the dense granules of newly formed merozoites (62). Within minutes after the invasion of a merozoite into an erythrocyte, the contents of the dense granules, including RESA, are discharged into the parasitophorous vacuole (63–65). From there, RESA is then exported to the iRBC and localizes at the iRBC cytoskeleton, where it remains for ~24 h (64, 65). At the cytoskeleton, RESA is phosphorylated (66, 67) and interacts with spectrin (68). A fragment of 108 amino acids has been identified to interact with repeat 16 of the β-chain of spectrin (here it is important to note that residues 663 to 770 correspond to only a partial DnaJ X domain and not to the DnaJ J domain). As a result of this interaction, the spectrin tetramers are stabilized and rigidify the iRBC (69); however, it needs to be proven whether this interaction and the accompanying rigidification would also occur with the full-length domain or full-length RESA protein.

There is controversy regarding whether this interaction impairs the invasion of merozoites, since one study with erythrocytes prepacked with a recombinant form of RESA showed that the RESA-spectrin interaction had no significant effect on invasion (70). The recombinant RESA used in this study contained residues 322 to 1073 and lacked the entire PHIST domain (residues 174 to 294) (70) (Fig. 3). However, using a similar setup, Pei et al. showed that an even shorter fragment of RESA (residues 663 to 770) was able to reduce the invasion efficiency (69). Importantly, this recombinant peptide lacked both the PHIST domain and the DnaJ domain and hence might have created an artificial inhibitory interaction.

A domain of 70 amino acids found in RESA shares 39% homology with the DnaJ heat shock protein of *Escherichia coli* (41). Proteins with a DnaJ domain belong to the HSP40 family and act as cochaperones to the DnaK/HSP70 chaperones, which are involved in protein assembly and trafficking (18, 41). Proteins with a DnaJ domain have been described to be membrane associated (41), a feature shared by RESA. Initially, it was proposed that RESA destabilizes the RBC cytoskeleton (64), but now there is evidence that RESA in fact does the contrary, namely, stabilizing the cytoskeleton with the effect that it rigidifies ring stage infected parasites (65, 69, 71). It has been shown that the RESA-spectrin interaction protects iRBCs from thermal damage (65, 69, 70), and it has been speculated that the DnaJ domain of RESA might prevent spectrin from unfolding at elevated temperatures, or it might directly bind to hydrophobic regions of partially unfolded spectrin molecules (70). This rigidification of ring stage parasite-infected erythrocytes, potentially impairing passage through the spleen (72), is rather surprising, but this might simply be a side effect of the protective function of RESA against thermal damage to the host cell.

At the end of each 48-h cycle, the iRBC ruptures and releases

FIG 6 Heat maps. (A) Heat map of *phist* gene expression of the *P. falciparum* 3D7 strain over the course of 53 h. Microarray data on transcript abundance were reported previously (46) (accessed through PlasmoDB, release 28, 31 March 2016). The heat map was constructed by using TMeV4.9 (170). *phist* genes were clustered into their respective subgroups and were then ordered by gene identification. Genes annotated "*phista*-like" or as "*phist*" genes were grouped together as "*phist* others." Yellow boxes to the right of the heat map indicate PHIST proteins present in the early gametocyte proteome (35), differentially expressed *phist* genes in pregnancy-associated malaria (29, 49, 50, 84, 92, 112) and in cerebral malaria (32, 34), or if variant expression has been reported (55). Green to red colors represent fold changes (log fold changes from −3 to 3). (B) For a number of *phist* genes, no expression data were available in the data set, and these genes were grouped first by PHIST subgroup and then by gene identification. Additional information for selected PHIST proteins is provided in Tables 1 to 5. The colored bars next to the gene identifications indicate the PHIST subgroup.

new merozoites. This event is accompanied by fever peaks that last for a few hours (73, 74). During these fever episodes, the parasites are in ring stages, and this correlates with the time when RESA interacts with the cytoskeleton, protecting it from thermal damage caused by fever. After ~24 h, RESA dissociates from spectrin (61), and other proteins might be responsible for further rigidification of the cytoskeleton (71). This apparent functional contradiction might be an evolutionary tradeoff between the need for survival during fever and costs of increased cell rigidity to a level that still allows passage through the spleen. The fact that less deformable ring stage parasite-iRBCs are cleared by the spleen supports this idea of a tradeoff (72).

While the function of the DnaJ domain in RESA has been described in much detail, the function of the PHIST domain still remains enigmatic.

PVX_093680 (CVC-81_{95})

The only PHIST protein not from *P. falciparum* that has been further characterized is the *P. vivax* PHIST CVC-81_{95} (PVX_093680). Caveola-vesicle complexes (CVCs) are parasite-induced indentations in *P. vivax*-infected erythrocyte cell membranes. The exact structure, protein composition, and function are not yet fully understood, but CVC-81_{95} is exported, is a predominant protein in these CVCs, and is found on tubular extensions going inwards from the CVC (75, 76). Its orthologue in *P. cynomolgi* shows a similar localization (75). CVC-81_{95} was found by Acharya et al. (77) in *P. vivax*-infected peripheral blood, and another study showed that over 80% of patient sera reacted positively with CVC-81_{95} (78). Based on these findings, CVC-81_{95} was suggested to be involved in immune evasion (78), as the PHIST protein family was previously suggested to be involved in this process (24). Therefore, in *P. vivax*, PHIST proteins also seem to be localized to parasite-induced structures in iRBCs and might be essential for host-parasite interactions. However, more functional analyses are required to fully understand the role of this PHIST protein in the CVC of *P. vivax*.

phist Gene Knockout Study

In a large gene knockout study in *P. falciparum* to functionally characterize exported proteins, 17 *phist* genes were targeted for deletion (44). These genes included 1 *phista* gene, 7 *phistb* genes, 6 *phistb-dnaJ* genes, and 3 *phistc* genes. Of these, all but four (PF3D7_0936800, PF3D7_0401800, PF3D7_0402100, and PF3D7_1149000) were successfully disrupted, indicating that the majority was dispensable for *in vitro* growth. Except for PF3D7_0731100 (PfPTP2), none of the *phist* knockout parasites from this study were analyzed in greater detail. Some were reported to have an influence on altered knob morphology (PF3D7_0424600-KO) or reduced (PF3D7_0102200/RESA-KO) or increased (PF3D7_0220100-KO) iRBC rigidity (44). Further phenotypic characterization of these parasite lines is urgently needed to better understand the role of PHIST proteins in host cell remodeling.

Structure and Function

It is highly conceivable that PHIST proteins might fulfill similar roles as chaperones, since a number of chaperones also contain DnaJ domains. They may also be responsible for the close association with the host cytoskeleton and cell membrane due to the intrinsic positive charge of many PHIST proteins. The few studies on PHISTs have looked mostly at the PHIST domain only; however, Tarr et al. (20) suggested that the PHIST domain alone is not sufficient to correctly target the protein to its destination, at least for those PHIST proteins investigated. Mayer et al. (56) analyzed the binding affinities of various PHIST domains for a number of ATS domains, but only the PHIST protein PF3D7_0532400 has been studied in greater detail with respect to structure and function (19, 56). This is rather surprising for a protein family comprising a large proportion of the complete exportome of *P. falciparum*.

CONCLUSION

The three major PHIST subfamilies not only differ in sequence but also seem to differ in function. PHISTb proteins mostly interact with and localize to the iRBC cytoskeleton and seem to be involved in changes of cell properties such as rigidity. PHISTc proteins seem to be involved mostly in protein trafficking of other exported proteins, while the PHISTa subfamily remains enigmatic, and there is not yet sufficient information available to draw a conclusion on function.

The presence of PHIST proteins at various localizations in the host cell makes them highly interesting candidates as interaction partners for other exported proteins, and therefore, it would be important to understand what determines the destination of PHIST proteins. The identification of export requirements for PHIST proteins would increase our understanding of the interaction network of exported proteins.

It seems that some PHIST proteins have at least two binding domains, the PHIST domain and a second one toward the C terminus, e.g., the MEC motif, the spectrin binding site, the band 3 interaction epitope, or a DnaJ domain. This would make PHIST proteins ideal molecules for multifunctional interactions at the iRBC cytoskeleton or in protein export with the PHIST domain serving as a general adaptor, while the C-terminal domain could function as a highly specific binding site. However, only a few additional binding motifs have been identified in some PHIST proteins, and more PHIST proteins remain to be studied.

Our knowledge of PHIST proteins is still very limited and based mainly on studies of the 3D7 laboratory strain, which does not suffice to understand the full extent of PHIST protein functions for *in vivo* parasite survival and malaria-associated disease and pathology. PHIST proteins should be studied in various disease presentations from mild to severe malaria as well as in pregnancy-associated malaria. Furthermore, the role of PHIST proteins in gametocytogenesis and also in mosquito stages remains completely enigmatic. Since many PHIST proteins seem to be central for host cell remodeling, it is essential to understand their function in this crucial process.

ACKNOWLEDGMENTS

We thank Beatrice Schibler and Alexander Oberli for carefully reading and commenting on the manuscript. We acknowledge Christoph Schmid and Anita Lerch for their help with the alignments and phylogenetic tree construction.

J.D.W. conducted the literature review. J.D.W., I.V., and H.-P.B. wrote the manuscript.

We claim no conflicting interests.

J.D.W. and H.-P.B. were supported by Swiss National Science Foundation grant number 31003A_149297/1. I.V. was supported by a Wellcome Trust RCD fellowship (088497/Z/09/Z). The funders had no role in determining the content of the paper or in the decision to submit this work for publication.

REFERENCES

1. **Boddey JA, Cowman AF.** 2013. Plasmodium nesting: remaking the erythrocyte from the inside out. Annu Rev Microbiol **67:**243–269. http://dx.doi.org/10.1146/annurev-micro-092412-155730.
2. **Tuteja R.** 2007. Malaria—an overview. FEBS J **274:**4670–4679. http://dx.doi.org/10.1111/j.1742-4658.2007.05997.x.
3. **WHO.** 2015. World malaria report 2015. WHO, Geneva, Switzerland.
4. **Amino R, Giovannini D, Thiberge S, Gueirard P, Boisson B, Dubremetz JF, Prevost MC, Ishino T, Yuda M, Menard R.** 2008. Host cell traversal is important for progression of the malaria parasite through the dermis to the liver. Cell Host Microbe **3:**88–96. http://dx.doi.org/10.1016/j.chom.2007.12.007.
5. **Sturm A, Amino R, van de Sand C, Regen T, Retzlaff S, Rennenberg A, Krueger A, Pollok JM, Menard R, Heussler VT.** 2006. Manipulation of host hepatocytes by the malaria parasite for delivery into liver sinusoids. Science **313:**1287–1290. http://dx.doi.org/10.1126/science.1129720.
6. **Gardner JP, Pinches RA, Roberts DJ, Newbold CI.** 1996. Variant antigens and endothelial receptor adhesion in Plasmodium falciparum. Proc Natl Acad Sci U S A **93:**3503–3508. http://dx.doi.org/10.1073/pnas.93.8.3503.
7. **Turner L, Lavstsen T, Berger SS, Wang CW, Petersen JE, Avril M, Brazier AJ, Freeth J, Jespersen JS, Nielsen MA, Magistrado P, Lusingu J, Smith JD, Higgins MK, Theander TG.** 2013. Severe malaria is associated with parasite binding to endothelial protein C receptor. Nature **498:**502–505. http://dx.doi.org/10.1038/nature12216.
8. **Bannister L, Mitchell G.** 2003. The ins, outs and roundabouts of malaria. Trends Parasitol **19:**209–213. http://dx.doi.org/10.1016/S1471-4922(03)00086-2.
9. **Marti M, Good RT, Rug M, Knuepfer E, Cowman AF.** 2004. Targeting malaria virulence and remodeling proteins to the host erythrocyte. Science **306:**1930–1933. http://dx.doi.org/10.1126/science.1102452.
10. **Hiller NL, Bhattacharjee S, van Ooij C, Liolios K, Harrison T, Lopez-Estrano C, Haldar K.** 2004. A host-targeting signal in virulence proteins reveals a secretome in malarial infection. Science **306:**1934–1937. http://dx.doi.org/10.1126/science.1102737.
11. **Boddey JA, Carvalho TG, Hodder AN, Sargeant TJ, Sleebs BE, Marapana D, Lopaticki S, Nebl T, Cowman AF.** 2013. Role of plasmepsin V in export of diverse protein families from the Plasmodium falciparum exportome. Traffic **14:**532–550. http://dx.doi.org/10.1111/tra.12053.
12. **Schulze J, Kwiatkowski M, Borner J, Schluter H, Bruchhaus I, Burmester T, Spielmann T, Pick C.** 2015. The Plasmodium falciparum exportome contains non-canonical PEXEL/HT proteins. Mol Microbiol **97:**301–314. http://dx.doi.org/10.1111/mmi.13024.
13. **Spielmann T, Gilberger TW.** 2010. Protein export in malaria parasites: do multiple export motifs add up to multiple export pathways? Trends Parasitol **26:**6–10. http://dx.doi.org/10.1016/j.pt.2009.10.001.
14. **Heiber A, Kruse F, Pick C, Gruring C, Flemming S, Oberli A, Schoeler H, Retzlaff S, Mesen-Ramirez P, Hiss JA, Kadekoppala M, Hecht L, Holder AA, Gilberger TW, Spielmann T.** 2013. Identification of new PNEPs indicates a substantial non-PEXEL exportome and underpins common features in Plasmodium falciparum protein export. PLoS Pathog **9:**e1003546. http://dx.doi.org/10.1371/journal.ppat.1003546.
15. **Sargeant TJ, Marti M, Caler E, Carlton JM, Simpson K, Speed TP, Cowman AF.** 2006. Lineage-specific expansion of proteins exported to erythrocytes in malaria parasites. Genome Biol **7:**R12. http://dx.doi.org/10.1186/gb-2006-7-2-r12.
16. **Frech C, Chen N.** 2013. Variant surface antigens of malaria parasites: functional and evolutionary insights from comparative gene family classification and analysis. BMC Genomics **14:**427. http://dx.doi.org/10.1186/1471-2164-14-427.
17. **Shi J, Blundell TL, Mizuguchi K.** 2001. FUGUE: sequence-structure homology recognition using environment-specific substitution tables and structure-dependent gap penalties. J Mol Biol **310:**243–257. http://dx.doi.org/10.1006/jmbi.2001.4762.
18. **Oakley MS, Kumar S, Anantharaman V, Zheng H, Mahajan B, Haynes JD, Moch JK, Fairhurst R, McCutchan TF, Aravind L.** 2007. Molecular factors and biochemical pathways induced by febrile temperature in intraerythrocytic Plasmodium falciparum parasites. Infect Immun **75:**2012–2025. http://dx.doi.org/10.1128/IAI.01236-06.
19. **Oberli A, Slater LM, Cutts E, Brand F, Mundwiler-Pachlatko E, Rusch S, Masik MF, Erat MC, Beck HP, Vakonakis I.** 2014. A Plasmodium falciparum PHIST protein binds the virulence factor PfEMP1 and comigrates to knobs on the host cell surface. FASEB J **28:**4420–4433. http://dx.doi.org/10.1096/fj.14-256057.
20. **Tarr SJ, Moon RW, Hardege I, Osborne AR.** 2014. A conserved domain targets exported PHISTb family proteins to the periphery of Plasmodium infected erythrocytes. Mol Biochem Parasitol **196:**29–40. http://dx.doi.org/10.1016/j.molbiopara.2014.07.011.
21. **Otto TD, Rayner JC, Bohme U, Pain A, Spottiswoode N, Sanders M, Quail M, Ollomo B, Renaud F, Thomas AW, Prugnolle F, Conway DJ, Newbold C, Berriman M.** 2014. Genome sequencing of chimpanzee malaria parasites reveals possible pathways of adaptation to human hosts. Nat Commun **5:**4754. http://dx.doi.org/10.1038/ncomms5754.
22. **Carlton JM, Adams JH, Silva JC, Bidwell SL, Lorenzi H, Caler E, Crabtree J, Angiuoli SV, Merino EF, Amedeo P, Cheng Q, Coulson RM, Crabb BS, Del Portillo HA, Essien K, Feldblyum TV, Fernandez-Becerra C, Gilson PR, Gueye AH, Guo X, Kang'a S, Kooij TW, Korsinczky M, Meyer EV, Nene V, Paulsen I, White O, Ralph SA, Ren Q, Sargeant TJ, Salzberg SL, Stoeckert CJ, Sullivan SA, Yamamoto MM, Hoffman SL, Wortman JR, Gardner MJ, Galinski MR, Barnwell JW, Fraser-Liggett CM.** 2008. Comparative genomics of the neglected human malaria parasite Plasmodium vivax. Nature **455:**757–763. http://dx.doi.org/10.1038/nature07327.
23. **Westenberger SJ, McClean CM, Chattopadhyay R, Dharia NV, Carlton JM, Barnwell JW, Collins WE, Hoffman SL, Zhou Y, Vinetz JM, Winzeler EA.** 2010. A systems-based analysis of Plasmodium vivax lifecycle transcription from human to mosquito. PLoS Negl Trop Dis **4:**e653. http://dx.doi.org/10.1371/journal.pntd.0000653.
24. **Bozdech Z, Mok S, Hu G, Imwong M, Jaidee A, Russell B, Ginsburg H, Nosten F, Day NP, White NJ, Carlton JM, Preiser PR.** 2008. The transcriptome of Plasmodium vivax reveals divergence and diversity of transcriptional regulation in malaria parasites. Proc Natl Acad Sci U S A **105:**16290–16295. http://dx.doi.org/10.1073/pnas.0807404105.
25. **Pain A, Bohme U, Berry AE, Mungall K, Finn RD, Jackson AP, Mourier T, Mistry J, Pasini EM, Aslett MA, Balasubrammaniam S, Borgwardt K, Brooks K, Carret C, Carver TJ, Cherevach I, Chillingworth T, Clark TG, Galinski MR, Hall N, Harper D, Harris D, Hauser H, Ivens A, Janssen CS, Keane T, Larke N, Lapp S, Marti M, Moule S, Meyer IM, Ormond D, Peters N, Sanders M, Sanders S, Sargeant TJ, Simmonds M, Smith F, Squares R, Thurston S, Tivey AR, Walker D, White B, Zuiderwijk E, Churcher C, Quail MA, Cowman AF, Turner CM, Rajandream MA, Kocken CH, et al.** 2008. The genome of the simian and human malaria parasite Plasmodium knowlesi. Nature **455:**799–803. http://dx.doi.org/10.1038/nature07306.
26. **Moreira CK, Naissant B, Coppi A, Bennett BL, Aime E, Franke-Fayard B, Janse CJ, Coppens I, Sinnis P, Templeton TJ.** 2016. The Plasmodium PHIST and RESA-like protein families of human and rodent malaria parasites. PLoS One **11:**e0152510. http://dx.doi.org/10.1371/journal.pone.0152510.
27. **Eksi S, Haile Y, Furuya T, Ma L, Su X, Williamson KC.** 2005. Identification of a subtelomeric gene family expressed during the asexual-sexual stage transition in Plasmodium falciparum. Mol Biochem Parasitol **143:**90–99. http://dx.doi.org/10.1016/j.molbiopara.2005.05.010.
28. **Scholz M, Fraunholz MJ.** 2008. A computational model of gene expression reveals early transcriptional events at the subtelomeric regions of the malaria parasite, Plasmodium falciparum. Genome Biol **9:**R88. http://dx.doi.org/10.1186/gb-2008-9-5-r88.
29. **Tuikue Ndam N, Bischoff E, Proux C, Lavstsen T, Salanti A, Guitard J, Nielsen MA, Coppee JY, Gaye A, Theander T, David PH, Deloron P.** 2008. Plasmodium falciparum transcriptome analysis reveals pregnancy malaria associated gene expression. PLoS One **3:**e1855. http://dx.doi.org/10.1371/journal.pone.0001855.
30. **Daily JP, Le Roch KG, Sarr O, Ndiaye D, Lukens A, Zhou YY, Ndir O, Mboup S, Sultan A, Winzeler EA, Wirth DF.** 2005. In vivo transcriptome of Plasmodium falciparum reveals overexpression of transcripts that encode surface proteins. J Infect Dis **191:**1196–1203. http://dx.doi.org/10.1086/428289.
31. **Claessens A, Adams Y, Ghumra A, Lindergard G, Buchan CC, Andisi C, Bull PC, Mok S, Gupta AP, Wang CW, Turner L, Arman M, Raza A, Bozdech Z, Rowe JA.** 2012. A subset of group A-like var genes encodes the malaria parasite ligands for binding to human brain endothelial cells. Proc Natl Acad Sci U S A **109:**E1772–E1781. http://dx.doi.org/10.1073/pnas.1120461109.
32. **Almelli T, Nuel G, Bischoff E, Aubouy A, Elati M, Wang CW, Dillies**

MA, Coppee JY, Ayissi GN, Basco LK, Rogier C, Ndam NT, Deloron P, Tahar R. 2014. Differences in gene transcriptomic pattern of Plasmodium falciparum in children with cerebral malaria and asymptomatic carriers. PLoS One **9:**e114401. http://dx.doi.org/10.1371/journal.pone.0114401.

33. **Mok BW, Ribacke U, Winter G, Yip BH, Tan CS, Fernandez V, Chen Q, Nilsson P, Wahlgren M.** 2007. Comparative transcriptomal analysis of isogenic Plasmodium falciparum clones of distinct antigenic and adhesive phenotypes. Mol Biochem Parasitol **151:**184–192. http://dx.doi.org/10.1016/j.molbiopara.2006.11.006.
34. **Bertin GI, Sabbagh A, Argy N, Salnot V, Ezinmegnon S, Agbota G, Ladipo Y, Alao JM, Sagbo G, Guillonneau F, Deloron P.** 2016. Proteomic analysis of Plasmodium falciparum parasites from patients with cerebral and uncomplicated malaria. Sci Rep **6:**26773. http://dx.doi.org/10.1038/srep26773.
35. **Silvestrini F, Lasonder E, Olivieri A, Camarda G, van Schaijk B, Sanchez M, Younis Younis S, Sauerwein R, Alano P.** 2010. Protein export marks the early phase of gametocytogenesis of the human malaria parasite Plasmodium falciparum. Mol Cell Proteomics **9:**1437–1448. http://dx.doi.org/10.1074/mcp.M900479-MCP200.
36. **Joice R, Narasimhan V, Montgomery J, Sidhu AB, Oh K, Meyer E, Pierre-Louis W, Seydel K, Milner D, Williamson K, Wiegand R, Ndiaye D, Daily J, Wirth D, Taylor T, Huttenhower C, Marti M.** 2013. Inferring developmental stage composition from gene expression in human malaria. PLoS Comput Biol **9:**e1003392. http://dx.doi.org/10.1371/journal.pcbi.1003392.
37. **Joice R, Nilsson SK, Montgomery J, Dankwa S, Egan E, Morahan B, Seydel KB, Bertuccini L, Alano P, Williamson KC, Duraisingh MT, Taylor TE, Milner DA, Marti M.** 2014. Plasmodium falciparum transmission stages accumulate in the human bone marrow. Sci Transl Med **6:**244re5. http://dx.doi.org/10.1126/scitranslmed.3008882.
38. **Oberli A, Zurbrugg L, Rusch S, Brand F, Butler ME, Day JL, Cutts EE, Lavstsen T, Vakonakis I, Beck HP.** 24 February 2016. Plasmodium falciparum PHIST proteins contribute to cytoadherence and anchor PfEMP1 to the host cell cytoskeleton. Cell Microbiol http://dx.doi.org/10.1111/cmi.12583.
39. **Kilili GK, LaCount DJ.** 2011. An erythrocyte cytoskeleton-binding motif in exported Plasmodium falciparum proteins. Eukaryot Cell **10:**1439–1447. http://dx.doi.org/10.1128/EC.05180-11.
40. **Proellocks NI, Herrmann S, Buckingham DW, Hanssen E, Hodges EK, Elsworth B, Morahan BJ, Coppel RL, Cooke BM.** 2014. A lysine-rich membrane-associated PHISTb protein involved in alteration of the cytoadhesive properties of Plasmodium falciparum-infected red blood cells. FASEB J **28:**3103–3113. http://dx.doi.org/10.1096/fj.14-250399.
41. **Bork P, Sander C, Valencia A, Bukau B.** 1992. A module of the DnaJ heat-shock proteins found in malaria parasites. Trends Biochem Sci **17:**129. http://dx.doi.org/10.1016/0968-0004(92)90319-5.
42. **Maier AG, Cooke BM, Cowman AF, Tilley L.** 2009. Malaria parasite proteins that remodel the host erythrocyte. Nat Rev Microbiol **7:**341–354. http://dx.doi.org/10.1038/nrmicro2110.
43. **Regev-Rudzki N, Wilson DW, Carvalho TG, Sisquella X, Coleman BM, Rug M, Bursac D, Angrisano F, Gee M, Hill AF, Baum J, Cowman AF.** 2013. Cell-cell communication between malaria-infected red blood cells via exosome-like vesicles. Cell **153:**1120–1133. http://dx.doi.org/10.1016/j.cell.2013.04.029.
44. **Maier AG, Rug M, O'Neill MT, Brown M, Chakravorty S, Szestak T, Chesson J, Wu Y, Hughes K, Coppel RL, Newbold C, Beeson JG, Craig A, Crabb BS, Cowman AF.** 2008. Exported proteins required for virulence and rigidity of Plasmodium falciparum-infected human erythrocytes. Cell **134:**48–61. http://dx.doi.org/10.1016/j.cell.2008.04.051.
45. **de Koning-Ward TF, Gilson PR, Boddey JA, Rug M, Smith BJ, Papenfuss AT, Sanders PR, Lundie RJ, Maier AG, Cowman AF, Crabb BS.** 2009. A newly discovered protein export machine in malaria parasites. Nature **459:**945–949. http://dx.doi.org/10.1038/nature08104.
46. **Llinas M, Bozdech Z, Wong ED, Adai AT, DeRisi JL.** 2006. Comparative whole genome transcriptome analysis of three Plasmodium falciparum strains. Nucleic Acids Res **34:**1166–1173. http://dx.doi.org/10.1093/nar/gkj517.
47. **Bozdech Z, Llinás M, Pulliam BL, Wong ED, Zhu J, DeRisi JL.** 2003. The transcriptome of the intraerythrocytic developmental cycle of Plasmodium falciparum. PLoS Biol **1:**e5. http://dx.doi.org/10.1371/journal.pbio.0000005.
48. **Foth BJ, Zhang N, Chaal BK, Sze SK, Preiser PR, Bozdech Z.** 2011. Quantitative time-course profiling of parasite and host cell proteins in the human malaria parasite Plasmodium falciparum. Mol Cell Proteomics **10:**M110.006411. http://dx.doi.org/10.1074/mcp.M110.006411.
49. **Francis SE, Malkov VA, Oleinikov AV, Rossnagle E, Wendler JP, Mutabingwa TK, Fried M, Duffy PE.** 2007. Six genes are preferentially transcribed by the circulating and sequestered forms of Plasmodium falciparum parasites that infect pregnant women. Infect Immun **75:**4838–4850. http://dx.doi.org/10.1128/IAI.00635-07.
50. **Mackinnon MJ, Li J, Mok S, Kortok MM, Marsh K, Preiser PR, Bozdech Z.** 2009. Comparative transcriptional and genomic analysis of Plasmodium falciparum field isolates. PLoS Pathog **5:**e1000644. http://dx.doi.org/10.1371/journal.ppat.1000644.
51. **Tiburcio M, Dixon MW, Looker O, Younis SY, Tilley L, Alano P.** 2015. Specific expression and export of the Plasmodium falciparum gametocyte exported protein-5 marks the gametocyte ring stage. Malar J **14:**334. http://dx.doi.org/10.1186/s12936-015-0853-6.
52. **Flueck C, Bartfai R, Volz J, Niederwieser I, Salcedo-Amaya AM, Alako BT, Ehlgen F, Ralph SA, Cowman AF, Bozdech Z, Stunnenberg HG, Voss TS.** 2009. Plasmodium falciparum heterochromatin protein 1 marks genomic loci linked to phenotypic variation of exported virulence factors. PLoS Pathog **5:**e1000569. http://dx.doi.org/10.1371/journal.ppat.1000569.
53. **Brancucci NM, Bertschi NL, Zhu L, Niederwieser I, Chin WH, Wampfler R, Freymond C, Rottmann M, Felger I, Bozdech Z, Voss TS.** 2014. Heterochromatin protein 1 secures survival and transmission of malaria parasites. Cell Host Microbe **16:**165–176. http://dx.doi.org/10.1016/j.chom.2014.07.004.
54. **Goldowitz IS.** 2015. Plasmodium's crossroads: deciphering the molecular pathway that leads to malaria transmission. Doctoral dissertation. Harvard University, Boston, MA.
55. **Rovira-Graells N, Gupta AP, Planet E, Crowley VM, Mok S, Ribas de Pouplana L, Preiser PR, Bozdech Z, Cortes A.** 2012. Transcriptional variation in the malaria parasite Plasmodium falciparum. Genome Res **22:**925–938. http://dx.doi.org/10.1101/gr.129692.111.
56. **Mayer C, Slater L, Erat MC, Konrat R, Vakonakis I.** 2012. Structural analysis of the Plasmodium falciparum erythrocyte membrane protein 1 (PfEMP1) intracellular domain reveals a conserved interaction epitope. J Biol Chem **287:**7182–7189. http://dx.doi.org/10.1074/jbc.M111.330779.
57. **Dixon MW, Thompson J, Gardiner DL, Trenholme KR.** 2008. Sex in Plasmodium: a sign of commitment. Trends Parasitol **24:**168–175. http://dx.doi.org/10.1016/j.pt.2008.01.004.
58. **Parish LA, Mai DW, Jones ML, Kitson EL, Rayner JC.** 2013. A member of the Plasmodium falciparum PHIST family binds to the erythrocyte cytoskeleton component band 4.1. Malar J **12:**160. http://dx.doi.org/10.1186/1475-2875-12-160.
59. **Fowler VM.** 2013. The human erythrocyte plasma membrane: a Rosetta Stone for decoding membrane-cytoskeleton structure. Curr Top Membr **72:**39–88. http://dx.doi.org/10.1016/B978-0-12-417027-8.00002-7.
60. **Lustigman S, Anders RF, Brown GV, Coppel RL.** 1990. The mature-parasite-infected erythrocyte surface antigen (MESA) of Plasmodium falciparum associates with the erythrocyte membrane skeletal protein, band 4.1. Mol Biochem Parasitol **38:**261–270. http://dx.doi.org/10.1016/0166-6851(90)90029-L.
61. **Brown GV, Culvenor JG, Crewther PE, Bianco AE, Coppel RL, Saint RB, Stahl HD, Kemp DJ, Anders RF.** 1985. Localization of the ring-infected erythrocyte surface antigen (RESA) of Plasmodium falciparum in merozoites and ring-infected erythrocytes. J Exp Med **162:**774–779. http://dx.doi.org/10.1084/jem.162.2.774.
62. **Aikawa M, Torii M, Sjolander A, Berzins K, Perlmann P, Miller LH.** 1990. Pf155/Resa antigen is localized in dense granules of Plasmodium falciparum merozoites. Exp Parasitol **71:**326–329. http://dx.doi.org/10.1016/0014-4894(90)90037-D.
63. **Riglar DT, Richard D, Wilson DW, Boyle MJ, Dekiwadia C, Turnbull L, Angrisano F, Marapana DS, Rogers KL, Whitchurch CB, Beeson JG, Cowman AF, Ralph SA, Baum J.** 2011. Super-resolution dissection of coordinated events during malaria parasite invasion of the human erythrocyte. Cell Host Microbe **9:**9–20. http://dx.doi.org/10.1016/j.chom.2010.12.003.
64. **Coppel RL, Lustigman S, Murray L, Anders RF.** 1988. MESA is a Plasmodium falciparum phosphoprotein associated with the erythrocyte membrane skeleton. Mol Biochem Parasitol **31:**223–232. http://dx.doi.org/10.1016/0166-6851(88)90152-1.
65. **Silva MD, Cooke BM, Guillotte M, Buckingham DW, Sauzet JP, Le**

Scanf C, Contamin H, David P, Mercereau-Puijalon O, Bonnefoy S. 2005. A role for the Plasmodium falciparum RESA protein in resistance against heat shock demonstrated using gene disruption. Mol Microbiol **56:**990–1003. http://dx.doi.org/10.1111/j.1365-2958.2005.04603.x.

66. **Anders R, Murray L, Thomas L, Davern K, Brown G, Kemp D.** 1987. Structure and function of candidate vaccine antigens in Plasmodium falciparum. Biochem Soc Symp **53:**103–114.
67. **Foley M, Murray LJ, Anders RF.** 1990. The ring-infected erythrocyte surface-antigen protein of Plasmodium falciparum is phosphorylated upon association with the host cell membrane. Mol Biochem Parasitol **38:**69–75. http://dx.doi.org/10.1016/0166-6851(90)90206-2.
68. **Foley M, Tilley L, Sawyer WH, Anders RF.** 1991. The ring-infected erythrocyte surface antigen of Plasmodium falciparum associates with spectrin in the erythrocyte membrane. Mol Biochem Parasitol **46:**137–147. http://dx.doi.org/10.1016/0166-6851(91)90207-M.
69. **Pei XH, Guo XH, Coppel R, Bhattacharjee S, Haldar K, Gratzer W, Mohandas N, An XL.** 2007. The ring-infected erythrocyte surface antigen (RESA) of Plasmodium falciparum stabilizes spectrin tetramers and suppresses further invasion. Blood **110:**1036–1042. http://dx.doi.org/10.1182/blood-2007-02-076919.
70. **Da Silva E, Foley M, Dluzewski AR, Murray LJ, Anders RF, Tilley L.** 1994. The Plasmodium falciparum protein RESA interacts with the erythrocyte cytoskeleton and modifies erythrocyte thermal stability. Mol Biochem Parasitol **66:**59–69. http://dx.doi.org/10.1016/0166-6851(94)90036-1.
71. **Mills JP, Diez-Silva M, Quinn DJ, Dao M, Lang MJ, Tan KS, Lim CT, Milon G, David PH, Mercereau-Puijalon O, Bonnefoy S, Suresh S.** 2007. Effect of plasmodial RESA protein on deformability of human red blood cells harboring Plasmodium falciparum. Proc Natl Acad Sci U S A **104:**9213–9217. http://dx.doi.org/10.1073/pnas.0703433104.
72. **Safeukui I, Correas JM, Brousse V, Hirt D, Deplaine G, Mule S, Lesurtel M, Goasguen N, Sauvanet A, Couvelard A, Kerneis S, Khun H, Vigan-Womas I, Ottone C, Molina TJ, Treluyer JM, Mercereau-Puijalon O, Milon G, David PH, Buffet PA.** 2008. Retention of Plasmodium falciparum ring-infected erythrocytes in the slow, open microcirculation of the human spleen. Blood **112:**2520–2528. http://dx.doi.org/10.1182/blood-2008-03-146779.
73. **Crutcher JM, Hoffman SL.** 1996. Malaria, chapter 83, p 997. *In* Baron S (ed), Medical microbiology, 4th ed. University of Texas Medical Branch at Galveston, Galveston, TX.
74. **Oakley MS, Gerald N, McCutchan TF, Aravind L, Kumar S.** 2011. Clinical and molecular aspects of malaria fever. Trends Parasitol **27:**442–449. http://dx.doi.org/10.1016/j.pt.2011.06.004.
75. **Akinyi S, Hanssen E, Meyer EVS, Jiang J, Korir CC, Singh B, Lapp S, Barnwell JW, Tilley L, Galinski MR.** 2012. A 95 kDa protein of Plasmodium vivax and P. cynomolgi visualized by three-dimensional tomography in the caveola-vesicle complexes (Schüffner's dots) of infected erythrocytes is a member of the PHIST family. Mol Microbiol **84:**816–831. http://dx.doi.org/10.1111/j.1365-2958.2012.08060.x.
76. **Anderson DC, Lapp SA, Akinyi S, Meyer EV, Barnwell JW, Korir-Morrison C, Galinski MR.** 2015. Plasmodium vivax trophozoite-stage proteomes. J Proteomics **115:**157–176. http://dx.doi.org/10.1016/j.jprot.2014.12.010.
77. **Acharya P, Pallavi R, Chandran S, Chakravarti H, Middha S, Acharya J, Kochar S, Kochar D, Subudhi A, Boopathi AP, Garg S, Das A, Tatu U.** 2009. A glimpse into the clinical proteome of human malaria parasites Plasmodium falciparum and Plasmodium vivax. Proteomics Clin Appl **3:**1314–1325. http://dx.doi.org/10.1002/prca.200900090.
78. **Lu F, Li J, Wang B, Cheng Y, Kong DH, Cui L, Ha KS, Sattabongkot J, Tsuboi T, Han ET.** 2014. Profiling the humoral immune responses to Plasmodium vivax infection and identification of candidate immunogenic rhoptry-associated membrane antigen (RAMA). J Proteomics **102:**66–82. http://dx.doi.org/10.1016/j.jprot.2014.02.029.
79. **Nyalwidhe J, Lingelbach K.** 2006. Proteases and chaperones are the most abundant proteins in the parasitophorous vacuole of Plasmodium falciparum-infected erythrocytes. Proteomics **6:**1563–1573. http://dx.doi.org/10.1002/pmic.200500379.
80. **Jiang H, Patel JJ, Yi M, Mu J, Ding J, Stephens R, Cooper RA, Ferdig MT, Su XZ.** 2008. Genome-wide compensatory changes accompany drug-selected mutations in the Plasmodium falciparum crt gene. PLoS One **3:**e2484. http://dx.doi.org/10.1371/journal.pone.0002484.
81. **Mwai L, Diriye A, Masseno V, Muriithi S, Feltwell T, Musyoki J, Lemieux J, Feller A, Mair GR, Marsh K, Newbold C, Nzila A, Carret CK.** 2012. Genome wide adaptations of Plasmodium falciparum in response to lumefantrine selective drug pressure. PLoS One **7:**e31623. http://dx.doi.org/10.1371/journal.pone.0031623.
82. **Mbengue A, Berry L, Braun-Breton C.** 2014. Establishment of Plasmodium falciparum extracellular compartments in its host erythrocyte, p 133–159. *In* Shonhai A, Blatch G (ed), Heat shock proteins of malaria. Springer, New York, NY.
83. **Crowley VM, Rovira-Graells N, Ribas de Pouplana L, Cortes A.** 2011. Heterochromatin formation in bistable chromatin domains controls the epigenetic repression of clonally variant Plasmodium falciparum genes linked to erythrocyte invasion. Mol Microbiol **80:**391–406. http://dx.doi.org/10.1111/j.1365-2958.2011.07574.x.
84. **Bertin GI, Sabbagh A, Guillonneau F, Jafari-Guemouri S, Ezinmegnon S, Federici C, Hounkpatin B, Fievet N, Deloron P.** 2013. Differential protein expression profiles between Plasmodium falciparum parasites isolated from subjects presenting with pregnancy-associated malaria and uncomplicated malaria in Benin. J Infect Dis **208:**1987–1997. http://dx.doi.org/10.1093/infdis/jit377.
85. **Buchholz K, Burke TA, Williamson KC, Wiegand RC, Wirth DF, Marti M.** 2011. A high-throughput screen targeting malaria transmission stages opens new avenues for drug development. J Infect Dis **203:**1445–1453. http://dx.doi.org/10.1093/infdis/jir037.
86. **Goel S, Muthusamy A, Miao J, Cui L, Salanti A, Winzeler EA, Gowda DC.** 2014. Targeted disruption of a ring-infected erythrocyte surface antigen (RESA)-like export protein gene in Plasmodium falciparum confers stable chondroitin 4-sulfate cytoadherence capacity. J Biol Chem **289:**34408–34421. http://dx.doi.org/10.1074/jbc.M114.615393.
87. **Natalang O, Bischoff E, Deplaine G, Proux C, Dillies MA, Sismeiro O, Guigon G, Bonnefoy S, Patarapotikul J, Mercereau-Puijalon O, Coppee JY, David PH.** 2008. Dynamic RNA profiling in Plasmodium falciparum synchronized blood stages exposed to lethal doses of artesunate. BMC Genomics **9:**388. http://dx.doi.org/10.1186/1471-2164-9-388.
88. **Cai H, Hong C, Gu J, Lilburn TG, Kuang R, Wang Y.** 2012. Module-based subnetwork alignments reveal novel transcriptional regulators in malaria parasite Plasmodium falciparum. BMC Syst Biol **6**(Suppl 3)**:**S5. http://dx.doi.org/10.1186/1752-0509-6-S3-S5.
89. **Vincensini L, Richert S, Blisnick T, Van Dorsselaer A, Leize-Wagner E, Rabilloud T, Braun Breton C.** 2005. Proteomic analysis identifies novel proteins of the Maurer's clefts, a secretory compartment delivering Plasmodium falciparum proteins to the surface of its host cell. Mol Cell Proteomics **4:**582–593. http://dx.doi.org/10.1074/mcp.M400176-MCP200.
90. **Lanzer M, Wickert H, Krohne G, Vincensini L, Braun Breton C.** 2006. Maurer's clefts: a novel multi-functional organelle in the cytoplasm of Plasmodium falciparum-infected erythrocytes. Int J Parasitol **36:**23–36. http://dx.doi.org/10.1016/j.ijpara.2005.10.001.
91. **Ralph SA, Bischoff E, Mattei D, Sismeiro O, Dillies MA, Guigon G, Coppee JY, David PH, Scherf A.** 2005. Transcriptome analysis of antigenic variation in Plasmodium falciparum—var silencing is not dependent on antisense RNA. Genome Biol **6:**R93. http://dx.doi.org/10.1186/gb-2005-6-11-r93.
92. **Vignali M, Armour CD, Chen J, Morrison R, Castle JC, Biery MC, Bouzek H, Moon W, Babak T, Fried M, Raymond CK, Duffy PE.** 2011. NSR-seq transcriptional profiling enables identification of a gene signature of Plasmodium falciparum parasites infecting children. J Clin Invest **121:**1119–1129. http://dx.doi.org/10.1172/JCI43457.
93. **Le Roch KG, Johnson JR, Florens L, Zhou Y, Santrosyan A, Grainger M, Yan SF, Williamson KC, Holder AA, Carucci DJ, Yates JR, III, Winzeler EA.** 2004. Global analysis of transcript and protein levels across the Plasmodium falciparum life cycle. Genome Res **14:**2308–2318. http://dx.doi.org/10.1101/gr.2523904.
94. **Wang D.** 2008. Discrepancy between mRNA and protein abundance: insight from information retrieval process in computers. Comput Biol Chem **32:**462–468. http://dx.doi.org/10.1016/j.compbiolchem.2008.07.014.
95. **Nair S, Nkhoma S, Nosten F, Mayxay M, French N, Whitworth J, Anderson T.** 2010. Genetic changes during laboratory propagation: copy number at the reticulocyte-binding protein 1 locus of Plasmodium falciparum. Mol Biochem Parasitol **172:**145–148. http://dx.doi.org/10.1016/j.molbiopara.2010.03.015.
96. **Sam-Yellowe TY.** 2009. The role of the Maurer's clefts in protein transport in Plasmodium falciparum. Trends Parasitol **25:**277–284. http://dx.doi.org/10.1016/j.pt.2009.03.009.

97. **Talevich E, Tobin AB, Kannan N, Doerig C.** 2012. An evolutionary perspective on the kinome of malaria parasites. Philos Trans R Soc Lond B Biol Sci **367:**2607–2618. http://dx.doi.org/10.1098/rstb.2012.0014.
98. **Mu J, Awadalla P, Duan J, McGee KM, Keebler J, Seydel K, McVean GA, Su XZ.** 2007. Genome-wide variation and identification of vaccine targets in the Plasmodium falciparum genome. Nat Genet **39:**126–130. http://dx.doi.org/10.1038/ng1924.
99. **LaCount DJ, Vignali M, Chettier R, Phansalkar A, Bell R, Hesselberth JR, Schoenfeld LW, Ota I, Sahasrabudhe S, Kurschner C, Fields S, Hughes RE.** 2005. A protein interaction network of the malaria parasite Plasmodium falciparum. Nature **438:**103–107. http://dx.doi.org/10.1038/nature04104.
100. **Spillman NJ, Beck JR, Goldberg DE.** 2015. Protein export into malaria parasite-infected erythrocytes: mechanisms and functional consequences. Annu Rev Biochem **84:**813–841. http://dx.doi.org/10.1146/annurev-biochem-060614-034157.
101. **Pallavi R, Acharya P, Chandran S, Daily JP, Tatu U.** 2010. Chaperone expression profiles correlate with distinct physiological states of Plasmodium falciparum in malaria patients. Malar J **9:**236. http://dx.doi.org/10.1186/1475-2875-9-236.
102. **Pavithra SR, Kumar R, Tatu U.** 2007. Systems analysis of chaperone networks in the malarial parasite Plasmodium falciparum. PLoS Comput Biol **3:**1701–1715.
103. **Oyelade J, Ewejobi I, Brors B, Eils R, Adebiyi E.** 2011. Computational identification of signalling pathways in Plasmodium falciparum. Infect Genet Evol **11:**755–764. http://dx.doi.org/10.1016/j.meegid.2010.11.006.
104. **Razak MR, Abdullah NR, Chomel R, Muhamad R, Ismail Z.** 2014. Effect of choline kinase inhibitor hexadecyltrimethylammonium bromide on Plasmodium falciparum gene expression. Southeast Asian J Trop Med Public Health **45:**259–266.
105. **Botha M, Pesce ER, Blatch GL.** 2007. The Hsp40 proteins of Plasmodium falciparum and other apicomplexa: regulating chaperone power in the parasite and the host. Int J Biochem Cell Biol **39:**1781–1803. http://dx.doi.org/10.1016/j.biocel.2007.02.011.
106. **Florens L, Liu X, Wang Y, Yang S, Schwartz O, Peglar M, Carucci DJ, Yates JR, III, Wu Y.** 2004. Proteomics approach reveals novel proteins on the surface of malaria-infected erythrocytes. Mol Biochem Parasitol **135:**1–11. http://dx.doi.org/10.1016/j.molbiopara.2003.12.007.
107. **Spielmann T, Hawthorne PL, Dixon MW, Hannemann M, Klotz K, Kemp DJ, Klonis N, Tilley L, Trenholme KR, Gardiner DL.** 2006. A cluster of ring stage-specific genes linked to a locus implicated in cytoadherence in Plasmodium falciparum codes for PEXEL-negative and PEXEL-positive proteins exported into the host cell. Mol Biol Cell **17:**3613–3624. http://dx.doi.org/10.1091/mbc.E06-04-0291.
108. **Siau A, Toure FS, Ouwe-Missi-Oukem-Boyer O, Ciceron L, Mahmoudi N, Vaquero C, Froissard P, Bisvigou U, Bisser S, Coppee JY, Bischoff E, David PH, Mazier D.** 2007. Whole-transcriptome analysis of Plasmodium falciparum field isolates: identification of new pathogenicity factors. J Infect Dis **196:**1603–1612. http://dx.doi.org/10.1086/522012.
109. **Penn WD.** 2010. Yeast two-hybrid analysis of host-parasite protein interactions in falciparum malaria. Doctoral dissertation. Purdue University, West Lafayette, IN.
110. **Fried M, Hixson KK, Anderson L, Ogata Y, Mutabingwa TK, Duffy PE.** 2007. The distinct proteome of placental malaria parasites. Mol Biochem Parasitol **155:**57–65. http://dx.doi.org/10.1016/j.molbiopara.2007.05.010.
111. **Hviid L.** 2011. The case for PfEMP1-based vaccines to protect pregnant women against Plasmodium falciparum malaria. Expert Rev Vaccines **10:**1405–1414. http://dx.doi.org/10.1586/erv.11.113.
112. **Nunes MC, Sterkers Y, Gamain B, Scherf A.** 2008. Investigation of host factors possibly enhancing the emergence of the chondroitin sulfate A-binding phenotype in Plasmodium falciparum. Microbes Infect **10:**928–932. http://dx.doi.org/10.1016/j.micinf.2008.05.006.
113. **Carret CK, Horrocks P, Konfortov E, Winzeler E, Qureshi M, Newbold C, Ivens A.** 2005. Microarray-based comparative genomic analyses of the human malaria parasite Plasmodium falciparum using Affymetrix arrays. Mol Biochem Parasitol **144:**177–186. http://dx.doi.org/10.1016/j.molbiopara.2005.08.010.
114. **Prajapati SK, Singh OP.** 2013. Remodeling of human red cells infected with Plasmodium falciparum and the impact of PHIST proteins. Blood Cells Mol Dis **51:**195–202. http://dx.doi.org/10.1016/j.bcmd.2013.06.003.
115. **Rodriguez LE, Curtidor H, Urquiza M, Cifuentes G, Reyes C, Patarroyo ME.** 2008. Intimate molecular interactions of P. falciparum merozoite proteins involved in invasion of red blood cells and their implications for vaccine design. Chem Rev **108:**3656–3705. http://dx.doi.org/10.1021/cr068407v.
116. **Gamboa D, Ho MF, Bendezu J, Torres K, Chiodini PL, Barnwell JW, Incardona S, Perkins M, Bell D, McCarthy J, Cheng Q.** 2010. A large proportion of P. falciparum isolates in the Amazon region of Peru lack pfhrp2 and pfhrp3: implications for malaria rapid diagnostic tests. PLoS One **5:**e8091. http://dx.doi.org/10.1371/journal.pone.0008091.
117. **Abdallah JF, Okoth SA, Fontecha GA, Torres RE, Banegas EI, Matute ML, Bucheli ST, Goldman IF, de Oliveira AM, Barnwell JW, Udhayakumar V.** 2015. Prevalence of pfhrp2 and pfhrp3 gene deletions in Puerto Lempira, Honduras. Malar J **14:**19. http://dx.doi.org/10.1186/s12936-014-0537-7.
118. **Gelhaus C, Fritsch J, Krause E, Leippe M.** 2005. Fractionation and identification of proteins by 2-DE and MS: towards a proteomic analysis of Plasmodium falciparum. Proteomics **5:**4213–4222. http://dx.doi.org/10.1002/pmic.200401285.
119. **Singh K, Agarwal A, Khan SI, Walker LA, Tekwani BL.** 2007. Growth, drug susceptibility, and gene expression profiling of Plasmodium falciparum cultured in medium supplemented with human serum or lipid-rich bovine serum albumin. J Biomol Screen **12:**1109–1114. http://dx.doi.org/10.1177/1087057107310638.
120. **Ribacke U, Mok BW, Wirta V, Normark J, Lundeberg J, Kironde F, Egwang TG, Nilsson P, Wahlgren M.** 2007. Genome wide gene amplifications and deletions in Plasmodium falciparum. Mol Biochem Parasitol **155:**33–44. http://dx.doi.org/10.1016/j.molbiopara.2007.05.005.
121. **Angus BJ, Chotivanich K, Udomsangpetch R, White NJ.** 1997. In vivo removal of malaria parasites from red blood cells without their destruction in acute falciparum malaria. Blood **90:**2037–2040.
122. **Dixon MW, Kenny S, McMillan PJ, Hanssen E, Trenholme KR, Gardiner DL, Tilley L.** 2011. Genetic ablation of a Maurer's cleft protein prevents assembly of the Plasmodium falciparum virulence complex. Mol Microbiol **81:**982–993. http://dx.doi.org/10.1111/j.1365-2958.2011.07740.x.
123. **Rug M, Maier AG.** 2011. The heat shock protein 40 family of the malaria parasite Plasmodium falciparum. IUBMB Life **63:**1081–1086. http://dx.doi.org/10.1002/iub.525.
124. **Le Roch KG, Johnson JR, Ahiboh H, Chung DW, Prudhomme J, Plouffe D, Henson K, Zhou Y, Witola W, Yates JR, Mamoun CB, Winzeler EA, Vial H.** 2008. A systematic approach to understand the mechanism of action of the bisthiazolium compound T4 on the human malaria parasite, Plasmodium falciparum. BMC Genomics **9:**513. http://dx.doi.org/10.1186/1471-2164-9-513.
125. **Acharya P, Kumar R, Tatu U.** 2007. Chaperoning a cellular upheaval in malaria: heat shock proteins in Plasmodium falciparum. Mol Biochem Parasitol **153:**85–94. http://dx.doi.org/10.1016/j.molbiopara.2007.01.009.
126. **Badaut C, Guyonnet L, Milet J, Renard E, Durand R, Viwami F, Sagbo G, Layla F, Deloron P, Bonnefoy S, Migot-Nabias F.** 2015. Immunoglobulin response to Plasmodium falciparum RESA proteins in uncomplicated and severe malaria. Malar J **14:**278. http://dx.doi.org/10.1186/s12936-015-0799-8.
127. **Caro F, Ahyong V, Betegon M, DeRisi JL.** 2014. Genome-wide regulatory dynamics of translation in the Plasmodium falciparum asexual blood stages. eLife **3:**e04106. http://dx.doi.org/10.7554/eLife.04106.
128. **Durand R, Migot-Nabias F, Andriantsoanirina V, Seringe E, Viwami F, Sagbo G, Lalya F, Deloron P, Mercereau-Puijalon O, Bonnefoy S.** 2012. Possible association of the Plasmodium falciparum T1526C resa2 gene mutation with severe malaria. Malar J **11:**128. http://dx.doi.org/10.1186/1475-2875-11-128.
129. **Pelle KG, Oh K, Buchholz K, Narasimhan V, Joice R, Milner DA, Brancucci NM, Ma S, Voss TS, Ketman K, Seydel KB, Taylor TE, Barteneva NS, Huttenhower C, Marti M.** 2015. Transcriptional profiling defines dynamics of parasite tissue sequestration during malaria infection. Genome Med **7:**19. http://dx.doi.org/10.1186/s13073-015-0133-7.
130. **Siau A, Silvie O, Franetich JF, Yalaoui S, Marinach C, Hannoun L, van Gemert GJ, Luty AJ, Bischoff E, David PH, Snounou G, Vaquero C, Froissard P, Mazier D.** 2008. Temperature shift and host cell contact up-regulate sporozoite expression of Plasmodium falciparum genes involved in hepatocyte infection. PLoS Pathog **4:**e1000121. http://dx.doi.org/10.1371/journal.ppat.1000121.

131. **Speake C, Duffy PE.** 2009. Antigens for pre-erythrocytic malaria vaccines: building on success. Parasite Immunol **31:**539–546. http://dx.doi.org/10.1111/j.1365-3024.2009.01139.x.
132. **Duffy PE, Fried M.** 2011. Pregnancy malaria: cryptic disease, apparent solution. Mem Inst Oswaldo Cruz **106**(Suppl 1):64–69. http://dx.doi.org/10.1590/S0074-02762011000900008.
133. **Davies DH, Duffy P, Bodmer JL, Felgner PL, Doolan DL.** 2015. Large screen approaches to identify novel malaria vaccine candidates. Vaccine **33:**7496–7505. http://dx.doi.org/10.1016/j.vaccine.2015.09.059.
134. **Radfar A, Diez A, Bautista JM.** 2008. Chloroquine mediates specific proteome oxidative damage across the erythrocytic cycle of resistant Plasmodium falciparum. Free Radic Biol Med **44:**2034–2042. http://dx.doi.org/10.1016/j.freeradbiomed.2008.03.010.
135. **Fatumo S, Adebiyi M, Adebiyi E.** 2013. In silico models for drug resistance. Methods Mol Biol **993:**39–65. http://dx.doi.org/10.1007/978-1-62703-342-8_4.
136. **Boddey JA, Hodder AN, Gunther S, Gilson PR, Patsiouras H, Kapp EA, Pearce JA, de Koning-Ward TF, Simpson RJ, Crabb BS, Cowman AF.** 2010. An aspartyl protease directs malaria effector proteins to the host cell. Nature **463:**627–631. http://dx.doi.org/10.1038/nature08728.
137. **Sam-Yellowe TY, Florens L, Wang T, Raine JD, Carucci DJ, Sinden R, Yates JR, III.** 2004. Proteome analysis of rhoptry-enriched fractions isolated from Plasmodium merozoites. J Proteome Res **3:**995–1001. http://dx.doi.org/10.1021/pr049926m.
138. **Baum E, Badu K, Molina DM, Liang X, Felgner PL, Yan G.** 2013. Protein microarray analysis of antibody responses to Plasmodium falciparum in western Kenyan highland sites with differing transmission levels. PLoS One **8:**e82246. http://dx.doi.org/10.1371/journal.pone.0082246.
139. **Andrews KT, Gupta AP, Tran TN, Fairlie DP, Gobert GN, Bozdech Z.** 2012. Comparative gene expression profiling of P. falciparum malaria parasites exposed to three different histone deacetylase inhibitors. PLoS One **7:**e31847. http://dx.doi.org/10.1371/journal.pone.0031847.
140. **Le Roch KG, Zhou Y, Blair PL, Grainger M, Moch JK, Haynes JD, De La Vega P, Holder AA, Batalov S, Carucci DJ, Winzeler EA.** 2003. Discovery of gene function by expression profiling of the malaria parasite life cycle. Science **301:**1503–1508. http://dx.doi.org/10.1126/science.1087025.
141. **Chookajorn T, Hartl DL.** 2006. Position-specific polymorphism of Plasmodium falciparum Stuttering motif in a PHISTc PFI1780w. Exp Parasitol **114:**126–128. http://dx.doi.org/10.1016/j.exppara.2006.02.019.
142. **Otto TD, Wilinski D, Assefa S, Keane TM, Sarry LR, Böhme U, Lemieux J, Barrell B, Pain A, Berriman M.** 2010. New insights into the blood-stage transcriptome of Plasmodium falciparum using RNA-Seq. Mol Microbiol **76:**12–24. http://dx.doi.org/10.1111/j.1365-2958.2009.07026.x.
143. **Carver T, Harris SR, Otto TD, Berriman M, Parkhill J, McQuillan JA.** 2013. BamView: visualizing and interpretation of next-generation sequencing read alignments. Brief Bioinform **14:**203–212. http://dx.doi.org/10.1093/bib/bbr073.
144. **Issar N, Roux E, Mattei D, Scherf A.** 2008. Identification of a novel posttranslational modification in Plasmodium falciparum: protein sumoylation in different cellular compartments. Cell Microbiol **10:**1999–2011. http://dx.doi.org/10.1111/j.1462-5822.2008.01183.x.
145. **Josling GA, Llinas M.** 2015. Sexual development in Plasmodium parasites: knowing when it's time to commit. Nat Rev Microbiol **13:**573–587. http://dx.doi.org/10.1038/nrmicro3519.
146. **Haase S, Herrmann S, Gruring C, Heiber A, Jansen PW, Langer C, Treeck M, Cabrera A, Bruns C, Struck NS, Kono M, Engelberg K, Ruch U, Stunnenberg HG, Gilberger TW, Spielmann T.** 2009. Sequence requirements for the export of the Plasmodium falciparum Maurer's clefts protein REX2. Mol Microbiol **71:**1003–1017. http://dx.doi.org/10.1111/j.1365-2958.2008.06582.x.
147. **Volz J, Carvalho TG, Ralph SA, Gilson P, Thompson J, Tonkin CJ, Langer C, Crabb BS, Cowman AF.** 2010. Potential epigenetic regulatory proteins localise to distinct nuclear sub-compartments in Plasmodium falciparum. Int J Parasitol **40:**109–121. http://dx.doi.org/10.1016/j.ijpara.2009.09.002.
148. **Lee AH, Symington LS, Fidock DA.** 2014. DNA repair mechanisms and their biological roles in the malaria parasite Plasmodium falciparum. Microbiol Mol Biol Rev **78:**469–486. http://dx.doi.org/10.1128/MMBR.00059-13.
149. **Taylor DW, Parra M, Chapman GB, Stearns ME, Rener J, Aikawa M, Uni S, Aley SB, Panton LJ, Howard RJ.** 1987. Localization of Plasmodium falciparum histidine-rich protein 1 in the erythrocyte skeleton under knobs. Mol Biochem Parasitol **25:**165–174. http://dx.doi.org/10.1016/0166-6851(87)90005-3.
150. **Watermeyer JM, Hale VL, Hackett F, Clare DK, Cutts EE, Vakonakis I, Fleck RA, Blackman MJ, Saibil HR.** 2016. A spiral scaffold underlies cytoadherent knobs in Plasmodium falciparum-infected erythrocytes. Blood **127:**343–351. http://dx.doi.org/10.1182/blood-2015-10-674002.
151. **Mundwiler-Pachlatko E, Beck HP.** 2013. Maurer's clefts, the enigma of Plasmodium falciparum. Proc Natl Acad Sci U S A **110:**19987–19994. http://dx.doi.org/10.1073/pnas.1309247110.
152. **Cyrklaff M, Sanchez CP, Frischknecht F, Lanzer M.** 2012. Host actin remodeling and protection from malaria by hemoglobinopathies. Trends Parasitol **28:**479–485. http://dx.doi.org/10.1016/j.pt.2012.08.003.
153. **Cyrklaff M, Sanchez CP, Kilian N, Bisseye C, Simpore J, Frischknecht F, Lanzer M.** 2011. Hemoglobins S and C interfere with actin remodeling in Plasmodium falciparum-infected erythrocytes. Science **334:**1283–1286. http://dx.doi.org/10.1126/science.1213775.
154. **Spycher C, Rug M, Klonis N, Ferguson DJ, Cowman AF, Beck HP, Tilley L.** 2006. Genesis of and trafficking to the Maurer's clefts of Plasmodium falciparum-infected erythrocytes. Mol Cell Biol **26:**4074–4085. http://dx.doi.org/10.1128/MCB.00095-06.
155. **Pachlatko E, Rusch S, Muller A, Hemphill A, Tilley L, Hanssen E, Beck HP.** 2010. MAHRP2, an exported protein of Plasmodium falciparum, is an essential component of Maurer's cleft tethers. Mol Microbiol **77:**1136–1152. http://dx.doi.org/10.1111/j.1365-2958.2010.07278.x.
156. **Hawthorne PL, Trenholme KR, Skinner-Adams TS, Spielmann T, Fischer K, Dixon MWA, Ortega MR, Anderson KL, Kemp DJ, Gardiner DL.** 2004. A novel Plasmodium falciparum ring stage protein, REX, is located in Maurer's clefts. Mol Biochem Parasitol **136:**181–189. http://dx.doi.org/10.1016/j.molbiopara.2004.03.013.
157. **Dietz O, Rusch S, Brand F, Mundwiler-Pachlatko E, Gaida A, Voss T, Beck HP.** 2014. Characterization of the small exported Plasmodium falciparum membrane protein SEMP1. PLoS One **9:**e103272. http://dx.doi.org/10.1371/journal.pone.0103272.
158. **Blisnick T, Eugenia M, Betoulle M, Barale JC, Uzureau P, Berry L, Desroses S, Fujioka H, Mattei D, Breton CB.** 2000. Pfsbp 1, a Maurer's cleft Plasmodium falciparum protein, is associated with the erythrocyte skeleton. Mol Biochem Parasitol **111:**107–121. http://dx.doi.org/10.1016/S0166-6851(00)00301-7.
159. **Rug M, Cyrklaff M, Mikkonen A, Lemgruber L, Kuelzer S, Sanchez CP, Thompson J, Hanssen E, O'Neill M, Langer C, Lanzer M, Frischknecht F, Maier AG, Cowman AF.** 2014. Export of virulence proteins by malaria-infected erythrocytes involves remodeling of host actin cytoskeleton. Blood **124:**3459–3468. http://dx.doi.org/10.1182/blood-2014-06-583054.
160. **Kats LM, Proellocks NI, Buckingham DW, Blanc L, Hale J, Guo X, Pei X, Herrmann S, Hanssen EG, Coppel RL, Mohandas N, An X, Cooke BM.** 2015. Interactions between Plasmodium falciparum skeleton-binding protein 1 and the membrane skeleton of malaria-infected red blood cells. Biochim Biophys Acta **1848:**1619–1628. http://dx.doi.org/10.1016/j.bbamem.2015.03.038.
161. **Külzer S, Rug M, Brinkmann K, Cannon P, Cowman A, Lingelbach K, Blatch GL, Maier AG, Przyborski JM.** 2010. Parasite-encoded Hsp40 proteins define novel mobile structures in the cytosol of the P. falciparum-infected erythrocyte. Cell Microbiol **12:**1398–1420. http://dx.doi.org/10.1111/j.1462-5822.2010.01477.x.
162. **Külzer S, Charnaud S, Dagan T, Riedel J, Mandal P, Pesce ER, Blatch GL, Crabb BS, Gilson PR, Przyborski JM.** 2012. Plasmodium falciparum-encoded exported hsp70/hsp40 chaperone/co-chaperone complexes within the host erythrocyte. Cell Microbiol **14:**1784–1795. http://dx.doi.org/10.1111/j.1462-5822.2012.01840.x.
163. **Edgar RC.** 2004. MUSCLE: multiple sequence alignment with high accuracy and high throughput. Nucleic Acids Res **32:**1792–1797. http://dx.doi.org/10.1093/nar/gkh340.
164. **Li W, Cowley A, Uludag M, Gur T, McWilliam H, Squizzato S, Park YM, Buso N, Lopez R.** 2015. The EMBL-EBI bioinformatics Web and programmatic tools framework. Nucleic Acids Res **43:**W580–W584. http://dx.doi.org/10.1093/nar/gkv279.
165. **Mitchell A, Chang HY, Daugherty L, Fraser M, Hunter S, Lopez R, McAnulla C, McMenamin C, Nuka G, Pesseat S, Sangrador-Vegas A, Scheremetjew M, Rato C, Yong SY, Bateman A, Punta M, Attwood TK, Sigrist CJ, Redaschi N, Rivoire C, Xenarios I, Kahn D, Guyot D, Bork P, Letunic I, Gough J, Oates M, Haft D, Huang H, Natale DA, Wu CH,**

Orengo C, Sillitoe I, Mi H, Thomas PD, Finn RD. 2015. The InterPro protein families database: the classification resource after 15 years. Nucleic Acids Res **43:**D213–D221. http://dx.doi.org/10.1093/nar/gku1243.

166. **Sievers F, Wilm A, Dineen D, Gibson TJ, Karplus K, Li W, Lopez R, McWilliam H, Remmert M, Soding J, Thompson JD, Higgins DG.** 2011. Fast, scalable generation of high-quality protein multiple sequence alignments using Clustal Omega. Mol Syst Biol **7:**539. http://dx.doi.org/10.1038/msb.2011.75.
167. **Hall TA.** 1999. BioEdit: a user-friendly biological sequence alignment editor and analysis program for Windows 95/98/NT. Nucleic Acids Symp Ser **41:**95–98.
168. **Cole C, Barber JD, Barton GJ.** 2008. The Jpred 3 secondary structure prediction server. Nucleic Acids Res **36:**W197–W201. http://dx.doi.org/10.1093/nar/gkn238.
169. **Cuff JA, Barton GJ.** 2000. Application of multiple sequence alignment profiles to improve protein secondary structure prediction. Proteins **40:**502–511. http://dx.doi.org/10.1002/1097-0134(20000815)40:3<502::AID-PROT170>3.0.CO;2-Q.
170. **Saeed AI, Bhagabati NK, Braisted JC, Liang W, Sharov V, Howe EA, Li J, Thiagarajan M, White JA, Quackenbush J.** 2006. TM4 microarray software suite. Methods Enzymol **411:**134–193. http://dx.doi.org/10.1016/S0076-6879(06)11009-5.

Jan D. Warncke obtained his B.Sc. in biology with an emphasis on microbiology from Brigham Young University—Idaho, Rexburg, ID. He then moved on to the Swiss Tropical and Public Health Institute and the University of Basel, Switzerland, where he received his M.Sc. in Infection Biology. Currently, he is enrolled in a Ph.D. program at the Swiss Tropical and Public Health Institute, working in the Molecular Parasitology and Epidemiology unit under the supervision of Professor Hans-Peter Beck. His interest is in exported proteins of *P. falciparum* and their role in host cell remodeling during the asexual blood stage of malaria.

Ioannis Vakonakis has a B.Sc. in Biology from the University of Crete. He obtained his Ph.D. in Biochemistry from Texas A&M University, where he pioneered the structural analysis of circadian clock proteins from cyanobacteria. His postdoctoral work at the University of Oxford focused on the mechanisms behind cell adhesion and the formation of the extracellular matrix in animals. He was trained in X-ray crystallography during a second postdoc at the Swiss Light Source prior to starting his own laboratory in Oxford Biochemistry as a Wellcome Trust Career Development Fellow. He is now an Associate Professor in Structural Biology and Biophysics at the University of Oxford. Over the last 6 years, his research has aimed to understand how large molecular machines form in cells, such as the cytoadherent assemblies created upon *P. falciparum* infection of human erythrocytes.

Hans-Peter Beck obtained his M.Sc. and Ph.D. in cell biology at the University of Tübingen. After his postdoc position at the Wellcome Centre of Molecular Parasitology in Edinburgh-Glasgow, where he worked on the bovine parasite *Theileria annulata*, he moved as a visiting scientist to the Walter and Eliza Hall Institute in Melbourne before he took up the position as group leader in Molecular Parasitology at the Papua New Guinean Institute of Medical Research. During this period, he pioneered molecular epidemiology for *P. falciparum* infections and established a research group working on the cell biology of these parasites. After 5 years in Papua New Guinea, he moved to the University of Witten-Herdecke, Germany, as group leader and subsequently moved to the Swiss Tropical and Public Health Institute, where he holds the position of unit head of a research group and holds a Professorship for Molecular Parasitology at the University of Basel. His research focus is on the molecular epidemiology and cell biology of the human malaria parasite *P. falciparum*. His research group in particular focuses on the interaction network of exported proteins of the parasite.

Chapter 4: PHIST BioID and Protein Interaction Network

Manuscript in preparation for submission

Exported Plasmodium falciparum PHIST proteins target the erythrocyte cytoskeleton

Jan D. Warncke[a,b], Lara Pérez-Martínez[c], Françoise Brand[a,b], Falk Butter[c], Hans-Peter Beck[a,b*]

[a] Department of Medical Parasitology and Infection Biology, Swiss Tropical and Public Health Institute, Basel, Switzerland

[b] University of Basel, Basel, Switzerland

[c] Quantitative Proteomics, Institute of Molecular Biology (IMB), Mainz, Germany

* corresponding author: Hans-Peter Beck, Swiss TPH, Socinstrasse 57, CH-4051 Basel, Switzerland, phone +41 61 284 81 16, fax: +41 61 284 81 01, hans-peter.beck@unibas.ch

ORCID IDs

Jan Warncke: 0000-0001-6852-4191

Falk Butter: 0000-0002-7197-7279

Hans-Peter Beck: 0000-0001-8326-4834

Summary

Remodeling of the erythrocyte is a hallmark feature of the asexual blood stages of *Plasmodium falciparum* and is the cause of all malaria-associated morbidity and mortality. Exported parasite proteins are the effectors facilitating this remodeling process. Plasmodium helical interspersed subtelomeric (PHIST) proteins, a family of exported proteins, have previously been suggested to play a role in host cell remodeling and particularly in cytoskeleton interactions. To elucidate their interactions and to better understand processes involved in remodeling, we selected 9 PHIST proteins for comprehensive analyses. We showed their localization at the erythrocyte cytoskeleton which was further confirmed for most candidates by solubilization studies and immuno-electron microscopy. Through a BioID approach and co-immunoprecipitations with subsequent mass spectrometry we identified potential interaction partners. Using this data we generated a network of PHIST protein interactions at the erythrocyte cytoskeleton involving both host and exported parasite proteins. We identified a number of so far uncharacterized exported parasite proteins that might also act as key players in host cell remodeling. The generation of this network of protein interactions of exported parasite proteins at the erythrocyte cytoskeleton adds to our better understanding of host cell remodeling and provides opportunities for further hypothesis driven studies.

Introduction

Upon invasion into the human erythrocyte, the malaria parasite *Plasmodium falciparum* extensively refurbishes its host cell. One hallmark of this refurbishment is the appearance of knobs, electron-dense protrusion on the surface of the infected red blood cell (iRBC) (1). PfEMP1, the major virulence protein of *P. falciparum* which is encoded by var genes is anchored in those knobs and mediates cytoadhesion to endothelial cells. This leads to sequestration of iRBCs in the microvasculature of human organs and is the cause of malaria-associated morbidity and mortality (2).

This host cell remodeling depends on the export of approximately 10% of the entire parasite proteome into the host cell. There are about 460 PEXEL-carrying proteins (3, 4) and an unknown number of PEXEL-negative exported proteins (PNEPs) (5, 6) destined for export into the host cell. Both classes of proteins are translocated into the parasitophorous vacuolar space and finally exported in the host cytosol through the Plasmodium translocon of exported proteins (PTEX) (7-9). A large number of the Plasmodium helical interspersed subtelomeric (PHIST) protein family members are amongst these exported proteins, which possess a ~150 amino acid domain which forms four consecutive alpha helices referred to as PHIST domain. Based on the presence and position of conserved tryptophan residues, the PHIST family is divided into several subgroups (10, 11).

Several PHISTb proteins previously have been shown to localize to the iRBC membrane or cytoskeleton (12). It was therefore suggested that PHIST proteins act as cross-linkers at the cytoskeleton, which was based on the capacity of the PHIST domain to target these proteins to the cytoskeleton and mediate binding to it (12). The PHISTb protein PF3D7_0532400 (Lysine-rich membrane-associated protein, LyMP) was specifically shown to bind to the intracellular ATS domain of PfEMP1 and seems to act as cross-linker to the remodeled iRBC cytoskeleton. Depletion of PF3D7_0532400 significantly affected anchoring of PfEMP1 and thus the strength of cytoadhesion (13-15).

Nine PHISTb proteins contain a cytoskeleton-binding motif first identified in MESA (16) and 7 PHISTb proteins possess a DnaJ domain which could assist in protein interactions at the cytoskeleton (11). One of these PHISTb-DnaJ proteins is RESA which has been shown to bind to spectrin and provides resistance to thermal stress during febrile episodes (17-19), emphasizing the importance of PHIST proteins for the parasite's survival. The PHISTc protein PfPTP2 (PF3D7_0731100) has been shown to be involved in trafficking of PfEMP1 to its final destination

within the host cell (20) whilst another PHISTc protein, PF3D7_0936800 (PFI1780w), was shown to interact at the host cytoskeleton similar to PHISTb proteins (13).

The cytoskeleton of the iRBC is a major target in the remodeling process and acts as interface between exported parasite and erythrocyte proteins. We therefore set out to investigate the role of PHIST proteins in this host cell remodeling process. Through pull-down experiments we identified potential interactions partners of selected PHITS proteins. As we expected a number of cytoskeletal proteins to be involved in these interactions that would be difficult to solubilize for immunoprecipitations, we used the proximity-dependent biotin identification (BioID) approach (21, 22). With the identification of potential interaction partners we were able to establish a network of protein interactions at the remodeled iRBC cytoskeleton which to our knowledge is the first network of exported parasite proteins at the erythrocyte cytoskeleton interface reported.

Methods

Parasite culture

In vitro culturing and transfection of *P. falciparum* 3D7 parasites was performed as described (23). Parasites were synchronized either with sorbitol treatment (24) or by a Percoll density gradient (23). Gelatin flotation was frequently used to select for presence of knobs on the parasite surface (25). Transgenic cell lines were cultured in 10 nM WR99210 (Jacobs Pharmaceuticals, Cologne, Germany) or 5 mg/ml Blasticidin S (Sigma).

Cloning

P. falciparum 3D7 cDNA was prepared using the ImProm-II Reverse transcriptase System (Promega, Switzerland). For the PHIST-GFP parasites, the coding region of the selected PHIST genes was amplified from cDNA and cloned into the pARL vector (26) using AflII and ClaI. To express PHIST-BirA*-3xHA-2A-BSD under the endogenous promoter, the SLI approach was used (27). For each PHIST, the last 300-600 bp of the coding region were selected as homology region (referred to as 3'HR) and cloned into the pSLI vector (27) which already contained the BirA* and HA tags. For the 0830600-3xHA cell line, the coding sequence was cloned via BamHI and NheI into the pBcamR plasmid containing the 3xHA tag. Primers are listed in Table S1.

Cell lysates, solubility assay, and Western blot

To obtain lysates, 10 ml cell culture of about 5% parasitemia were pelleted, lysed in 4 ml 0.03% Saponin/PBS for 10 min on ice, washed in PBS, and then resuspended in 100-200 µl Laemmli buffer. Sample preparation for the solubility assay was done as described (28). Parasite lysates were boiled at 95°C for 5 min, and 10-15 µl were loaded onto a 4-12% NOVEX NuPAGE Bis-Tris gel and run in MOPS or MES buffer and then blotted with the iBlot 2 (all from Life Technologies). Membranes were blocked in 5% milk/TNT (100 mM Tris, 150 mM NaCl, 43 mM HCl, and 0.1% Tween 20). All antibodies were diluted in 5% milk/TNT: rat anti-HA (1:500; Roche), mouse anti-GFP (1:250; Roche), mouse anti-GAPDH (1:10'000), and mouse anti-MAHRP1 (1:500). Goat anti-mouse-HRP (1:10'000; Pierce), goat anti-rabbit-HRP (1:5000; Jackson Immunology), and goat anti-rat-HRP (1:10'000; Southern Biotech) were used as secondary antibodies.

Immunofluorescence assays (IFA)

Thin smears were prepared, fixed in methanol/acetone (60:40) for 2 min at -20°C and then blocked with 3% BSA/PBS followed by antibody staining. To retain the three dimensional structure, cell were cross-linked with 4% paraformaldehyde/0.01% glutaraldehyde as described by Tonkin et al. (29) and then probed with antibodies. Primary antibodies used for IFA were rat anti-HA (1:100; Roche), rabbit anti-GFP (1:200; Abcam), mouse anti-GFP (1:250; Roche), mouse anti-MAHRP1 (1:500), rabbit a-MAHRP2 (1:500), rabbit anti-MESA (1:200), and mouse anti-KAHRP (1:100). Goat anti-mouse, anti-rabbit, or anti-rat conjugated with one of the Alexa Flourophores 405, 488, or 594 (all 1:200; Invitrogen) were used as secondary antibodies. Nuclei were stained with DAPI (Vector Laboratories, Inc.) and membranes with Cellmask deep red plasma membrane stain (Invitrogen). Images were acquired with a Leica DM 5000 B in combination with the LAS 4.9.0 software or with a Zeiss LSM700 upright confocal microscope, using the ZEN 2010 software and processed with Omero 5.3.3, Imaris 8.4, and ImageJ 1.48v. Deconvolution of confocal images was done with Huygens Remote Manager 3.4 and colocalization analysis was then performed using the JACoP plugin for ImageJ (30).

Electron microscopy

For immunoelectron microscopy (iEM), mature iRBCs were knob-selected and subsequently purified by Percoll density gradient,fixed in 2% PFA/0.2% glutaraldehyde in phosphate buffer pH7.4, and then embedded according to Tokuyasu et al. (31). Ultrathin sections (70 nm) were prepared on a FC7/UC7-ultramicrotome (Leica) at -120°C. The sections were immuno-labeled with rabbit anti-HA (dilution 1:30; Invitrogen) and rabbit anti-mouse (1:350; Rockland) antibodies and finally decorated with 5 or 10 nm protein A-gold (1:70; UMC, Utrecht, The Netherlands). Sections were stained with 4% uranyl acetate/methylcellulose (1:9) and examined with a Tecnai G2 Spirit or CM100 Philips transmission electron microscope at 80 kV (31).

BioID and co-Immunoprecipitation (Co-IP)

For BioID assays, biotin was added to 150 ml ring stage parasite culture (~7-8% parasitemia) to a final concentration of 50 µM to for 24 hours. An equal cell culture volume was left untreated to be used as negative control. Trophozoite-iRBCs were harvested by Percoll flotation, pelleted, and washed once in PBS. Cells were pelleted, lysed in 2 ml lysis buffer (50 mM Tris-HCl (pH 7.4), 500 mM NaCl, 0.2% SDS, 2% Triton X-100, 1x Protease Inhibitor Cocktail (PIC), 1 mM DTT), and sonicated in 30 s intervals for 15 min at setting 'high' (Bioruptor, Diagenode). After centrifugation (20'000 g, 4°C) 500 µl supernatant was added to 50 µl Pierce streptavidin magnetic beads (Thermo Fisher), which were washed three times in lysis buffer. Four identical technical replicates were set up for both the BioID and the negative control IP. Samples were incubated over night at 4°C on a rotator, the beads were collected using a magnetic stand and the supernatant was removed. Beads were washed three times with 500 µl lysis buffer and then two times with 500 µl wash buffer (50 mM Tris (pH 7.4), 150 mM NaCl) and then resuspended in 30 µl 1x LDS sample buffer (Pierce), boiled for 5 min, and processed for LC-MS/MS analysis.

For Co-IP assays, Percoll isolated trophozoite stage iRBCs from 300 ml cell culture at 5% hematocrit and ~7-8% parasitemia were used. Cells were resuspended in 20 ml 1% paraformaldehyde/PBS. After 30 min at 37°C, the reaction was stopped by adding 4.1 ml 2.5 M glycine. Cells were pelleted, lysed in 150 µl 0.03% Saponin in PBS for 10 min at 4°C, washed, resuspended in 5.2 ml sonication buffer (50 mM Tris-HCl (pH 8.0), 10 mM EDTA, 1% SDS, 1x PIC), and sonicated in 30 s intervals for 15 min at setting 'high' (Bioruptor, Diagenode). After centrifugation (20'000 g, 4°C) 650 µl supernatant was added to 50 µl Pierce anti-HA magnetic beads (Thermo Fisher), which were washed three times in 1x binding buffer. Four identical

technical replicates were set up for both the PHIST co-IP and the negative control co-IP. For the PHIST co-IP, 650 µl 2x binding buffer (50 mM Tris (pH 7.4), 300 mM NaCl, 2% Nonidet P40, 1x PIC) were added to the supernatant/bead suspension. The negative control co-IP was supplemented with 450 µl 2x binding buffer and 200 µl HA peptide in 1x binding buffer at 0.5 mg/ml. Samples were incubated over night at 4°C on a rotator, the beads were collected using a magnetic stand and the supernatant was removed. Beads were washed three times with 500 µl wash buffer (50 mM Tris (pH 7.4), 150 mM NaCl, 1 mM EDTA, 1% Nonidet P40, 1x PIC). Proteins were eluted in a molar excess of HA-peptide (30 µl of 0.5 mg/ml HA-peptide in 1x binding buffer) while rotating for two hours. The eluate was transferred to a new tube containing 6 µl 4x LDS sample buffer (Pierce). Samples were boiled for 5 min and processed for LC-MS/MS analysis.

Mass-spectrometry

Samples were loaded onto a 4%-12% gradient Bis-Tris gel (Thermo) and run in 1x MOPS buffer at 180 V for 10 min. Each lane was sliced, minced and transferred to a reaction tube. In-gel digest with trypsin was performed as previously described (32), and samples were stored on StageTips (33) until measurement. Digested peptides to be measured were separated on a 25 cm reverse-phase capillary (75 µM inner diameter, New Objective) packed with Reprosil C18 material (Dr. Maisch GmbH) and peptides were eluted with a 2 h gradient from 2%-40% acetonitrile buffer followed by a 95% acetonitrile wash-out at 200 nl/min on the Easy LC1000 HPLC system (Thermo). Mass spectrometry measurements were performed with a Q Exactive Plus mass spectrometer (Thermo) operated with a Top10 data-dependent MS/MS acquisition method per full scan. Spray voltage was set to 2.2-2.4 kV.

Raw MS data was analyzed using MaxQuant v1.5.2.8 (34) with standard settings and activated match between runs and LFQ quantitation features. The search was performed against the human Uniprot database (81,194 entries) and the *Plasmodium falciparum* database (PlasmoDB 9.3, 5,538 entries). The proteinGroups file was filtered for known contaminants and proteins identified from the reversed database were removed prior to statistical analysis. Non-measured data points were imputed by a beta distribution at the limit of quantitation. Data was plotted as a volcano plot using the R environment with in-house scripts: log2 fold enrichment was calculated as median from the four replicates and the p-value was determined by a two-sided unpaired t-test Welch. The threshold line for enriched proteins is defined with p = 0.05, enrichment = 2 and s0 = 1.

Generation of protein interaction network

First, the exportome of *Plasmodium falciparum* was defined by creating a table containing all known PEXEL proteins (35, 36) and published PNEPs (5, 28, 37-42). PlasmoDB Release 40 was searched for "PfEMP1", "PNEP", and "exported". In total, we assigned 739 proteins as part of the *P. falciparum* exportome (Table S2).

To focus on protein interactions occurring within the iRBC involving exported parasite and human RBC proteins, the complete list of all proteins found to be positively enriched in MS experiments (Table S3) was filtered using the previously defined exportome to remove all non-exported *P. falciparum* proteins, leaving only human and exported parasite proteins in the final selection for the network. Proteins from each IP were sorted by the –log10 (p-value) and from each IP the top 15 entries were included in the network which was generated using Cytoscape 3.6.

Results

Subcellular localization of PHIST proteins

To confirm export and determine localization of the nine selected PHIST proteins, cell lines were generated episomally expressing the respective PHIST-GFP fusion protein (Figure 1A). All PHIST proteins were exported to the iRBC periphery as shown by Immunofluorescence assays (Figure 1B). A dotted pattern alongside the iRBC membrane was observed for most of these PHISTs and KAHRP was used for co-labeling to test whether the dotted pattern was similar to that of knobs. In some transgenic parasites, the signal was partially overlapping but none co-localized completely (Figure S1).

Solubility of each PHIST-GFP fusion protein was tested by sequential protein extractions to obtain fractions of soluble, membrane-associated, transmembrane, and insoluble proteins. Six out of the selected PHIST proteins were membrane-associated and soluble in carbonate buffer (0401800-GFP, 0402000-GFP, 0424600-GFP, 0937000-GFP, 1038800-GFP, and 1476200-GFP). The PHIST protein 0201600-GFP was found insoluble whilst 0402100-GFP and 0830600-GFP were never detected in any of the fractions (Figure 1C). This could be expected for 0830600 as the episomally expressed 0830600-3xHA protein was previously found to be soluble and washed out of the iRBC during saponin lysis (Figure 1D). We therefore concluded that all 9 PHIST proteins are exported into the host cell, and localize to the proximity of the erythrocyte cytoskeleton, but are most likely not part of the knob structures.

Time course expression pattern

After we had confirmed that all 9 PHISTs were exported, we wanted to identify interaction partners by performing immunoprecipitations. For this we generated new cell lines with the endogenous PHISTs tagged with a biotin-ligase and a 3xHA tag (BirA*-3xHA) under the endogenous promoter followed by the viral 2A split peptide, giving rise to a co-translational cleaved off Blasticidin S deaminase (BSD) and conferring resistance to Blasticidin S (27) (Figure S2A-C). The promiscuous BirA* was fused to the 3' of the PHIST genes and allowed proximity-dependent biotin identification (BioID) followed by immunoprecipitation and mass-spectrometry to identify potential interaction partners (21). We successfully established 5 transgenic cell lines (0201600-BirA*-HA, 0402000-BirA*-HA, 0830600-BirA*-HA, 1038800-BirA*-HA, and 1476200-BirA*-HA) but were unable to obtain the other 4 cell lines (0401800-BirA*HA, 0402100-BirA*-HA, 0424600-BirA*-HA, and 0937000-BirA*-HA) after at least three independent transfections. They were then removed from the study as well as 1038800-BirA*-HA which grew in culture but plasmid integration into the endogenous locus could not be proven. For the remaining four parasite lines, correct integration of the plasmid into the endogenous gene locus was confirmed by PCR (Figure S2).

To determine the expression time and localization pattern of each of the four remaining PHIST-BirA*-HA proteins, we prepared IFA slides and lysates for Western blot every eight hours over the course of the 48 hour intra-erythrocytic development cycle. Smears were fixed and probed with anti-HA antibodies. Fluorescence images were acquired from all eight time points of each parasite line and processed with identical microscope settings to compare signal intensities. All PHIST-BirA*-HA proteins were found to be expressed and exported latest 17-24 hpi. The localization for 0402000-BirA*-HA and 1476200-BirA*-HA was similar to the episomally expressed GFP-tagged proteins whilst 0201600-BirA*-HA and 0830600-BirA*-HA showed a dotted pattern throughout the iRBC (Figure 2) unlike in the respective IFAs. Parasite lysates of the same time points were used for Western blots and labeled with anti-HA antibody. Throughout the life cycle, increasing protein abundance was observed for each cell line. In most cases, a double band was observed corresponding to the predicted sizes of the PHIST-BirA*-HA and the uncleaved PHIST-BirA*-HA-2A-BSD, indicating that a proportion of the fusion proteins were not successfully cleaved at the 2A split peptide (Figure S3).

To study the peripheral localization of the PHIST-BirA*-HA proteins in more detail ultra-thin sections from the two parasite lines 0201600-BirA*-HA and 0402000-BirA*-HA were immuno-gold

labeled and visualized by electron microscopy. In both cases the gold labeling of was found underneath the iRBC membrane (Figure 3). The immuno-labelling for 0201600-BirA*-HA resembled the IFA pattern observed with the episomally expressed GFP tagged protein but was discrepant to the IFA observed with the endogenous 0201600-BirA*-HA PHIST which was rather dotted and spread throughout the iRBC (Figure 2).

Identification of interaction partners

We performed BioID and Co-IP experiments with trophozoite stage infected iRBCs when the respective PHIST proteins have reached their destination and most likely interact with their potential binding partners. As control for a protein with known interaction partners we included a cell line expressing MESA-BirA*-HA (PF3D7_0500800). MESA is an exported *P. falciparum* protein binding to the erythrocyte cytoskeleton but does not belong to the PHIST family (11, 43). With all established parasite lines we performed BioID or co-IP followed by mass spectrometry for protein enrichment to identify potential interaction partners. The respective bait protein together with a larger number of additional proteins was enriched in all positive immunoprecipitations when compared to negative control fractions (Figure 4A, Table S3).

Based on these data we generated a network of protein interactions occurring at the remodeled iRBC cytoskeleton. We included all proteins that were found in the previously defined *P. falciparum* exportome (Table S2) and all proteins derived from the human host. Thereby, all non-exported *P. falciparum* proteins were excluded as they do not contribute to protein interactions at the remodeled iRBC cytoskeleton (Table S3). From each co-IP the fifteen candidates with the highest p-value were included in the network (Figure 4B), resulting in a network comprising 55 nodes and 58 edges with an arbitrary edge length.

With this network we show that the three PHIST proteins (0201600, 0830600, and 1476200) are not directly connected but share common potential interaction partners that mediate a connection. In contrast, 0830600 and MESA were the only two bait proteins that shared a significant direct, uni-directional connection in the present network. There was also evidence that the two bait proteins 1476200 and MESA directly interacte as they pulled down each other but this is not represented in the network because this interaction fell below the significance threshold.,Six subunits of the TCP-1 complex were found amongst the top fifteen candidates of 0830600 and MESA. Two of these subunits (TCP-1 eta and TCP-1 theta) were shared between the

two parasite proteins. 1476200 was the only bait to pull down TCP-1 theta (not part of the top fifteen candidates) while subunit alpha was never identified.

The PHIST protein 0201600-BirA*-HA was co-labeled with MAHRP1 and MAHRP2 in immunofluorescence. Although MAHRP2 was found amongst the top fifteen potential interaction partners of 0201600 it could not be shown to colocalize (Figure 4C). In contrast, a high degree of colocalization was found between 0201600-BirA*-HA and MAHRP1 (Figure 4C) which was also detected in the co-IP but reached a lower significance level and was excluded from the network. The interaction with MAHRP1 and MAHRP2 of 0201600 suggests that it might be a Maurer's cleft protein.

Discussion

PHIST proteins comprise almost 20% of the known exportome of *Plasmodium falciparum*. It has been suggested that PHIST proteins are involved in host cell remodeling by targeting the erythrocyte cytoskeleton that already has been confirmed in some cases (13-15). Here we selected 9 PHIST proteins and showed that they were exported into the host cell in blood stage parasites. In most cases they localized to the vicinity of the iRBC membrane or cytoskeleton. We also identified potential interaction partners for three of the PHIST proteins as well as for MESA, another exported *P. falciparum* protein to generate an interaction network of human and exported parasite proteins at the iRBC cytoskeleton.

We were primarily interested in interactions occurring at the iRBC cytoskeleton and probably involved in its modification. Because the BioID system requires incubation times of 20h with biotin (44) proteins from young ring stage to mid-trophozoites were biotinylated. Hence we expected that proteins along the export pathway probably would be also biotinylated in a 10 nm radius of the BirA* ligase, resulting in positive enrichment of non-exported proteins. This pitfall of the BioID method could have been overcome with the availability of a much faster BirA* variant that has been recently published (45, 46). To remove those non-exported parasite proteins from the network, we defined the Plasmodium falciparum exportome and used this to filter the prey proteins identified by mass spectrometry.

Since cytoskeleton remodeling upon infection is a dynamic process, a more rapid biotinylation would allow the creation of a proteomic time series to investigate the temporal modification of this process. In addition, smaller versions of BirA* seem to improve localization of

fusion proteins (46). Wrongly targeted BirA* fusion proteins could explain the differences seen between GFP-tagged and BirA*-tagged 0201600 and 0402000 fusion proteins, and it also could explain the export deficiency in 1252700.

Amongst the prey proteins detected in the different co-IP were subunits of the group II chaperonin T-complex polypeptide-1 (TCP-1 complex). TCP-1 was reported to interact with the erythrocyte cytoskeleton during elevated temperature (47). The strong presence of almost all TCP-1 subunits amongst the potential binding partners suggests that these exported parasite proteins seem to interact with the human TCP-1 complex. However, the role of this chaperonin complex during the remodeling process of the erythrocyte cytoskeleton remains elusive but it is strong evidence for its interaction with parasite proteins. The *P. falciparum* TCP-1 complex called PfTRiC was previously reported to traffic exported proteins to their final destination in the iRBC (48) but a later report argued that PfTRiC is not exported and thus could not shuttle proteins inside the iRBC cytosol (49).

One third of the parasite proteins shown in the network belong to the PHIST protein family. Their strong presence at the remodeled iRBC cytoskeleton supports the hypothesis that PHIST proteins play a central role in erythrocyte cytoskeleton remodeling during a *P. falciparum* infection. The elucidation of their detailed function and interaction can pave the path of understanding the role of the massively expanded gene family in *P. falciparum*.

Despite the limitations of our approach the dataset clearly shows that a large number of exported proteins target the iRBC cytoskeleton. To the best of our knowledge this is the first protein interaction network on the iRBC cytoskeleton and provides the basis for further research. Reverse co-IPs as well as additional colocalization and interaction studies are required to confirm these protein interactions. Identification of parasite proteins that target the erythrocyte cytoskeleton and determination of essential interactions provide a deeper insight and understanding of the host cell remodeling process and could lead to new targets to interfere with intracellular parasite growth and survival.

Funding Information

This project was supported by the Swiss National Science Foundation Grant Number SNSF 31003A_169347. The funders had no role in determining the content of the paper or in the decision to submit this work for publication.

Author contributions

JW and HPB designed the project and wrote the manuscript. Experiments were designed and carried out by JW and FBr. LP and FBu performed mass spectrometry.

Conflict of Interest

The authors declare no conflict of interest.

Acknowledgement

We acknowledge Alexia Loynton-Ferrand, Kai Schleicher, and Henning Stahlberg at the Imaging Core Facility (IMCF) and C-CINA, Biozentrum, University of Basel, for access to confocal and electron microscopes as well as their support with image acquisition and analysis. We also thank Mario Dejung from the Proteomics Core Facility at the IMB, Mainz, for providing the R Script for analysis of MS data and his assistance in the analysis process. Furthermore, we thank the following colleagues for sharing antibodies: Claudia Daubenberger (anti-GAPDH), Diane Taylor (anti-KAHRP), and Tobias Spielmann for providing the pSLI plasmid. We thank Armin Passecker for critical reading and commenting of the manuscript.

Bibliografie

1. **Watermeyer JM, Hale VL, Hackett F, Clare DK, Cutts EE, Vakonakis I, Fleck RA, Blackman MJ, Saibil HR.** 2016. A spiral scaffold underlies cytoadherent knobs in Plasmodium falciparum-infected erythrocytes. Blood **127:**343-351.
2. **Hviid L, Jensen ATR.** 2015. Chapter Two-PfEMP1–A Parasite Protein Family of Key Importance in Plasmodium falciparum Malaria Immunity and Pathogenesis. Advances in Parasitology **88:**51-84.
3. **Hiller NL, Bhattacharjee S, van Ooij C, Liolios K, Harrison T, Lopez-Estrano C, Haldar K.** 2004. A host-targeting signal in virulence proteins reveals a secretome in malarial infection. Science **306:**1934-1937.
4. **Marti M, Good RT, Rug M, Knuepfer E, Cowman AF.** 2004. Targeting malaria virulence and remodeling proteins to the host erythrocyte. Science **306:**1930-1933.
5. **Heiber A, Kruse F, Pick C, Gruring C, Flemming S, Oberli A, Schoeler H, Retzlaff S, Mesen-Ramirez P, Hiss JA, Kadekoppala M, Hecht L, Holder AA, Gilberger TW, Spielmann T.** 2013. Identification of new PNEPs indicates a substantial non-PEXEL exportome and underpins common features in Plasmodium falciparum protein export. PLoS Pathog **9:**e1003546.
6. **Spielmann T, Gilberger TW.** 2010. Protein export in malaria parasites: do multiple export motifs add up to multiple export pathways? Trends Parasitol **26:**6-10.
7. **de Koning-Ward TF, Gilson PR, Boddey JA, Rug M, Smith BJ, Papenfuss AT, Sanders PR, Lundie RJ, Maier AG, Cowman AF, Crabb BS.** 2009. A newly discovered protein export machine in malaria parasites. Nature **459:**945-949.
8. **de Koning-Ward TF, Dixon MW, Tilley L, Gilson PR.** 2016. Plasmodium species: master renovators of their host cells. Nat Rev Microbiol **14:**494-507.
9. **Przyborski JM, Nyboer B, Lanzer M.** 2016. Ticket to ride: export of proteins to the Plasmodium falciparum-infected erythrocyte. Mol Microbiol **101:**1-11.
10. **Sargeant TJ, Marti M, Caler E, Carlton JM, Simpson K, Speed TP, Cowman AF.** 2006. Lineage-specific expansion of proteins exported to erythrocytes in malaria parasites. Genome Biol **7:**R12.
11. **Warncke JD, Vakonakis I, Beck HP.** 2016. Plasmodium Helical Interspersed Subtelomeric (PHIST) Proteins, at the Center of Host Cell Remodeling. Microbiol Mol Biol Rev **80:**905-927.
12. **Tarr SJ, Moon RW, Hardege I, Osborne AR.** 2014. A conserved domain targets exported PHISTb family proteins to the periphery of Plasmodium infected erythrocytes. Mol Biochem Parasitol **196:**29-40.
13. **Oberli A, Slater LM, Cutts E, Brand F, Mundwiler-Pachlatko E, Rusch S, Masik MF, Erat MC, Beck HP, Vakonakis I.** 2014. A Plasmodium falciparum PHIST protein binds the virulence factor PfEMP1 and comigrates to knobs on the host cell surface. FASEB J **28:**4420-4433.

14. **Oberli A, Zurbrugg L, Rusch S, Brand F, Butler ME, Day JL, Cutts EE, Lavstsen T, Vakonakis I, Beck HP.** 2016. Plasmodium falciparum PHIST Proteins Contribute to Cytoadherence and Anchor PfEMP1 to the Host Cell Cytoskeleton. Cell Microbiol doi: 10.1111/cmi.12583.

15. **Proellocks NI, Herrmann S, Buckingham DW, Hanssen E, Hodges EK, Elsworth B, Morahan BJ, Coppel RL, Cooke BM.** 2014. A lysine-rich membrane-associated PHISTb protein involved in alteration of the cytoadhesive properties of Plasmodium falciparum-infected red blood cells. FASEB J **28:**3103-3113.

16. **Kilili GK, LaCount DJ.** 2011. An erythrocyte cytoskeleton-binding motif in exported Plasmodium falciparum proteins. Eukaryot Cell **10:**1439-1447.

17. **Da Silva E, Foley M, Dluzewski AR, Murray LJ, Anders RF, Tilley L.** 1994. The Plasmodium falciparum protein RESA interacts with the erythrocyte cytoskeleton and modifies erythrocyte thermal stability. Mol Biochem Parasitol **66:**59-69.

18. **Pei X, Guo X, Coppel R, Bhattacharjee S, Haldar K, Gratzer W, Mohandas N, An X.** 2007. The ring-infected erythrocyte surface antigen (RESA) of Plasmodium falciparum stabilizes spectrin tetramers and suppresses further invasion. Blood **110:**1036-1042.

19. **Silva MD, Cooke BM, Guillotte M, Buckingham DW, Sauzet JP, Le Scanf C, Contamin H, David P, Mercereau-Puijalon O, Bonnefoy S.** 2005. A role for the Plasmodium falciparum RESA protein in resistance against heat shock demonstrated using gene disruption. Mol Microbiol **56:**990-1003.

20. **Regev-Rudzki N, Wilson DW, Carvalho TG, Sisquella X, Coleman BM, Rug M, Bursac D, Angrisano F, Gee M, Hill AF, Baum J, Cowman AF.** 2013. Cell-cell communication between malaria-infected red blood cells via exosome-like vesicles. Cell **153:**1120-1133.

21. **Roux KJ, Kim DI, Raida M, Burke B.** 2012. A promiscuous biotin ligase fusion protein identifies proximal and interacting proteins in mammalian cells. J Cell Biol **196:**801-810.

22. **Roux KJ.** 2013. Marked by association: techniques for proximity-dependent labeling of proteins in eukaryotic cells. Cell Mol Life Sci **70:**3657-3664.

23. **Moll K, Kaneko A, Scherf A, Wahlgren M.** 2013. Methods in Malaria Reserch, 6th Edition ed. American Type Culture Collection, 10801 University Boulevard, Manassas, VA 20110-2209.

24. **Lambros C, Vanderberg JP.** 1979. Synchronization of Plasmodium falciparum erythrocytic stages in culture. J Parasitol **65:**418-420.

25. **Ménard R.** 2013. Malaria - Methods and Protocols, 2 ed doi:10.1007/978-1-62703-026-7. Humana Press.

26. **Crabb BS, Rug M, Gilberger T-W, Thompson JK, Triglia T, Maier AG, Cowman AF.** 2004. Transfection of the human malaria parasite Plasmodium falciparum, p 263-276, Parasite Genomics Protocols. Springer.

27. **Birnbaum J, Flemming S, Reichard N, Soares AB, Mesen-Ramirez P, Jonscher E, Bergmann B, Spielmann T.** 2017. A genetic system to study Plasmodium falciparum protein function. Nat Methods **14:**450-456.

28. **Pachlatko E, Rusch S, Muller A, Hemphill A, Tilley L, Hanssen E, Beck HP.** 2010. MAHRP2, an exported protein of Plasmodium falciparum, is an essential component of Maurer's cleft tethers. Mol Microbiol **77:**1136-1152.

29. **Tonkin CJ, van Dooren GG, Spurck TP, Struck NS, Good RT, Handman E, Cowman AF, McFadden GI.** 2004. Localization of organellar proteins in Plasmodium falciparum using a novel set of transfection vectors and a new immunofluorescence fixation method. Mol Biochem Parasitol **137:**13-21.

30. **Bolte S, Cordelieres FP.** 2006. A guided tour into subcellular colocalization analysis in light microscopy. J Microsc **224:**213-232.

31. **Tokuyasu KT.** 1973. A technique for ultracryotomy of cell suspensions and tissues. J Cell Biol **57:**551-565.

32. **Bluhm A, Casas-Vila N, Scheibe M, Butter F.** 2016. Reader interactome of epigenetic histone marks in birds. Proteomics **16:**427-436.

33. **Rappsilber J, Mann M, Ishihama Y.** 2007. Protocol for micro-purification, enrichment, pre-fractionation and storage of peptides for proteomics using StageTips. Nat Protoc **2:**1896-1906.

34. **Cox J, Mann M.** 2008. MaxQuant enables high peptide identification rates, individualized p.p.b.-range mass accuracies and proteome-wide protein quantification. Nat Biotechnol **26:**1367-1372.

35. **Boddey JA, Carvalho TG, Hodder AN, Sargeant TJ, Sleebs BE, Marapana D, Lopaticki S, Nebl T, Cowman AF.** 2013. Role of plasmepsin V in export of diverse protein families from the Plasmodium falciparum exportome. Traffic **14:**532-550.

36. **Schulze J, Kwiatkowski M, Borner J, Schluter H, Bruchhaus I, Burmester T, Spielmann T, Pick C.** 2015. The Plasmodium falciparum exportome contains non-canonical PEXEL/HT proteins. Mol Microbiol **97:**301-314.

37. **Spycher C, Rug M, Pachlatko E, Hanssen E, Ferguson D, Cowman AF, Tilley L, Beck HP.** 2008. The Maurer's cleft protein MAHRP1 is essential for trafficking of PfEMP1 to the surface of Plasmodium falciparum–infected erythrocytes. Mol Microbiol **68:**1300-1314.

38. **Dietz O, Rusch S, Brand F, Mundwiler-Pachlatko E, Gaida A, Voss T, Beck HP.** 2014. Characterization of the small exported Plasmodium falciparum membrane protein SEMP1. PLoS One **9:**e103272.

39. **Spielmann T, Hawthorne PL, Dixon MW, Hannemann M, Klotz K, Kemp DJ, Klonis N, Tilley L, Trenholme KR, Gardiner DL.** 2006. A cluster of ring stage-specific genes linked to a locus implicated in cytoadherence in Plasmodium falciparum codes for PEXEL-negative and PEXEL-positive proteins exported into the host cell. Mol Biol Cell **17:**3613-3624.

40. **Hodder AN, Maier AG, Rug M, Brown M, Hommel M, Pantic I, Puig-de-Morales-Marinkovic M, Smith B, Triglia T, Beeson J, Cowman AF.** 2009. Analysis of structure and function of the giant protein Pf332 in Plasmodium falciparum. Mol Microbiol **71:**48-65.

41. **Saridaki T, Fröhlich KS, Braun–Breton C, Lanzer M.** 2009. Export of PfSBP1 to the Plasmodium falciparum Maurer's clefts. Traffic **10:**137-152.

42. **Blisnick T, Eugenia M, Betoulle M, Barale JC, Uzureau P, Berry L, Desroses S, Fujioka H, Mattei D, Breton CB.** 2000. Pfsbp 1, a Maurer's cleft Plasmodium falciparum protein, is associated with the erythrocyte skeleton. Molecular and Biochemical Parasitology **111:**107-121.

43. **Coppel R, Lustigman S, Murray L, Anders R.** 1988. MESA is a Plasmodium falciparum phosphoprotein associated with the erythrocyte membrane skeleton. Molecular and Biochemical Parasitology **31:**223-231.

44. **Khosh-Naucke M, Becker J, Mesen-Ramirez P, Kiani P, Birnbaum J, Frohlke U, Jonscher E, Schluter H, Spielmann T.** 2017. Identification of novel parasitophorous vacuole proteins in P. falciparum parasites using BioID. Int J Med Microbiol doi:10.1016/j.ijmm.2017.07.007.

45. **Ramanathan M, Majzoub K, Rao DS, Neela PH, Zarnegar BJ, Mondal S, Roth JG, Gai H, Kovalski JR, Siprashvili Z.** 2018. RNA–protein interaction detection in living cells. Nature methods **15:**207.

46. **Kim DI, Jensen SC, Noble KA, Kc B, Roux KH, Motamedchaboki K, Roux KJ.** 2016. An improved smaller biotin ligase for BioID proximity labeling. Mol Biol Cell **27:**1188-1196.

47. **Wagner CT, Lu IY, Hoffman MH, Sun WQ, Trent JD, Connor J.** 2004. T-complex polypeptide-1 interacts with the erythrocyte cytoskeleton in response to elevated temperatures. J Biol Chem **279:**16223-16228.

48. **Mbengue A, Vialla E, Berry L, Fall G, Audiger N, Demettre−Verceil E, Boteller D, Braun−Breton C.** 2015. cNew export pathway in Plasmodium falciparum−infected erythrocytes: role of the parasite group II chaperonin, PfTRiC. Traffic.

49. **Spillman NJ, Beck JR, Ganesan SM, Niles JC, Goldberg DE.** 2017. The chaperonin TRiC forms an oligomeric complex in the malaria parasite cytosol. Cell Microbiol **19**.

Figure legends

Figure 1 – Over-expression of PHIST-GFP fusion proteins from episomes

(A) Schematic representation of the plasmid used for transfection. (B) IFA of PHIST-GFP cell lines probed with anti-GFP. Nuclei were stained with DAPI. Differential interference contrast (DIC) and an overlay of all channels (columns 3 and 4) (scale bar = 5 μm). (C) Four fractions obtained from solubility assays (hypotonic lysis, Carbonate, Triton X-100, and SDS) were probed in Western blots with anti-GFP for the presence of the PHIST-GFP fusion proteins. Anti-GAPDH and anti-MAHRP1 were used as the controls for the soluble and transmembrane fractions, respectively. (D) Supernatant and pellet from saponin lysed PF3D7_0830600-3xHA iRBCs were probed in a Western blot with anti-HA and anti-GAPDH.

Figure 2 - Time Course IFA of PHIST-BirA-HA parasite lines*

PHIST-BirA*-HA-tagged proteins were labeled with anti-HA (first column). The second column shows nuclei stained with DAPI, followed by a merge of the fluorescent channels and an overlay of all channels. Each row corresponds to an 8 hour time interval (scale bar = 5 μm).

Figure 3 - Electron microscopy images of two PHIST-BirA-HA parasite lines*

Immuno-gold labeling of ultrathin sections of iRBCs were probed with anti-HA antibodies and imaged with an electron microscope. (A) 0201600-BirA*-HA and (B) 0402000-BirA*-HA (scale bars = 500 nm).

Figure 4 - BioID and mass spectrometry data

(A) Volcano plots indicating protein enrichment from BioID assays after immunoprecipitation and mass-spectrometry. The right side of each plot indicates proteins enriched in the experiment, the left side shows proteins enriched in the control. Red: bait proteins; blue: significantly enriched proteins ($p < 0.05$, enrichment > 2, s0 = 1); green: background. (B) Interaction network of host cytoskeleton and exported parasite proteins. Dark blue: parasite proteins; light blue inlay: PHIST proteins; red: erythrocyte proteins. Bait proteins are indicated by a larger circle. Edge length is random and not to scale. (C) IFA co-labeling of PF3D7_0201600-BirA*-HA with antibodies as

indicated. Pearson's correlation and the two Mander's coefficients for colocalization are provided in the table (scale bars = 5 µm).

Figure S1 - Co-labeling of GFP and KAHRP in IFA

The first column shows the DIC, followed by fluorescence images with anti-GFP and anti-KAHRP antibodies, a merge of the fluorescence images and an overlay of all channels (scale bar = 5 µm).

Figure S2 – PCR-confirmation of PHIST-BirA-HA integration into the wild-type locus*

Schematic representations indicating primer binding sites for (A) the PHIST locus in 3D7 wild-type parasites, (B) the plasmid used for transfection and integration, and (C) the modified PHIST locus with the integrated plasmid. (D) to (G) PCR was done on DNA extracted from the transgenic PHIST-BirA*-HA parasites (lanes 1-3), the 3D7 wild-type (Lanes 4-6), and the transfection plasmid (lane 7). The primers correspond to those indicated in (A and B). (H) Table showing the expected lengths of the PCR products.

Figure S3 - Time course Western blot

Over the course of one intra-erythrocytic cycle, cell lysates were prepared every eight hours and then probed in Western blots with anti-HA.

Table S1 – List of primers

Summary of all cloning and sequencing primers used to generate the cell lines included in this project. Restriction sites and additional descriptions for the primers are included.

Table S2 – Exportome Table

List of all exported *P. falciparum* proteins that were used for the filtering of protein for the network.

Table S3 – Complete Mass Spec Data Table

All proteins found to be enriched in the positive or negative co-IP fractions of all immunoprecipitation experiments are listed in this table along with descriptive information such as protein accession number, name, p-value, and fold change. This table is accessible under the following DOI: 10.5281/zenodo.2582949.

Figure 1

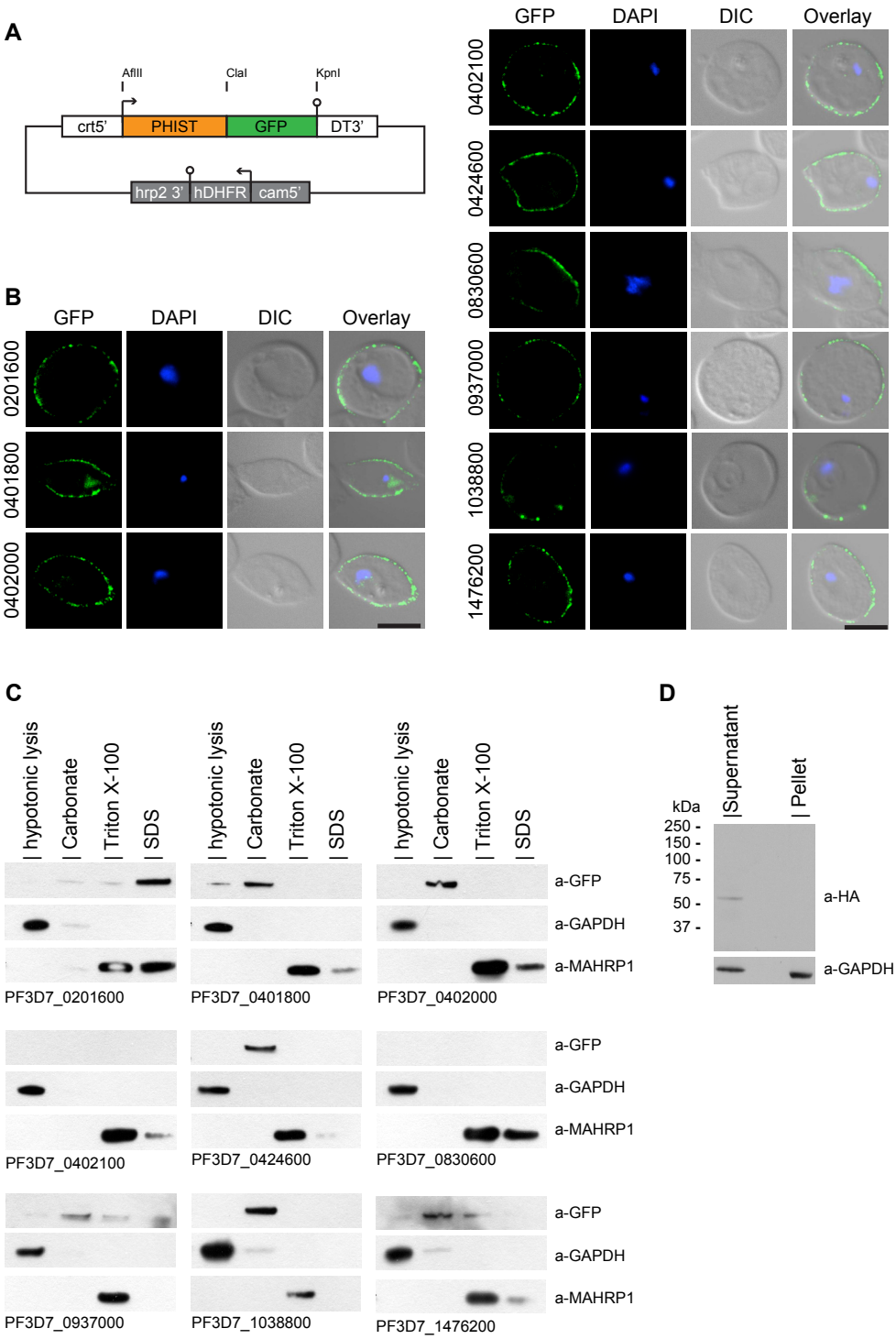
A
AflII
ClaI
KpnI
crt5'
PHIST
GFP
DT3'
hrp2 3'
hDHFR
cam5'
B
GFP
DAPI
DIC
Overlay
0201600
0401800
0402000
0402100
0424600
0830600
0937000
1038800
1476200
C
hypotonic lysis
Carbonate
Triton X-100
SDS
a-GFP
a-GAPDH
a-MAHRP1
PF3D7_0201600
PF3D7_0401800
PF3D7_0402000
PF3D7_0402100
PF3D7_0424600
PF3D7_0830600
PF3D7_0937000
PF3D7_1038800
PF3D7_1476200
D
kDa
250 -
150 -
100 -
75 -
50 -
37 -
Supernatant
Pellet
a-HA
a-GAPDH

Figure 2

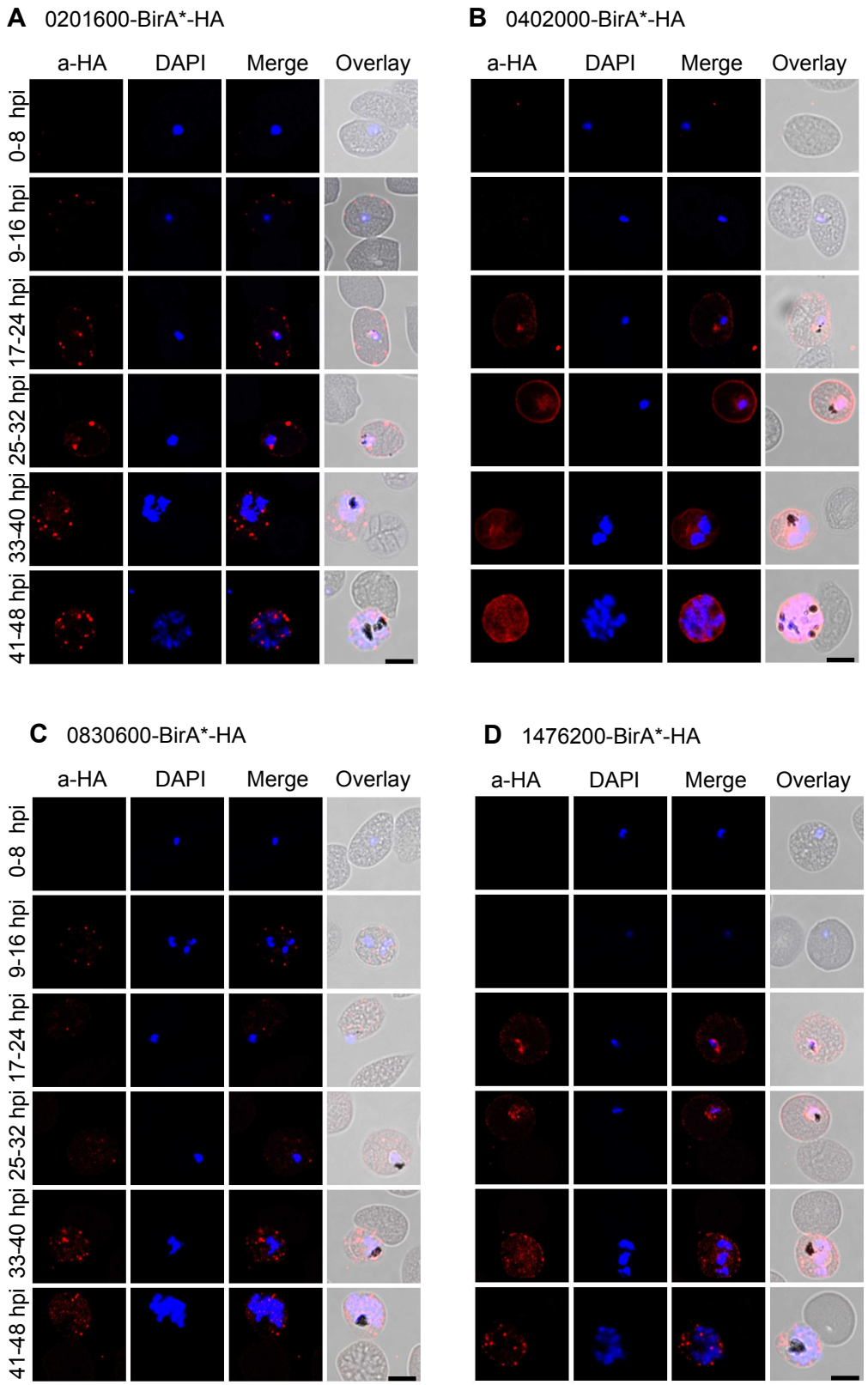
A 0201600-BirA*-HA
B 0402000-BirA*-HA
C 0830600-BirA*-HA
D 1476200-BirA*-HA
a-HA
DAPI
Merge
Overlay
0-8 hpi
9-16 hpi
17-24 hpi
25-32 hpi
33-40 hpi
41-48 hpi

Figure 3

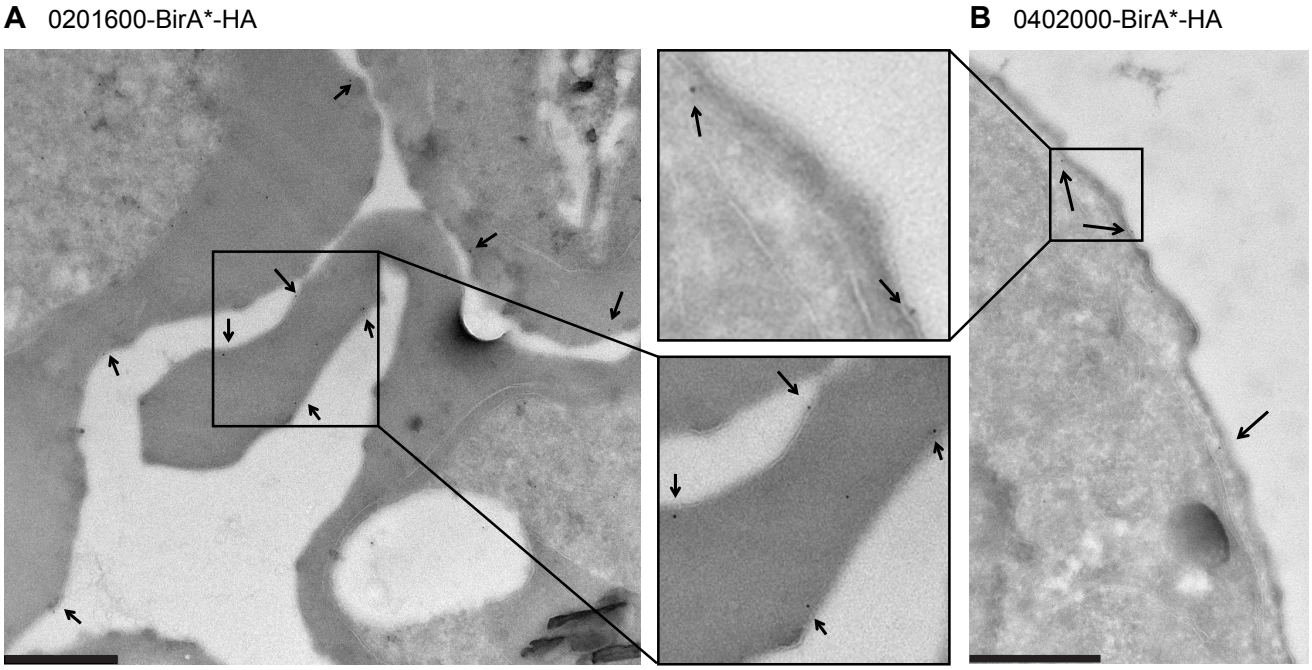

Figure 4

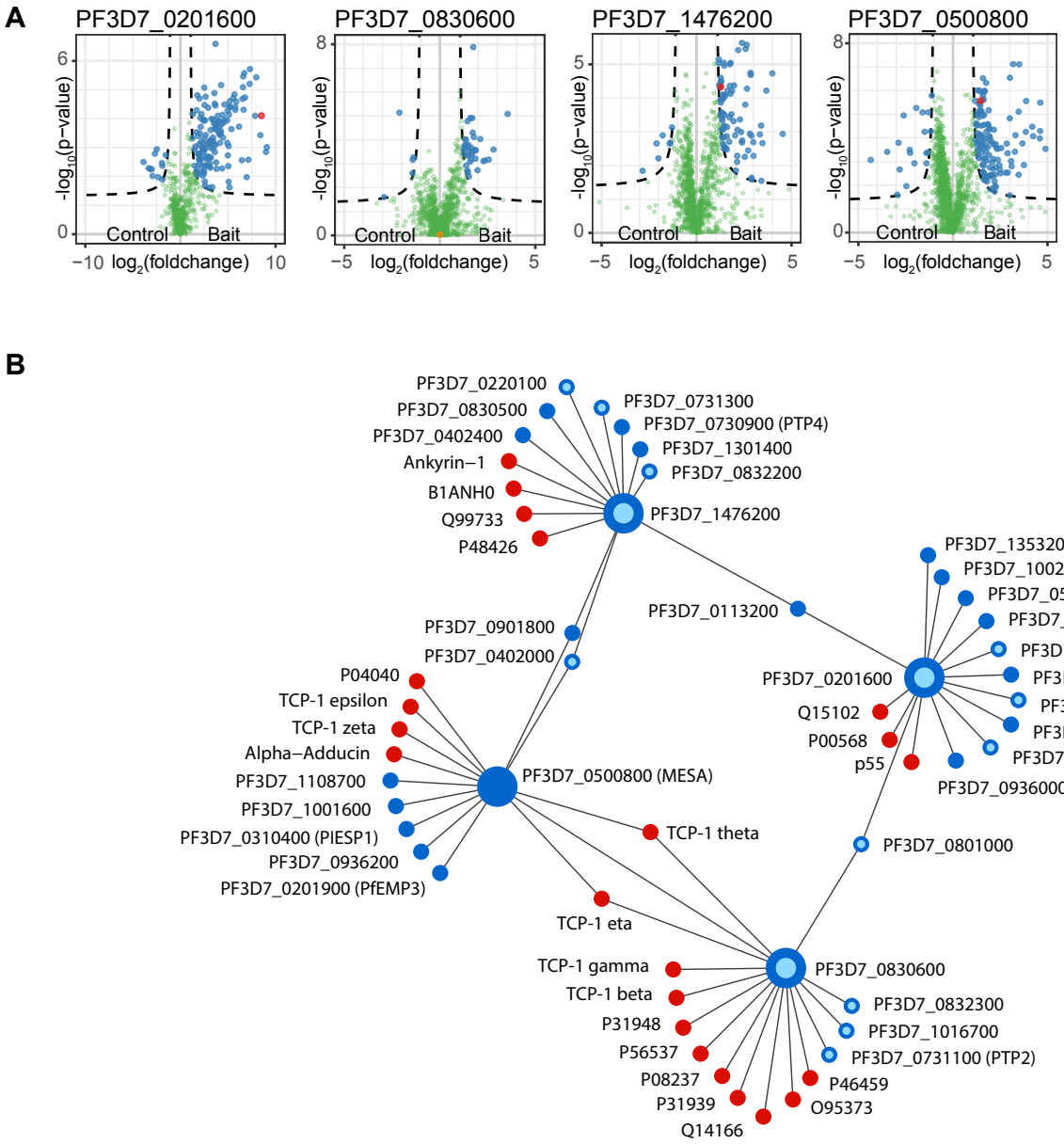

Coefficients	MAHRP1	MAHRP2
Pearson's	0.87	0.14
Mander's 1	0.97	0.19
Mander's 2	0.87	0.99

Figure S1

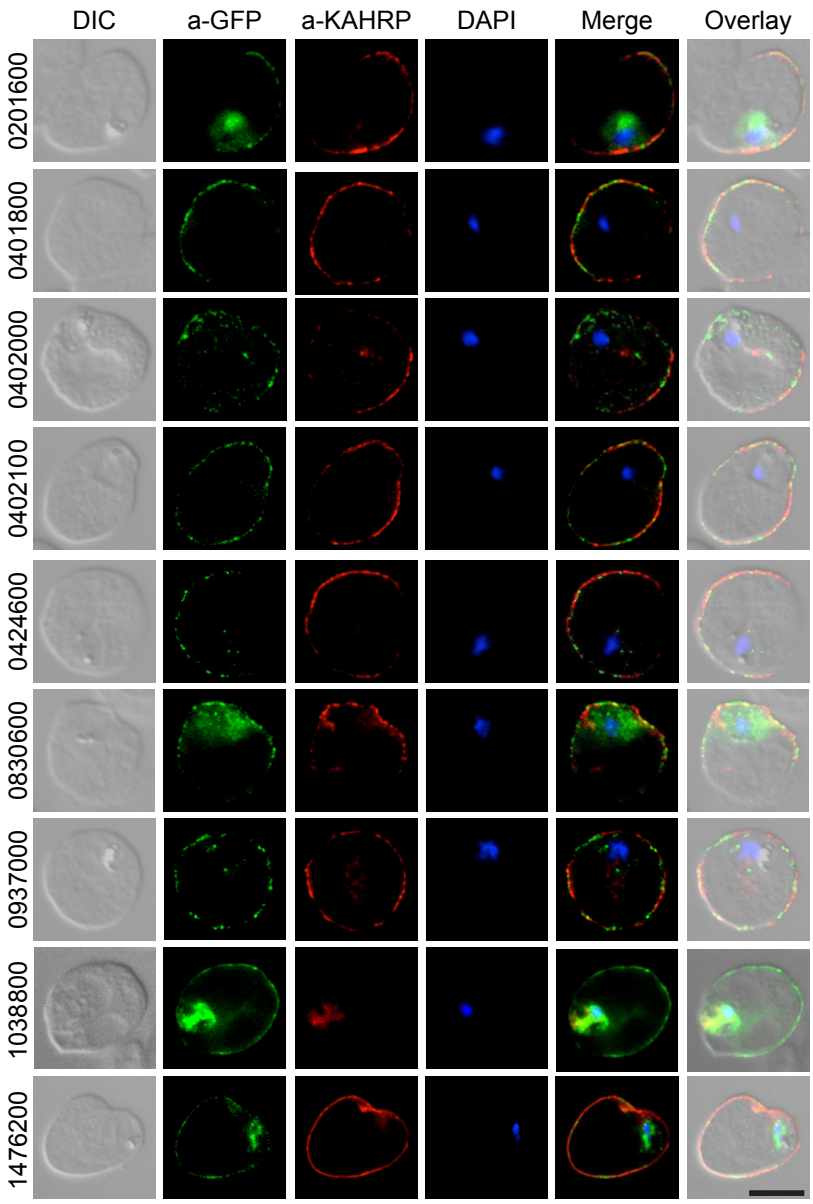
DIC
a-GFP
a-KAHRP
DAPI
Merge
Overlay
0201600
0401800
0402000
0402100
0424600
0830600
0937000
1038800
1476200

Figure S2

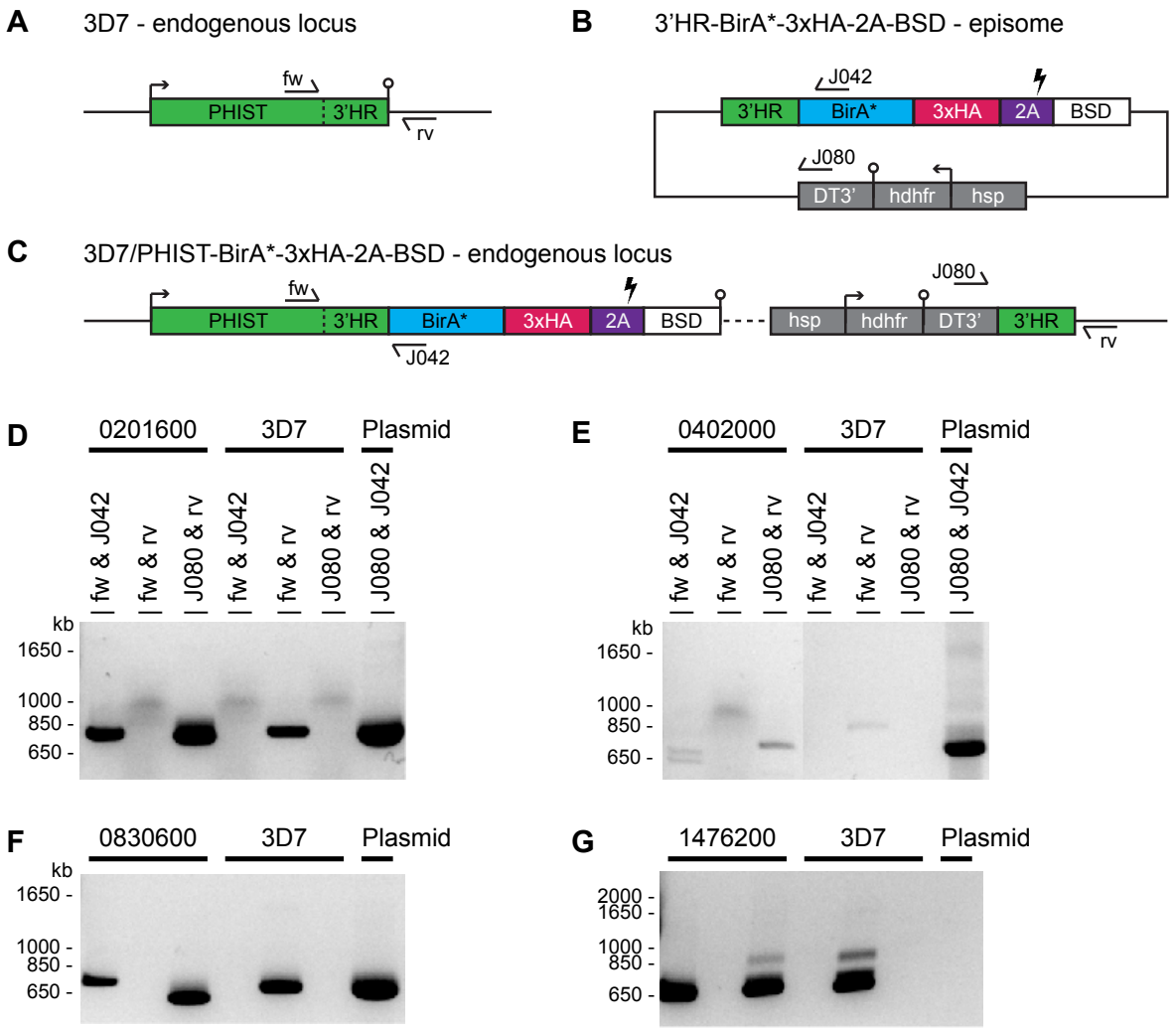

H

		PHIST gDNA fw	PHIST gDNA rv	PHIST gDNA fw	PHIST gDNA rv	PHIST gDNA fw	PHIST gDNA rv	3D7 gRNA fw	3D7 gRNA rv	3D7 gRNA fw	3D7 gRNA rv	3D7 gRNA fw	3D7 gRNA rv	Maxi Plasmid fw	Maxi Plasmid rv
PF3D7_0201600	Primer	J120	J042	J120	J121	J080	J121	J120	J042	J120	J121	J080	J121	J080	J042
	Tm	55	57	55	54	54	54	55	57	55	54	54	54	54	57
	length		869		9114		830		n/a		858		n/a		841
PF3D7_0402000	Primer	J122	J042	J122	J123	J080	J123	J122	J042	J122	J123	J080	J123	J080	J042
	Tm	53	57	53	53	54	53	53	57	53	53	54	53	54	57
	bp		727		8998		856		n/a		854		n/a		729
PF3D7_0830600	Primer	J124	J042	J124	J125	J080	J125	J124	J042	J124	J125	J080	J125	J080	J042
	Tm	55	57	55	54	54	54	55	57	55	54	54	54	54	57
	bp		849		8993		729		n/a		796		n/a		782
PF3D7_1476200	Primer	J128	J042	J128	J129	J080	J129	J128	J042	J128	J129	J080	J129	J080	J042
	Tm	53	57	53	53	54	53	53	57	53	53	54	53	54	57
	bp		792		8996		789		n/a		746		n/a		835

Figure S3

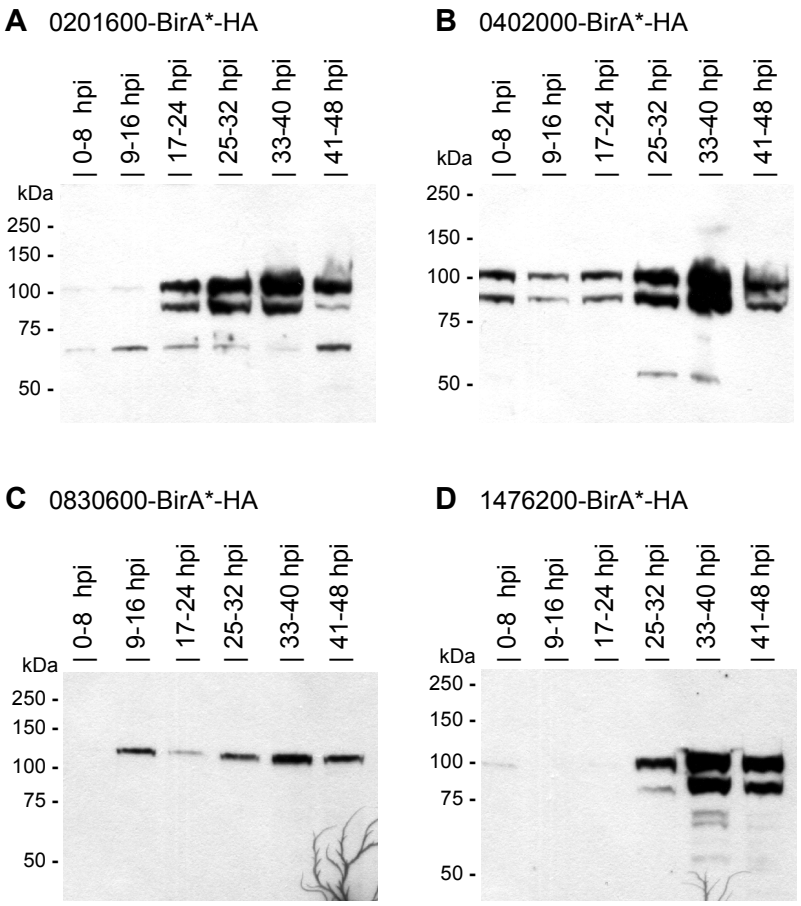
A 0201600-BirA*-HA
B 0402000-BirA*-HA
C 0830600-BirA*-HA
D 1476200-BirA*-HA
0-8 hpi
9-16 hpi
17-24 hpi
25-32 hpi
33-40 hpi
41-48 hpi
kDa
250
150
100
75
50

Table S1

Primer Name	Sequence (5′ -> 3′)
Cloning Primers pARL constructs	
PF3D7_0201600	ataactcgagcttaagATGAAGACCTATAATAGGAATAATAATTGT
	cctttactcatatcgatTAAATTAAATCTTACTTTTTTTATTGGTTT
PF3D7_0401800	ataactcgagcttaagATGAAGATAATAAGCAACCTAGGAAGTATG
	cctttactcatatcgatATCTTGTATCATGACTTTAGATTCTTCTTG
PF3D7_0402000	ataactcgagcttaagATGTGTAATAAATTGTCAAGGGGTAGTAAT
	cctttactcatatcgatATTGTTTTTTTTTAATTCTTTTTTCACCTCTT
PF3D7_0402100	ataactcgagcttaagATGGGAAAAGCATTTTTATTTAAATCTTTA
	cctttactcatatcgatTTGCTCATCATTCAAAGTTGACATATTATTTCC
PF3D7_0424600	ataactcgagcttaagATGAAGTTTTTTAACGGATCAAGCTTT
	cctttactcatatcgatTATATCAATAAAATTTTTACTACGCATGA
PF3D7_0601500	ataactcgagcttaagATGAGTCAAGGAACATATTTTAATTGGTTGT
	cctttactcatatcgatATTATTTATAATGTTATGCATATATACCTCAT
PF3D7_0830600	ataactcgagcttaagATGGAATATTTAAAAAAGACTTTATTTATTTCTG
	cctttactcatatcgatTTGTACATAATTTTTAAAATTTTTTTCGAGT
PF3D7_0937000	ataactcgagcttaagATGAAAGGAATGAATTTTTTTAGAAGTATTTCAC
	cctttactcatatcgatTTCTTCATCTATATATGGTGCATTTATTAGAC
PF3D7_1038800	ataactcgagcttaagATGAAATGTTTAAAATTATTTTCTTTTAAATCAT
	cctttactcatatcgatATCCTTTTGGTTCCTACTCCTTATTCT
PF3D7_1476200	ataactcgagcttaagATGTGTATTAGGTATATAAATATTATTAAAATTA
	cctttactcatatcgatTTTCCAAGTTTTAATTTTATTTTTAGTTTCC
Cloning Primers BirA*-HA constructs	
pH_BirA*-3xHA	ctgaaaaaagcggccgctacccgtacgacgtc
pH_BirA*-3xHA	ccctagatgagtcgacttaggcataatctggaac
PF3D7_0201600	cagggtaggcggccctgcagCAAAAATAATGTATATTTAGATG
	tgctagcacaggatccTAAATTAAATCTTACTTTTTTTATTGGTTTATCT

Primer Name	Sequence (5′ -> 3′)
PF3D7_0401800	cagggtaggcggccctgcagGAAGGTAGTAACGTAGATATTA
	tgctagcacaggatccATCTTGTATCATGACTTTAGATTCTTCTTG
PF3D7_0402000	cagggtaggcggccctgcagGTTCATGAAAATGATTATACTG
	tgctagcacaggatccATTGTTTTTTTTTAATTCTTTTTTCACCTCTTC
PF3D7_0402100	cagggtaggcggccctgcagGATTTGGAATATGAAAAAGAAG
	tgctagcacaggatccTTGCTCATCATTCAAAGTTGACATATTATTTCC
PF3D7_0424600	cagggtaggcggccctgcagACCATTGGTAATTTATTTGAAG
	tgctagcacaggatccTATATCAATAAAATTTTTACTACGCATGATAG
PF3D7_0601500	cagggtaggcggccctgcagATTTATTAAAAGAAGAACTAC
	tgctagcacaggatccATTATTTATAATGTTATGCATATATACCTCATC
PF3D7_0830600	cagggtaggcggccctgcagATAATAATAATATTAGATCAAC
	tgctagcacaggatccTTGTACATAATTTTTAAAATTTTTTTCGAGTG
PF3D7_0937000	cagggtaggcggccctgcagGATATATTCTTTAAATTCAAATG
	tgctagcacaggatccTTCTTCATCTATATATGGTGCATTTATTAGAC
PF3D7_1038800	cagggtaggcggccctgcagTAAATAATTGTAGTAAGGTTAC
	tgctagcacaggatccATCCTTTTGGTTCCTACTCCTTATTCTTG
PF3D7_1476200	cagggtaggcggccctgcagAATAGACTATAATAATTTGTCT
	tgctagcacaggatccTTTCCAAGTTTTAATTTTATTTTTAGTTTCCTTC

Cloning Primers SLI constructs

PF3D7_0201600	gtaggcggccatcgctgcagCAAAAATAATGTATATTTAGAT
PF3D7_0401800	gtaggcggccatcgctgcagGAAGGTAGTAACGTAGATAT
PF3D7_0402000	gtaggcggccatcgctgcagGTTCATGAAAATGATTATAC
PF3D7_0402100	gtaggcggccatcgctgcagGATTTGGAATATGAAAAAG
PF3D7_0424600	gtaggcggccatcgctgcagACCATTGGTAATTTATTTGAAG
PF3D7_0830600	gtaggcggccatcgctgcagATAATAATAATATTAGATCAAC
PF3D7_0937000	gtaggcggccatcgctgcagGATATATTCTTTAAATTCAAATG
PF3D7_1038800	gtaggcggccatcgctgcagTAAATAATTGTAGTAAGGTTAC

Primer Name	Sequence (5′ -> 3′)
PF3D7_1476200	gtaggcggccatcgctgcagAATAGACTATAATAATTTGTCT
all	cgctaccataactagtggcataatctggaacatcgtaag
Sequencing Primers	
PF3D7_0201600	TATTATATGTTATCAGGAAATAGTG
PF3D7_0401800	TTCAACAACACGATCAGCATCAACA
PF3D7_0402000	AATTAAGTCAGGACTATAATGATGT
PF3D7_0402100	GAAGAAAATATGAAAATCTGAGAGA
PF3D7_0601500	TGATGAGATATGTAAAAAATATTGC
PF3D7_0830600	CCGAAAGTAACGTAGATTATGTTGT
PF3D7_1038800	TCTAAATATTTATCTTTAATACATC
PF3D7_1038800	AGTCCATCCTATAGATTTTAAAATG
PF3D7_1476200	AAAGAATTTATGGAATGGGATGATG
pARL_fwd	TATTTTTAGACTATAATATCCG
5'GFP_rev (pARL)	ATTTGTGCCCATTAACATCACCATC
pH_BirA_fwd	gagacagctcaattctttatgtcca
pH_BirA_tag_rv	ctattattaaataagcttaatcattc
pH_BirA_ins_rv	cctaatgtttcacctaattgttcacctg
pH_BirA_fwd2	atgagaagagtagaagaatcagtag
pH_BirA_ins_rv2	ccaatctcttaatgtttgtatatgt
pH-2A-fw	caattctttatgtccacaacatcatc
pH-2A-rv after BSD	gcttaatcattcttctcatatacttc
seq of BirA	gctagcatgaaagataatacagtac
0830600-3xHA	ATTAggatccATGGAATATTTAAAAAAGACTTTATTTATTTC
0830600-3xHA	ATATgctagcTTGTACATAATTTTTAAAATTTTTTTCGAG

Table S2

PF3D7_0100100	PF3D7_0200500	PF3D7_0300300	PF3D7_0408800	PF3D7_0600800	PF3D7_0712000
PF3D7_0100300	PF3D7_0200600	PF3D7_0300400	PF3D7_0408900	PF3D7_0601000	PF3D7_0712300
PF3D7_0100500	PF3D7_0200700	PF3D7_0300500	PF3D7_0410000	PF3D7_0601100	PF3D7_0712400
PF3D7_0100600	PF3D7_0200800	PF3D7_0300600	PF3D7_0412400	PF3D7_0601200	PF3D7_0712500
PF3D7_0100700	PF3D7_0201000	PF3D7_0300700	PF3D7_0412700	PF3D7_0601300	PF3D7_0712600
PF3D7_0100800	PF3D7_0201100	PF3D7_0300800	PF3D7_0412900	PF3D7_0601400	PF3D7_0712800
PF3D7_0100900	PF3D7_0201200	PF3D7_0300900	PF3D7_0413100	PF3D7_0601500	PF3D7_0712900
PF3D7_0101000	PF3D7_0201300	PF3D7_0301100	PF3D7_0413200	PF3D7_0601700	PF3D7_0713000
PF3D7_0101100	PF3D7_0201400	PF3D7_0301200	PF3D7_0413300	PF3D7_0601900	PF3D7_0713100
PF3D7_0101200	PF3D7_0201500	PF3D7_0301300	PF3D7_0413400	PF3D7_0603400	PF3D7_0713200
PF3D7_0101300	PF3D7_0201600	PF3D7_0301400	PF3D7_0420700	PF3D7_0607300	PF3D7_0713300
PF3D7_0101400	PF3D7_0201700	PF3D7_0301500	PF3D7_0420900	PF3D7_0608100	PF3D7_0716300
PF3D7_0101500	PF3D7_0201800	PF3D7_0301600	PF3D7_0421100	PF3D7_0609100	PF3D7_0717000
PF3D7_0101600	PF3D7_0201900	PF3D7_0301700	PF3D7_0421200	PF3D7_0611000	PF3D7_0719800
PF3D7_0101700	PF3D7_0202000	PF3D7_0301800	PF3D7_0421300	PF3D7_0615300	PF3D7_0721100
PF3D7_0101800	PF3D7_0202100	PF3D7_0302200	PF3D7_0421500	PF3D7_0617400	PF3D7_0726100
PF3D7_0101900	PF3D7_0202200	PF3D7_0302300	PF3D7_0421600	PF3D7_0617600	PF3D7_0726700
PF3D7_0102000	PF3D7_0202300	PF3D7_0302500	PF3D7_0422000	PF3D7_0617700	PF3D7_0726800
PF3D7_0102300	PF3D7_0202900	PF3D7_0304600	PF3D7_0424000	PF3D7_0624700	PF3D7_0730800
PF3D7_0102600	PF3D7_0207000	PF3D7_0310400	PF3D7_0424500	PF3D7_0625400	PF3D7_0730900
PF3D7_0102700	PF3D7_0210800	PF3D7_0312500	PF3D7_0424600	PF3D7_0631100	PF3D7_0731100
PF3D7_0104000	PF3D7_0215000	PF3D7_0315900	PF3D7_0424700	PF3D7_0631200	PF3D7_0731200
PF3D7_0104400	PF3D7_0215300	PF3D7_0316300	PF3D7_0424800	PF3D7_0631300	PF3D7_0731300
PF3D7_0106000	PF3D7_0217000	PF3D7_0318300	PF3D7_0424900	PF3D7_0631400	PF3D7_0731400
PF3D7_0106100	PF3D7_0219300	PF3D7_0321200	PF3D7_0425000	PF3D7_0631500	PF3D7_0731700
PF3D7_0107300	PF3D7_0219700	PF3D7_0323900	PF3D7_0425100	PF3D7_0631600	PF3D7_0732000
PF3D7_0107400	PF3D7_0219800	PF3D7_0324000	PF3D7_0425200	PF3D7_0631800	PF3D7_0732100
PF3D7_0107700	PF3D7_0219900	PF3D7_0324100	PF3D7_0425250	PF3D7_0631900	PF3D7_0732200
PF3D7_0111400	PF3D7_0220000	PF3D7_0324200	PF3D7_0425300	PF3D7_0632000	PF3D7_0732300
PF3D7_0112100	PF3D7_0220100	PF3D7_0324300	PF3D7_0425400	PF3D7_0632100	PF3D7_0732400
PF3D7_0112800	PF3D7_0220200	PF3D7_0324400	PF3D7_0425500	PF3D7_0632200	PF3D7_0732500
PF3D7_0112900	PF3D7_0220300	PF3D7_0324500	PF3D7_0425800	PF3D7_0632300	PF3D7_0732600
PF3D7_0113000	PF3D7_0220400	PF3D7_0324600	PF3D7_0426000	PF3D7_0632400	PF3D7_0732700
PF3D7_0113200	PF3D7_0220500	PF3D7_0324700	PF3D7_0500100	PF3D7_0632500	PF3D7_0732800
PF3D7_0113300	PF3D7_0220600	PF3D7_0324800	PF3D7_0500200	PF3D7_0632600	PF3D7_0733000
PF3D7_0113400	PF3D7_0220700	PF3D7_0324900	PF3D7_0500400	PF3D7_0632800	PF3D7_0800100
PF3D7_0113700	PF3D7_0220900	PF3D7_0400100	PF3D7_0500500	PF3D7_0700100	PF3D7_0800200
PF3D7_0113900	PF3D7_0221000	PF3D7_0400200	PF3D7_0500600	PF3D7_0700200	PF3D7_0800300
PF3D7_0114000	PF3D7_0221100	PF3D7_0400300	PF3D7_0500800	PF3D7_0700400	PF3D7_0800500
PF3D7_0114100	PF3D7_0221200	PF3D7_0400400	PF3D7_0500900	PF3D7_0700500	PF3D7_0800600
PF3D7_0114200	PF3D7_0221300	PF3D7_0400600	PF3D7_0501000	PF3D7_0700600	PF3D7_0800750
PF3D7_0114300	PF3D7_0221400	PF3D7_0400800	PF3D7_0501100	PF3D7_0700800	PF3D7_0800800
PF3D7_0114400	PF3D7_0221600	PF3D7_0400900	PF3D7_0501100	PF3D7_0700900	PF3D7_0800900
PF3D7_0114500	PF3D7_0221650	PF3D7_0401000	PF3D7_0501200	PF3D7_0701000	PF3D7_0801000
PF3D7_0114600	PF3D7_0221700	PF3D7_0401100	PF3D7_0501300	PF3D7_0701400	PF3D7_0807700
PF3D7_0114700	PF3D7_0221900	PF3D7_0401300	PF3D7_0505300	PF3D7_0701500	PF3D7_0808600
PF3D7_0114800	PF3D7_0222000	PF3D7_0401400	PF3D7_0530500	PF3D7_0701600	PF3D7_0808700
PF3D7_0114900	PF3D7_0222100	PF3D7_0401500	PF3D7_0532200	PF3D7_0701700	PF3D7_0808800
PF3D7_0115100	PF3D7_0222200	PF3D7_0401600	PF3D7_0532300	PF3D7_0701800	PF3D7_0808900
PF3D7_0115150	PF3D7_0222300	PF3D7_0401600	PF3D7_0532400	PF3D7_0701900	PF3D7_0809100
PF3D7_0115200	PF3D7_0222500	PF3D7_0401700	PF3D7_0532500	PF3D7_0702000	PF3D7_0823800
PF3D7_0115300	PF3D7_0222700	PF3D7_0401800	PF3D7_0532600	PF3D7_0702100	PF3D7_0824700
PF3D7_0115400	PF3D7_0222800	PF3D7_0401900	PF3D7_0532700	PF3D7_0702300	PF3D7_0825200
PF3D7_0115500	PF3D7_0222900	PF3D7_0402000	PF3D7_0532900	PF3D7_0702400	PF3D7_0825300
PF3D7_0115600	PF3D7_0223100	PF3D7_0402100	PF3D7_0533100	PF3D7_0702500	PF3D7_0827900
PF3D7_0115700	PF3D7_0223200	PF3D7_0402400	PF3D7_0600100	PF3D7_0702600	PF3D7_0830300
PF3D7_0200100	PF3D7_0223300	PF3D7_0402500	PF3D7_0600200	PF3D7_0703100	PF3D7_0830400
PF3D7_0200200	PF3D7_0223400	PF3D7_0402600	PF3D7_0600400	PF3D7_0707300	PF3D7_0830500
PF3D7_0200300	PF3D7_0223500	PF3D7_0402800	PF3D7_0600500	PF3D7_0710300	PF3D7_0830600
PF3D7_0200400	PF3D7_0300100	PF3D7_0404900	PF3D7_0600600	PF3D7_0711700	PF3D7_0830700

PF3D7_0830900
PF3D7_0831000
PF3D7_0831300
PF3D7_0831400
PF3D7_0831500
PF3D7_0831600
PF3D7_0831700
PF3D7_0831750
PF3D7_0831900
PF3D7_0832000
PF3D7_0832200
PF3D7_0832200
PF3D7_0832250
PF3D7_0832300
PF3D7_0832400
PF3D7_0832500
PF3D7_0832700
PF3D7_0832900
PF3D7_0833000
PF3D7_0833200
PF3D7_0833300
PF3D7_0833400
PF3D7_0833500
PF3D7_0900100
PF3D7_0900200
PF3D7_0900300
PF3D7_0900400
PF3D7_0900500
PF3D7_0900600
PF3D7_0900700
PF3D7_0900800
PF3D7_0900900
PF3D7_0901000
PF3D7_0901100
PF3D7_0901200
PF3D7_0901300
PF3D7_0901400
PF3D7_0901500
PF3D7_0901600
PF3D7_0901700
PF3D7_0901800
PF3D7_0902100
PF3D7_0902300
PF3D7_0902400
PF3D7_0902600
PF3D7_0902700
PF3D7_0904200
PF3D7_0904700
PF3D7_0907800
PF3D7_0908300
PF3D7_0910300
PF3D7_0916200
PF3D7_0918000
PF3D7_0927900
PF3D7_0928200
PF3D7_0929400
PF3D7_0929800
PF3D7_0931500
PF3D7_0935500
PF3D7_0935700
PF3D7_0935800
PF3D7_0935900
PF3D7_0936000
PF3D7_0936200
PF3D7_0936300
PF3D7_0936400
PF3D7_0936500
PF3D7_0936600
PF3D7_0936800
PF3D7_0936900
PF3D7_0937000
PF3D7_0937100
PF3D7_0937300
PF3D7_0937400
PF3D7_0937600
PF3D7_0937800
PF3D7_1000100
PF3D7_1000300
PF3D7_1000400
PF3D7_1000500
PF3D7_1000600
PF3D7_1000700
PF3D7_1000900
PF3D7_1001000
PF3D7_1001300
PF3D7_1001400
PF3D7_1001600
PF3D7_1001700
PF3D7_1001800
PF3D7_1001900
PF3D7_1002000
PF3D7_1002100
PF3D7_1002300
PF3D7_1005000
PF3D7_1016300
PF3D7_1016400
PF3D7_1016500
PF3D7_1016600
PF3D7_1016700
PF3D7_1016800
PF3D7_1016900
PF3D7_1018300
PF3D7_1019600
PF3D7_1024800
PF3D7_1028100
PF3D7_1028200
PF3D7_1028700
PF3D7_1029500
PF3D7_1029700
PF3D7_1031600
PF3D7_1034800
PF3D7_1038400
PF3D7_1038500
PF3D7_1038600
PF3D7_1038700
PF3D7_1038800
PF3D7_1039000
PF3D7_1039100
PF3D7_1039200
PF3D7_1039400
PF3D7_1039600
PF3D7_1039700
PF3D7_1039800
PF3D7_1039900
PF3D7_1040000
PF3D7_1040100
PF3D7_1040200
PF3D7_1040300
PF3D7_1040400
PF3D7_1040500
PF3D7_1040600
PF3D7_1040700
PF3D7_1040800
PF3D7_1040900
PF3D7_1041000
PF3D7_1041100
PF3D7_1041300
PF3D7_1100100
PF3D7_1100200
PF3D7_1100400
PF3D7_1100500
PF3D7_1100600
PF3D7_1100800
PF3D7_1100900
PF3D7_1101000
PF3D7_1101200
PF3D7_1101300
PF3D7_1101500
PF3D7_1101600
PF3D7_1101700
PF3D7_1101800
PF3D7_1101900
PF3D7_1102100
PF3D7_1102200
PF3D7_1102300
PF3D7_1102500
PF3D7_1102600
PF3D7_1102900
PF3D7_1104100
PF3D7_1104800
PF3D7_1106100
PF3D7_1108700
PF3D7_1109900
PF3D7_1110000
PF3D7_1112000
PF3D7_1116000
PF3D7_1116700
PF3D7_1116800
PF3D7_1121000
PF3D7_1121600
PF3D7_1125000
PF3D7_1127400
PF3D7_1127500
PF3D7_1133300
PF3D7_1136900
PF3D7_1148700
PF3D7_1148800
PF3D7_1148900
PF3D7_1149000
PF3D7_1149100
PF3D7_1149200
PF3D7_1149300
PF3D7_1149400
PF3D7_1149500
PF3D7_1149600
PF3D7_1149700
PF3D7_1149800
PF3D7_1149900
PF3D7_1150000
PF3D7_1150200
PF3D7_1150400
PF3D7_1200100
PF3D7_1200200
PF3D7_1200300
PF3D7_1200400
PF3D7_1200500
PF3D7_1200600
PF3D7_1200800
PF3D7_1200900
PF3D7_1201000
PF3D7_1201100
PF3D7_1201200
PF3D7_1201300
PF3D7_1201400
PF3D7_1210000
PF3D7_1212100
PF3D7_1215900
PF3D7_1219300
PF3D7_1219400
PF3D7_1219500
PF3D7_1221700
PF3D7_1221900
PF3D7_1225100
PF3D7_1232000
PF3D7_1233800
PF3D7_1234400
PF3D7_1239500
PF3D7_1240100
PF3D7_1240200
PF3D7_1240300
PF3D7_1240400
PF3D7_1240600
PF3D7_1240900
PF3D7_1241600
PF3D7_1250100
PF3D7_1252200
PF3D7_1252300
PF3D7_1252500
PF3D7_1252700
PF3D7_1252800
PF3D7_1252900
PF3D7_1253000
PF3D7_1253100
PF3D7_1253300
PF3D7_1253500
PF3D7_1253700
PF3D7_1253800
PF3D7_1253900
PF3D7_1254000
PF3D7_1254100
PF3D7_1254200
PF3D7_1254300
PF3D7_1254400
PF3D7_1254500
PF3D7_1254600
PF3D7_1254900
PF3D7_1255000
PF3D7_1255100
PF3D7_1255200
PF3D7_1300100
PF3D7_1300200
PF3D7_1300300
PF3D7_1300400
PF3D7_1300500
PF3D7_1300600
PF3D7_1300700
PF3D7_1300800
PF3D7_1300900
PF3D7_1301100
PF3D7_1301200
PF3D7_1301300
PF3D7_1301400
PF3D7_1301500
PF3D7_1301700
PF3D7_1301900
PF3D7_1302000
PF3D7_1302300
PF3D7_1303000
PF3D7_1306200
PF3D7_1316300
PF3D7_1323700
PF3D7_1330700
PF3D7_1333200
PF3D7_1334300
PF3D7_1334400
PF3D7_1334500
PF3D7_1334600
PF3D7_1334700
PF3D7_1335900
PF3D7_1338900
PF3D7_1346100
PF3D7_1351300
PF3D7_1352900
PF3D7_1353100
PF3D7_1353200
PF3D7_1367800
PF3D7_1368000
PF3D7_1369000
PF3D7_1370300
PF3D7_1371700
PF3D7_1371800
PF3D7_1371900
PF3D7_1372000
PF3D7_1372100
PF3D7_1372200
PF3D7_1372300
PF3D7_1372500
PF3D7_1372700
PF3D7_1372800
PF3D7_1372900
PF3D7_1373000
PF3D7_1373200
PF3D7_1373300
PF3D7_1373400
PF3D7_1373500
PF3D7_1400100
PF3D7_1400200
PF3D7_1400300
PF3D7_1400400
PF3D7_1400500
PF3D7_1400600
PF3D7_1400700
PF3D7_1400800
PF3D7_1400900
PF3D7_1401000
PF3D7_1401050
PF3D7_1401100
PF3D7_1401200
PF3D7_1401300
PF3D7_1401600
PF3D7_1404300
PF3D7_1404700
PF3D7_1404800
PF3D7_1407800
PF3D7_1413500
PF3D7_1416700
PF3D7_1416800
PF3D7_1421900
PF3D7_1427200
PF3D7_1429600
PF3D7_1430200
PF3D7_1439300
PF3D7_1446400
PF3D7_1455900
PF3D7_1458000
PF3D7_1463900
PF3D7_1464400
PF3D7_1465700
PF3D7_1469000
PF3D7_1471100
PF3D7_1472300
PF3D7_1475300
PF3D7_1476100
PF3D7_1476200
PF3D7_1476300
PF3D7_1476600
PF3D7_1476900
PF3D7_1477000
PF3D7_1477100
PF3D7_1477200
PF3D7_1477300
PF3D7_1477400
PF3D7_1477500
PF3D7_1477700
PF3D7_1478000
PF3D7_1478100
PF3D7_1478200
PF3D7_1478300
PF3D7_1478400
PF3D7_1478500
PF3D7_1478600
PF3D7_1478700
PF3D7_1478800
PF3D7_1479000
PF3D7_1479100
PF3D7_1479200
PF3D7_1479300
PF3D7_1479400
PF3D7_1479500
PF3D7_1479600
PF3D7_1479700
PF3D7_1479800
PF3D7_1479900
PF3D7_1480000
PF3D7_1480100

Chapter 5: Humanized Parasites

Manuscript in preparation for submission

Plasmodium falciparum expresses and exports human cytoskeleton proteins for protein-protein interaction studies

Jan D. Warncke[a,b], Sabina Beilstein[a,b], Matthias Wyss[a,b], Armin Passecker[a,b], Anke Gabel[a,b], , Hans-Peter Beck[a,b*]

[a] Department of Medical Parasitology and Infection Biology, Swiss Tropical and Public Health Institute, Basel, Switzerland

[b] University of Basel, Basel, Switzerland

* corresponding author: Hans-Peter Beck, Swiss TPH, Socinstrasse 57, CH-4051 Basel, Switzerland, phone +41 61 284 81 16, fax: +41 61 284 81 01, hans-peter.beck@unibas.ch

ORCID IDs

Jan Warncke: 0000-0001-6852-4191

Armin Passecker: 0000-0002-5970-3339

Hans-Peter Beck: 0000-0001-8326-4834

Abstract

The extensive host cell remodeling of human erythrocytes during the course of *Plasmodium falciparum* infection is facilitated by a large number of exported parasite proteins. The function of the majority of these proteins remains elusive but we showed by immunoprecipitation that erythrocyte cytoskeleton proteins are potential interaction partners for many exported parasite proteins. Reverse precipitations to confirm these interactions are a major challenge due to the lack of a nucleus in the terminally differentiated erythrocyte. We constructed transgenic parasite lines which express and export different tagged human cytoskeleton proteins. These human proteins were designed to be soluble within the cytosol of the infected erythrocyte. They are expected to bind their putative parasite binding partners either during transport to or at their final destination within the erythrocyte. This approach allows us to use human proteins as bait for immunoprecipitations but also to potentially modify these proteins within the infected cell. Here we show the expression and export of these transgenic proteins and show that several different N-terminal export sequences can be used to successfully target the proteins for export into the host cytosol. This humanized parasite approach thus offers immense potential for studying interactions between human cytoskeleton and exported parasite proteins.

Introduction

During the course of intraerythrocytic asexual development, the malaria parasite *P. falciparum* extensively remodels the red blood cell to make it a suitable host cell. This is facilitated by ~550 parasite proteins known or predicted to be exported. The majority of these proteins possess the *Plasmodium* Export Element (PEXEL), a pentameric N-terminal amino acid motif which targets them for export (1-3). Inside the endoplasmic reticulum (ER), the PEXEL motif is co-translationally cleaved by the parasite protease Plasmepsin V and the new N-terminus is acetylated (4-6). Once discharged into the parasitophorous vacuole, PEXEL proteins are translocated across the parasitophorous vacuole membrane (PVM) by the *Plasmodium* translocon of exported proteins (PTEX) (7). PEXEL-negative exported proteins (PNEP) lack a known export motif (8, 9). Less is known about their export pathway, but it also seems to include translocation by the PTEX (10). Once inside the cytosol of the infected red blood cell (iRBC), chaperones assist in refolding and exported proteins are trafficked to their final destination such as Maurer's clefts, the iRBC cytoskeleton or membrane, or remain as soluble proteins inside the iRBC cytosol (reviewed in (11)).

Exported proteins are central to surface presentation of the major virulence factor PfEMP1 (12, 13). On the cytoplasmic side, exported proteins such as KAHRP and PHIST family members make up surface protrusions called knobs in which PfEMP1 is anchored to the cytoskeleton (14, 15). PfEMP1 confers binding to the endothelial cells of the deep vasculature, a process referred to as cytoadhesion, sequestering the iRBCs and preventing their passage through the spleen. This process not only allows the parasite to rapidly multiply in its host but is also the major contributor to pathology and morbidity (16). To understand essential mechanism of the erythrocyte remodeling could provide new strategies to interfere with these crucial processes.

Studies of host-parasite protein interactions often used co-immunoprecipitations (co-IP) to identify potential interaction partners for proteins of interest. Mostly in these studies parasite proteins were used as bait since they are easily tagged or manipulated by molecular cloning techniques (7, 14). Using tagged erythrocyte cytoskeleton proteins as bait is more of a challenge because the lack of a nucleus in the erythrocyte makes it refractory to genetic manipulation. To circumvent this, erythrocyte precursor cells have been genetically manipulated and subsequently differentiated into erythrocytes (17). While genetic manipulation of hematopoietic stem cells with CRISPR/Cas9 or Zink finger nuclease–based approaches has shown promising results in correcting

the sickle cell trait (18) and hemoglobinopathies (19), the cost of producing larger amounts of erythrocytes required for cell culture and co-IP remain very high at the moment.

Alternatively, we created a versatile system that allows for genetic manipulation of human cytoskeleton proteins to be used for reverse co-IPs to confirm potential interactions with exported parasite proteins. We transfected *P. falciparum* parasites with plasmids to overexpress fusion proteins containing a N-terminal export sequence of a PEXEL protein and the codon optimized coding sequence of human cytoskeleton proteins fused to a molecular tag. Fusion proteins were designed to be soluble in the iRBC cytosol and we removed transmembrane domains or truncated the proteins to express only fragments implicated to interact with parasite proteins. Here we show that a number of different export sequences successfully target human proteins expressed by *P. falciparum* into the iRBC cytosol.

Methods

Parasite Culture

In vitro culturing of *P. falciparum* 3D7 parasites was performed according to Moll et al., 2008 (20). Parasites were synchronized either by sorbitol treatment (21) or by using a Percoll density gradient (22) and were selected for presence of knobs by gelatin flotation (23). Transfection was performed on ring stages (24) and transgenic cell lines were cultured on 10 nM WR99210 (Jacobs Pharmaceuticals, Cologne, Germany) or 5 mg/ml blasticidin (Sigma).

Cloning

Genes were synthesized by Eurofins (Munich, Germany) and GenScript (Piscataway, NJ, USA) and the sequences codon-optimized for expression in *P. falciparum*: band 3 (nucleotides 1-1137 coding for amino acids 1-379), band 4.1 (full length), band 4.2 (full length), band 7 (full length), and ankyrin (nucleotides 1-2481 coding for amino acids 1-827).

To generate overexpression constructs, the pARL vector was used (Figure S1A) (24). Band3_1-379 was first inserted into a cloning plasmid containing the HA-tag- Band3_1-379_HA was then cloned into the pARL vector with AflII and KpnI (Figure S1B). To generate a band3_1-379_myc, the HA-tag was replaced by the myc-tag through multiple PCR reactions and then inserted via the AflII and KpnI restriction sites (Figure S1C). The band3_1-379_myc plasmid

was digested with SpeI and NheI/BmtI to insert band4.1_FL, band4.2_FL, band7_FL, and Ankyrin_1-827. For the GFP-tagged constructs, the amplified genes were cloned into pARLmGFP, using AflII and ClaI (Figure S1D). In addition, truncated versions of band 7 lacking the transmembrane domain were generated: band7_55-288_GFP/myc.

To test different export sequences, PF13_0275 of pARL_band3_1-379_myc was replaced via XhoI and SpeI cloning with three other sequences: PFI1780w (aa 1-90), PFE1605w (aa 1-111 and aa 1-149) (Figure S1E). The export signal from REX3 (aa 1-70) was cloned into pARL_band3_1-379, 4.2_FL, 7_55-288, and Ankyrin_1-827 (all myc-tagged) via XhoI and SpeI (Figure S1F). The export sequences were amplified from *P. falciparum* 3D7 cDNA that was prepared using the ImProm-II Reverse transcriptase System (Promega, Switzerland).

Truncations of Ankyrin_myc containing only aa 1-400 or aa 401-827 were generated using SpeI and BmtI. Band7_myc was further reduced to aa 85-218 (SpeI and BmtI). A V197P point mutation in band7_55-288_myc was generated and inserted via SpeI and KpnI (Figure S1G). The glmS sequence was inserted after the myc-tag for band 3 and band 4.1 via *Xho*I and *Spe*I (Figure S1H). All ligations were done via InFusion ligation (Clontech, USA). Primers are listed in Table S1.

Western blot

iRBCs obtained from Percoll purification (20) were lysed in 0.03% Saponin/PBS for 5 or 10 min on ice and then centrifuged (5 min, 20'000 g, 4°C). Supernatant and pellet were separated and each resuspended in 100-200 µl Laemmli-buffer supplemented with 1 x Protease Inhibitor Complete (PIC) (Roche, Switzerland) and DNase (1:100; Sigma). Lysates were sonicated for 5 min (30 sec intervals and high intensity) and stored at -20 °C until further use. Sample preparation for the solubility assay was done as previously described (25). For SDS-PAGE parasite lysates were heated at 95 °C for 5 min, pulse-vortexed and centrifuged at full speed for 1 min. 10-15 µl were loaded onto a NOVEX NuPAGE Bis-Tris gel (12% or 4-12%), run in MOPS or MES buffer, and then blotted with the iBlot2 (all from Life Technologies). Membranes were blocked in 5% milk/TNT (100 mM Tris, 150 mM NaCl, 43 mM HCl, and 0.1% Tween 20). All antibodies were diluted in 5% milk/TNT. The following primary antibodies were used: rat anti-HA (1:500; Roche), mouse anti-GFP (1:500; Roche), rat anti-myc (1:1000; Abcam), mouse anti-GAPDH (1:10'000), and rabbit anti-PFE1605w (1:1000). Goat anti-mouse-HRP (1:10'000; Pierce), goat anti-rabbit-HRP (1:5000; Jackson Immunology), and goat anti-rat-HRP (1:10'000; Southern Biotech) were used as secondary antibodies.

Microscopy

For immunofluorescence assays (IFA) thin smears were prepared, fixed in methanol/acetone (60:40) for 2 min at -20°C and then blocked with 3% BSA/PBS followed by antibody staining. For confocal microscopy and to retain the three dimensional structure, cells were treated with paraformaldehyde (26) and then stained with antibodies. Primary antibodies were rat anti-HA (1:100; Roche), mouse anti-GFP (1:100; Roche), and rat anti-myc (1:100; Abcam). Goat anti-mouse, anti-rabbit, or anti-rat with Alexa Fluorophores 405, 488, or 594 (all 1:200; Invitrogen) were used as secondary antibodies, respectively. Nuclei were stained with DAPI (Vector Laboratories, Inc.) and membranes were stained with Cellmask deep red plasma membrane stain (1:200, Invitrogen). Images were acquired with a Leica DM 5000 B in combination with the LAS 4.9.0 software or with a Zeiss LSM700 upright confocal microscope, using the ZEN 2010 software and processed with Omero 5.3.3 and Imaris 8.4.

Microsphiltration

Microsphiltration was performed as described by Lavazec et al. (27) with ring stages (12-16 hpi) and trophozoites (36-40 hpi) that had been cultured for at least four cycles with or without 2.5 mM glucosamine (GlcN; Sigma). Parasite cultures were adjusted to approximately 3-4% parasitemia at 1.5% hematocrit in culture medium supplemented with 0.5 % Albumax II. Six hundred µl were injected per column and washed through the column with 5 ml medium at a flow rate of 60 ml/h. For each experiment and parasite line, six columns were loaded. Parasitemia was determined by FACS. Input and flow through samples were centrifuged and the pellet was resuspended in 100 µl SYBR® green (Sigma) diluted 1:5,000 in FACS Flow (Becton Dickinson) and incubated in the dark at 37°C for 15 min. The pellet was subsequently washed once in 850 µl FACS Flow, resuspended in 850 µl FACS Flow, and then subjected to measurement. Per sample, 100,000 events were measured on a FACS Calibur (Becton Dickinson) and analyzed using Cell Quest V5.2.1 (BD Biosciences).

Results

To target recombinant human cytoskeleton proteins expressed by *Plasmodium falciparum* for export into the host cell, an export sequence was added. The N-terminal part of PF13_0275 comprising residues 1-110, which includes the signal peptide and PEXEL motif, has been previously used to target the ATS domain of PfEMP1 variants for export into the iRBC (14). We therefore fused this export sequence upstream of the N-terminus of selected human cytoskeleton proteins and fused an HA-, GFP-, or myc-tag to the C-terminus. For band 3 we selected the N-terminal intracellular loop up to the first transmembrane (TM) domain (nucleotides 1-1137 coding for residues 1-379) which was previously shown to interact with the PHIST protein PF3D7_0532400 (PFE1605w/LyMP) (14). As band 4.1 and band 4.2 do not contain any TM domains, both were used as full length proteins. The TM of band 7 was removed and the remaining residues 55-288 (nucleotides 166-864) were selected. Ankyrin was truncated to contain only residues 1-827 (nucleotides 1-2481), a region that has been shown to be involved in interactions with membrane protein band 3 and cytoskeleton protein band 4.2 (28) (Figure S1 B-D).

Band3_1-379 was tested with each of the three tags while band4.1_FL, band4.2_FL, band7_55-288, and Ankyrin_1-827 were only tested with GFP- and myc-tags. Except for parasites transfected with band4.2_FL_GFP or _myc all transgenic parasites lines could be expanded after transfection.

The correct size of each fusion protein was tested by lysing the cells and analyzing the resulting supernatants and pellets by Western blot using the respective antibodies against the tags. The supernatant fractions were supposed to contain soluble proteins while membrane associated or insoluble complexes should remain in the pellet. All of our fusion proteins were detected near the predicted molecular weight. For most fusion proteins, bands were detected in both fractions. Band4.1_FL_GFP was only present in the supernatant fraction. Ankyrin_1-827_GFP and band7_55-288_myc were mostly detected in the pellet. For Ankyrin_1-827_myc, detected bands sowed at a much lower molecular weight than expected. The GAPDH loading control was detected in both fractions indicating partial lysis of late stage parasite (Figure 1A).

Next we wanted to determine the localization of the exported human fusion proteins. Initially, we hardly detected band3_1-379_GFP/myc in IFAs on methanol/acetone fixed parasites (Figure S2). Since previous Western blots had shown that the fusion proteins were partially soluble and washed out of the iRBC during lysis we cross-linked the proteins with paraformaldehyde prior to lysis and antibody labeling, also retaining the three dimensional shape of the iRBC. Confocal

microscope revealed band 3 and band 4.1 fusion proteins to be exported. Fusion proteins expressed from all three band 3 constructs were evenly distributed in the iRBC cytosol. The pattern observed for band 4.1 was also evenly distributed but showed a more granular distribution. Ankyrin_1-827_GFP showed a very weak signal at the iRBC membrane but most of the signal was detected within the parasite, Ankyrin_1-827_myc as well as band7_55-288_GFP and _myc were not exported (Figure 1B).

We performed a solubility assay for band3_1-379_GFP and _myc and sequentially extracted proteins from the iRBC based on their solubility characteristics. When analyzing all fractions by Western blot, we detected band3_1-379_GFP or _myc in the Saponin supernatant which contains soluble proteins from the iRBC cytosol. There was no GAPDH in this fraction indicating that the parasites membranes were not lysed. Thus, the band3_1-379_GFP and _myc proteins were exported and soluble in the iRBCs cytosol. No signal for these two proteins was detected after hypotonic lysis which ruptures all membranes, indicating that no soluble fusion protein was retained within the parasite. Band3_1-379_GFP and _myc fusion proteins were again detected in the following carbonate fraction, identifying them to be cytoskeleton or membrane associated (Figure 1C). Based on these findings we conclude that the band3_1-379_GFP and _myc fusion proteins occupy two different subcellular localizations within the host cell as some of the protein is capable of binding to the cytoskeleton while some remains soluble in the iRBC cytosol.

From the previous transfection series, not all fusion proteins were exported and one cell line never grew after transfection. We therefore wanted to test other N-termini of PEXEL proteins to see if they would also qualify as export sequences. Having achieved good export for band 3, we tested these other N-termini with band3_1-379 first, to be able to compare the new export sequences to the previously used PF13_0275 sequence. We replaced the export sequence of PF13_0275_band3_1-379_myc with the N-termini the two previously investigated PHIST proteins PFI1780w (PF3D7_0936800) and PFE1605w (PF3D7_0532400). As PFE1605w possesses two PEXEL motives, two versions were designed including only the first or both of the PEXEL motives (Figure S1E). Correct molecular masses of the fusion proteins were confirmed by Western blot (Figure 2A) and export was confirmed by confocal microscopy, showing the same homogenous distribution of the signal throughout the entire iRBC (Figure 2B) as observed with PF13_0275_band3_1-379_myc. This data demonstrate that four different N-termini from three different PEXEL proteins were able to target human proteins for export from the parasite into the iRBC.

We next selected the N-terminus of the non-canonical PEXEL protein REX3, which is exported and soluble. Residues 1-70 suffice to export GFP into the iRBC cytosol (29, 30) and were therefore used as export sequence for band4.2_FL, band7_55-288, and Ankyrin_1-827, with the myc-tag was added to each fusion protein. Band3_1-379 was included in this group as control (Figure S1F). The correct molecular sizes were confirmed by Western blot. For each of the fusion proteins, most signal was detected in the pellet fraction with the exception of the band 3 fusion protein which showed most signal in the supernatant fraction (Figure 2A). Only band3_1-379_myc was clearly exported. Ankyrin_1-827_myc showed signal at the iRBC membrane and within the parasite. Band4.2_FL_myc and band7_55-288_myc were again not exported (Figure 2C). So far, band 3_1-379 was exported into the host cell with any of the tested export sequences while the different Ankyrin_1-827 and band7_55-288 constructs showed only little or no export.

To test if shorter fragments would enhance export, we split Ankyrin_1-827 into two fragments (amino acids 1-400 and 401-827; Figure S1G).. Both showed the correct molecular weight in Western blot (Figure 3A), but only PF13_0275_Ankyrin_401-827_myc was found to be exported to the iRBC in confocal microscopy, similar to the PF13_0275_Anykrin_1-827_GFP and REX3_Ankyrin_1-827_myc parasite lines. In agreement with findings from the PF13_0275_Ankyrin _1-827_GFP and REX3_Ankyrin_1-827_myc cell lines, the signal presented as a ring around the iRBC which overlaps with the iRBC membrane stain Cellmask (Figure 3B).

We reduced the recombinant band 7 protein to contain only the stomatin domain (amino acids 85-218) and also generated a construct expressing band7_55-288 with a V197P point mutation which was reported to prevent band 7 dimerization (31). Both were fused to the PF13_0275 export sequence and a myc tag (Figure S1G). Confirmation of correct molecular weight by Western blot (Figure 3A) was followed by confocal microscopy to test for protein export. Band7_85-218_myc was found to be evenly distributed throughout the entire iRBC while Band7_55-288_V197P_myc was not exported (Figure 3B).

To assure that overexpression of the recombinant human proteins is not detrimental to intracellular parasite growth we included an inducible expression system into our approach. We established this system with those two proteins that were exported in previous experiments and also with band 4.2, which was never exported so far. We added the glmS ribozyme sequence to the band3_1-379, band4.1_FL, and band4.2_FL constructs with the PF13_0275 export sequence and the myc tag (Figure S1H). When treated with glucosamine (GlcN), glmS is activated and the mRNA self-cleaves, resulting in fast and efficient reduction of protein levels (32). Without GlcN we

detected the proteins by Western blot and showed that they were exported by confocal microscopy (Figure 4A-B). Upon addition of GlcN, band band4.1_FL_myc_glmS was not detected and protein levels of band3_1-379_myc_glmS were strongly reduced (Figure 4A-B).

Since Band 4.1 has no transmembrane domain we expressed it as a non-truncated version and the recombinantly expressed band4.1_FL protein could potentially bind to band 4.1 binding sites competing with the endogenous erythrocyte band 4.1 for binding to its partners. In contrast, band 3 is a multipass transmembrane protein and we therefore expressed only the N-terminal cytosolic part comprising amino acids 1-397. Since this cytosolic part is involved in the interaction with Ankyrin (33, 34) and also has been shown to interact with PHIST proteins (14), the recombinant band3_1-379 could also compete with its endogenous erythrocyte counterpart. Because these additional interactions could have an effect on iRBC cytoskeleton rigidity we performed microsphiltration experiments with the conditional knock-down clones expressing band3_1-379_myc_glmS and band4.1_FL_myc_glmS, at two time points in the asexual cycle (12 and 36 hpi) to measure potential changes in iRBC deformability. There was no substantial difference at both time points with both parasite lines with or without GlcN (Figure 4C).

Discussion

Here we present a transgenic system which allows expression and export of human erythrocyte proteins by *P. falciparum*. Several different *P. falciparum* export sequences were able to target these fusion proteins with different molecular tags for export. The glmS ribozyme-based conditional expression system also worked well.

In summary, fusion proteins band3_1-379 and band4.1_FL were always exported into the host cell, irrespective of export sequence or molecular tag. Transgenic cell lines expressing band4.2_FL could either not be established or the fusion protein was not exported. A band 7 fusion protein (residue 55-288) was expressed from various plasmids with different export sequences and tags, but none were exported. In contrast, the stomatin domain comprising only residues 85-218 was exported into the iRBC cytosol. We were unable to identify sequence signatures determining whether a protein is exported or not. It is conceivable that certain sequences prevent unfolding as is required to translocate through the PTEX (7, 35). It is interesting to note that the tag fused to the chimeric protein seems to strongly influence the destination of the protein. Band4.1_FL protein fused to a GFP tag was completely soluble whilst the same protein expressed from a

construct with a myc tag was to a large degree found membrane associated as shown by Western blot. It is possible that the larger GFP-tag might sterically hinder the interaction of band4.1_FL with its binding partners at the cytoskeleton.

We obtained inconclusive results with Ankyrin when only weak signals from the PF13_0275_Ankyrin_1-827 GFP-tagged fusion protein were seen exported whilst the same construct with a myc-tag was not exported. In contrast, when the export sequence was changed, REX3_Ankyrin_1-827_myc and PF13_0275_Ankyrin_401-827_myc showed much better export signals, however, the other half of the shortened Ankyrin molecule (PF13_0275_Ankyrin_1-400_myc) was not exported. From these experiments it is clear that yet no prediction can be made for whether a transgenic protein will be exported or not. Whether this is determined by structure, sequence, or other features of respective proteins remains elusive. Transport across the plasma and parasitophorus vacuole membranes has been shown to be complex and partially unknown (11). It is clear that a number of other proteins such as chaperons or heat shock proteins (36-38) are interacting with export cargo, and this process might be disturbed generally with the addition of a tag (39) or with fragments of chimeric and heterologous proteins. It also has been shown that correct folding and unfolding might be highly specific for a particular protein and these conditions might not be available in the system presented (40).

Once exported, these recombinant human proteins could engage with the iRBC cytoskeleton by binding to additional free binding sites which in turn might alter cytoskeleton rigidity. Microsphiltration to test for such changes showed that there was no difference in rigidity in the presence of recombinantly expressed exported cytoskeleton proteins. Except for the band4.1_FL_myc_glmS parasite strain at 36 hpi we obtained retention rates similar to what had been previously reported in the range of 15-25% and 80-100% for the 12 and 36 hpi time points, respectively (41, 42). The difference at 36 hpi might be explained by the fact that we used the 3D7 strain cultured in Albumax and not the NF54 cultured in serum

We showed that the presented humanized parasite approach could be a versatile system to study function and interaction of a number of human erythrocyte proteins that mostly are nonmalleable by genetic means.

Funding Information

This project was supported by the Swiss National Science Foundation (31003A_169347) to HPB. The funders had no role in study design, data collection, data analysis, manuscript preparation, and publication.

Acknowledgement

We thank Alexander Oberli who was involved in starting the idea of humanized parasites. We acknowledge Alexia Loynton-Ferrand and Kai Schleicher at the IMCF, Biozentrum, University of Basel, for their support with image acquisition and analysis. We thank Igor Niederwieser and Sylwia Boltryk for providing the glmS plasmid and Claudia Daubenberger for the anti-GAPDH antibody.

Author contributions

JW and HPB designed the project. Experiments were designed and carried out by JW, SB, MW, and AP with the assistance of AG. LP and FB performed mass spectrometry. Data analysis and the rendering of the figures were done by JW. The manuscript was written by JW and HPB.

Conflict of Interest

The authors declare no conflict of interest.

Bibliografie

1. **Marti M, Good RT, Rug M, Knuepfer E, Cowman AF.** 2004. Targeting malaria virulence and remodeling proteins to the host erythrocyte. Science **306:**1930-1933.
2. **Hiller NL, Bhattacharjee S, van Ooij C, Liolios K, Harrison T, Lopez-Estrano C, Haldar K.** 2004. A host-targeting signal in virulence proteins reveals a secretome in malarial infection. Science **306:**1934-1937.
3. **Spielmann T, Gilberger TW.** 2015. Critical Steps in Protein Export of Plasmodium falciparum Blood Stages. Trends Parasitol **31:**514-525.
4. **Boddey JA, O'Neill MT, Lopaticki S, Carvalho TG, Hodder AN, Nebl T, Wawra S, van West P, Ebrahimzadeh Z, Richard D, Flemming S, Spielmann T, Przyborski J, Babon JJ, Cowman AF.** 2016. Export of malaria proteins requires co-translational processing of the PEXEL motif independent of phosphatidylinositol-3-phosphate binding. Nat Commun **7:**10470.
5. **Russo I, Babbitt S, Muralidharan V, Butler T, Oksman A, Goldberg DE.** 2010. Plasmepsin V licenses Plasmodium proteins for export into the host erythrocyte. Nature **463:**632-636.
6. **Chang HH, Falick AM, Carlton PM, Sedat JW, DeRisi JL, Marletta MA.** 2008. N-terminal processing of proteins exported by malaria parasites. Mol Biochem Parasitol **160:**107-115.
7. **de Koning-Ward TF, Gilson PR, Boddey JA, Rug M, Smith BJ, Papenfuss AT, Sanders PR, Lundie RJ, Maier AG, Cowman AF, Crabb BS.** 2009. A newly discovered protein export machine in malaria parasites. Nature **459:**945-949.
8. **Heiber A, Kruse F, Pick C, Gruring C, Flemming S, Oberli A, Schoeler H, Retzlaff S, Mesen-Ramirez P, Hiss JA, Kadekoppala M, Hecht L, Holder AA, Gilberger TW, Spielmann T.** 2013. Identification of new PNEPs indicates a substantial non-PEXEL exportome and underpins common features in Plasmodium falciparum protein export. PLoS Pathog **9:**e1003546.
9. **Spielmann T, Gilberger TW.** 2010. Protein export in malaria parasites: do multiple export motifs add up to multiple export pathways? Trends Parasitol **26:**6-10.
10. **Elsworth B, Matthews K, Nie CQ, Kalanon M, Charnaud SC, Sanders PR, Chisholm SA, Counihan NA, Shaw PJ, Pino P, Chan J-A, Azevedo MF, Rogerson SJ, Beeson JG, Crabb BS, Gilson PR, de Koning-Ward TF.** 2014. PTEX is an essential nexus for protein export in malaria parasites. Nature **511:**587-591.
11. **de Koning-Ward TF, Dixon MW, Tilley L, Gilson PR.** 2016. Plasmodium species: master renovators of their host cells. Nat Rev Microbiol **14:**494-507.
12. **Maier AG, Rug M, O'Neill MT, Brown M, Chakravorty S, Szestak T, Chesson J, Wu Y, Hughes K, Coppel RL, Newbold C, Beeson JG, Craig A, Crabb BS, Cowman AF.** 2008. Exported proteins required for virulence and rigidity of Plasmodium falciparum-infected human erythrocytes. Cell **134:**48-61.
13. **Maier AG, Cooke BM, Cowman AF, Tilley L.** 2009. Malaria parasite proteins that remodel the host erythrocyte. Nat Rev Microbiol **7:**341-354.

14. **Oberli A, Zurbrugg L, Rusch S, Brand F, Butler ME, Day JL, Cutts EE, Lavstsen T, Vakonakis I, Beck HP.** 2016. Plasmodium falciparum PHIST Proteins Contribute to Cytoadherence and Anchor PfEMP1 to the Host Cell Cytoskeleton. Cell Microbiol doi: 10.1111/cmi.12583.

15. **Watermeyer JM, Hale VL, Hackett F, Clare DK, Cutts EE, Vakonakis I, Fleck RA, Blackman MJ, Saibil HR.** 2016. A spiral scaffold underlies cytoadherent knobs in Plasmodium falciparum-infected erythrocytes. Blood **127:**343-351.

16. **White NJ.** 2017. Malaria parasite clearance. Malar J **16:**88.

17. **Gruszczyk J, Kanjee U, Chan L-J, Menant S, Malleret B, Lim NT, Schmidt CQ, Mok Y-F, Lin K-M, Pearson RD.** 2018. Transferrin receptor 1 is a reticulocyte-specific receptor for Plasmodium vivax. Science **359:**48-55.

18. **Hoban MD, Cost GJ, Mendel MC, Romero Z, Kaufman ML, Joglekar AV, Ho M, Lumaquin D, Gray D, Lill GR, Cooper AR, Urbinati F, Senadheera S, Zhu A, Liu PQ, Paschon DE, Zhang L, Rebar EJ, Wilber A, Wang X, Gregory PD, Holmes MC, Reik A, Hollis RP, Kohn DB.** 2015. Correction of the sickle cell disease mutation in human hematopoietic stem/progenitor cells. Blood **125:**2597-2604.

19. **Dever DP, Bak RO, Reinisch A, Camarena J, Washington G, Nicolas CE, Pavel-Dinu M, Saxena N, Wilkens AB, Mantri S, Uchida N, Hendel A, Narla A, Majeti R, Weinberg KI, Porteus MH.** 2016. CRISPR/Cas9 beta-globin gene targeting in human haematopoietic stem cells. Nature **539:**384-389.

20. **Moll K, Ljungström I, Perlmann H, Scherf A, Wahlgren M.** 2008. Methods in Malaria Reserch. American Type Culture Collection, 10801 University Boulevard, Manassas, VA 20110-2209.

21. **Lambros C, Vanderberg JP.** 1979. Synchronization of Plasmodium falciparum erythrocytic stages in culture. J Parasitol **65:**418-420.

22. **Moll K, Kaneko A, Scherf A, Wahlgren M.** 2013. Methods in Malaria Reserch, 6th Edition ed. American Type Culture Collection, 10801 University Boulevard, Manassas, VA 20110-2209.

23. **Ménard R.** 2013. Malaria - Methods and Protocols, 2 ed doi:10.1007/978-1-62703-026-7. Humana Press.

24. **Crabb BS, Rug M, Gilberger T-W, Thompson JK, Triglia T, Maier AG, Cowman AF.** 2004. Transfection of the human malaria parasite Plasmodium falciparum, p 263-276, Parasite Genomics Protocols. Springer.

25. **Pachlatko E, Rusch S, Muller A, Hemphill A, Tilley L, Hanssen E, Beck HP.** 2010. MAHRP2, an exported protein of Plasmodium falciparum, is an essential component of Maurer's cleft tethers. Mol Microbiol **77:**1136-1152.

26. **Tonkin CJ, van Dooren GG, Spurck TP, Struck NS, Good RT, Handman E, Cowman AF, McFadden GI.** 2004. Localization of organellar proteins in Plasmodium falciparum using a novel set of transfection vectors and a new immunofluorescence fixation method. Mol Biochem Parasitol **137:**13-21.

27. **Lavazec C, Deplaine G, Safeukui I, Perrot S, Milon G, Mercereau-Puijalon O, David PH, Buffet P.** 2013. Microsphiltration: a microsphere matrix to explore erythrocyte deformability. Methods Mol Biol **923:**291-297.

28. **Kümpornsin K, Jiemsup S, Yongkiettrakul S, Chookajorn T.** 2011. Characterization of band 3–ankyrin–Protein 4.2 complex by biochemical and mass spectrometry approaches. Biochemical and biophysical research communications **406:**332-335.

29. **Spielmann T, Hawthorne PL, Dixon MW, Hannemann M, Klotz K, Kemp DJ, Klonis N, Tilley L, Trenholme KR, Gardiner DL.** 2006. A cluster of ring stage-specific genes linked to a locus implicated in cytoadherence in Plasmodium falciparum codes for PEXEL-negative and PEXEL-positive proteins exported into the host cell. Mol Biol Cell **17:**3613-3624.

30. **Schulze J, Kwiatkowski M, Borner J, Schluter H, Bruchhaus I, Burmester T, Spielmann T, Pick C.** 2015. The Plasmodium falciparum exportome contains non-canonical PEXEL/HT proteins. Mol Microbiol **97:**301-314.

31. **Brand J, Smith ES, Schwefel D, Lapatsina L, Poole K, Omerbasic D, Kozlenkov A, Behlke J, Lewin GR, Daumke O.** 2012. A stomatin dimer modulates the activity of acid-sensing ion channels. EMBO J **31:**3635-3646.

32. **Prommana P, Uthaipibull C, Wongsombat C, Kamchonwongpaisan S, Yuthavong Y, Knuepfer E, Holder AA, Shaw PJ.** 2013. Inducible knockdown of Plasmodium gene expression using the glmS ribozyme. PloS one **8:**e73783.

33. **Willardson BM, Thevenin BJ, Harrison ML, Kuster WM, Benson MD, Low PS.** 1989. Localization of the ankyrin-binding site on erythrocyte membrane protein, band 3. J Biol Chem **264:**15893-15899.

34. **Chang SH, Low PS.** 2003. Identification of a critical ankyrin-binding loop on the cytoplasmic domain of erythrocyte membrane band 3 by crystal structure analysis and site-directed mutagenesis. J Biol Chem **278:**6879-6884.

35. **Gehde N, Hinrichs C, Montilla I, Charpian S, Lingelbach K, Przyborski JM.** 2009. Protein unfolding is an essential requirement for transport across the parasitophorous vacuolar membrane of Plasmodium falciparum. Mol Microbiol **71:**613-628.

36. **Charnaud SC, Dixon MWA, Nie CQ, Chappell L, Sanders PR, Nebl T, Hanssen E, Berriman M, Chan JA, Blanch AJ, Beeson JG, Rayner JC, Przyborski JM, Tilley L, Crabb BS, Gilson PR.** 2017. The exported chaperone Hsp70-x supports virulence functions for Plasmodium falciparum blood stage parasites. PLoS One **12:**e0181656.

37. **Külzer S, Charnaud S, Dagan T, Riedel J, Mandal P, Pesce ER, Blatch GL, Crabb BS, Gilson PR, Przyborski JM.** 2012. Plasmodium falciparum−encoded exported hsp70/hsp40 chaperone/co−chaperone complexes within the host erythrocyte. Cell Microbiol **14:**1784-1795.

38. **Batinovic S, McHugh E, Chisholm SA, Matthews K, Liu B, Dumont L, Charnaud SC, Schneider MP, Gilson PR, de Koning-Ward TF, Dixon MWA, Tilley L.** 2017. An exported protein-interacting complex involved in the trafficking of virulence determinants in Plasmodium-infected erythrocytes. Nat Commun **8:**16044.

39. **Saiz-Baggetto S, Méndez E, Quilis I, Igual JC, Bañó MC.** 2017. Chimeric proteins tagged with specific 3xHA cassettes may present instability and functional problems. PloS one **12:**e0183067.

40. **Nagai N, Hosokawa M, Itohara S, Adachi E, Matsushita T, Hosokawa N, Nagata K.** 2000. Embryonic lethality of molecular chaperone hsp47 knockout mice is associated with defects in collagen biosynthesis. The Journal of cell biology **150:**1499-1506.

41. **Sanyal S, Egee S, Bouyer G, Perrot S, Safeukui I, Bischoff E, Buffet P, Deitsch KW, Mercereau-Puijalon O, David PH, Templeton TJ, Lavazec C.** 2012. Plasmodium falciparum STEVOR proteins impact erythrocyte mechanical properties. Blood **119:**e1-8.

42. **Deplaine G, Safeukui I, Jeddi F, Lacoste F, Brousse V, Perrot S, Biligui S, Guillotte M, Guitton C, Dokmak S, Aussilhou B, Sauvanet A, Cazals Hatem D, Paye F, Thellier M, Mazier D, Milon G, Mohandas N, Mercereau-Puijalon O, David PH, Buffet PA.** 2011. The sensing of poorly deformable red blood cells by the human spleen can be mimicked in vitro. Blood **117:**e88-95.

Figure legends

Figure 1

Characterization of human fusion proteins expressed from the pARL_PF13_0275 vector. (A) Western blot of supernatants (SN) and pellets (P) from each lysed parasite line were probed with antibodies as indicated. Expected molecular weights of the fusion proteins are indicated underneath the blots. Anti-GAPDH was used as loading control. (B) Confocal images of transgenic parasite lines. Differential interference contrast (DIC) and DAPI images are shown in the first column followed by anti-myc, anti-GFP, or anti-HA staining. Column three depicts Cellmask staining and column 4 and 5 the merge of fluorescence channels and overlay of all channels, respectively (scale bar = 5 μm). (C) Solubility assay of selected exported recombinant human cytoskeleton proteins. Fusion proteins were labeled with anti-myc. GAPDH and PFE1605w were used as controls for the saponin and carbonate fractions, respectively. PFE1605w was also found occasionally in the SDS fraction.

Figure 2

Characterization of exported human cytoskeleton fusion proteins with different export sequences. (A) Western blots of supernatants (SN) and pellets (P) from lysed parasites were probed with anti-myc antibodies. Anti-GAPDH was used as loading control. Expected molecular weights of the fusion proteins are indicated underneath the blots. (B) and (C) Confocal images of transgenic cell lines. Differential interference contrast (DIC) and DAPI images are shown in the first column followed by anti-myc staining. Column three depicts Cellmask staining and column 4 and 5 the merge of fluorescence channels and overlay of all channels, respectively (scale bar = 5 μm).

Figure 3

Characterization of humanized parasites with truncated or mutated cytoskeleton proteins (A) Western blots of supernatants (SN) and pellets (P) from lysed parasites were probed with anti-myc antibodies. GAPDH was used as loading control. The expected molecular weights of the fusion proteins are indicated underneath the blots. (B) Differential interference contrast (DIC) and DAPI images are shown in the first column followed anti-myc staining. Column three depicts Cellmask

staining and column 4 and 5 the merge of fluorescence channels and overlay of all channels, respectively (scale bar = 5 µm).

Figure 4

Characterization of humanized parasites with conditionally expressed cytoskeleton proteins. (A) Western blots of supernatants (SN) and pellets (P) from lysed parasites were probed with anti-myc antibodies. GAPDH was used as loading control. The expected molecular weights of the fusion proteins are indicated underneath the blots. (B) Differential interference contrast (DIC) and DAPI images are shown in the first column followed anti-myc staining. Column three depicts Cellmask staining and column 4 and 5 the merge of fluorescence channels and overlay of all channels, respectively (scale bar = 5 µm). (C) Microsphiltration of parasites with conditionally expressed and exported recombinant human cytoskeleton proteins. The small bar indicates the mean of the six technical replicates. The mean values from the six technical replicates are summarized for both time points and cell lines in the table. Hpi: hours post invasion. On and off refers to the presence or absence of GlcN in the cell culture medium, respectively.

Figure S1

Schematic representation of all types and variations of plasmids used to transfect *P. falciparum* 3D7 parasites. GOI: gene of interest, export seq.: export sequence, glmS: glucosamine-6-phosphate riboswitch ribozyme. The dashed lines in (C) to (H) represent the plasmid backbone from (B). The arrow indicates the start codon and the circle the stop codon. Restriction sites that were used for cloning are indicated.

Figure S2

Immunofluorescence images of methanol/acetone fixed PF13_0275_band3_1-379_GFP/myc cells that were probed with antibodies against the respective molecular tags. DIC (first column) is followed by anti-GFP or anti-myc signal, the nuclear stain DAPI, a merge of the fluorescence images and finally an overlay of all channels (scale bar = 5 µm).

Figure 1

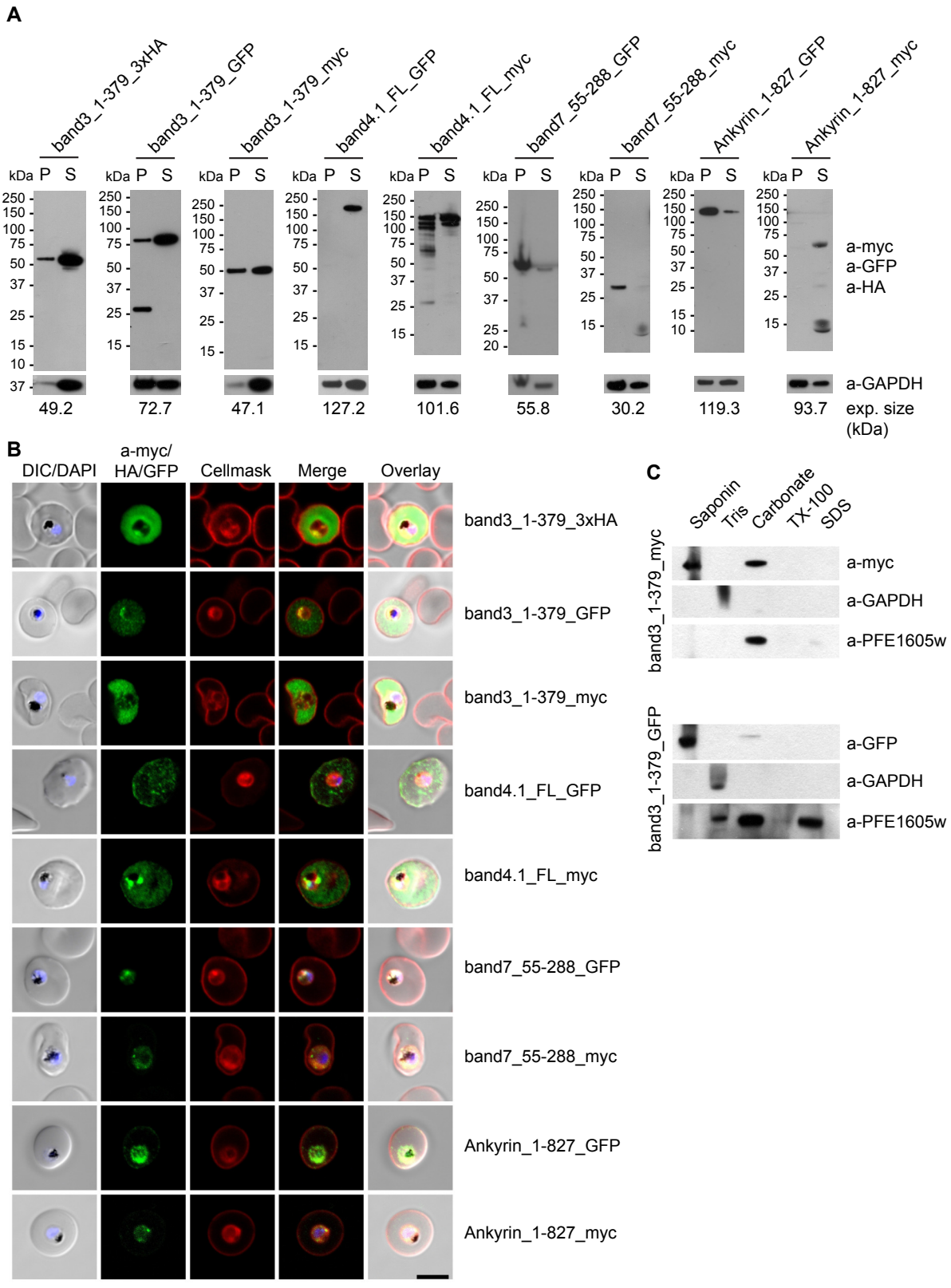
A
band3_1-379_3xHA
band3_1-379_GFP
band3_1-379_myc
band4.1_FL_GFP
band4.1_FL_myc
band7_55-288_GFP
band7_55-288_myc
Ankyrin_1-827_GFP
Ankyrin_1-827_myc
kDa P S
a-myc
a-GFP
a-HA
a-GAPDH
49.2
72.7
47.1
127.2
101.6
55.8
30.2
119.3
93.7
exp. size (kDa)
B
DIC/DAPI
a-myc/ HA/GFP
Cellmask
Merge
Overlay
band3_1-379_3xHA
band3_1-379_GFP
band3_1-379_myc
band4.1_FL_GFP
band4.1_FL_myc
band7_55-288_GFP
band7_55-288_myc
Ankyrin_1-827_GFP
Ankyrin_1-827_myc
C
Saponin
Tris
Carbonate
TX-100
SDS
band3_1-379_myc
a-myc
a-GAPDH
a-PFE1605w
band3_1-379_GFP
a-GFP
a-GAPDH
a-PFE1605w

Figure 2

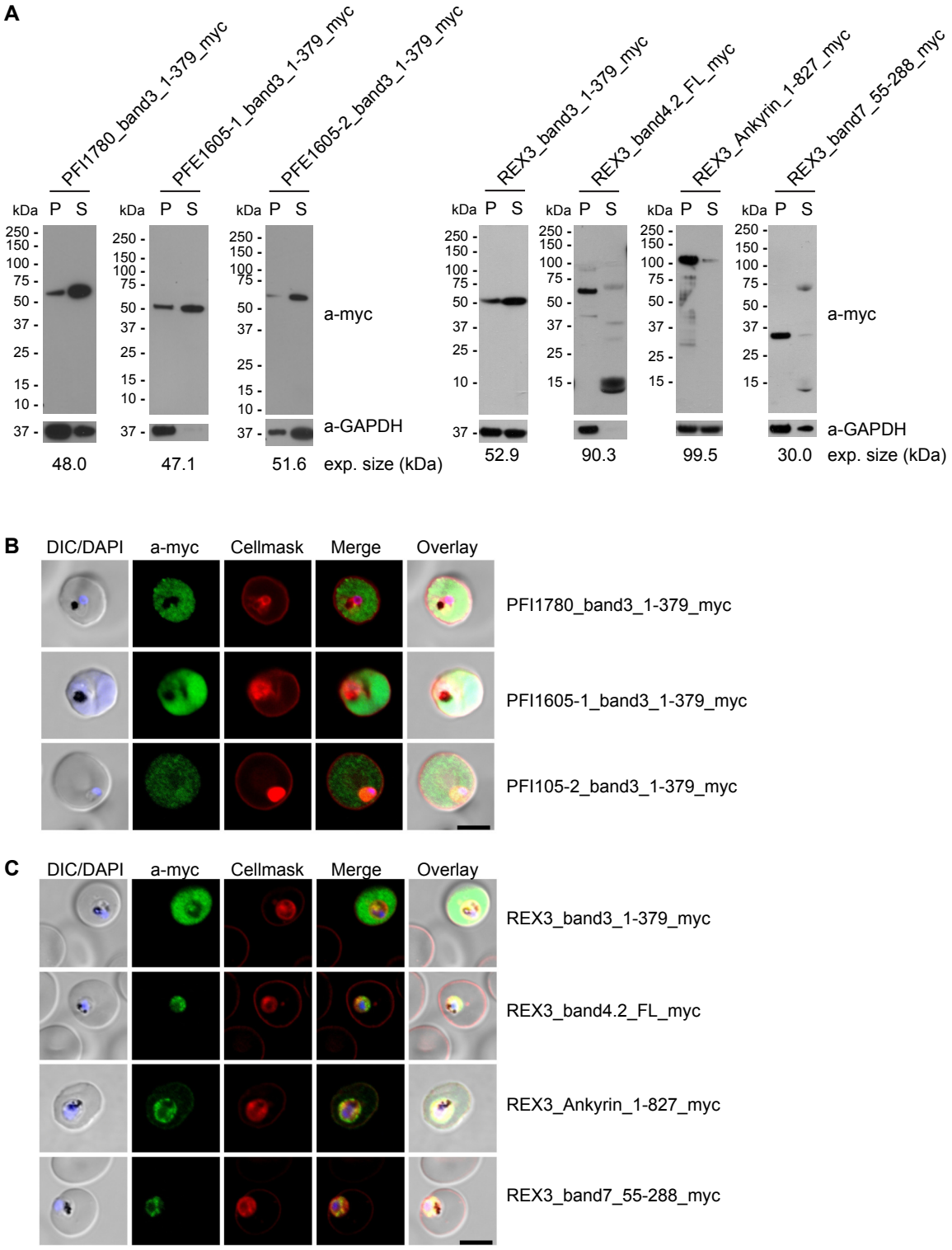
A
PFI1780_band3_1-379_myc
PFE1605-1_band3_1-379_myc
PFE1605-2_band3_1-379_myc
REX3_band3_1-379_myc
REX3_band4.2_FL_myc
REX3_Ankyrin_1-827_myc
REX3_band7_55-288_myc
kDa P S
250 150 100 75 50 37 25 15 10
a-myc
a-GAPDH
48.0
47.1
51.6
exp. size (kDa)
52.9
90.3
99.5
30.0
exp. size (kDa)
B
DIC/DAPI
a-myc
Cellmask
Merge
Overlay
PFI1780_band3_1-379_myc
PFI1605-1_band3_1-379_myc
PFI105-2_band3_1-379_myc
C
DIC/DAPI
a-myc
Cellmask
Merge
Overlay
REX3_band3_1-379_myc
REX3_band4.2_FL_myc
REX3_Ankyrin_1-827_myc
REX3_band7_55-288_myc

Figure 3

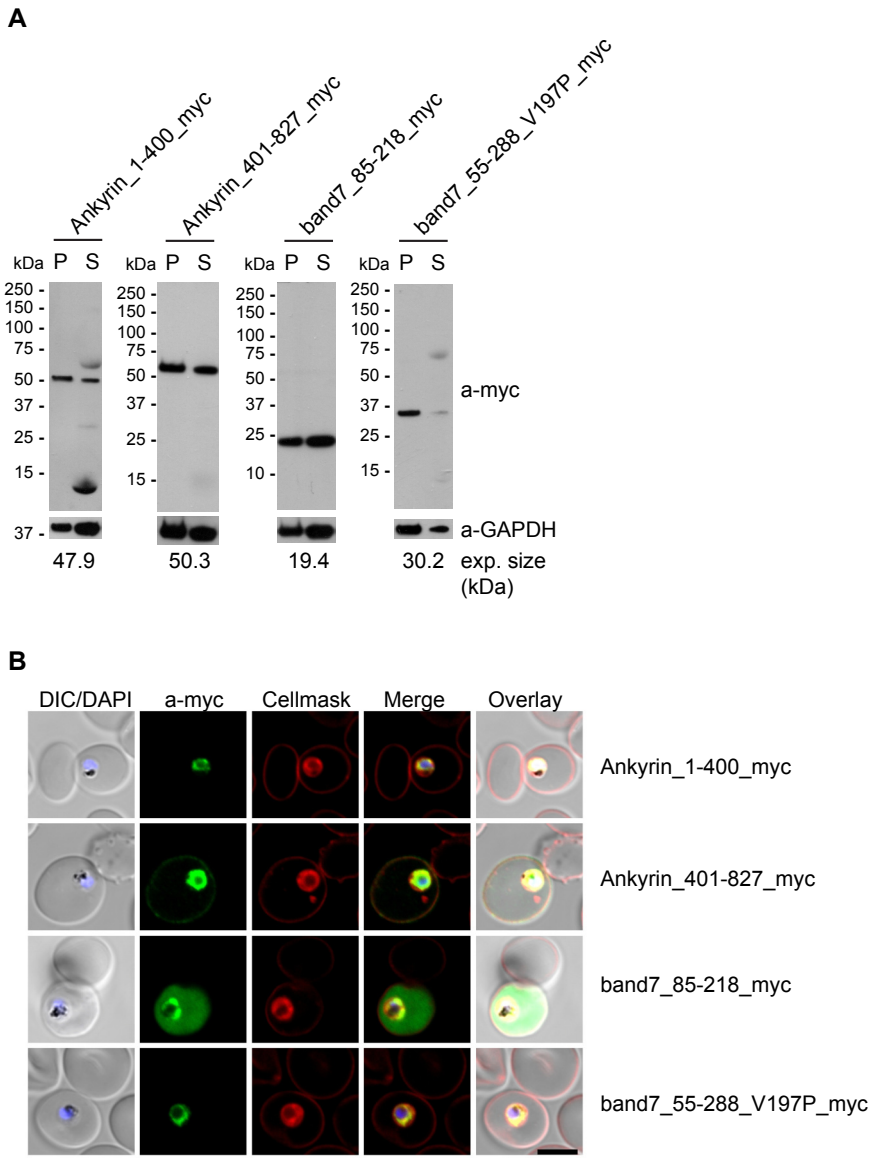
A
Ankyrin_1-400_myc
Ankyrin_401-827_myc
band7_85-218_myc
band7_55-288_V197P_myc
kDa P S
250
150
100
75
50
37
25
15
10
a-myc
a-GAPDH
47.9
50.3
19.4
30.2
exp. size (kDa)
B
DIC/DAPI
a-myc
Cellmask
Merge
Overlay
Ankyrin_1-400_myc
Ankyrin_401-827_myc
band7_85-218_myc
band7_55-288_V197P_myc

Figure 4

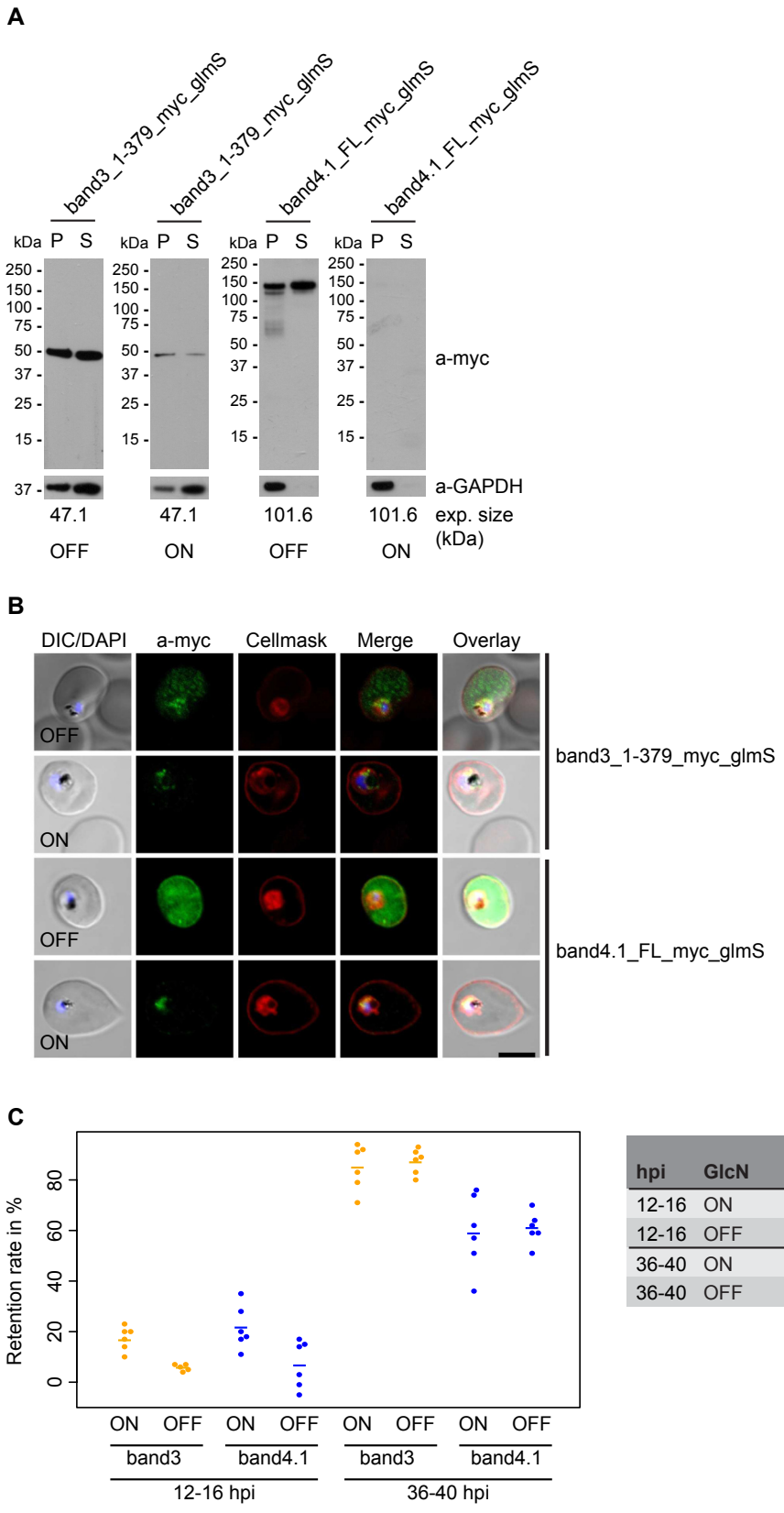

hpi	GlcN	mean retention rates in % band3	band4.1
12-16	ON	17	22
12-16	OFF	6	7
36-40	ON	85	59
36-40	OFF	87	61

Figure S1

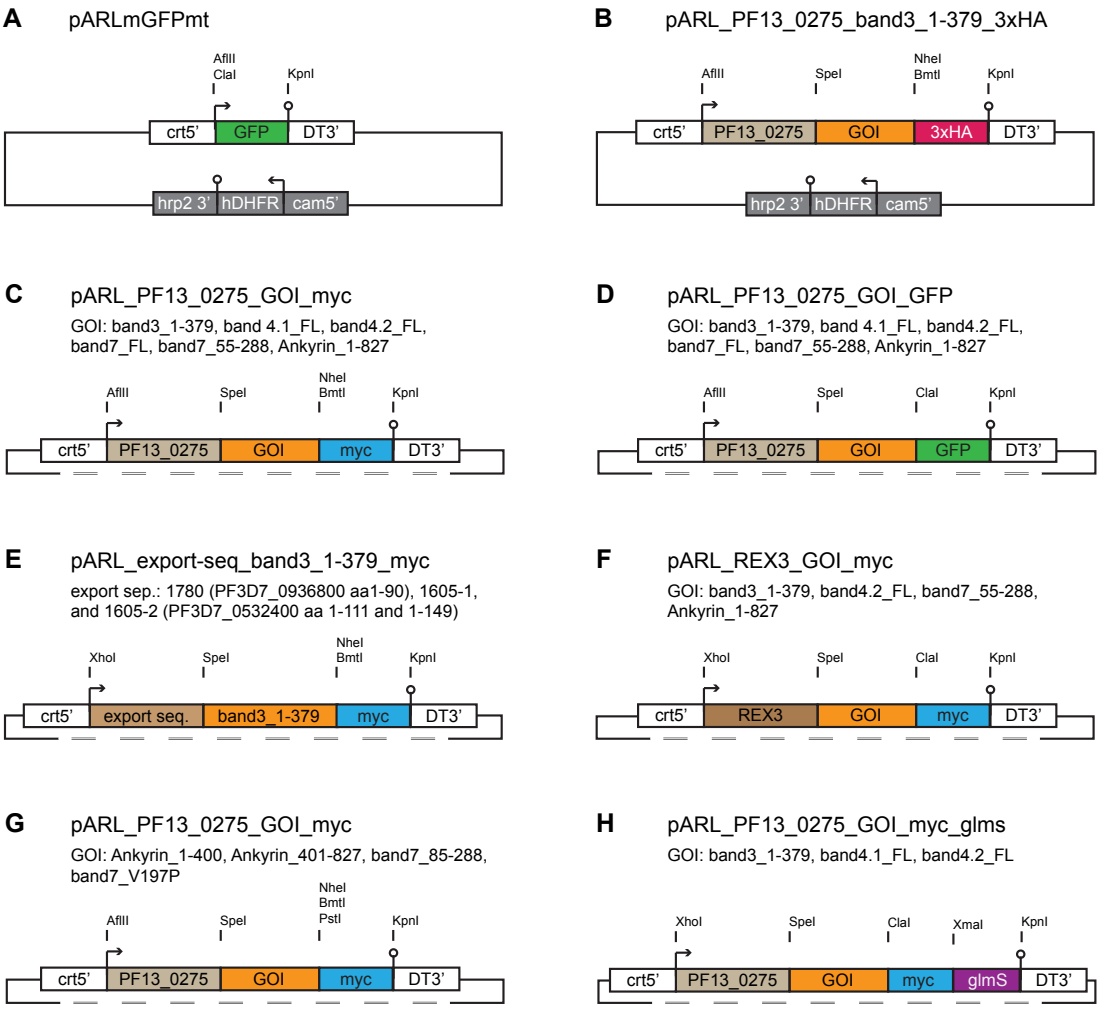
A
pARLmGFPmt
AflII
ClaI
KpnI
crt5'
GFP
DT3'
hrp2 3'
hDHFR
cam5'
B
pARL_PF13_0275_band3_1-379_3xHA
AflII
SpeI
NheI
BmtI
KpnI
crt5'
PF13_0275
GOI
3xHA
DT3'
hrp2 3'
hDHFR
cam5'
C
pARL_PF13_0275_GOI_myc
GOI: band3_1-379, band 4.1_FL, band4.2_FL, band7_FL, band7_55-288, Ankyrin_1-827
AflII
SpeI
NheI
BmtI
KpnI
crt5'
PF13_0275
GOI
myc
DT3'
D
pARL_PF13_0275_GOI_GFP
GOI: band3_1-379, band 4.1_FL, band4.2_FL, band7_FL, band7_55-288, Ankyrin_1-827
AflII
SpeI
ClaI
KpnI
crt5'
PF13_0275
GOI
GFP
DT3'
E
pARL_export-seq_band3_1-379_myc
export sep.: 1780 (PF3D7_0936800 aa1-90), 1605-1, and 1605-2 (PF3D7_0532400 aa 1-111 and 1-149)
XhoI
SpeI
NheI
BmtI
KpnI
crt5'
export seq.
band3_1-379
myc
DT3'
F
pARL_REX3_GOI_myc
GOI: band3_1-379, band4.2_FL, band7_55-288, Ankyrin_1-827
XhoI
SpeI
ClaI
KpnI
crt5'
REX3
GOI
myc
DT3'
G
pARL_PF13_0275_GOI_myc
GOI: Ankyrin_1-400, Ankyrin_401-827, band7_85-288, band7_V197P
AflII
SpeI
NheI
BmtI
PstI
KpnI
crt5'
PF13_0275
GOI
myc
DT3'
H
pARL_PF13_0275_GOI_myc_glms
GOI: band3_1-379, band4.1_FL, band4.2_FL
XhoI
SpeI
ClaI
XmaI
KpnI
crt5'
PF13_0275
GOI
myc
glmS
DT3'

Figure S2

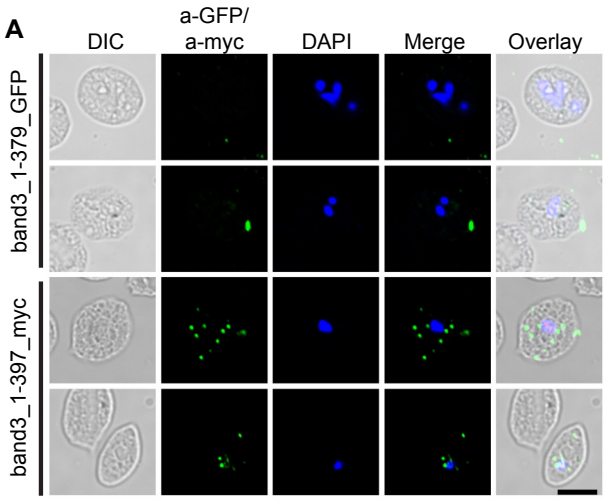
A
DIC
a-GFP/
a-myc
DAPI
Merge
Overlay
band3_1-379_GFP
band3_1-397_myc

Table S1

Primer Name	Sequence (5′ -> 3′)
Cloning Primers pARL constructs	
band3_1-379_GFP/ HA/myc	ATAACTCGAGCTTAAtccATGAAGACATACAATTC
band3_1-379_GFP	CCTTTACTCATATCGATAAACAATTGACCAGTTTGCTG
band3_1-379_HA	CCTCGACCCGGGATGGTACCTCAGGCATAATCTGGAACATCG
band3_1-379_myc	CCTCGACCCGGGATGgtacctcataaatcttcttcacttattaatttttg
band3_1-379_myc	TCATAAATCTTCTTCACTTATTAATTTTTGTTCCCTAAGCACCACGCTA G
band3_1-379_myc	TCTTCACTTATTAATTTTTGTTCCCTAAGCACCACGCTAG
band_4.2_FL_myc	TGGAGAACGTACTAGTATGGGACAAGGAGAACCAAGTCAAAG
band_4.2_FL_myc	TAAGCACCACGCTAGCGGCACTTAACTCTGGTGCTAC
band 7_FL_myc	TGGAGAACGTACTAGTATGGCAGAAAAGAGACATACAAGAGATAG
band 7_FL_myc	TAAGCACCACGCTAGCCCCTAAATGTGAATGTTTAGCAC
band 7_55-288_myc	TGGAGAACGTACTAGTAAAATTATTAAAGAGTATGAAAGAGCC
band 7_55-288_myc	CCTCGACCCGGGATGGTACCTC
band4.1_FL_myc	TGGAGAACGTACTAGTATGACAACAGAAAAAAG
band4.1_FL_myc	tccctaagcaccacgctagcTTCATCAGCTAT
Ankyrin_1-827_myc	TGGAGAACGTACTAGTATGCCATATAGTGTTGG
Ankyrin_1-827_myc	tccctaagcaccacgctagcAAATGATATTAATTCTTC
band4.2_FL and 7_FL_GFP	ataactcgagcttaagATGAAGACATACAATTCTTTAAAT
band4.2_GFP	cctttactcatatcgatGGCACTTAACTCTGGTG
band7_FL_GFP	cctttactcatatcgatCCCTAAATGTGAATGTTTAG
band 7_55-288_GFP	TGGAGAACGTACTAGTAAAATTATTAAAGAGTATGAAAGAGCC
band 7_55-288_GFP	CCTCGACCCGGGATGGTACCAG
band4.1_FL and Ankyrin_1-827_GFP	ataactcgagcttaagATGAAGACATACAATTCTTTAAAT

Primer Name	Sequence (5′ -> 3′)
band4.1_FL_GFP	cctttactcatatcgatTTCATCAGCTATTTCTGTTTC
Ankyrin_1-827_GFP	cctttactcatatcgatAAATGATATTAATTCTTCTCCTTC
band3_1-379 and 4.1_FL_myc_glms	AAGAAGATTTATGAGGTACCTCTTGTTCTTATTTTCTCAATAG
band3_1-379 and 4.1_FL_myc_glms	TATCCCTCGACCCGGGATTTTTCTTCCTCCTAAGATTG

Cloning Primers Export Sequences

1780_b3_1-379_myc	aaactcgagATGGCTGTTAGTACATATAATAATAC
1780_b3_1-379_myc	aaaactagtTATTTCGTCACTTAATGATTTC
1605_1/2_band3_myc	AAACTCGAGATGAGGTTTACTAATTCATTATATTCG
1605_1_band3_myc	AAAACTAGTAGATGCAATAAACATATCAGG
1605_2_band3_myc	ATATATACACTAGTATAAGGTACTTTATTATG
band3,4.2,7,Ank_myc	TTACATATAACTCGAGATGCAAACCCGTAAATATAATAAGATG
band7_55-288_myc	TAATAATTTTACTAGTTGCTTCTATATGTGATGACTCTGC
band4.2_FL_myc	CTGTTGTCATACTAGTTGCTTCTATATGTGATGACTCTGC
band3_1-379_myc	ATTCTTCCATACTAGTTGCTTCTATATGTGATGACTCTGC
ankyrin1-827_myc	TATATGGCATACTAGTTGCTTCTATATGTGATGACTCTGC

Cloning Primers Mutations and Truncations

band7_85-218_myc	TGGAGAACGTACTAGTCTTCCATGTACAGATAGTTTTATAAAAGTAG
band7_85-218_myc	taagcaccacgctagcTCTTGCTTCACGACTAGCTTCTGC
b7_55-288_myc_V179P	GAAGTTGTACAGGTAATTTTGGGTCTTTTATC
b7_55-288_myc_V179P	GACTAGCTTCTGCTTCTGCAGCCATTGCTCTTTGAAGTTGTACAGGTA
Ankyrin_1-400_myc	TGGAGAACGTACTAGTATGCCATATAGTGTTGGTTTTAGAG

Primer Name	Sequence (5′ -> 3′)
Ankyrin_1-400_myc	taagcaccacgctagcAACAGCATCAATACTTGCACCTG
Ankyrin_401-827_myc	TGGAGAACGTACTAGTACAGAATCAGGATTAACACCATTAC
Ankyrin_401-827_myc	taagcaccacgctagcAAATGATATTAATTCTTCTCCTTCATC

Sequencing Primers

pARL_fwd	TATATATATATATATATTTATAATATGTATATTTTAAACTAGAAAAGG
pARL_rv	AAAAATTCATATGTATTTTTTTTGTAATTTCTGTGTTTATG
multiple	CATACTAGCCATTTTATGTGTGTAAAG
pARL_fwd	TATTTTTAGACTATAATATCCG
5'GFP_rev (pARL)	ATTTGTGCCCATTAACATCACCATC
pARL_rv	GTTCATAATTTTAGCTATTTACATG
band 4.2	CATTTCCCATATCTTCATTAGGTG
band 4.2	TGTTAGGAAGTTGTGATTTAGTAC
band 7	TTCGATTAGGTAGGATATTACAAG
band 3	AGAGTATTTACCAAAGGAACTGTG
b4.1FL_GFP	GATTTACATTCATTAAGTTCAG
b4.1FL_GFP	TTTAGGAGTTTGTAGTTCAG
Ank_1-827_myc	AGGTCATGAAAATGTTGTAG
Ank_1-827_myc	AAATGCAAAAGCTAAAGATG

Chapter 6: Gametocyte PHIST Protein GEXP02

Manuscript in preparation for submission

The PHIST Protein GEXP02 Targets the Host Cytoskeleton During Sexual Development of *Plasmodium falciparum*

Jan D. Warncke[a,b,#], Armin Passecker[a,b,#], Enja Kipfer[a,b,c], Françoise Brand[a,b], Lara Pérez-Martínez[d], Nicholas I. Proellochs[e], Taco W.A. Kooij[e], Falk Butter[d], Till S. Voss[a,b*], Hans-Peter Beck[a,b*]

[a] Department of Medical Parasitology and Infection Biology, Swiss Tropical and Public Health Institute, Basel, Switzerland

[b] University of Basel, Basel, Switzerland

[c] Department of Dermatology, Inselspital, Bern University Hospital, University of Bern, Switzerland

[d] Quantitative Proteomics, Institute of Molecular Biology (IMB), Mainz, Germany

[e] Medical Microbiology, Radboud Institute for Molecular Life Sciences, Radboud University Medical Center, PO Box 9101, 6500 HB Nijmegen, The Netherlands

[#] these authors contributed equally [*] corresponding authors:

Hans-Peter Beck, Swiss TPH, Socinstrasse 57, CH-4051 Basel, Switzerland, phone +41 61 284 81 16, fax: +41 61 284 81 01, hans-peter.beck@unibas.ch

Till Voss, Swiss TPH, Socinstrasse 57, CH-4051 Basel, Switzerland, phone +41 61 284 81 61, fax: +41 61 284 81 01, till.voss@swisstph.ch

ORCID IDs

Jan Warncke: 0000-0001-6852-4191

Armin Passecker: 0000-0002-5970-3339

Enja Kipfer: 0000-0001-5870-6784

Taco WA Kooij: 0000-0002-8547-7523

Falk Butter: 0000-0002-7197-7279

Till Voss: 0000-0002-1464-4988

Hans-Peter Beck: 0000-0001-8326-4834

Nicholas Proellochs: 0000-0003-3750-1135

Abstract

A hallmark of the biology of *Plasmodium falciparum* blood stage parasites is their extensive host cell remodeling, facilitated by parasite proteins which are exported into the erythrocyte. Although this area has received extensive attention, only a few exported parasite proteins have been analyzed in detail and much of this remodeling process remains unknown, particularly for gametocyte development. Recent advances to induce high rates of sexual commitment enable the production of large numbers of gametocytes. We used this approach to study the Plasmodium helical interspersed subtelomeric (PHIST) protein GEXP02, which is expressed during sexual development. We show by immunofluorescence that GEXP02 is exported to the gametocyte-infected host cell periphery. Co-immunoprecipitation revealed potential interactions between GEXP02 and components of the erythrocyte cytoskeleton as well as other exported parasite proteins. This indicates that GEXP02 targets the erythrocyte cytoskeleton and is likely involved in its remodeling. GEXP02 knock-out parasites show no obvious phenotype during gametocyte maturation, transmission through mosquitoes, and hepatocyte infection, suggesting auxiliary or redundant functions for this protein. In summary, we performed a detailed cellular and biochemical analysis of a sexual stage-specific exported parasite protein using a novel experimental approach that is broadly applicable to study the biology of *P. falciparum* gametocytes.

Introduction

Despite major elimination efforts, the death toll due to malaria was more than 400,000 in 2017, mostly attributed to *Plasmodium falciparum* and occurring in Sub-Saharan Africa (1). A major hurdle in elimination programs is the transmission of parasites to the anopheline vector. While pathogenicity of malaria is exclusively linked to asexually replicating blood-stage parasites, gametocytes are required for malaria transmission (2). In each replication cycle during blood infection, a small sub-population of schizont stage parasites commit to sexual development, releasing merozoites that will differentiate into either male or female gametocytes upon red blood cell (RBC) invasion (3-6). During gametocytogenesis, *P. falciparum* parasites differentiate through five distinct morphological stages within approximately 10 to 12 days (7) into mature stage V gametocytes that are infective to the mosquito vector.

Proteins which are exported from the parasite into the host cell play a central role in *P. falciparum* biology and are important for parasite survival and virulence. During export, they have to cross the parasite plasma membrane and parasitophorous vacuole membrane. A pentameric amino acid motif termed Plasmodium export element (PEXEL) is found in most exported proteins and targets them for export (8, 9). These proteins enter the secretory pathway and are discharged into the parasitophorous vacuole from where they are translocated by the Plasmodium translocon of exported proteins (PTEX) into the erythrocyte cytosol (10). Some exported PEXEL-negative proteins (PNEP) have been identified. While less is known about the export pathway of PNEPs, it seems to converge with that of PEXEL proteins. Once in the host cell cytosol, exported proteins are further trafficked to their final destination where they are involved in processes such as remodeling of the cytoskeleton, formation of knobs, rigidification, and cytoadhesion in asexual intraerythrocytic stages (11-13). Amongst the proteins known or predicted to be exported are 89 which belong to the Plasmodium helical interspersed subtelomeric (PHIST) family (8, 9, 14, 15). Several PHIST proteins have been shown to localize to and interact with the erythrocyte cytoskeleton in asexual stages of *P. falciparum* (15-18) and have thus been proposed to play a role in the remodeling of the erythrocyte cytoskeleton.

While little is known about the role of exported proteins in asexual stages, even less is known about their function during gametocytogenesis. However, it seems that the cytoskeleton of the gametocyte-infected erythrocyte (GIE) is extensively remodeled from early stage I to mature stage V. Host cell rigidity increases to reach its maximum in stage III and then drops during maturation from stage IV to stage V (19, 20). Only the deformable banana-shaped stage V gametocytes are

found in peripheral circulation whilst stage I-IV gametocytes sequester in the bone marrow (21-23). Gametocyte sequestration and the resulting protection from host immunity might be facilitated by this cytoskeleton remodeling, enabling the parasite to complete its sexual maturation. Understanding the processes underlying the changes in GIE rigidity and sequestration properties could lead to new ways of interfering with malaria transmission. Although, exported Plasmodium proteins are expected to drive many of the involved modifications and interactions with the GIE cytoskeleton, there is a clear lack of knowledge about the role of exported proteins in host cell remodeling during gametocyte development (24, 25).

Here, we studied PF3D7_1102500 (GEXP02), one of several early gametocyte exported proteins, which belongs to the PHISTb protein family (26). We show that GEXP02 is expressed throughout gametocyte development and demonstrate that it localizes at and associates with the GIE cytoskeleton. Through co-immunoprecipitation (co-IP) followed by liquid chromatography tandem mass spectrometry (LC-MS/MS), we identified potential GEXP02 interaction partners and validated two of these interactions with dual-labeling confocal imaging. gexp02 knock-out parasites showed no changes in cell deformability, retained the capacity to exflagellate, infect mosquitoes, and produce viable sporozoites that were able to infect liver cells. Hence, GEXP02 seems to be another dispensable exported protein in *P. falciparum*, which underpins the point that parasites employ redundant mechanisms for crucial biological processes.

Methods

Parasite Culture

Parasites were cultured according to established standard methods (27). Synchronous parasites were obtained by sorbitol lysis of late stage asexual parasites (28) or Percoll density gradient centrifugation (29). 3D7/GDV1-GFP-DD parasites (30) (here renamed 3D7GDV1) were cultured in parasite culture medium (PCM) supplemented with 0.5% Albumax II (Gibco) in presence of 5 nM WR99210 (Jacob Pharmaceuticals, Cologne, Germany). 3D7GDV1/GEXP02-HA, 3D7GDV1/GEXP02-tdTomato, 3D7/GEXP02-HA/0424600-GFP and 3D7GDV1/GEXP02-KO parasites were cultured on 5 nM WR99210 and 2.5 µg/ml Blasticidin-S-hydrochloride (BSD) (Sigma). NF54/GEXP02-KO was cultured in PCM supplemented with 10% heat-inactivated human serum (AB+) on 2.5 µg/ml BSD (Sigma).

Induction of gametocytogenesis of 3D7GDV1, 3D7GDV1/GEXP02-HA and 3D7GDV1/GEXP02-KO was performed as described previously (30). Briefly, synchronized ring stage parasites were seeded to a parasitemia of 1.5% at 5% hematocrit and treated with 337.5 nM Shield-1 for 48 hours to stabilize GDV1-GFP-DD expression. During re-invasion, cultures were kept under shaking conditions at 45 rpm to enrich for single parasite RBC infections. After re-invasion, parasites were cultured without selection drug in PCM supplemented with 50 mM GlcNAc for five days to eliminate asexual stages. Gametocyte cultures were then maintained in PCM until the desired gametocyte stages were observed in Giemsa smears. 3D7/GEXP02-HA/0424600-GFP gametocytes were generated by overgrowing a synchronous parasite population leading to the death of asexual parasites and the survival of developing gametocytes.

For NF54 and NF54/GEXP02-KO parasites, gametocytogenesis was induced as previously published (31). In brief, late stage parasites were obtained using a Percoll density gradient, allowed to re-invade fresh RBCs and synchronized eight hours later by sorbitol treatment. At 24-30 hours post invasion (hpi), parasites were washed once and then cultured in minimal fatty acid medium (RPMI-1640 medium supplemented with 25 mM HEPES, 100 µM hypoxanthine, 24 mM $NaHCO_3$, 390 mg/100 ml fatty acid-free BSA, 30 µM palmitic acid, 30 µM oleic acid). Upon re-invasion, parasites were fed with serum-supplemented PCM containing 50 mM GlcNAc for five days to eliminate asexual stages and afterwards parasites were fed every second day with serum-supplemented PCM.

Cloning

3D7GDV1/GEXP02-HA parasites were obtained by single crossover integration of the pB_GEXP02-HA plasmid into the parasite genome. To obtain pB_GEXP02-HA, pBcam(3xHA)M1 (32) was digested with BglII and BmtI and the vector backbone pB_3xHA was purified from an agarose gel to remove the fragment containing the promoter and mahrp1 coding sequence. The 1,600 bp 3' homology region from gexp02 was PCR amplified using primers GsePb1 forward (#1) and GsePb1 reverse (#2) and cloned into the purified pB_3xHA backbone using T4 ligase. After transfection, parasites were selected on 2.5 µg/ml BSD until a stable population was obtained. To enrich for parasites carrying the integrated plasmid BSD pressure was removed for four weeks (OFF BSD) followed by re-challenge with 2.5 µg/ml BSD (ON BSD). This OFF/ON BSD cycle was repeated two more times. After PCR confirmation of plasmid integration, these parasites were

transfected with pHcam-GDV1-GFP-DD (30) to obtain the GEXP02-HA-tagged inducible gametocyte producing cell line 3D7GDV1/GEXP02-HA.

3D7GDV1/GEXP02-tdTomato parasites were generated as described above by single crossover integration of the pARL_GEXP02-tdTomato plasmid. pARL_GEXP02-tdTomato was cloned by replacing the crt promoter and gfp in the pARL_mGFP vector (33) with a multi-cloning site into which the 3' homology region of gexp02 (primers GsePb1 forward tomato (#3) and GsePb1 reverse tomato (#4)) was inserted using PstI/SalI, followed by insertion of a synthetic *P. falciparum* codon-optimized tdtomato sequence PCR-amplified from pEX-K4-Tomato_opt (Eurofins genomics, Germany) with primers TdT_F_SalI (#21) and TdT_R_KpnI (#22) (Document S1) using SalI/KpnI. Upon PCR confirmation of plasmid integration, these parasites were transfected with pHcam-GDV1-GFP-DD (30) to obtain the GEXP02-tdTomato-tagged inducible gametocyte producing cell line 3D7GDV1/GEXP02-tdTomato.

To generate 3D7GDV1/GEXP02-KO and NF54/GEXP02-KO parasites, the respective wild type parasites were transfected with the CRISPR-Cas9 plasmid p_gC-GEXP02KO. To obtain p_gC-GEXP02KO, three PCR products comprising 5' (346 bp) and 3' (331 bp) homology boxes flanking a blasticidin deaminase resistance cassette were inserted into EcoRI/HindIII-digested p_gC (30) using Gibson cloning (34). The homology regions were amplified from 3D7 gDNA (5' box, primers #5 and #6; 3' box, primers #9 and #10) and the resistance cassette was amplified from pBcam(3xHA)M1 (32) (primers #7 and #8). Finally, two complementary oligonucleotides (#11 and #12) encoding the guide RNA (nucleotides +811 to +831 with respect to gexp02 start codon) and appropriate single-stranded overhangs were annealed and ligated into the gRNA expression cassette in this intermediate BsaI-digested vector using T4 ligase. After transfection with this CRISPR-Cas9 KO vector parasites were selected on 2.5 µg/ml BSD until drug-resistant stable 3D7/GEXP02-KO and NF54/GEXP02-KO populations were obtained. The successful gexp02 knock-out was confirmed by PCR. 3D7/GEXP02-KO parasites were further transfected with pHcam-GDV1-GFP-DD (30) to obtain the inducible gametocyte producing GEXP02-KO cell line 3D7GDV1/GEXP02-KO. For the PF3D7_0424600-GFP construct, *P. falciparum* 3D7 cDNA was prepared using the ImProm-II Reverse transcriptase System (Promega, Switzerland). The coding region of pf3d7_0424600 was amplified from cDNA and cloned into the pARL_mGFP vector (33) using AflII and ClaI. The episomal pARL_0424600-GFP vector was transfected into 3D7/GEXP02-HA parasites followed by selection on 5nM WR99210 and 2.5 µg/ml BSD until stably propagating

double transgenic 3D7/GEXP02-HA/0424600-GFP parasites were obtained. All primers are listed in Table S1.

Western blots

For Western blots, 500 µl blood pellets from ring stage, trophozoite, schizont, and stage I to III gametocyte cultures were harvested and lysed, whereas 1.5 ml and 3 ml blood pellets were harvested for stage IV and stage V gametocytes, respectively. RBC pellets were lysed in eight pellet volumes 0.03% saponin in PBS on ice for 10 min. The washed parasite pellets were dissolved in 200 µl sample loading buffer supplemented with 1x Complete Protease Inhibitor (PIC; Roche) and DNase I (75ug/ml) (Sigma). Samples were sonicated for 5 min at 30 sec intervals at high intensity (Bioruptor, Diagenode) and stored at -20°C until further use. Sample preparation for solubility assays was done as described previously (35).

Parasite lysates were thawed and boiled at 95°C for 5 min, pulse-vortexed and centrifuged at full speed for 1 min. 10 µl of supernatant were loaded onto a 4-12% or 12% NOVEX NuPAGE Bis-Tris gel and run in MOPS or MES buffer (Life Technologies). Proteins were blotted using the iBlot 2 (Life Technologies) at program P0 and subsequently membranes were blocked in 5% milk in TNT (100 mM Tris, 150 mM NaCl, 43 mM HCl, and 0.1% Tween 20). Antibodies were diluted in milk/TNT. Mouse anti-MAHRP1 (1:500), mouse anti-GAPDH (1:10,000), rabbit anti-GEXP02 (1: 1000, (36)), and rat anti-HA 3F10 (1:500; Roche), were used as primary antibodies. Goat anti-mouse-HRP (1:10,000; Pierce), goat anti-rabbit-HRP (1:5000; Jackson Immunology), and goat anti-rat-HRP (1:10,000; Southern Biotech) were used as secondary antibodies. Silver staining of gels was done with the SilverQuest Staining Kit (Invitrogen).

Trypsin Cleavage Assay

Stage III gametocytes were purified using a Percoll density gradient (29) and washed in PBS. The pellet was split and one aliquot was treated with 100 µg/ml trypsin (Sigma)/PBS for 15 min at 37°C and the control was incubated in PBS only (500 µl each). The reaction was stopped by adding 500 µl 2 mg/ml soybean trypsin inhibitor (Sigma) and samples were incubated for 15 min at room temperature. Subsequently, samples were washed once in 1 ml PBS and the pellets were lysed in 1 ml 1% Triton X-100/1 mM DTT/PBS for 5 min on ice. After two wash steps in lysis buffer the proteins were extracted in 200 µl 2% SDS/10 mM DTT/1xPIC/PBS for 30 min under vigorous

shaking at room temperature. Finally, samples were centrifuged at 16,000 g for 20 min and the supernatants were subjected to SDS-PAGE. Subsequently, proteins were blotted and the membrane was probed with rat anti-HA 3F10 (1:1000; Roche) and rat anti-Glycophorin A (1:1000 Thermo Scientific). Goat anti-mouse-HRP (1:10,000; Pierce) and goat anti-rabbit-HRP (1:5000; Jackson Immunology) were used as secondary antibodies.

Microsphiltration

Microsphiltration was performed as described by Lavazec et al. (37). Cultures were adjusted to approximately 3-4% gametocytemia at 1.5% hematocrit and 600 µl samples were injected per column. Samples were washed through the column with 5 ml medium at a flow rate of 60 ml/h. For each experiment and cell line six columns were loaded and Giemsa smears were prepared from the flow through and input samples. To determine the parasitemias of the flow through and input samples at least 1,000 cells were counted per slide. Experiments were conducted in complete PCM supplemented with 10% heat-inactivated serum. For mature gametocytes, the collection tubes were placed in a water bath at 37°C to inhibit gametocyte activation and exflagellation. No activated or exflagellated gametocytes were detected.

Exflagellation

The exflagellation capacity of NF54 and NF54/GEXP02-KO was assessed as published by Delves et al. (38). In brief, 10 µl of mature gametocyte culture at 5% hematocrit were mixed with an equal volume of exflagellation medium (100 µM xanthurenic acid in complete serum-complemented PCM) and loaded into a Neubauer improved chamber. The chamber was covered with a wet tissue and incubated for 15 minutes at room temperature. Subsequently, exflagellation centers were counted in the four outermost grids of a 5x5 16-field grid using 40x magnification on a Leica DM1000 LED microscope (Leica Microsystems, Wetzlar, Germany). RBC counts were obtained by counting the total number of RBCs in the same grids.

The percentage of exflagellating cells was obtained by dividing the number of exflagellation centers/ml (mean number of four grids x 2 (dilution factor) x 104) by the number of RBCs/ml (mean number of four grids x 2 (dilution factor) x 25 x 104) multiplied by 100 (38). The large squares in which exflagellation centers were counted contain 100 nl each, whereas the small squares in which RBCs were counted contain 4 nl each, thus the latter value was multiplied by the

factor 25 to adjust for the volume. Gametocytemia was determined by counting at least 1,000 RBCs on a Giemsa smear of the same culture.

Standard Membrane-Feeding Assay

Anopheles stephensi mosquitoes were reared with a 12 hour day/night cycle at 30°C and 70-80% humidity. Female mosquitoes at ages 1-5 days were used in standard membrane-feeding assay (SMFA) (39, 40). *P. falciparum* NF54 gametocytes from both parental and NF54/GEXP02-KO lines were obtained from a starting culture of 0.5% parasitemia and cultured with continuous shaking for two weeks in an automated suspension culture system (41). On day 14 the number of mature gametocytes and the male:female ratio was estimated using Giemsa-stained thin smears and by counting exflagellation centers. The SMFA was prepared using 1 ml gametocyte culture that was added to 600 µl of washed packed RBCs. Cells were spun down for 20 sec at 10,000 rpm and resuspended in 600 µl of pre-warmed normal human sera (37°C). Samples were added to pre-warmed glass feeding devices and 100-150 laboratory raised female mosquitoes were allowed to feed for 10 min. Subsequently, all non-fed mosquitoes were removed and the remaining blood fed mosquitoes were kept at 26°C and 70-80% humidity. On day 7 post feeding 10-20 mosquitoes were collected and dissected. The midgut contents were stained with 1% mercurochrome for oocysts counts. On day 14 post feeding the salivary glands of a minimum of 30 mosquitoes were collected and pooled into 1 ml PBS and sporozoites were counted in a Bürker Türk counting chamber for a total of four counts per parasite line.

NF54wt and the NF54/GEXP02-KO parasites lines were allowed to passage through mosquitoes (as described above) with slavery gland sporozoites collected on day 15. Primary human hepatocytes were incubated with either 10,000 sporozoites for traversal (42) or 50,000 sporozoites (43) per well as previously described from both the knockout and parental line. Briefly, sporozoites for the traversal assay were incubated in conjunction with fluorescein isothiocyanate (FITC)-dextran and positive (traversed) hepatocytes counted via flow cytometry (42). For the invasion assay infected hepatocytes were fixed in and permeabilised and detected with 3SP2-FITC antibodies (43) and counted by flow cytometry.

Microscopy

For live cell imaging, 0.5 ml culture was centrifuged at 1200 rpm for 2 min and the pellet was resuspended in 0.5 ml pre-warmed PCM. Two µl Hoechst stain (500 µg/ml) were added to the sample and incubated for 15 min at 37°C in the dark, after which the cells were pelleted, washed and resuspended in one pellet volume PCM. Three µl of Vectashield mounting solution was added to 3 µl cell suspension and covered with a coverslip.

Immunofluorescence assays (IFA) were performed either on methanol-fixed thin blood smears (100% methanol, -20°C, 2 min) or, to retain the three dimensional structure of the GIEs, on cells cross-linked with 4% paraformaldehyde/0.01% glutaraldehyde as described by Tonkin et al. (44). Sheared GIEs as described by Dearnley et al. (24) were blocked with 3% BSA in PBS and subsequently incubated with antibodies. The shearing of infected erythrocytes was done as previously described (24, 45). Immediately after shearing the slides were blocked in 3%BSA/PBS and then probed with antibodies. In all microscopy assays rat anti-HA 3F10 (1:100; Roche), mouse anti-Pfs16 (1:500), rabbit anti-GFP (1:200; Abcam), rabbit anti-GEXP02 (1:1000 (36)), mouse anti-PFI1780w (1:1000; (17)), and mouse anti-glycophorin A (1:200; Abcam) were used as primary antibodies, and the matching combination of goat anti-mouse, anti-rabbit, or anti-rat conjugated with Alexa Flourophores 405, 488, or 594 (all 1:200; Invitrogen) were used as secondary antibodies. Nuclei were stained with DAPI (Vector Laboratories, Inc.) and membranes with Cellmask deep red plasma membrane stain (Invitrogen). Images were acquired with a Leica DM 5000 B in combination with the LAS 4.9.0 software or with a Zeiss LSM700 upright confocal microscope, using the ZEN 2010 software and processed with Omero 5.3.3, Imaris 8.4, and ImageJ 1.48v.

Electron Microscopy

For immuno-electron microscopy (iEM) stage III gametocytes were purified by Percoll density gradient, fixed in 2% PFA/0.2% glutaraldehyde in phosphate buffer pH7.4, and then embedded according to Tokuyasu et al. (46). Ultrathin sections (70 nm) were prepared on a FC7/UC7-ultramicrotome (Leica) at -120°C. The sections were immuno-gold labeled with rabbit anti-HA (1:30; Invitrogen), mouse anti-Pfs16 (1:100) and rabbit anti-mouse antibodies (1:350; Rockland) as secondary antibody against anti-Pfs16 and finally decorated with 5 or 10 nm protein A-gold, respectively (1:70; UMC, Utrecht, The Netherlands). Sections were stained with 4% uranyl acetate/

methylcellulose (1:9) and examined with a Tecnai G2 Spirit or CM100 Philips transmission electron microscope at 80 kV.

Co-Immunoprecipitation

The 3D7GDV1/GEXP02-HA parasite line was treated with Shield-1 to induce sexual conversion. 300 ml of parasite culture at 5% hematocrit and ~7-8% gametocytemia was harvested at stage III and GIEs were separated by Percoll density gradient. The pellet was resuspended in 20 ml 1% paraformaldehyde/PBS. After 30 min at 37°C the reaction was stopped by adding 4.1 ml 2.5 M glycine. Cells were pelleted, lysed in 150 µl 0.03% Saponin in PBS for 10 min at 4°C, washed, resuspended in 5.2 ml sonication buffer (50 mM Tris-HCl (pH 8.0), 10 mM EDTA, 1% SDS, 1xPIC), and sonicated in 30 s intervals for 15 min at setting 'high' (Bioruptor, Diagenode). After centrifugation (20,000 g, 4°C) 650 µl supernatant was added to 50 µl magnetic anti-HA beads (Pierce), which were washed three times in 1x binding buffer. Four identical technical replicates were set up for both the GEXP02-HA co-IP and the negative control co-IP. For the GEXP02-HA co-IP, 650 µl 2x binding buffer (50 mM Tris (pH 7.4), 300 mM NaCl, 2% Nonidet P40, 1x PIC) were added to the supernatant/bead suspension. The negative control co-IP was supplemented with 450 µl 2x binding buffer and 200 µl HA peptide in 1x binding buffer at 0.5 mg/ml. Samples were incubated over night at 4°C on a rotator, the beads were collected using a magnetic stand and the supernatant was removed. Beads were washed three times with 500 µl wash buffer (50 mM Tris (pH 7.4), 150 mM NaCl, 1 mM EDTA, 1% Nonidet P40, 1x PIC) and then washed twice in ddH2O. Beads were resuspended in 1x LDS sample buffer (Pierce), boiled for 5 min, and processed for LC-MS/MS analysis.

For the native co-IP, the 3D7GDV1/GEXP02-HA parasite line was treated with Shield-1 to induce sexual conversion. 300 ml of parasite culture at 5% hematocrit and ~7-8% gametocytemia was harvested at stage III and GIEs were separated by Percoll density gradient. The pellet was lysed in 1 ml 0.03% Saponin in PBS for 10 min at 4°C, washed, resuspended in 2 ml extraction buffer (0.2% Triton X-100 in PBS, 1 mM EDTA, 1x PIC), incubated on ice for 60 min and then pelleted (5 min, 4°C, 16,000 g). The supernatant was used to set up the co-IP using Pierce anti-HA magnetic beads that were washed three times in a 1:1 mixture of extraction and 2x binding buffer (2x binding buffer: 50 mM Tris-HCl (pH 7.4), 300 mM NaCl, 2% Nonidet P40, 1x PIC). For the GEXP02-HA co-IP, 250 µl supernatant were mixed with 250 µl 2x binding buffer and then applied to 50 µl washed beads. For the negative co-IP control, 250 µl supernatant, 170 µl 2x binding

buffer, and 80 µl HA-peptide (0.5 mg/ml in 1x binding buffer) were added to 50 µl beads. For the GEXP-02 co-IP and the negative control, four technical replicates were done each. Samples were incubated over night at 4°C on a rotator, the beads were collected using a magnetic stand and the supernatant was removed. Beads were washed three times with 500 µl wash buffer (50 mM Tris (pH 7.4), 150 mM NaCl, 1 mM EDTA, 1% Nonidet P40, 1x PIC). Proteins were then eluted with 30 µl HA-peptide and 10 µl 4x LDS sample buffer was added to the eluate which was then prepared for analysis by mass spectrometry.

LC-MS/MS analysis

Samples were loaded onto a 4%-12% gradient Bis-Tris gel (Thermo) and run in 1x MOPS buffer at 180 V for 10 min. Each lane was sliced, minced and transferred to a reaction tube, in-gel digest was then performed as previously described (47), and samples were stored on StageTips (48) until measurement. Digested peptides to be measured were separated on a 25 cm reverse-phase capillary (75 µM inner diameter, New Objective) packed with Reprosil C18 material (Dr. Maisch GmbH) and eluted with a 2 h gradient from 2%-40% acetonitrile buffer followed by a 95% acetonitrile wash-out at 200 nl/min on the Easy nLC1000 HPLC system (Thermo). Mass spectrometry measurements were performed with a Q Exactive Plus mass spectrometer (Thermo) operated with a Top10 data-dependent MS/MS acquisition method per full scan. Spray voltage was set to 2.2-2.4 kV.

Raw MS data was analyzed using MaxQuant v1.5.2.8 (49) with standard settings except match between runs and LFQ quantitation was activated. The search was performed against the human Uniprot database (81,194 entries) and the *Plasmodium falciparum* database (PlasmoDB 9.3, 5,538 entries). The proteinGroups file was filtered for known contaminants and proteins identified from the reversed database were removed prior to statistical analysis. Non-measured data points were imputed by a beta distribution at the limit of quantitation. Data was plotted as a volcano plot using the R environment with in-house scripts: log2 fold enrichment was calculated as median from the four replicates and the p-value was determined by a two-sided unpaired t-test Welch. The threshold line for enriched proteins is defined with $p = 0.05$, enrichment = 2 and $s0 = 1$.

Results

Expression and localization of GEXP02

GEXP02 is one of few PHIST proteins expressed in early gametocytes and present throughout gametocyte development (26, 50). To study GEXP02 in gametocytes we used our recently established approach to obtain high gametocyte numbers through conditional over-expression of GDV1. This system employs parasites carrying an episomal GDV1-GFP-DD expression cassette (3D7GDV1) (30). Upon addition of Shield-1, GDV1-GFP-DD is stabilized, resulting in sexual conversion rates of 50-60% (30). Hence, to test for export and localization of GEXP02, we generated the 3D7GDV1/GEXP02-tdTomato cell line, which expresses GEXP02-tdTomato under control of the endogenous promoter and contains the pHcam-GDV1-GFP-DD episomal plasmid (30). Correct tagging of the gexp02 gene was confirmed by PCR on genomic DNA (gDNA) (Figure 1A). Live fluorescence microscopy revealed that GEXP02-tdTomato localizes to the periphery of the GIE in all five gametocyte stages (Figure 1B).

We also generated a similar cell line (3D7GDV1/GEXP02-HA) where GEXP02 is tagged with a triple HA-tag because of its smaller size. Correct integration was confirmed by PCR (Figure 1A). Similar to GEXP02-tdTomato, GEXP02-HA localizes to the GIE periphery in all stages as shown by immunofluorescence assays (IFA) with a signal also observed within the parasite. We used antibodies against Pfs16, a gametocyte-specific protein localizing to the parasitophorous vacuolar membrane (PVM) (51), to confirm that GEXP02-HA was exported into the RBC in sexual stages (Figure S1A).

To compare protein abundance of GEXP02-HA in different intra-erythrocytic stages, cell lysates were prepared from each stage and run on a SDS-PAGE followed by immunoblotting. Almost no signal was detected in asexual stages, while all gametocyte stages showed strong signals. The strongest signal was detected in stage I gametocytes and signal strength declined continuously throughout the following stages (Figure 1C). To compare the total protein amount loaded for each stage, the nitrocellulose membrane was stained with Ponceau S prior to being probed with anti-HA antibodies.

We confirmed the peripheral localization of GEXP02-HA in negatively stained ultrathin sections of stage III gametocytes by immunoelectron microscopy. GEXP02-HA was decorated with 5 nm gold particles and found to be evenly distributed underneath the entire GIE membrane, while Pfs16 was decorated with 10 nm gold particles at the PVM (Figure 1D). Using differential

protein extraction from Percoll-purified 3D7/GEXP02-HA gametocytes, GEXP02-HA was extracted in carbonate buffer suggesting GEXP02 to be a membrane-associated protein (Figure 1E). Considering that both our localization and solubility data indicated that GEXP02 localizes to the GIE membrane, we wanted to determine if it associates with the cytoskeleton or whether it is exposed on the surface of the GIE. After trypsin digestion of intact, Percoll-purified stage III 3D7/GEXP02-HA GIEs, Western blot analysis showed no cleavage of GEXP02-HA in stage III GIEs confirming that GEXP02 is not surface exposed. In contrast, the abundant erythrocyte surface protein glycophorin A (52) was found cleaved in the trypsin fraction as its surface exposed C-terminus could not be detected with an anti-glycophorin A antibody that recognizes the C-terminus (Figure 1F).

All localization data suggested close proximity of GEXP02 to the cytoskeleton. To test whether there are physical interactions of GEXP02 with the cytoskeleton, we applied controlled shear forces to eliminate most of the cell structure and leave behind the cell membrane, cytoskeleton, and other structures firmly attached to it (24, 45). After probing with anti-HA antibodies and an antibody targeting the extracellular domain of glycophorin A, a substantial number of retained structures were filled with red dots (GEXP02-HA) whilst nearly all stained positive for glycophorin A, suggesting that GEXP02 binds to the cytoskeleton strongly enough to remain attached even under shearing conditions (Figure 1G). Due to the lack of a gametocyte marker that associates with the GIE cytoskeleton, we were not able to confirm that all structures derived from GIEs were GEXP02-HA-positive.

Co-immunoprecipitation of GEXP02

Purified stage III 3D7GDV1/GEXP02-HA GIEs were treated with paraformaldehyde to crosslink protein-protein interactions and processed for co-IP to identify potential interaction partners of GEXP02. After preparation of the lysate, anti-HA beads were added and half of the suspension was saturated with a molar excess of soluble HA-peptides to be used as negative control. Four technical replicates of the GEXP02-HA co-IP sample and negative control co-IP were simultaneously prepared. After washing and elution of bound proteins, samples were analyzed on a silver-stained SDS-PAGE gel. More protein bands were detected in the elution fraction of the probe than in the elution fraction of the negative control (Figure 2A). After LC/MS-MS analysis of the elution fractions a total of 570 proteins were detected among all eight samples. Of these, 66 were significantly enriched in the GEXP02-HA co-IP eluates, while only seven proteins were

enriched in the negative control co-IP (Figure 2B, Table S2). The ten erythrocyte or parasite proteins with the lowest p-value are shown in Figure 2C. In parallel, we performed another co-IP experiment under native conditions without crosslinking and only four proteins were found to be enriched, namely ankyrin, band 3, and both subunits of spectrin, all of which are part of the human band 3 complex that anchors the erythrocyte cytoskeleton to the membrane (Figure 2D) (53). The dual identification of these four cytoskeleton proteins in both immunoprecipitations (Table S2) provides strong evidence for true interactions between GEXP02 and these RBC cytoskeleton proteins.

Co-labeling of potential interaction partners

As GEXP02 is a PHIST protein, we wanted to colocalize it with other PHIST proteins that were detected in the cross-linked co-IP samples. PF3D7_0800600 and PF3D7_0115100 have the lowest p-value but also nearly identical sequences. We therefore selected PF3D7_0424600 and PF3D7_0936800 (PFI1780w), two other PHIST proteins that were also among our top ten putative GEXP02-interacting candidates (Figure 2C). We transfected 3D7/GEXP02-HA with an episomal plasmid encoding PF3D7_0424600-GFP under the regulation of the pfcrt promoter (Figure 3A) and gametocytes were obtained by overgrowing highly synchronized cultures. Stage III gametocytes were prepared for confocal microscopy and probed with anti-HA (GEXP02) and anti-GFP (PF3D7_0424600). Both localized to the GIE periphery with the latter also showing a signal within the parasite. Anti-Pfs16 was used for two reasons, first to show that the cells positive for GEXP02 are indeed gametocytes, and second to label the PVM and thus show that the GEXP02 and PF3D7_0424600 proteins localise outside the PVM. By staining membranes with CellMask we could further confirm the peripheral localization of GEXP02 and a fraction of PF3D7_0424600 (Figure 3B and Suppl. Figure 1B). Next, we labeled these double-transfected stage III GIEs with antibodies against the HA and GFP tags as well as antibodies against PFI1780w, a PHISTc protein that is exported to the iRBC membrane in asexual parasites (17). PFI1780w showed a distribution highly similar to that of GEXP02-HA, also localizing close to the GIE membrane (Figure 3C and Suppl. Figure 1C). A three-dimensional rendering was obtained from z-stacks of stage III gametocytes labeled with antibodies against GEXP02-HA, PF3D7_0424600-GFP, and PFI1780w. A surface reconstruction of signals of these three proteins showed that all three proteins localize to the same space (Figure 3D and Supplementary Video). To further confirm the colocalization of GEXP02-HA and PFI1780w at the GIE cytoskeleton, erythrocyte shearing experiments were

performed with 3D7GDV1/GEXP02-HA and co-labeled with antibodies against HA and PFI1780w, showing a nearly complete overlap of those two signals (Figure 3E) and suggesting that they act in concert on the GIE cytoskeleton.

GEXP02 is not essential for gametocyte maturation in vitro

To study the role of GEXP02 during gametocyte development and cytoskeleton remodeling, we generated two knock-out lines using CRISPR-Cas9-based gene editing: 3D7GDV1/GEXP02-KO and NF54/GEXP02-KO. Successful deletion of the gexp02 gene was confirmed by PCR (Figure 4A) and absence of GEXP02 expression from 3D7GDV1/GEXP02-KO and NF54/GEXP02-KO was confirmed by Western blotting using GEXP02-specific antibodies (36) (Figure 4B). Subsequently, the anti-GEXP02 antibody was used for fluorescence microscopy and wild-type 3D7 parasites showed strong signals for GEXP02 while only weak background signals were detected in 3D7GDV1/GEXP02-KO (Figure 4C). Compared to wild-type parasites, both knock-out parasite lines showed no obvious morphological aberrations or developmental delays over the course of all five gametocyte stages when stained with Giemsa (Figure 4D).

Gametocyte deformability, exflagellation, and mosquito and liver cell infectiousness of GEXP02-KO parasites

Next we assessed the effect of GEXP02 depletion on GIE rigidity throughout sexual stage development. Gametocyte conversion was induced in synchronized NF54wt and NF54/GEXP02-KO cultures and asexual parasites were removed by a five day treatment with GlcNAc (41). To determine the deformability of GIEs, microsphiltration experiments were performed. The retention rate in the column is positively correlated to GIE deformability (37). Microsphiltration was done with stage III and stage V gametocytes since GIE stiffness reaches the maximum during stage III and is lost in stage V gametocytes (19, 54). NF54/GEXP02-KO parasites showed no significant differences in retention rates when compared to NF54wt (Figure 4E), indicating that depletion of GEXP02 does not affect cytoskeleton rigidity and deformability in stage III or stage V gametocytes.

To test if exflagellation is impaired in absence of GEXP02, we activated stage V gametocytes of NF54/GEXP02-KO and NF54wt with xanthurenic acid and quantified exflagellation rates in biological triplicates. In all three exflagellation experiments, there was no pronounced difference

in the number of exflagellation centers in NF54/GEXP02-KO parasites compared to NF54wt, suggesting that the knock-out parasites are equally capable of exflagellating as the wild-type parasites (Figure 4F).

To further explore if the absence of GEXP02 impairs sexual stage development in the mosquito vector, we performed standard membrane feeding assays (SMFA). Stage V gametocytes of NF54/GEXP02-KO and NF54wt were fed to mosquitoes and oocysts were counted. There was no difference in oocyst numbers or numbers of sporozoites produced per oocyst, indicating that both parasite lines can be transmitted to and develop in the mosquito with similar efficiency (Figure 4G). Furthermore, sporozoites from both parasite lines were able to traverse and invade hepatocytes (Figure 4H). Combined, these data show that GEXP02 is not required for maturation of gametocytes *in vitro*, transmission to mosquitoes, sporozoite production, and hepatocyte infection.

Discussion

There is only a small number of PHIST proteins that have been shown to be expressed in gametocytes and very little is known about their function, localization, or interaction partners. Therefore, the expression of the exported PHISTb protein GEXP02 throughout all stages of gametocyte development and its localization at the host cell cytoskeleton make it an interesting candidate to study host-parasite protein interactions in gametocytes. We also detected weak signals for GEXP02 in asexual parasites by Western blot but the most likely source of GEXP02 in these samples are the small numbers of gametocytes that are always present in *in vitro* cultures. Lasonder et al. found a significant increase of GEXP02 protein levels in male compared to female gametocytes (55); however, we did not detect substantial differences in the abundance of GEXP02 by IFA analysis among individual gametocytes in GDV1-induced cultures where all gametocytes stained positive for GEXP02 with similar fluorescence intensities. While our IFA results suggest that both male and female gametocytes express GEXP02, we have not quantified GEXP02 protein abundance and cannot therefore rule out a slight difference between the sexes.

Maier and colleagues could generate gexp02 knock-out parasites in the CS2 strain background and PfEMP1 presentation and iRBC rigidity was not affected (36). Similarly, we readily obtained gexp02 knock-out parasites in 3D7 and NF54 parasites and did not observe any growth-related phenotypes in both mutants. This is not surprising given that GEXP02 is not expressed to

appreciable levels in asexual blood stage parasites. Similar to the observation in asexual parasites, depletion of GEXP02 also does not seem to affect gametocytogenesis *in vitro*. GEXP02 knock-out and wild-type gametocytes showed similar deformability properties, were able to exflagellate, infected mosquitoes with similar rates of oocyst and sporozoite production, and also showed comparable levels of hepatocyte traversal and invasion. Although there is no discernable phenotype in the GEXP02 knock-out parasite, we provide some evidence that GEXP02 might play a role in host-cell remodeling. Its localization in close proximity to the GIE membrane as shown by IFAs and immunoelectron microscopy, its solubility attributes, and the potential RBC cytoskeletal interaction partners identified by co-IP followed by LC-MS/MS analysis all suggest that GEXP02 interacts with the GIE cytoskeleton. This is strongly supported our co-purification of four host cell cytoskeleton and membrane proteins (spectrin alpha, spectrin beta, ankyrin, and band 3) with GEXP02 in both cross-linked and native co-IP experiments. The lack of an obvious loss-of-function phenotype after GEXP02 depletion might be explained by functional redundancy of proteins of the PHIST family. In *P. falciparum* 89 PHIST proteins have been identified (14, 15) and it is conceivable that other proteins containing PHIST domains could compensate for the loss of GEXP02 *in vitro*. In fact, we identified two PHIST proteins that co-localized with GEXP02 and might fulfill identical or similar roles as GEXP02. It is noteworthy that all hitherto examined PHISTb proteins target the host cytoskeleton as has been shown with several episomally over-expressed PHISTb-GFP fusion proteins (including GEXP02) (18). It is also important to realize that all gametocyte experiments reported here were performed *in vitro*, and it is conceivable that GEXP02 may play an important role in the biology of gametocytes *in vivo*, which is currently extremely difficult if not impossible to be measured for reasons of technical limitations.

This is one of the first studies to describe and characterize an exported *P. falciparum* protein in gametocytes that is involved in host cell remodeling during gametocytogenesis. It also proves the excellent value provided by a novel tool to produce large numbers of synchronous gametocytes via conditional expression of GDV1 as described by Filarsky and colleagues (30) for the detailed molecular analysis of gametocyte proteins and better understanding of gametocyte biology.

Acknowledgments

We acknowledge Alexia Loynton-Ferrand and Kai Schleicher at the IMCF, Biozentrum, University of Basel, for their support with image acquisition and analysis. We thank Henning Stahlberg and his team at C-CINA, Biozentrum, University of Basel, for the access to the EM facility. Furthermore we thank Beatrice Schibler and Eva Hitz, Swiss TPH, for assistance with the microsphiltration and exflagellation experiments, respectively. We also thank Mario Dejung from the Proteomics Core Facility at the IMB, Mainz, for providing the R Script for analysis of MS data and his assistance in the analysis process. We thank the following colleagues for sharing antibodies: Alex Maier (anti-GEXP02), Claudia Daubenberger (anti-GAPDH), and Robert Sauerwein (anti-Pfs16). Also we are thankful to Geert-Jan van Gemert and Marga van de Vegte-Bolmer for their expert assistance in the SMFA and mosquito work.

Authors contribution

JW, AP, TSV, and HPB designed the project. JW, AP, EK performed most experiments. FBr performed electron microscopy. Mosquito feeding experiments were designed by NIP and analyzed by TWAK and NIP. LP and FBu performed the LC-MS/MS experiments. JW, AP, TSV and HPB wrote the manuscript.

Conflict of interest

All authors declare no conflict of interest.

Funding Information

HPB was funded by the Swiss National Science Foundation (grant number SNF 31003A_169347). TSV received funding from the Swiss Vaccine Research Institute and the Swiss National Science Foundation (grant number BSCGI0_157729). TWAK was funded by Netherlands Organization for Scientific Research (NWO-VIDI 864.13.009) and NIP was supported by a Marie-Slodowska-Curie grant No 790085. The funders had no role in study design, data collection and analysis, decision to publish, or preparation of the manuscript.

References

1. **WHO.** 2018. World Malaria Report 2018. WHO,
2. **Aingaran M, Zhang R, Law SK, Peng Z, Undisz A, Meyer E, Diez-Silva M, Burke TA, Spielmann T, Lim CT, Suresh S, Dao M, Marti M.** 2012. Host cell deformability is linked to transmission in the human malaria parasite Plasmodium falciparum. Cell Microbiol **14:**983-993.
3. **Inselburg J.** 1983. Gametocyte formation by the progeny of single Plasmodium falciparum schizonts. J Parasitol **69:**584-591.
4. **Silvestrini F, Alano P, Williams JL.** 2000. Commitment to the production of male and female gametocytes in the human malaria parasite Plasmodium falciparum. Parasitology **121 Pt 5:**465-471.
5. **Smith TG, Lourenco P, Carter R, Walliker D, Ranford-Cartwright LC.** 2000. Commitment to sexual differentiation in the human malaria parasite, Plasmodium falciparum. Parasitology **121 (Pt 2):**127-133.
6. **Kooij TW, Matuschewski K.** 2007. Triggers and tricks of Plasmodium sexual development. Curr Opin Microbiol **10:**547-553.
7. **Hawking F, Wilson ME, Gammage K.** 1971. Evidence for cyclic development and short-lived maturity in the gametocytes of Plasmodium falciparum. Trans R Soc Trop Med Hyg **65:**549-559.
8. **Hiller NL, Bhattacharjee S, van Ooij C, Liolios K, Harrison T, Lopez-Estrano C, Haldar K.** 2004. A host-targeting signal in virulence proteins reveals a secretome in malarial infection. Science **306:**1934-1937.
9. **Marti M, Good RT, Rug M, Knuepfer E, Cowman AF.** 2004. Targeting malaria virulence and remodeling proteins to the host erythrocyte. Science **306:**1930-1933.
10. **de Koning-Ward TF, Gilson PR, Boddey JA, Rug M, Smith BJ, Papenfuss AT, Sanders PR, Lundie RJ, Maier AG, Cowman AF, Crabb BS.** 2009. A newly discovered protein export machine in malaria parasites. Nature **459:**945-949.
11. **Przyborski JM, Nyboer B, Lanzer M.** 2016. Ticket to ride: export of proteins to the Plasmodium falciparum-infected erythrocyte. Mol Microbiol **101:**1-11.
12. **Watermeyer JM, Hale VL, Hackett F, Clare DK, Cutts EE, Vakonakis I, Fleck RA, Blackman MJ, Saibil HR.** 2016. A spiral scaffold underlies cytoadherent knobs in Plasmodium falciparum-infected erythrocytes. Blood **127:**343-351.
13. **de Koning-Ward TF, Dixon MW, Tilley L, Gilson PR.** 2016. Plasmodium species: master renovators of their host cells. Nat Rev Microbiol **14:**494-507.
14. **Sargeant TJ, Marti M, Caler E, Carlton JM, Simpson K, Speed TP, Cowman AF.** 2006. Lineage-specific expansion of proteins exported to erythrocytes in malaria parasites. Genome Biol **7:**R12.

15. **Warncke JD, Vakonakis I, Beck HP.** 2016. Plasmodium Helical Interspersed Subtelomeric (PHIST) Proteins, at the Center of Host Cell Remodeling. Microbiol Mol Biol Rev **80:**905-927.

16. **Proellocks NI, Herrmann S, Buckingham DW, Hanssen E, Hodges EK, Elsworth B, Morahan BJ, Coppel RL, Cooke BM.** 2014. A lysine-rich membrane-associated PHISTb protein involved in alteration of the cytoadhesive properties of Plasmodium falciparum-infected red blood cells. FASEB J **28:**3103-3113.

17. **Oberli A, Slater LM, Cutts E, Brand F, Mundwiler-Pachlatko E, Rusch S, Masik MF, Erat MC, Beck HP, Vakonakis I.** 2014. A Plasmodium falciparum PHIST protein binds the virulence factor PfEMP1 and comigrates to knobs on the host cell surface. FASEB J **28:**4420-4433.

18. **Tarr SJ, Moon RW, Hardege I, Osborne AR.** 2014. A conserved domain targets exported PHISTb family proteins to the periphery of Plasmodium infected erythrocytes. Mol Biochem Parasitol **196:**29-40.

19. **Tiburcio M, Niang M, Deplaine G, Perrot S, Bischoff E, Ndour PA, Silvestrini F, Khattab A, Milon G, David PH, Hardeman M, Vernick KD, Sauerwein RW, Preiser PR, Mercereau-Puijalon O, Buffet P, Alano P, Lavazec C.** 2012. A switch in infected erythrocyte deformability at the maturation and blood circulation of Plasmodium falciparum transmission stages. Blood **119:**e172-180.

20. **Dixon MW, Dearnley MK, Hanssen E, Gilberger T, Tilley L.** 2012. Shape-shifting gametocytes: how and why does P. falciparum go banana-shaped? Trends Parasitol **28:**471-478.

21. **Alano P.** 2007. Plasmodium falciparum gametocytes: still many secrets of a hidden life. Mol Microbiol **66:**291-302.

22. **Nilsson SK, Childs LM, Buckee C, Marti M.** 2015. Targeting Human Transmission Biology for Malaria Elimination. PLoS Pathog **11:**e1004871.

23. **Tiburcio M, Sauerwein R, Lavazec C, Alano P.** 2015. Erythrocyte remodeling by Plasmodium falciparum gametocytes in the human host interplay. Trends Parasitol **31:**270-278.

24. **Dearnley M, Chu T, Zhang Y, Looker O, Huang C, Klonis N, Yeoman J, Kenny S, Arora M, Osborne JM, Chandramohanadas R, Zhang S, Dixon MW, Tilley L.** 2016. Reversible host cell remodeling underpins deformability changes in malaria parasite sexual blood stages. Proc Natl Acad Sci U S A **113:**4800-4805.

25. **Naissant B, Dupuy F, Duffier Y, Lorthiois A, Duez J, Scholz J, Buffet P, Merckx A, Bachmann A, Lavazec C.** 2016. Plasmodium falciparum STEVOR phosphorylation regulates host erythrocyte deformability enabling malaria parasite transmission. Blood **127:**e42-53.

26. **Silvestrini F, Lasonder E, Olivieri A, Camarda G, van Schaijk B, Sanchez M, Younis Younis S, Sauerwein R, Alano P.** 2010. Protein export marks the early phase of gametocytogenesis of the human malaria parasite Plasmodium falciparum. Mol Cell Proteomics **9:**1437-1448.

27. **Moll K, Ljungström I, Perlmann H, Scherf A, Wahlgren M.** 2008. Methods in Malaria Reserch. American Type Culture Collection, 10801 University Boulevard, Manassas, VA 20110-2209.

28. **Lambros C, Vanderberg JP.** 1979. Synchronization of Plasmodium falciparum erythrocytic stages in culture. J Parasitol **65:**418-420.

29. **Moll K, Kaneko A, Scherf A, Wahlgren M.** 2013. Methods in Malaria Reserch, 6th Edition ed. American Type Culture Collection, 10801 University Boulevard, Manassas, VA 20110-2209.

30. **Filarsky M, Fraschka SA, Niederwieser I, Brancucci NMB, Carrington E, Carrio E, Moes S, Jenoe P, Bartfai R, Voss TS.** 2018. GDV1 induces sexual commitment of malaria parasites by antagonizing HP1-dependent gene silencing. Science **359:**1259-1263.

31. **Brancucci NMB, Gerdt JP, Wang C, De Niz M, Philip N, Adapa SR, Zhang M, Hitz E, Niederwieser I, Boltryk SD, Laffitte MC, Clark MA, Gruring C, Ravel D, Blancke Soares A, Demas A, Bopp S, Rubio-Ruiz B, Conejo-Garcia A, Wirth DF, Gendaszewska-Darmach E, Duraisingh MT, Adams JH, Voss TS, Waters AP, Jiang RHY, Clardy J, Marti M.** 2017. Lysophosphatidylcholine Regulates Sexual Stage Differentiation in the Human Malaria Parasite Plasmodium falciparum. Cell **171:**1532-1544 e1515.

32. **Spycher C, Rug M, Pachlatko E, Hanssen E, Ferguson D, Cowman AF, Tilley L, Beck HP.** 2008. The Maurer's cleft protein MAHRP1 is essential for trafficking of PfEMP1 to the surface of Plasmodium falciparum–infected erythrocytes. Mol Microbiol **68:**1300-1314.

33. **Crabb BS, Rug M, Gilberger T-W, Thompson JK, Triglia T, Maier AG, Cowman AF.** 2004. Transfection of the human malaria parasite Plasmodium falciparum, p 263-276, Parasite Genomics Protocols. Springer.

34. **Gibson DG, Young L, Chuang RY, Venter JC, Hutchison CA, 3rd, Smith HO.** 2009. Enzymatic assembly of DNA molecules up to several hundred kilobases. Nat Methods **6:**343-345.

35. **Pachlatko E, Rusch S, Muller A, Hemphill A, Tilley L, Hanssen E, Beck HP.** 2010. MAHRP2, an exported protein of Plasmodium falciparum, is an essential component of Maurer's cleft tethers. Mol Microbiol **77:**1136-1152.

36. **Maier AG, Rug M, O'Neill MT, Brown M, Chakravorty S, Szestak T, Chesson J, Wu Y, Hughes K, Coppel RL, Newbold C, Beeson JG, Craig A, Crabb BS, Cowman AF.** 2008. Exported proteins required for virulence and rigidity of Plasmodium falciparum-infected human erythrocytes. Cell **134:**48-61.

37. **Lavazec C, Deplaine G, Safeukui I, Perrot S, Milon G, Mercereau-Puijalon O, David PH, Buffet P.** 2013. Microsphiltration: a microsphere matrix to explore erythrocyte deformability. Methods Mol Biol **923:**291-297.

38. **Delves MJ, Straschil U, Ruecker A, Miguel-Blanco C, Marques S, Dufour AC, Baum J, Sinden RE.** 2016. Routine in vitro culture of P. falciparum gametocytes to evaluate novel transmission-blocking interventions. Nat Protoc **11:**1668-1680.

39. **van der Kolk M, De Vlas SJ, Saul A, van de Vegte-Bolmer M, Eling WM, Sauerwein RW.** 2005. Evaluation of the standard membrane feeding assay (SMFA) for the

determination of malaria transmission-reducing activity using empirical data. Parasitology **130:**13-22.

40. **Ponnudurai T, Lensen AH, Van Gemert GJ, Bensink MP, Bolmer M, Meuwissen JH.** 1989. Infectivity of cultured Plasmodium falciparum gametocytes to mosquitoes. Parasitology **98 Pt 2:**165-173.

41. **Ponnudurai T, Lensen AH, Meis JF, Meuwissen JH.** 1986. Synchronization of Plasmodium falciparum gametocytes using an automated suspension culture system. Parasitology **93 (Pt 2):**263-274.

42. **Yang ASP, O'Neill MT, Jennison C, Lopaticki S, Allison CC, Armistead JS, Erickson SM, Rogers KL, Ellisdon AM, Whisstock JC, Tweedell RE, Dinglasan RR, Douglas DN, Kneteman NM, Boddey JA.** 2017. Cell Traversal Activity Is Important for Plasmodium falciparum Liver Infection in Humanized Mice. Cell Rep **18:**3105-3116.

43. **Mendes AM, Machado M, Goncalves-Rosa N, Reuling IJ, Foquet L, Marques C, Salman AM, Yang ASP, Moser KA, Dwivedi A, Hermsen CC, Jimenez-Diaz B, Viera S, Santos JM, Albuquerque I, Bhatia SN, Bial J, Angulo-Barturen I, Silva JC, Leroux-Roels G, Janse CJ, Khan SM, Mota MM, Sauerwein RW, Prudencio M.** 2018. A Plasmodium berghei sporozoite-based vaccination platform against human malaria. NPJ Vaccines **3:**33.

44. **Tonkin CJ, van Dooren GG, Spurck TP, Struck NS, Good RT, Handman E, Cowman AF, McFadden GI.** 2004. Localization of organellar proteins in Plasmodium falciparum using a novel set of transfection vectors and a new immunofluorescence fixation method. Mol Biochem Parasitol **137:**13-21.

45. **Shi H, Liu Z, Li A, Yin J, Chong AG, Tan KS, Zhang Y, Lim CT.** 2013. Life cycle-dependent cytoskeletal modifications in Plasmodium falciparum infected erythrocytes. PLoS One **8:**e61170.

46. **Tokuyasu KT.** 1973. A technique for ultracryotomy of cell suspensions and tissues. J Cell Biol **57:**551-565.

47. **Bluhm A, Casas-Vila N, Scheibe M, Butter F.** 2016. Reader interactome of epigenetic histone marks in birds. Proteomics **16:**427-436.

48. **Rappsilber J, Mann M, Ishihama Y.** 2007. Protocol for micro-purification, enrichment, pre-fractionation and storage of peptides for proteomics using StageTips. Nat Protoc **2:**1896-1906.

49. **Cox J, Mann M.** 2008. MaxQuant enables high peptide identification rates, individualized p.p.b.-range mass accuracies and proteome-wide protein quantification. Nat Biotechnol **26:**1367-1372.

50. **Lasonder E, Rijpma SR, van Schaijk BC, Hoeijmakers WA, Kensche PR, Gresnigt MS, Italiaander A, Vos MW, Woestenenk R, Bousema T.** 2016. Integrated transcriptomic and proteomic analyses of P. falciparum gametocytes: molecular insight into sex-specific processes and translational repression. Nucleic acids research **44:**6087-6101.

51. **Eksi S, Williamson KC.** 2011. Protein targeting to the parasitophorous vacuole membrane of Plasmodium falciparum. Eukaryot Cell **10:**744-752.

52. **Chasis JA, Mohandas N.** 1992. Red blood cell glycophorins. Blood **80:**1869-1879.

53. **Bennett V, Stenbuck PJ.** 1979. The membrane attachment protein for spectrin is associated with band 3 in human erythrocyte membranes. Nature **280:**468-473.

54. **Tiburcio M, Dixon MW, Looker O, Younis SY, Tilley L, Alano P.** 2015. Specific expression and export of the Plasmodium falciparum Gametocyte EXported Protein-5 marks the gametocyte ring stage. Malar J **14:**334.

55. **Lasonder E, Rijpma SR, van Schaijk BC, Hoeijmakers WA, Kensche PR, Gresnigt MS, Italiaander A, Vos MW, Woestenenk R, Bousema T, Mair GR, Khan SM, Janse CJ, Bartfai R, Sauerwein RW.** 2016. Integrated transcriptomic and proteomic analyses of P. falciparum gametocytes: molecular insight into sex-specific processes and translational repression. Nucleic Acids Res **44:**6087-6101.

Figure Legends

Figure 1.

Expression, export, and localization of GEXP02: (A) Schematic representation of the endogenous and transgenic gexp02 loci indicating location of the homology region (HR) and the tdTomato- or HA-tag. Arrows indicate primer sites used to confirm integration of the plasmids into the gexp02 locus (the plasmid backbone is indicated as a dotted line). Right panel shows PCR products confirming plasmid integration. PCR primers A-C are indicated in the left panel. HA, 3D7GDV1/GEXP02-HA; tdT, 3D7GDV1/GEXP02-tdTomato; 3D7, 3D7 wild-type. (B) Live fluorescence microscopy of all gametocyte stages of the 3D7GDV1/GEXP02-tdTomato parasite line. First column shows differential interference contrast (DIC); second column shows tdTomato fluorescence; third column shows nuclei stained with Hoechst; fourth column shows an overlay of all fluorescence channels; fifth column shows a merge with all images (scale bar = 5 μm). (C) Western blot analyses of 3D7GDV1/GEXP02-HA parasite lysates probed with anti-HA antibodies. The Ponceau S-stained membrane shows comparable amounts of total protein loaded in each lane. (D) Immunoelectron micrograph of negatively stained ultrathin sections of 3D7GDV1/GEXP02-HA. GEXP02 was probed with anti-HA (5 nm gold, indicated by arrows) and Pfs16 with anti-Pfs16 (10 nm gold). PVM: parasitophorous vacuole membrane, GIE: gametocyte-infected erythrocyte (white scale bar = 1 μm, black scale bar = 200 nm). (E) Western blot analysis of protein extracts obtained from the serial solubility assay probed with antibodies as indicated. Anti-MAHRP1 (35) and anti-GAPDH served as controls for the respective fractions. (F) Western blot analysis of lysed cell pellets of trypsin-treated (right lane) and untreated (left lane) 3D7/GEXP02-HA stage III gametocytes probed with antibodies against the HA-tag and against glycophorin A. (G) IFA using sheared GIEs probed with antibodies against the HA-tag and glycophorin A (GYPA) (scale bar = 10 μm).

Figure 2.

Co-immunoprecipitation (co-IP) and LC-MS/MS: (A) Silver-stained SDS gel of the input, flow through (FT), wash, and elution fractions of the co-IP experiment. +, GEXP02 co-IP; -, negative control co-IP. (B) Volcano plot showing proteins enriched in the GEXP02-HA and negative control Co-IPs using cross-linked samples. Proteins significantly enriched ($p < 0.05$, enrichment > 2, s0 = 1) are marked in blue, GEXP02 is highlighted in red. (C) Table showing the ten most significantly

enriched exported partners identified by Co-IP using crosslinked samples. The complete list of identified proteins can be found in the Supplementary Table 2. (D) Table showing the four proteins identified in the native GEXP02-HA co-IP.

Figure 3.

Colocalization of GEXP02 with potential interaction partners. (A) Vector map of the plasmid used for episomal over-expression of PF3D7_0424600-GFP. Crt: crt promoter; GFP: green fluorescent protein. The arrow indicates the start of the coding sequence and the circle the end. (B) and (C) Confocal microscopy images of 3D7/GEXP02-HA stage III gametocytes expressing PF3D7_0424600-GFP. Antibodies against the epitope tags or native proteins are indicated (scale bar = 5 µm). (D) Three dimensional rendering of a stage III gametocyte of the same parasite line probed with anti-HA (red), anti-GFP (blue), and anti-PFI1780w (green). The signal of each channel is shown as a surface reconstruction (scale bar = 5 µm). An animated 3D image can be found in the Supplementary Video. (E) IFAs of sheared stage III gametocytes of 3D7GDV1/GEXP02-HA parasites probed with antibodies as indicated (scale bar = 10 µm).

Figure 4.

Characterization of GEXP02 knock-out parasites: (A) Schematic representation of the endogenous loci of 3D7GDV1, NF54wt, 3D7GDV1/GEXP02-KO, and NF54/GEXP02-KO parasite lines. Primer positions used for PCR confirmation of integration are indicated by arrows. Right panel: PCR products for 3D7GDV1 (3D7) and NF54 and the corresponding knock-out lines (KO) to confirm successful deletion of GEXP02. PCR primers A-F are indicated in the left panel. (B) Western blot of 3D7GDV1, 3D7GDV1/GEXP02-HA, and 3D7GDV1/GEXP02–KO as well as NF54wt and NF54/GEXP02-KO lysates probed with anti-GEXP02 antibodies to confirm absence of GEXP02 in the KO lines. Anti-GAPDH was used as loading control. (C) IFAs of 3D7GDV1 and 3D7GDV1/GEXP02-KO using an antibody against GEXP02 to confirm the absence of GEXP02 in the knock-out cell line. DAPI was used to stain nuclei (scale bar = 5 µm). (D) Giemsa-stained blood smears of all five gametocyte stages from NF54 and NF54/GEXP02-KO as well as 3D7GDV1 and 3D7GDV1/GEXP02-KO parasites. (E) Retention rates of stage III and stage V NF54 and NF54/GEXP02-KO gametocytes as measured by microsphiltration. (F) Bar chart showing data from three biological replicates of exflagellation assays. All measurements were normalized to the

exflagellation rates determined for NF54. (G) Summary of the results obtained from mosquito feeding experiments. (H) Summary of results from liver infectivity experiments, which measured traversal and hepatocyte invasion. The values are in percent.

Figure S1.

Co-labeling in immunofluorescence assays: (A) IFAs of all five gametocyte stages of 3D7GDV1/GEXP02-HA parasites. The first column represents the differential interference contrast (DIC) image, the second column shows anti-HA signal labeling GEXP02-HA, the third column shows anti-Pfs16 staining, the fourth column depicts a fluorescence overlay and the fifth column is a merge of all images. All stages were imaged with the same microscope setting, but because the anti-HA signal in gametocyte stages IV and V was weaker the signal was digitally increased post-acquisition to improve its visibility (scale bar = 5 μm). (B) Confocal microscopy IFAs of 3D7/GEXP02-HA gametocytes also expressing PF3D7_0424600-GFP. First column shows DIC; second column shows anti-GEXP02; third column shows anti-GFP; fourth column shows anti-Pfs16; fifth column shows the membrane stain CellMask; sixth column shows an overlay of anti-GEXP02, anti-GFP, and anti-Pfs16. The seventh column shows an overlay of all fluorescence images and the final column shows a merge of all images. (C) Confocal microscopy IFAs of 3D7/GEXP02-HA gametocytes also expressing PF3D7_0424600-GFP. First column shows DIC; second column shows anti-HA; third column shows anti-GFP; fourth column shows anti-PFI1780w; fifth column shows an overlay of the fluorescent images and the sixth column shows a merge of all images (scale bars = 5 μm).

Document S1

Nucleotide Sequences and alignment of the wild-type and the *P. falciparum* codon-optimized sequences encoding the tdTomato tag.

Figure 1

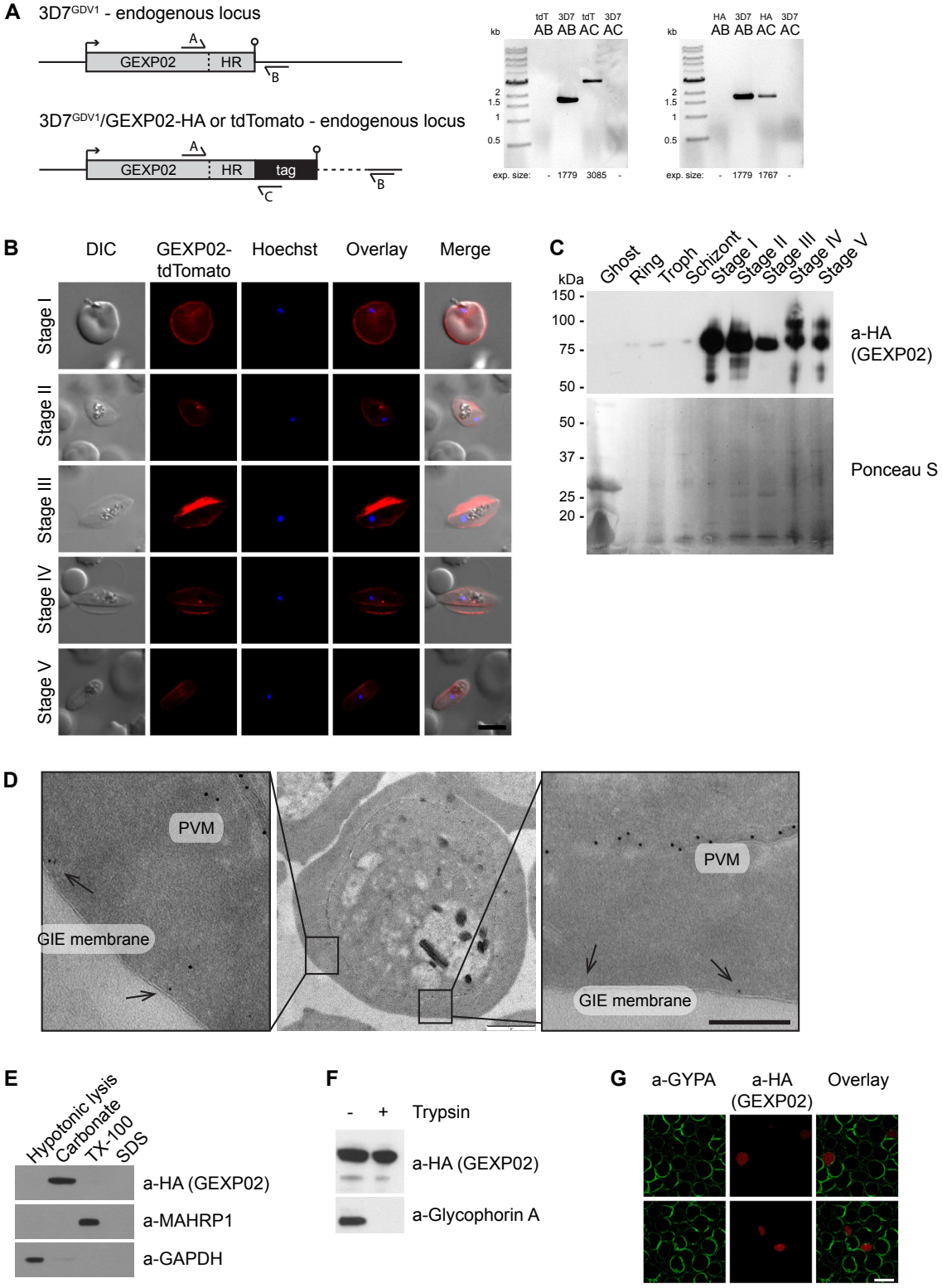
A
3D7GDV1 - endogenous locus
GEXP02
HR
A
B
3D7GDV1/GEXP02-HA or tdTomato - endogenous locus
GEXP02
HR
tag
A
B
C
tdT 3D7 tdT 3D7
AB AB AC AC
kb
2
1.5
1
0.5
exp. size: - 1779 3085 -
HA 3D7 HA 3D7
AB AB AC AC
kb
2
1.5
1
0.5
exp. size: - 1779 1767 -
B
DIC
GEXP02-tdTomato
Hoechst
Overlay
Merge
Stage I
Stage II
Stage III
Stage IV
Stage V
C
kDa
Ghost
Ring
Troph
Schizont
Stage I
Stage II
Stage III
Stage IV
Stage V
150 -
100 -
75 -
50 -
a-HA (GEXP02)
50 -
37 -
25 -
20 -
Ponceau S
D
PVM
GIE membrane
PVM
GIE membrane
E
Hypotonic lysis
Carbonate
TX-100
SDS
a-HA (GEXP02)
a-MAHRP1
a-GAPDH
F
- + Trypsin
a-HA (GEXP02)
a-Glycophorin A
G
a-GYPA
a-HA (GEXP02)
Overlay

Figure 2

A

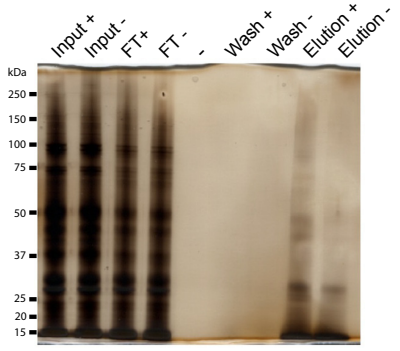

B

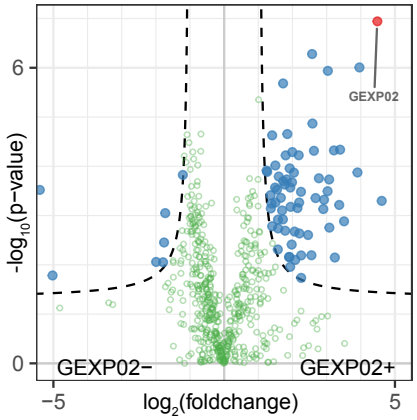

C

Protein ID	Protein Name	p-value	fold change
PF3D7_1102500	GEXP02	1.16E-10	4.49
P16157	Ankyrin-1	5.26E-10	2.57
PF3D7_0800600; PF3D7_0115100	PHISTa; PHISTa	9.85E-7	3.96
PF3D7_0936800	PFI1780w	1.15E-6	3.04
P11277	Spectrin beta	2.80E-6	1.72
P02549	Spectrin alpha	2.35E-5	1.41
PF3D7_0114000	Exported protein family 1	9.36E-5	1.50
P16452	band 4.2	1.33E-4	3.90
PF3D7_0424600	PHISTb	1.85E-4	3.07
P11171	band 4.1	2.11E-4	1.99

D

Protein ID	Protein Name	p-value	fold change
P11277	Spectrin beta	0.009	6.49
P02549	Spectrin alpha	0.013	7.52
P16157	Ankyrin-1	0.018	7.64
P02730	band 3	0.037	5.74

Figure 3

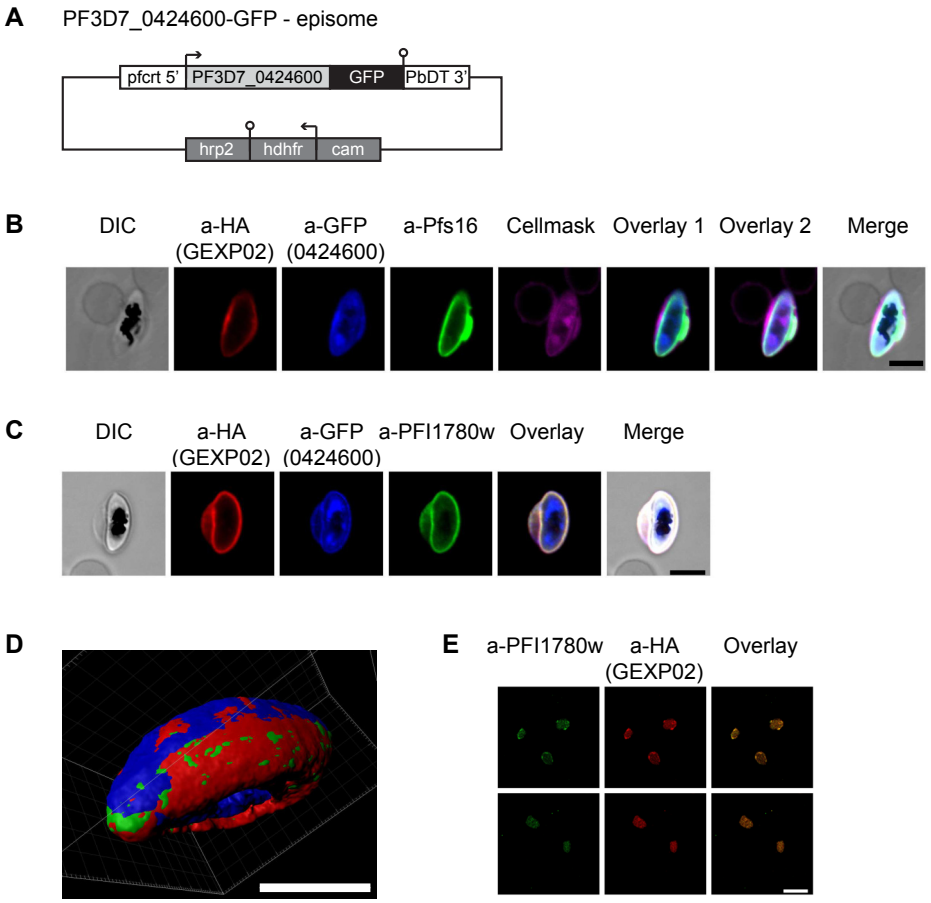
A
PF3D7_0424600-GFP - episome
pfcrt 5'
PF3D7_0424600
GFP
PbDT 3'
hrp2
hdhfr
cam
B
DIC
a-HA (GEXP02)
a-GFP (0424600)
a-Pfs16
Cellmask
Overlay 1
Overlay 2
Merge
C
DIC
a-HA (GEXP02)
a-GFP (0424600)
a-PFI1780w
Overlay
Merge
D
E
a-PFI1780w
a-HA (GEXP02)
Overlay

Figure 4

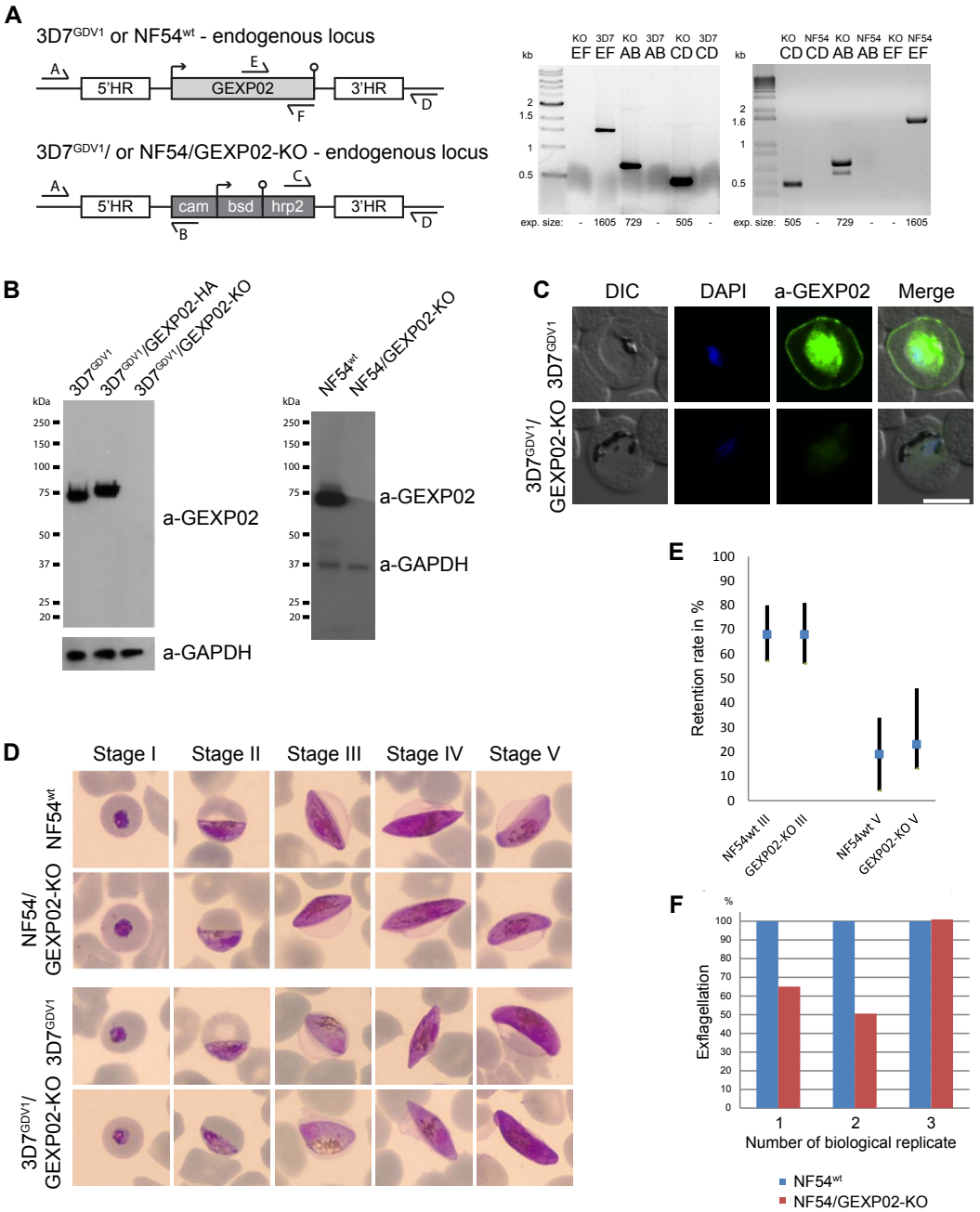

G

#	Cell line	Oocysts/ mosquito	Sporozoites/ oocyst
1	NF54	11.7	4,922
1	GEXP02-KO	9.1	4,057
2	NF54	10	2,750
2	GEXP02-KO	11	3,242

H

	Medium Control	NF54wt	NF54/ GEXP02-KO
Traversal (% of liver cells)	0.14	39.53	46.08
Invasion (% cells invaded)	0.61	13.93	18.85

Figure S1

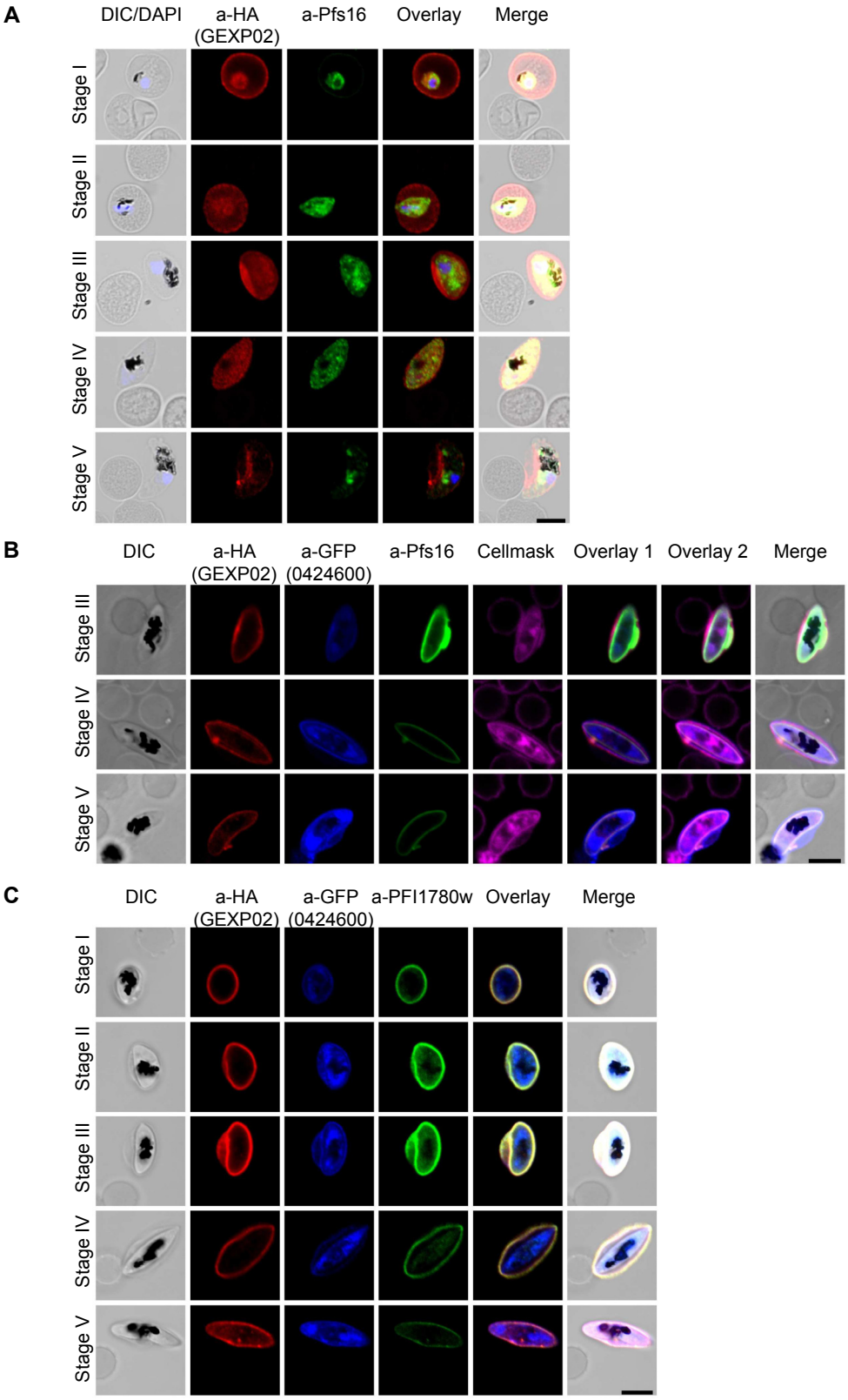
A
DIC/DAPI
a-HA (GEXP02)
a-Pfs16
Overlay
Merge
Stage I
Stage II
Stage III
Stage IV
Stage V
B
DIC
a-HA (GEXP02)
a-GFP (0424600)
a-Pfs16
Cellmask
Overlay 1
Overlay 2
Merge
Stage III
Stage IV
Stage V
C
DIC
a-HA (GEXP02)
a-GFP (0424600)
a-PFI1780w
Overlay
Merge
Stage I
Stage II
Stage III
Stage IV
Stage V

Table S1

Primer Name	Sequence (5′ -> 3′)
GsePb1 forward	aaaAGATCTGTTAACACTAGAGAACATGG
GsePb1 reverse	aaaGCTAGCACCTATATAAGGAGCTTCTG
GsePb1 tomato fw	aaaCTGCAGGTTAACACTAGAGAACATGG
GsePb1 tomato rv	aaaGTCGACACCTATATAAGGAGCTTCTG
GsePb1 HR1 fwd	TCAGGGTAGCTGATATCGGATCCGTATATGGAAATAAGAACGAGC
GsePb1 HR1 rev	TTCTATAAATTGATGTGGAATAACATAATACATGTATG
GsePb1 RES fwd	TTATGTTATTCCAC ATCAATTTATAGAAACAAAATATATAC
GsePb1 RES rev	ATCATTTAGAGTTTGTCTAGATTTAATAAATATGTTCTTATA
GsePb1 HR2 fwd	TTATTAAATCTAGACAAACTCTAAATGATTATCCAAAG
GsePb1 HR2 rev	GCGAGGAAGCGGAAGCTTTAAGTATATACATCTGTTGATGATAA
GsePb1 gRNA +	TATTGGGAAATTAGGAGTAAGAAG
GsePb1 gRNA -	AAACCTTCTTACTCCTAATTTCCC
GsePb1 forward	aaaAGATCTGTTAACACTAGAGAACATGG
GsePb1 reverse	aaaGCTAGCACCTATATAAGGAGCTTCTG
HA integr	GACATAAAGTTGTTAGAGCTC
tdTomato integr	TACCTTACTTATATAATTCATCC
GsePb1 KO rev	ttactttatattccatgtgtag
camR_KO	ttatacaagtatatattttgtttctataaattg
GsePb1 KO fwd	gtatcttatgttctataattgttc
hrp2F_KO	catgttttgtaatttatgggatagcg
PF3D7_0424600 fw	ataactcgagcttaagATGAAGTTTTTTAACGGATCAAGCTTT
PF3D7_0424600 rv	cctttactcatatcgatTATATCAATAAAATTTTTACTACGCATGA
TdT_F_SalI	aaagtcgacATGGTTAGTAAAGGAGAAGAAG
TdT_R_KpnI	aaaggtaccttaCTTATATAATTCATCCATACC

Table S2

Table with LC/MSMS data from cross-linked and native co-immunoprecipitations available under the following DOI: 10.5281/zenodo.2582927.

Supplementary Video

Transgenic *Plasmodium falciparum* stage III gametocyte expressing GEXP02-HA and PF3D7_0424600-GFP treated with paraformaldehyde and glutaraldehyde and then labeled with antibodies against PF3D7_0936800 (green), HA-tag (red), and GFP-tag (blue). Sections obtained with a confocal microscope were visualized in Imaris and a surface resconstruction of all three channels was obtained.

This video can be accessed under the following DOI: 0.5281/zenodo.2579764.

Document S1

Wild-type TdTomato:

atggtgagcaagggcgaggaggtcatcaaagagttcatgcgcttcaaggtgcgcatggagggctccatgaacggccacgagttcg
agatcgagggcgagggcgagggccgcccctacgagggcacccagaccgccaagctgaaggtgaccaagggcggccccctgcc
cttcgcctgggacatcctgtccccccagttcatgtacggctccaaggcgtacgtgaagcaccccgccgacatccccgattacaagaagc
tgtccttccccgagggcttcaagtgggagcgcgtgatgaacttcgaggacggcggtctggtgaccgtgacccaggactcctccctgc
aggacggcacgctgatctacaaggtgaagatgcgcggcaccaacttcccccccgacggccccgtaatgcagaagaagaccatggg
ctgggaggcctccaccgagcgcctgtacccccgcgacggcgtgctgaagggcgagatccaccaggccctgaagctgaaggacgg
cggccactacctggtggagttcaagaccatctacatggccaagaagcccgtgcaactgcccggctactactacgtggacaccaagct
ggacatcacctcccacaacgaggactacaccatcgtggaacagtacgagcgctccgagggccgccaccacctgttcctggggcatg
gcaccggcagcaccggcagcggcagctccggcaccgcctcctccgaggacaacaacatggccgtcatcaaagagttcatgcgcttc
aaggtgcgcatggagggctccatgaacggccacgagttcgagatcgagggcgagggcgagggccgcccctacgagggcaccca
gaccgccaagctgaaggtgaccaagggcggccccctgccttcgcctgggacatcctgtccccccagttcatgtacggctccaaggc
gtacgtgaagcaccccgccgacatccccgattacaagaagctgtccttccccgagggcttcaagtgggagcgcgtgatgaacttcga
ggacggcggtctggtgaccgtgacccaggactcctccctgcaggacggcacgctgatctacaaggtgaagatgcgcggcaccaact
tcccccccgacggccccgtaatgcagaagaagaccatgggctgggaggcctccaccgagcgcctgtacccccgcgacggcgtgct
gaagggcgagatccaccaggccctgaagctgaaggacggcggccactacctggtggagttcaagaccatctacatggccaagaag
cccgtgcaactgcccggctactactacgtggacaccaagctggacatcacctcccacaacgaggactacaccatcgtggaacagtacg
agcgctccgagggccgccaccacctgttcctgtacggcatggacgagctgtacaagtaa

P. falciparum Codon optimized tdTomato:

atggttagtaaaggagaagaagtaataaaagaatttatgagatttaaggtacgaatggaaggatcaatgaatggacatgagtttgaaa
ttgaaggagaaggagaaggtagaccttatgaaggtacgcaaacggctaaattgaaagtaacaaaaggaggtccattacccttgcat
gggatatattaagtccacaatttatgtatggaagtaaagcatatgtaaaacatccagctgatatacctgattacaagaagttgagttttcca
gagggttttaaatgggaacgtgttatgaattttgaggatggaggtttagtaacagttacacaagattctagtttacaagacgggactctta
tatataaagtgaaaatgagaggaactaattttcctcctgatggaccagtaatgcaaaagaaaacaatgggatgggaggcaagtaccg
aaagattatatcctagagatggagtgttgaaaggagaaatacatcaagcacttaaattaaaagacggtggacactatttggtagaattta
aaactatatatatggccaagaaaccagtacagttacctggatattattatgtagacacgaagttagatattacatcacataatgaagattat
actatagttgaacaatatgaaagaagtgaaggaaggcatcatttattcttaggtcatgggacgggtagtactggtagtggaagttctgg
tactgcttcaagtgaagataacaatatggctgttattaaagaattcatgagatttaaagttagaatggaaggaagtatgaatggtcatga
atttgaaatagagggagaaggtgaaggtcgtccatatgaaggaacacaaaccgcaaaattaaaggtaacaaagggtggaccattac
catttgcttgggatattttatctcctcaatttatgtacggatcaaaagcttatgtaaagcatcccgcagatataccagattataagaaattatc
atttccagaaggtttcaaatgggagagagtaatgaattttgaagatggtggattagttaccgtaactcaagattcttctttacaagatggg
acattaatttataaggttaaaatgcgagggacaaattttccacccgatggtcctgttatgcagaagaaaactatgggttgggaggcatct
acagaaaggttatatcctagggatggtgtgttaaaaggtgaaattcatcaagctttgaaattaaaagatggaggtcactatttagtagaa
ttcaaaacaatatacatggcaaagaaaccagttcaattaccaggttattattatgttgatacaaaattagatataacaagtcataatgagga
ttatacaattgtggaacaatatgagagatctgaagggcgtcatcatttgtttctttatggtatggatgaattatataagta

Multiple sequence allignment

```
TdTomato          MVSKGEEVIKEFMRFKVRMEGSMNGHEFEIEGEGEGRPYEGTQTAKLKVTKGGPLPFAWD  60
TdTomato_opt      MVSKGEEVIKEFMRFKVRMEGSMNGHEFEIEGEGEGRPYEGTQTAKLKVTKGGPLPFAWD  60
                  ************************************************************

TdTomato          ILSPQFMYGSKAYVKHPADIPDYKKLSFPEGFKWERVMNFEDGGLVTVTQDSSLQDGTLI  120
TdTomato_opt      ILSPQFMYGSKAYVKHPADIPDYKKLSFPEGFKWERVMNFEDGGLVTVTQDSSLQDGTLI  120
                  ************************************************************

TdTomato          YKVKMRGTNFPPDGPVMQKKTMGWEASTERLYPRDGVLKGEIHQALKLKDGGHYLVEFKT  180
TdTomato_opt      YKVKMRGTNFPPDGPVMQKKTMGWEASTERLYPRDGVLKGEIHQALKLKDGGHYLVEFKT  180
                  ************************************************************

TdTomato          IYMAKKPVQLPGYYYVDTKLDITSHNEDYTIVEQYERSEGRHHLFLGHGTGSTGSGSSGT  240
TdTomato_opt      IYMAKKPVQLPGYYYVDTKLDITSHNEDYTIVEQYERSEGRHHLFLGHGTGSTGSGSSGT  240
                  ************************************************************

TdTomato          ASSEDNNMAVIKEFMRFKVRMEGSMNGHEFEIEGEGEGRPYEGTQTAKLKVTKGGPLPFA  300
TdTomato_opt      ASSEDNNMAVIKEFMRFKVRMEGSMNGHEFEIEGEGEGRPYEGTQTAKLKVTKGGPLPFA  300
                  ************************************************************

TdTomato          WDILSPQFMYGSKAYVKHPADIPDYKKLSFPEGFKWERVMNFEDGGLVTVTQDSSLQDGT  360
TdTomato_opt      WDILSPQFMYGSKAYVKHPADIPDYKKLSFPEGFKWERVMNFEDGGLVTVTQDSSLQDGT  360
                  ************************************************************

TdTomato          LIYKVKMRGTNFPPDGPVMQKKTMGWEASTERLYPRDGVLKGEIHQALKLKDGGHYLVEF  420
TdTomato_opt      LIYKVKMRGTNFPPDGPVMQKKTMGWEASTERLYPRDGVLKGEIHQALKLKDGGHYLVEF  420
                  ************************************************************

TdTomato          KTIYMAKKPVQLPGYYYVDTKLDITSHNEDYTIVEQYERSEGRHHLFLYGMDELYK   476
TdTomato_opt      KTIYMAKKPVQLPGYYYVDTKLDITSHNEDYTIVEQYERSEGRHHLFLYGMDELYK   476
                  ***********************************************************
```

Chapter 7: General Discussion

Malaria remains one of the deadliest infectious diseases worldwide (1) with *Plasmodium falciparum* being accountable for most deaths (2). About halfway into the 48 hour intraerythrocytic asexual developmental cycle, the major parasite derived virulence factor PfEMP1 is inserted into the infected red blood cell (iRBC) membrane (3). PfEMP1-mediated cytoadhesion to endothelial cells allows parasites to sequester in the vasculature and thus escape splenic clearance (4, 5), a mechanisms that is linked to severe malaria (6, 7). On the cytosolic side of the iRBC membrane, PfEMP1 is anchored to the cytoskeleton in electron-dense protrusions called knobs (8, 9). This anchoring requires major refurbishment of the erythrocyte which is devoid of any protein translation or trafficking machinery. It requires cellular reorganization and a general modulation of the cytoskeleton that results in altered iRBC deformability and rigidity. Hence, the parasite has to establish a protein trafficking machinery to export parasite proteins into the iRBC where they carry out their function (10). Several exported proteins have been shown to target the iRBC cytoskeleton during asexual intraerythrocytic stages. Amongst these are MESA (11, 12), Pf332 (13, 14), PfEMP3 (15, 16), as well as members of the Plasmodium helical interspersed subtelomeric (PHIST) family, namely RESA (17, 18), PF3D7_0402000 (19, 20), PF3D7_0532400 (LyMP or PFE1605w) and PF3D7_0936800 (PFI1780w) (21-23). Less is known about protein export and the extent of cytoskeleton remodeling in gametocytes. One example of an exported protein targeting the gametocyte-infected erythrocyte (GIE) cytoskeleton is STEVOR, which has been shown to modulate the deformability of the GIE, a process that is linked to gametocyte sequestration (24). Hence, the cytoskeleton is the target of many exported proteins and therefore represents an interface of host-parasite interactions during all intraerythrocytic stages. Identifying and understanding the key players and process involved in cytoskeleton remodeling will contribute to a more detailed understanding of the intracellular survival mechanisms of the malaria parasite.

In this study, we therefore set out to understand the function of the PHIST protein family and establish an interaction network of exported proteins. The first project presents findings from a study on selected members of the large family of exported proteins, the PHIST protein family (25, 26). A new approach to express and export recombinant human proteins in *P. falciparum* to be used in interaction studies between host and parasite proteins is presented in the second project. In the third project, we investigated the exported PHIST protein GEXP02 (PF3D7_1102500) and its potential role in host cell remodeling during gametocyte development. In addition, I conducted two extensive literature reviews on the PHIST protein family and iRBC cytoskeleton remodeling to combine and analyze existing knowledge with the aim of drawing new conclusions and gaining an even deeper understanding of host cell remodeling during *P. falciparum* infection.

With 89 members, the PHIST family comprises ~14% of the PEXEL proteins (25, 26). It is therefore to be expected that its members play an important role in host cell remodeling. Previous immunoprecipitations with the Maurer's cleft protein MAHRP1 identified a number of PHIST proteins (unpublished and (27)) and started the interest of our lab in the PHIST family. While it was not feasible to investigate all of them at once, a selection has been made that was based on the presence of the MESA-erythrocyte cytoskeleton binding motif (28) or previous reports of peripheral localization in the iRBC (29). I could show that most of the selected PHIST proteins localize to the iRBC cytoskeleton which is in agreement with previous studies on PHIST proteins (21, 23, 29) and supported our hypothesis that this protein family might play a central role in host cell remodeling.

To study the interactions of the selected proteins, BioID was used because it does not require protein-protein interactions to remain intact, a feature needed to sufficiently solubilize cytoskeletal proteins for immunoprecipitations. The biotin ligase BirA* is fused to the bait protein and covalently biotinylates proximal protein (30). While BioID proved to be a fairly simple way to screen for potential interaction partners, its limitations also became obvious. The low activity of the BirA* ligase required 20 hours incubation (31) and resulted in the labeling and identification of many proteins involved in translation and trafficking, proteins that are only temporary interaction partners, but not the final target of the bait. Further improvements to BioID such as a drastic reduction of the incubation time are required to make this an even more powerful tool. Nevertheless, I used the data obtained with BioID in combination with data from previous immunoprecipitation studies to generate a network of interactions between erythrocyte cytoskeleton and exported *P. falciparum* parasite proteins. The presence of cytoskeletal proteins in each BioID or immunoprecipitation again confirmed our hypothesis that the investigated PHIST proteins target the cytoskeleton. At the same time, a number of other exported parasite proteins were identified. Their recurrence in multiple experiments and their resulting interconnected status in the protein interaction network suggest that they interact in concert with the investigated proteins. This network forms the basis for further research on iRBC cytoskeleton remodeling. Since proximity does not necessarily result in a physical interaction, each of the proposed interactions from the network must be confirmed in the future on an individual basis using techniques such as reverse immunoprecipitations, colocalization analyses, or biochemical interaction studies.

Having identified potential protein-protein interactions, their verification would be the next step. Adding molecular tags to potential interaction partners and performing co-localization

analyses or reverse immunoprecipitations would be two frequently employed approaches. An interesting facet of iRBC cytoskeleton remodeling is the interaction between proteins from two different species and types of cells. In this context, the human erythrocyte presents additional challenges as it is terminally differentiated and lacks a nucleus, making the genetic manipulation of erythrocytes and thus the generation of fusion proteins difficult. One workaround would be to manipulate erythrocyte precursor cells (32-34), which is cost-intensive and yields only small amounts of cells preventing large-scale cultures required for immunoprecipitations. As alternative, I have successfully designed and established a method which allows the expression of recombinant erythrocyte proteins in the parasite and targets these proteins for export into the host cell via its own established protein trafficking machinery. This humanized parasite approach was designed in a way that these recombinant human proteins should be soluble in the erythrocyte cytosol. This would eliminate the problem of releasing cytoskeleton proteins in immunoprecipitations from the skeleton. While in the iRBC cytosol, the fusion proteins are expected to bind their putative parasite interaction partners on their way to their final destination within the host cell. Thus, they can be used to screen for new or confirm potential interaction partners.

We showed that different N-termini from exported proteins including the signal peptide and PEXEL motif target recombinant erythrocyte cytoskeleton proteins for export into the host cell. For some of our fusion proteins, namely band3_1-379 and band4.1_FL, any combination of export sequence and tag resulted in efficient protein export. However, other proteins were hardly exported at all, regardless of which export sequence of tag was added. PEXEL proteins are translocated through the PTEX (35, 36) and protein unfolding is necessary in this process (37). It is therefore conceivable that sequence and structure of the selected human proteins might influence their ability to be unfolded prior to translocation though the PTEX. The ankyrin repeat is a very stably folded structural motif (38) and is present 23 times in the Ankyrin_1-827 construct and over 10 times in each of both truncated Ankyrin_1-400 and Ankyrin_401-827 constructs (InterPro search using ankyrin accession number P16157). Inefficient or unsuccessful unfolding could explain the observed partial export while most of the protein seems to be retained in the parasite or parasitophorous vacuole. While band7_55-288 was not exported, the stomatin domain alone (band7_85-218) was well exported into the host cell indicating that some features of band7_55-288 might interfere with export. In general, the humanized parasite approach offers new ways to express and export recombinant erythrocyte proteins in the malaria parasite *P. falciparum* to study host-parasite protein interactions or other features requiring heterologous

genes being expressed as recently has been shown with human redox reporter (39). While most research on exported *P. falciparum* proteins has focused on asexual stages, less is known about the extent of protein export and especially the role and function of exported proteins during gametocyte development. Understanding the mechanisms that play a role in rigidity and deformability changes during gametocyte development (40) that lead to sequestration in extravascular spaces of the bone marrow (41) would therefore be important for the identification of new targets in the effort to stop gametocyte development and thus transmission to the mosquito vector.

Taking advantage of recent advances in achieving high sexual conversion rates *in vitro* (42), I set out to investigate the role of GEXP02, a PHIST protein that has been reported to be expressed early in gametocytes (43). Here I have shown that GEXP02, along with two other PHIST proteins that were identified as potential interaction partners, targets the GIE cytoskeleton. While no function could be attributed to GEXP02 yet, our work shows that exported proteins target the GIE cytoskeleton and thus play a potential role in host cell remodeling at this stage as well. Despite initially finding fewer exflagellation centers *in vitro*, we could not observe an effect in biological replicates. Although it is tantalizing to consider a more male centered function of GEXP02 because of the previously observed increased expression in male gametocytes (44) we need to assume that even if a small effect would be due to the lack of GEXP02, it has no significance for natural infections.

Major differences in cytoskeleton remodeling between asexual stages and gametocytes have been observed, e.g. gametocytes lack knobs (45), which eliminates the need to locally restructure the cytoskeleton for their anchoring. In contrast, gametocytes present STEVOR on their surface, which has been implicated in the continuous increase of GIE rigidity up to stage IV. When transitioning from stage IV to stage V, STEVOR is lost from the surface and rigidity decreases (40, 46). Interestingly, immunofluorescence analyses suggest that GEXP02 it partially internalized during stages IV and V, which coincides with the loss of STEVOR from the surface and the decreased rigidity. Although the mechanisms of this switch in GIE rigidity has not yet been solved, it shows that cytoskeleton remodeling does occur in gametocytes. The peripheral localization of exported proteins in gametocytes as shown by our study adds further evidence to their involvement in host cytoskeleton remodeling also during these stages.

Erythrocyte cytoskeleton remodeling seems to occur in both asexual and sexual stages. The PHIST protein PFI1780w for example was previously found at the cytoskeleton of asexual stages

(21) and could now also be detected in this study. It is conceivable that protein such as PFI1780w might fulfil a general role in all intraerythrocytic stages, such as a general modulation or regulation of cytoskeletal integrity and stability. The presence of knobs in asexual stages (45) implies that some remodeling is specific to asexual stages whilst sexual stage-specific expression and presence of GEXP02 at the GIE cytoskeleton in turn suggests that some exported proteins might remodel the cytoskeleton only in gametocytes.

In addition to the experimental data generated in this study, I performed two extensive literature reviews. One review focused on the molecular mechanisms of erythrocyte cytoskeleton remodeling during *P. falciparum* infection. Combining findings from nearly 200 publications, a more detailed picture of the remodeling process was gained. It became apparent that remodeling is highly stage-specific to meet the requirements of the growing parasite at specific times within its life cycle. Understanding these requirements will help to formulate and test new hypotheses for future research.

In my second review I focused on the PHIST protein family, which has been central to the experimental studies on iRBC cytoskeleton remodeling conducted in this thesis work. Although PHIST proteins have been described as protein family over a decade ago, there has not been a global study on the entire PHIST family. Many research articles on exported proteins and host remodeling mention one or more members of the PHIST family. Collecting individual references to PHIST proteins form primary literature and accompanying supplementary data and using various protein identifications, I was able to collect comprehensive information on this large protein family. Although it is yet impossible to clearly attribute specific functions or roles to most PHIST proteins or to the different subgroups, the combined data strongly supports the notion that PHIST proteins play an important role in iRBC cytoskeleton remodeling.

In conclusion, the present thesis underlines the relevance of investigating exported *P. falciparum* proteins in the context of host cell remodeling. I could show that several PHIST proteins target the iRBC or GIE cytoskeleton. Furthermore, with the humanized parasite approach, I have designed and developed a system to express erythrocyte cytoskeleton proteins in *P. falciparum* and to export them into the host cell cytosol. With the exported gametocyte protein GEXP02, I present a detailed analysis of a previously uncharacterized PHIST protein.

References

1. **Fauci AS, Morens DM.** 2012. The perpetual challenge of infectious diseases. N Engl J Med **366:**454-461.
2. **WHO.** 2017. World Malaria Report 2017. WHO,
3. **Kriek N, Tilley L, Horrocks P, Pinches R, Elford BC, Ferguson DJ, Lingelbach K, Newbold CI.** 2003. Characterization of the pathway for transport of the cytoadherence-mediating protein, PfEMP1, to the host cell surface in malaria parasite-infected erythrocytes. Mol Microbiol **50:**1215-1227.
4. **Cranston HA, Boylan CW, Carroll GL, Sutera SP, Williamson JR, Gluzman IY, Krogstad DJ.** 1984. Plasmodium falciparum maturation abolishes physiologic red cell deformability. Science **223:**400-403.
5. **Hviid L, Jensen ATR.** 2015. Chapter Two-PfEMP1–A Parasite Protein Family of Key Importance in Plasmodium falciparum Malaria Immunity and Pathogenesis. Advances in Parasitology **88:**51-84.
6. **Dondorp AM, Ince C, Charunwatthana P, Hanson J, van Kuijen A, Faiz MA, Rahman MR, Hasan M, Bin Yunus E, Ghose A, Ruangveerayut R, Limmathurotsakul D, Mathura K, White NJ, Day NP.** 2008. Direct in vivo assessment of microcirculatory dysfunction in severe falciparum malaria. J Infect Dis **197:**79-84.
7. **Wahlgren M, Goel S, Akhouri RR.** 2017. Variant surface antigens of Plasmodium falciparum and their roles in severe malaria. Nat Rev Microbiol **15:**479-491.
8. **Pologe LG, Pavlovec A, Shio H, Ravetch JV.** 1987. Primary structure and subcellular localization of the knob-associated histidine-rich protein of Plasmodium falciparum. Proceedings of the National Academy of Sciences **84:**7139-7143.
9. **Watermeyer JM, Hale VL, Hackett F, Clare DK, Cutts EE, Vakonakis I, Fleck RA, Blackman MJ, Saibil HR.** 2016. A spiral scaffold underlies cytoadherent knobs in Plasmodium falciparum-infected erythrocytes. Blood **127:**343-351.
10. **Maier AG, Cooke BM, Cowman AF, Tilley L.** 2009. Malaria parasite proteins that remodel the host erythrocyte. Nat Rev Microbiol **7:**341-354.
11. **Lustigman S, Anders RF, Brown GV, Coppel RL.** 1990. The mature-parasite-infected erythrocyte surface antigen (MESA) of Plasmodium falciparum associates with the erythrocyte membrane skeletal protein, band 4.1. Mol Biochem Parasitol **38:**261-270.
12. **Waller KL, Nunomura W, An X, Cooke BM, Mohandas N, Coppel RL.** 2003. Mature parasite-infected erythrocyte surface antigen (MESA) of Plasmodium falciparum binds to the 30-kDa domain of protein 4.1 in malaria-infected red blood cells. Blood **102:**1911-1914.
13. **Waller KL, Stubberfield LM, Dubljevic V, Buckingham DW, Mohandas N, Coppel RL, Cooke BM.** 2010. Interaction of the exported malaria protein Pf332 with the red blood cell membrane skeleton. Biochim Biophys Acta **1798:**861-871.

14. **Hodder AN, Maier AG, Rug M, Brown M, Hommel M, Pantic I, Puig-de-Morales-Marinkovic M, Smith B, Triglia T, Beeson J, Cowman AF.** 2009. Analysis of structure and function of the giant protein Pf332 in Plasmodium falciparum. Mol Microbiol **71:**48-65.

15. **Waller KL, Stubberfield LM, Dubljevic V, Nunomura W, An X, Mason AJ, Mohandas N, Cooke BM, Coppel RL.** 2007. Interactions of Plasmodium falciparum erythrocyte membrane protein 3 with the red blood cell membrane skeleton. Biochim Biophys Acta **1768:**2145-2156.

16. **Pei X, Guo X, Coppel R, Mohandas N, An X.** 2007. Plasmodium falciparum erythrocyte membrane protein 3 (PfEMP3) destabilizes erythrocyte membrane skeleton. J Biol Chem **282:**26754-26758.

17. **Foley M, Tilley L, Sawyer WH, Anders RF.** 1991. The ring-infected erythrocyte surface antigen of Plasmodium falciparum associates with spectrin in the erythrocyte membrane. Mol Biochem Parasitol **46:**137-147.

18. **Da Silva E, Foley M, Dluzewski AR, Murray LJ, Anders RF, Tilley L.** 1994. The Plasmodium falciparum protein RESA interacts with the erythrocyte cytoskeleton and modifies erythrocyte thermal stability. Mol Biochem Parasitol **66:**59-69.

19. **Parish LA, Mai DW, Jones ML, Kitson EL, Rayner JC.** 2013. A member of the Plasmodium falciparum PHIST family binds to the erythrocyte cytoskeleton component band 4.1. Malar J **12:**160.

20. **Shakya B, Penn WD, Nakayasu ES, LaCount DJ.** 2017. The Plasmodium falciparum exported protein PF3D7_0402000 binds to erythrocyte ankyrin and band 4.1. Mol Biochem Parasitol **216:**5-13.

21. **Oberli A, Slater LM, Cutts E, Brand F, Mundwiler-Pachlatko E, Rusch S, Masik MF, Erat MC, Beck HP, Vakonakis I.** 2014. A Plasmodium falciparum PHIST protein binds the virulence factor PfEMP1 and comigrates to knobs on the host cell surface. FASEB J **28:**4420-4433.

22. **Oberli A, Zurbrugg L, Rusch S, Brand F, Butler ME, Day JL, Cutts EE, Lavstsen T, Vakonakis I, Beck HP.** 2016. Plasmodium falciparum PHIST Proteins Contribute to Cytoadherence and Anchor PfEMP1 to the Host Cell Cytoskeleton. Cell Microbiol doi: 10.1111/cmi.12583.

23. **Proellocks NI, Herrmann S, Buckingham DW, Hanssen E, Hodges EK, Elsworth B, Morahan BJ, Coppel RL, Cooke BM.** 2014. A lysine-rich membrane-associated PHISTb protein involved in alteration of the cytoadhesive properties of Plasmodium falciparum-infected red blood cells. FASEB J **28:**3103-3113.

24. **Naissant B, Dupuy F, Duffier Y, Lorthiois A, Duez J, Scholz J, Buffet P, Merckx A, Bachmann A, Lavazec C.** 2016. Plasmodium falciparum STEVOR phosphorylation regulates host erythrocyte deformability enabling malaria parasite transmission. Blood **127:**e42-53.

25. **Sargeant TJ, Marti M, Caler E, Carlton JM, Simpson K, Speed TP, Cowman AF.** 2006. Lineage-specific expansion of proteins exported to erythrocytes in malaria parasites. Genome Biol **7:**R12.

26. **Warncke JD, Vakonakis I, Beck HP.** 2016. Plasmodium Helical Interspersed Subtelomeric (PHIST) Proteins, at the Center of Host Cell Remodeling. Microbiol Mol Biol Rev **80:**905-927.

27. **Kumar V, Kaur J, Singh AP, Singh V, Bisht A, Panda JJ, Mishra PC, Hora R.** 2018. PHISTc protein family members localize to different subcellular organelles and bind Plasmodium falciparum major virulence factor PfEMP−1. The FEBS journal **285:**294-312.

28. **Kilili GK, LaCount DJ.** 2011. An erythrocyte cytoskeleton-binding motif in exported Plasmodium falciparum proteins. Eukaryot Cell **10:**1439-1447.

29. **Tarr SJ, Moon RW, Hardege I, Osborne AR.** 2014. A conserved domain targets exported PHISTb family proteins to the periphery of Plasmodium infected erythrocytes. Mol Biochem Parasitol **196:**29-40.

30. **Roux KJ, Kim DI, Raida M, Burke B.** 2012. A promiscuous biotin ligase fusion protein identifies proximal and interacting proteins in mammalian cells. J Cell Biol **196:**801-810.

31. **Khosh-Naucke M, Becker J, Mesen-Ramirez P, Kiani P, Birnbaum J, Frohlke U, Jonscher E, Schluter H, Spielmann T.** 2017. Identification of novel parasitophorous vacuole proteins in P. falciparum parasites using BioID. Int J Med Microbiol doi:10.1016/j.ijmm.2017.07.007.

32. **Panichakul T, Sattabongkot J, Chotivanich K, Sirichaisinthop J, Cui L, Udomsangpetch R.** 2007. Production of erythropoietic cells in vitro for continuous culture of Plasmodium vivax. International journal for parasitology **37:**1551-1557.

33. **Hoban MD, Cost GJ, Mendel MC, Romero Z, Kaufman ML, Joglekar AV, Ho M, Lumaquin D, Gray D, Lill GR, Cooper AR, Urbinati F, Senadheera S, Zhu A, Liu PQ, Paschon DE, Zhang L, Rebar EJ, Wilber A, Wang X, Gregory PD, Holmes MC, Reik A, Hollis RP, Kohn DB.** 2015. Correction of the sickle cell disease mutation in human hematopoietic stem/progenitor cells. Blood **125:**2597-2604.

34. **Dever DP, Bak RO, Reinisch A, Camarena J, Washington G, Nicolas CE, Pavel-Dinu M, Saxena N, Wilkens AB, Mantri S, Uchida N, Hendel A, Narla A, Majeti R, Weinberg KI, Porteus MH.** 2016. CRISPR/Cas9 beta-globin gene targeting in human haematopoietic stem cells. Nature **539:**384-389.

35. **de Koning-Ward TF, Gilson PR, Boddey JA, Rug M, Smith BJ, Papenfuss AT, Sanders PR, Lundie RJ, Maier AG, Cowman AF, Crabb BS.** 2009. A newly discovered protein export machine in malaria parasites. Nature **459:**945-949.

36. **Przyborski JM, Nyboer B, Lanzer M.** 2016. Ticket to ride: export of proteins to the Plasmodium falciparum-infected erythrocyte. Mol Microbiol **101:**1-11.

37. **Gehde N, Hinrichs C, Montilla I, Charpian S, Lingelbach K, Przyborski JM.** 2009. Protein unfolding is an essential requirement for transport across the parasitophorous vacuolar membrane of Plasmodium falciparum. Mol Microbiol **71:**613-628.

38. **Main ER, Jackson SE, Regan L.** 2003. The folding and design of repeat proteins: reaching a consensus. Curr Opin Struct Biol **13:**482-489.

39. **Schuh AK, Rahbari M, Heimsch KC, Mohring F, Gabryszewski SJ, Weder S, Buchholz K, Rahlfs S, Fidock DA, Becker K.** 2018. Stable integration and comparison of hGrx1-

roGFP2 and sfroGFP2 redox probes in the malaria parasite Plasmodium falciparum. ACS infectious diseases.

40. **Tiburcio M, Niang M, Deplaine G, Perrot S, Bischoff E, Ndour PA, Silvestrini F, Khattab A, Milon G, David PH, Hardeman M, Vernick KD, Sauerwein RW, Preiser PR, Mercereau-Puijalon O, Buffet P, Alano P, Lavazec C.** 2012. A switch in infected erythrocyte deformability at the maturation and blood circulation of Plasmodium falciparum transmission stages. Blood **119:**e172-180.

41. **Farfour E, Charlotte F, Settegrana C, Miyara M, Buffet P.** 2012. The extravascular compartment of the bone marrow: a niche for Plasmodium falciparum gametocyte maturation? Malar J **11:**285.

42. **Filarsky M, Fraschka SA, Niederwieser I, Brancucci NMB, Carrington E, Carrio E, Moes S, Jenoe P, Bartfai R, Voss TS.** 2018. GDV1 induces sexual commitment of malaria parasites by antagonizing HP1-dependent gene silencing. Science **359:**1259-1263.

43. **Silvestrini F, Lasonder E, Olivieri A, Camarda G, van Schaijk B, Sanchez M, Younis Younis S, Sauerwein R, Alano P.** 2010. Protein export marks the early phase of gametocytogenesis of the human malaria parasite Plasmodium falciparum. Mol Cell Proteomics **9:**1437-1448.

44. **Lasonder E, Rijpma SR, van Schaijk BC, Hoeijmakers WA, Kensche PR, Gresnigt MS, Italiaander A, Vos MW, Woestenenk R, Bousema T, Mair GR, Khan SM, Janse CJ, Bartfai R, Sauerwein RW.** 2016. Integrated transcriptomic and proteomic analyses of P. falciparum gametocytes: molecular insight into sex-specific processes and translational repression. Nucleic Acids Res **44:**6087-6101.

45. **Tiburcio M, Sauerwein R, Lavazec C, Alano P.** 2015. Erythrocyte remodeling by Plasmodium falciparum gametocytes in the human host interplay. Trends Parasitol **31:**270-278.

46. **Sanyal S, Egee S, Bouyer G, Perrot S, Safeukui I, Bischoff E, Buffet P, Deitsch KW, Mercereau-Puijalon O, David PH, Templeton TJ, Lavazec C.** 2012. Plasmodium falciparum STEVOR proteins impact erythrocyte mechanical properties. Blood **119:**e1-8.

Appendix

Publications

Plasmodium Helical Interspersed Subtelomeric (PHIST) Proteins, at the Center of Host Cell Remodeling
Warncke JD, Vakonakis I, Beck HP. 2016. Microbiol Mol Bio Rev. 80:905–927. doi:10.1128/MMBR.00014-16.

Conferences and Meetings

2018	**Molecular Parasitology Meeting**, Woods Hole, MA, USA Talk: „Using Humanized Malaria Parasites to Study Interactions at the Erythrocyte Cytoskeleton“
	Poster: „Using Humanized Malaria Parasites to Study Interactions at the Erythrocyte Cytoskeleton“
	BioMalPar Conference, Heidelberg, Germany Poster: „A PHIST Protein of *Plasmodium falciparum* Targets the Host Cytoskeleton During Sexual Development“
	Malaria Speed Talks, Basel, Switzerland Speed Talk: „Interaction Network Between Exported *Plasmodium* Proteins and the Erythrocyte Cytoskeleton“
2017	**Joint Annual SSTMP Meeting**, Basel, Switzerland
2016	**BioMalPar Conference**, Heidelberg, Germany Poster: „PHIST Proteins and the Host Cell Cytoskeleton - At the Center of Host Cell Remodeling“
2015	**European Congress on Tropical Medicine and International Health**, Basel, Switzerland

Teaching and Training Experiences

2018	**Supervision of Master Students,** Swiss TPH, Basel, Switzerland Training and supervision of two master students during the 12 months long lab and thesis work with the title „Using humanized malaria parasites to study protein interactions at the erythrocyte cytoskeleton“
2017	**Supervision of Master Student**, Swiss TPH, Basel, Switzerland Training and supervision of one master student during the 12 months long lab and thesis work with the title „PHISTb proteins and their interactions with the human cytoskeleton“

Block Course for Bachelor Students, Swiss TPH, Basel, Switzerland
Training and supervision of 4 bachelor students during a two week course in a molecular biology lab, working on *Plasmodium falciparum*

2016 **Supervision of Master Student**, Swiss TPH, Basel, Switzerland
Training and supervision of one master student during the 12 months long lab and thesis work with the title „Studies on interaction of PHIST proteins with the host cytoskeleton and the VAR2CSA-encoded PfEMP1"

Block Course for Bachelor Students, Swiss TPH, Basel, Switzerland
Training and supervision of 3 bachelor students during a two week course in a molecular biology lab, working on *Plasmodium falciparum*

2015 **Block Course for Bachelor Students**, Swiss TPH, Basel, Switzerland
Training and supervision of 4 bachelor students during a two week course in a molecular biology lab, working on *Plasmodium falciparum*